

Univerzita Karlova v Praze

1. lékařská fakulta

Studijní program: Vývojová a buněčná biologie



Ing. Matyáš Flemr

Stabilita mRNA a aktivita mikroRNA v myších oocytech

Messenger RNA stability and microRNA activity in mouse oocytes

Disertační práce

Školitel:

Mgr. Petr Svoboda, PhD

Praha, 2012

Prohlášení:

Prohlašuji, že jsem disertační práci zpracoval samostatně a že jsem řádně uvedl a citoval všechny použité prameny a literaturu. Současně prohlašuji, že práce nebyla využita k získání jiného nebo stejného titulu

Souhlasím s trvalým uložením elektronické verze mé práce v databázi systému meziuniverzitního projektu Theses.cz za účelem soustavné kontroly podobnosti kvalifikačních prací.

V Praze, 24.02.2012

Matyáš Flemr

Identifikační záznam:

FLEMR, Matyáš. *Stabilita mRNA a aktivita mikroRNA v myších oocytech. [Messenger RNA stability and microRNA activity in mouse oocytes]*. Praha, 2012. 140 s. Disertační práce. Univerzita Karlova v Praze, 1. lékařská fakulta / Akademie Věd České Republiky, Ústav Molekulární Genetiky. Školitel Svoboda, Petr.

Klíčová slova:

mRNA; post-transkripční regulace; mikroRNA; oocyt

Keywords:

mRNA; post-transcriptional regulation; microRNA; oocyte

ACKNOWLEDGEMENT

I dedicate this thesis to my parents.

Their never-ending support allowed me to concentrate all the effort on my work. Without them, I would not be able to enjoy my lab life and my scientific progress in such a pleasant, intensive and undistracting way.

My special thanks go to Petr for setting up a lab in Prague addressing the cutting edge topics in short RNA field, and for taking me on board to participate on the adventurous voyage of starting the lab from scratch. The experience I have gained during this process is invaluable.

I thank other members of captain Svoboda's crew for making the journey pleasant and amusing. The positive attitude, after all, is one of the most important driving forces when working in a lab.

I thank Richard Schultz, Jun Ma and Paula Stein for nice and fruitful collaboration.

I thank my co-workers from the IMG animal facility and from IMG service facilities, who make the life of a researcher at the IMG much easier.

I thank the rest of my family and my friends for reminding me constantly that a joyful live also exists outside of the institute's walls...

And last, but not least, I want to acknowledge Radio Nova at novaplanet.com and all the amazing musicians that contribute to its playlist. A large part of the presented data were generated while listening to the positive vibes of this station.

TABLE OF CONTENTS

Souhrn v českém jazyce	6
Abstract	7
1. Introduction	8
1.1 Overview of mouse oogenesis and oocyte-to-zygote transition	9
1.2 Post-transcriptional regulation of maternal mRNAs	13
1.3 Control of maternal mRNA stability and degradation	15
1.4 MicroRNAs and Processing bodies	18
1.5 MicroRNAs and other small RNAs in the oocyte-to-zygote transition	22
2. Aims of the project	25
3. Summary of results and discussion	26
3.1 Optimization of methods to study ribonucleoprotein complexes in mouse oocytes (Supplement 1)	26
3.2 P-body dynamics during oocyte growth and mRNA storage domains in fully-grown oocytes (Supplement 2)	28
3.3 Role of decapping in maternal mRNA degradation (Supplement 3)	31
3.4 MicroRNA pathway suppression in mouse oocytes (Supplement 4)	34
3.5 Regulation of Dicer-dependent pathways during mouse oocyte-to-zygote transition (Supplement 5)	37
4. Conclusions	40
5. References	41
Supplement 1	47
Supplement 2	59
Supplement 3	76
Supplement 4	100
Supplement 5	124
List of publications	139
Curriculum vitae	140

SOUHRN

Přerod oocyty v zygotu představuje jediný fyziologický děj během životního cyklu savců, při kterém se z diferenciované buňky stává buňka pluripotentní. Toto buněčné přeprogramování je z velké většiny závislé na bezchybné post-transkripční regulaci maternálních mRNA. Porozumění mechanismům post-transkripční regulace v oocytech proto povede k významnému rozšíření našeho poznání v otázce buněčného přeprogramování. Mezi důležité post-transkripční regulátory v širokém spektru buněčných a vývojových procesů patří nedávno objevené krátké nekódující mikroRNA. Jejich funkce spočívá v represi cílených mRNA za pomoci proteinových komplexů, které spouštějí deadenylaci a odstranění ochranné čepičky z 5'-konce. Zmíněné komplexy se za normálních okolností sdružují v tzv. procesních tělíscích (P-tělíska) v cytoplasmě. Tato práce přináší nečekané zjištění, že mikroRNA dráha je umlčena v plně dorostlých myších oocytech i během přerodu oocyty do zygoty. Toto zjištění je v souladu s pozorovaným rozpadem P-tělísk závislých na funkci mikroRNA během růstu oocyty a jejich absenci v plně dorostlých oocytech. Některé proteiny běžně obsažené v P-těliscích lokalizují v plně dorostlých oocytech do kortikální oblasti. Spolu s dalšími RNA-vazebnými faktory vytvářejí tyto proteiny ve finální fázi oocytárního růstu sub-kortikální domény, v nichž je uložena maternální mRNA. Dalším důležitým zjištěním je fakt, že součástí komplexu odpovědného za odstranění čepičky z 5'-konce mRNA jsou kódované umlčenými maternálními mRNA, které dávají vzniknout proteinům teprve během meiotického zrání oocyty. Aktivace tohoto komplexu během meiotického zrání přispívá k první vlně degradace maternálních mRNA. Uvedené výsledky významně přispívají k našemu chápání post-transkripční regulace maternálních mRNA, protože ozřejmují některé z mechanismů, jež mají podíl na udržování stabilního prostředí nutného pro akumulaci maternálních mRNA během oocytárního růstu a zároveň v průběhu meiotického zrání přepínají toto prostředí na degradační.

ABSTRACT

The oocyte-to-zygote transition represents the only physiological event in mammalian life cycle, during which a differentiated cell is reprogrammed to become pluripotent. For its most part, the reprogramming relies on the accurate post-transcriptional control of maternally deposited mRNAs. Therefore, understanding the mechanisms of post-transcriptional regulation in the oocyte will help improve our knowledge of cell reprogramming. Short non-coding microRNAs have recently emerged as an important class of post-transcriptional regulators in a wide range of cellular and developmental processes. MicroRNAs repress their mRNA targets via recruitment of deadenylation and decapping complexes, which typically accumulate in cytoplasmic Processing bodies (P-bodies). The presented work uncovers an unexpected feature of the microRNA pathway which is found to be suppressed in fully-grown mouse oocytes and through the entire process of oocyte-to-zygote transition. This finding is consistent with the observation that microRNA-related P-bodies disassemble early during oocyte growth and are absent in fully-grown oocytes. Some of the proteins normally associated with P-bodies localize to the oocyte cortex. At the final stage of oocyte growth, these proteins, together with other RNA-binding factors, form subcortical maternal mRNA storage domains. Furthermore, we find that components of the decapping complex are encoded by dormant maternal transcripts and their activation during meiotic maturation is a prerequisite for the initial wave of maternal mRNA clearance. Together, these data contribute to our understanding of maternal mRNA regulation by elucidating some of the mechanisms responsible for the maintenance of mRNA stabilizing environment during mouse oocyte growth and the switch to mRNA degradation during meiotic maturation.

1. INTRODUCTION

'Ex ovo omnia'

The famous suggestion by William Harvey established female germ cells as the origin of a living organism already in the mid 17th century [1]. Although his preformationist idea was disproved long ago and might raise a smile confronting our current knowledge, the general meaning of these words has remained legitimate. From the meeting of developmental and reproductive biology with modern molecular genetics we learned that oocytes carry the information required for the initiation of embryonic development upon fertilization or related artificial procedures. Detailed studies of mammalian oogenesis revealed the processes underlying the acquisition of developmental competence during oocyte maturation. This in turn enabled the development of laboratory techniques such as *in vitro* fertilization, which is nowadays widely used in human reproductive medicine or livestock industry. The exploration of alternative ways to activate the oocyte contributed significantly to our understanding of embryonic stem cell biology and cell reprogramming. In a seminal work on *Xenopus* model system, the oocyte was shown to be capable of reprogramming an introduced somatic cell nucleus [2]. This technique termed somatic cell nuclear transfer was later used to generate cloned mammals [3], bringing the ultimate support for Harvey's postulate. The reprogramming of a somatic cell to pluripotent state has been recently also achieved by the expression of a defined set of exogenously delivered transcription factors [4]. The resulting induced pluripotent stem cells (iPSC) hold great promises regarding their use in personalized regenerative medicine, diagnostics or generation of disease cell models. However, despite tremendous efforts put into iPSC research in recent years, the cellular processes accompanying reprogramming are still far from being completely elucidated. Derivation of iPSCs from terminally differentiated cells, such as fibroblasts, remains a very inefficient method. Moreover, use of current reprogramming methods often leads to suboptimal iPSCs that possess unwanted features interfering with their intended purpose [5]. The oocyte-to-zygote transition, being the only naturally occurring cell reprogramming from a more differentiated state towards pluripotent state, represents a perfect model system for studying the molecular mechanisms that ensure proper and efficient establishment of pluripotency. Indeed, maternal factors are being identified that significantly improve reprogramming efficiency when used together

with the previously defined factors [6]. It is well documented that the driving force for reprogramming resides in the cytoplasm of a developmentally competent oocyte [7]. Therefore, dissecting the processes occurring in the ooplasm during oocyte-to-zygote transition, including the post-transcriptional control of maternal mRNAs, will help complete the mosaic of cell reprogramming.

1.1 Overview of mouse oogenesis and oocyte-to-zygote transition

The journey of mouse female germ cells begins during gastrulation in E7.25 embryos when a group of cells is recruited to create a population of primordial germ cells (PGCs). Upon subsequent migration PGCs enter the forming gonadal ridge at approximately E10.5. Through Wnt signalling activation the gonadal ridges of XX genotype transform into ovaries and the PGCs within them undergo intense division phase. At E12.5 PGCs enter meiosis in response to retinoic acid signal and arrest at diplotene stage of meiosis I in which they remain until folliculogenesis in postnatal ovaries (reviewed in [8]).

Folliculogenesis is a tightly regulated process during which the oocyte is recruited to the growth phase and with the support of surrounding follicular granulosa cells it acquires developmental competence and eventually leaves the ovary upon ovulation. Prior to follicle formation, oocytes are resting in ovaries clustered within germ cell cysts. Those oocytes that survive the germ cell cyst breakdown in newborn ovaries become individually surrounded by a single layer of flattened pre-granulosa cells, together forming primordial follicles. The resting pool of primordial follicles represents a finite reserve of oocytes available throughout the female reproductive life span. At the stage of primordial follicle formation specific transcription factors expressed exclusively in oocytes start to orchestrate the oocyte development. Thus, FIGLA ensures the primordial follicle formation and maintenance, while NOBOX, SOHLH1 and SOHLH2 govern the primordial oocyte activation and transition to primary follicles (reviewed in [8]). This recruitment of a limited number of follicles for growth phase, which occurs in post-pubertal cycles, is accompanied by significant changes in the oocyte transcriptome and expression of oocyte specific factors required for follicle development [9]. Among these, members of the transforming growth factor β family GDF9 and BMP15 act as essential paracrine signals in the communication of the oocyte with surrounding granulosa cells during primary to secondary follicle transition, which first appears in mice 10-12 days after birth.

Subsequently, cyclically released pituitary gonadotropins follicle stimulating hormone (FSH) and luteinizing hormone (LH) become the master regulators of antral development and ovulation. During antral folliculogenesis a fluid-filled cavity forms within the follicle and separates granulosa cells into two distinct populations, cumulus cells surrounding the oocyte and mural granulosa cells at the follicle periphery. Proliferation of these cells is stimulated by FSH-activated cyclic AMP (cAMP)/protein kinase A pathway. In oocytes, the same pathway ensures inactive state of the maturation promoting factor (MPF) consisting of CDK1 and cyclin B that controls the G2/M transition. Thus, the elevated levels of follicular cAMP keep the oocyte arrested at the first meiotic prophase throughout growth phase until the point when LH surge triggers meiotic maturation (reviewed in [8]).

The final stage of oocyte growth before the resumption of meiosis is characterized by a large-scale chromatin rearrangement within germinal vesicle (GV), which is a common designation for the oocyte nucleus. For the most part of the growth phase chromosomes are dispersed in the nucleus with a large portion of chromatin being in the active euchromatin conformation. However, at the stage just prior to meiotic re-entry the entire chromatin content of the GV undergoes heterochromatinization, forming a densely packed heterochromatin ring around the oocyte nucleolus. Thereby, fully-grown GV oocytes are categorized based on their chromatin conformation as non-surrounded nucleolus (NSN) or surrounded nucleolus (SN) oocytes (reviewed in [10]). When fully-grown GV oocytes with a diameter of 70-80 μm are isolated from mouse ovaries, approximately 50% possess SN conformation. The remaining NSN oocytes are expected to acquire the SN conformation just prior to the resumption of meiosis [11]. The two types of GV oocytes can be easily distinguished under a microscope after staining with any commonly used DNA stain, such as DAPI. Although the molecular mechanism responsible for the global chromatin remodelling remains elusive, changes occurring within the oocyte during this process are essential for the acquisition of developmental competence. *In vitro*, both SN and NSN oocytes are capable of meiotic maturation and zygote formation. However, only eggs originating from SN oocytes can support further development, while the fertilized eggs of NSN origin arrest at the 2-cell stage [12]. Detailed investigation of the reciprocal GV transfer between NSN and SN oocytes and its impact on developmental competence revealed that SN ooplasm highly increases the meiotic maturation efficiency of NSN GVs, but is incapable of overcoming the preimplantation development block. This block is not caused by the chromatin composition of NSN oocytes itself, as metaphase II plates arising

from NSN GV oocytes can give rise to zygotes capable of completing full-term development when introduced into enucleated MII eggs of SN origin [13]. Therefore, changes in the cytoplasm and nucleus of SN GV oocytes, which are not directly related to chromatin, contribute to the acquisition of full developmental competence. A recent study suggested that SN specific translation activation of Oct4, a master transcriptional regulator of pluripotency, might explain the difference in developmental competence of NSN and SN oocytes [14]. However, additional experiments are required to confirm this hypothesis and to test whether translation activation of other maternal factors takes place in SN oocytes.

As mentioned above, the resumption of meiosis in fully-grown GV oocytes is triggered by a transient wave of LH signal. LH acts through the activation of phosphodiesterase PDE3A, which decreases cAMP levels in the oocyte, thereby promoting the activation of CDK1 and cell cycle progression (reviewed in [15]). The same cascade of events is set off spontaneously after the release of the oocyte from its natural follicular environment. For practical purposes, selective inhibitors of PDE3A, such as 3-isobutyl-1-methylxanthine (IBMX), can be added to the medium to maintain high levels of cAMP and prevent meiotic maturation during *in vitro* manipulation of fully-grown GV oocytes. The resumption of meiosis is characterized by a rapid germinal vesicle break down (GVBD), condensed chromosome segregation and asymmetric division of the cytoplasm, resulting in the first polar body extrusion. Meiosis proceeds directly to a second division during which a MOS kinase-containing cytostatic factor complex inhibits anaphase-promoting complex (APC) and arrests the oocyte at metaphase II (MII). Subsequently, ovulation occurs and the MII egg is released from its follicle in order to be fertilized by sperm in the oviduct (reviewed in [8]). Fertilization induces the completion of second meiotic division of the oocyte followed by parental pronuclei formation. Both pronuclei replicate their DNA content and approximately 20 hours post fertilization the first zygotic cleavage gives rise to two blastomeres of a 2-cell embryo, each equipped with a diploid nucleus containing one set of paternal and one set of maternal chromosomes. At this stage mouse zygotic genome is activated and the newly formed embryo discharges the maternal program and takes control of the further preimplantation development. This includes a second wave of genome activation at the 8-cell stage, when the embryo undergoes the process of compaction, in which loosely associated blastomeres create tightly connected cell mass of the morula, resulting in the formation of polarized epithelium. Preimplantation development is

completed after the differentiation of the morula into the blastocyst, composed of the outer layer of differentiated trophoectoderm cells that represent the origin of extraembryonic tissues and pluripotent cells of the inner cell mass (ICM) that will give rise to the embryo proper (reviewed in [16]). ICM cells are the natural equivalent and the source of *in vitro* cultured embryonic stem cells (ESCs).

The most part of mouse oocyte growth during folliculogenesis is characterized by significant transcriptional activity, resulting in a large maternal mRNA pool present in fully-grown GV oocytes. However, in the course of NSN to SN chromatin remodelling the oocytes become transcriptionally quiescent and the transcription remains shut down throughout the oocyte-to-zygote transition until the zygotic genome activation (ZGA) in the 2-cell embryo (reviewed in [16]). Thus, the whole process of oocyte meiotic maturation, fertilization, zygote formation and switch from meiotic to mitotic cell cycle during the first zygotic cleavage runs without transcription. Given the negligible contribution of non-DNA material by the sperm, the transition depends entirely on the maternal mRNAs synthesized during the oocyte growth phase. Therefore, an mRNA stabilizing environment needs to be created in the growing oocyte to enable maternal mRNA accumulation. In addition, a precise mechanism of post-transcriptional mRNA regulation ensuring timely translation and elimination of maternal transcripts is vital for correct orchestration of the oocyte-to-zygote transition.

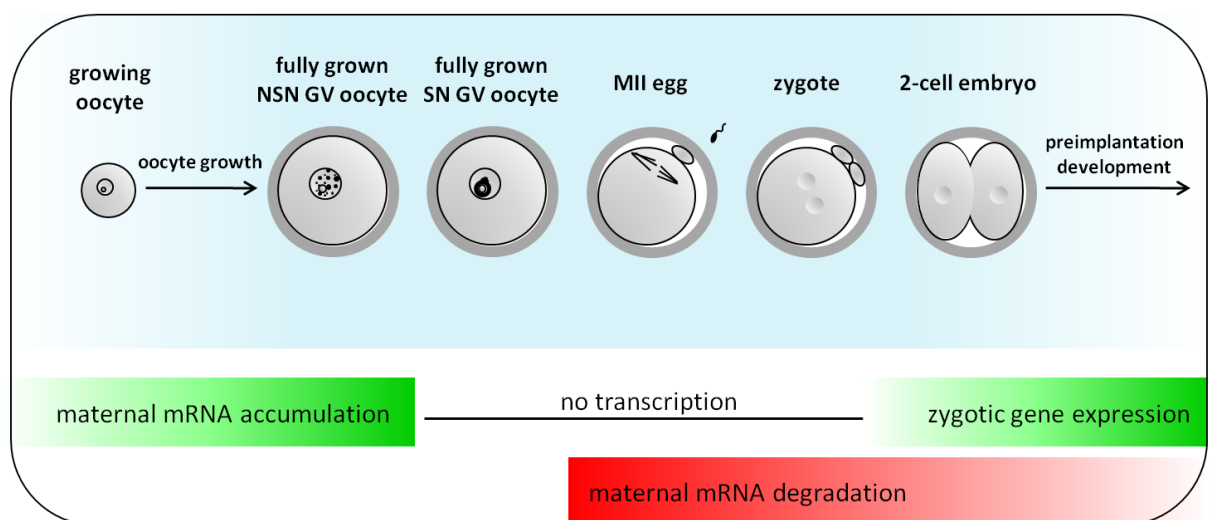


Figure 1. mRNA synthesis and degradation during mouse oocyte-to-zygote transition

1.2 Post-transcriptional regulation of maternal mRNAs

The mechanisms of post-transcriptional maternal mRNA control have started to be dissected by initial findings in *Xenopus* oocytes that translational activity is regulated by cytoplasmic polyadenylation [17]. Further research revealed that cytoplasmic polyadenylation is well conserved in both invertebrate and vertebrate oocytes, including mammals. However, as the resources of mammalian oocytes are limited and do not enable collection of sufficient amounts of material for biochemical studies, most of the molecular mechanisms underlying cytoplasmic polyadenylation have been elucidated using *Xenopus* oocyte maturation as a model system [18].

The investigation of potential regulatory motifs in 3'UTRs of maternal mRNAs identified two elements responsible for cytoplasmic polyadenylation. A conserved polyadenylation hexanucleotide (Hex) AAUAAA is a common sequence motif in all mRNAs required also for nuclear polyadenylation. In post-transcriptionally regulated maternal mRNAs, an additional cytoplasmic polyadenylation element (CPE) with consensus sequence UUUUUAU was found in the proximity of Hex motif. CPE is recognized by CPE binding protein (CPEB), which is currently considered a master regulator of cytoplasmic polyadenylation (reviewed in [19]). CPEB is found in oocytes within a large ribonucleoprotein (RNP) complex containing a cytoplasmic form of the multisubunit factor CPSF (cleavage and polyadenylation specificity factor) bound to the Hex, and the cytoplasmic poly(A) polymerase GLD-2. CPEB plays a dual role in the regulation of maternal mRNAs during oogenesis. In growing oocytes, when maternal mRNAs are synthesized and stored in a translationally inactive state, CPEB serves as a translation repressor. CPE-containing mRNAs are polyadenylated in the nucleus following transcription and subsequently deadenylated after transport to the cytoplasm by the action of poly(A)-ribonuclease (PARN). In immature oocytes, PARN directly binds to CPEB in RNP complexes also containing CPSF and GLD-2. It was suggested that competition between GLD-2 and PARN activity maintains the polyA tail of CPE-containing transcripts shortened, thereby interfering with translation. During meiotic maturation, CPEB becomes a target of Aurora A kinase, switching from a repressor to an activator function. Phosphorylation of CPEB impairs the interaction with PARN, which in turn leads to efficient polyadenylation of CPEB-bound mRNAs by GLD2, and to translation activation (reviewed in [20]). Alternative CPEB repressive mechanisms have been suggested and

CPEB was found to interact with other RNA-binding proteins, for example the well characterized translational repressor Xp54 (DDX6) [21].

During oocyte growth not all CPE-containing mRNAs are kept in a translationally repressed state. Likewise, the stimulation of translation does not occur uniformly for all CPE-containing mRNAs during meiotic maturation. Aurora A-mediated phosphorylation of CPEB induces the initial wave of cytoplasmic polyadenylation, which activates factors required for meiotic progression. Later during maturation around metaphase I, CPEB is hyperphosphorylated by CDC2, leading to CPEB degradation and a second wave of polyadenylation (reviewed in [20]). Recently, a combinatorial code has been proposed for the prediction of maternal mRNA behaviour that takes into account the number of CPEs and their position within 3'UTR relative to Hex motif [22]. Alternatively, the timing of maternal mRNA polyadenylation might depend on the interplay of different regulatory elements and their position within the same 3'UTR (reviewed in [20]).

The mechanisms of CPEB-regulated polyadenylation have not been extensively studied in mouse oocytes. However, CPEB-mediated control of meiotic maturation similar to that found in *Xenopus* has been well established and conserved CPE-containing targets, such as *c-Mos* and *Ccnb1*, were identified [23, 24]. Downregulation of CPEB during oocyte growth revealed that critical targets under CPEB control are the above mentioned MOS kinase and TGF β family member GDF9, as the CPEB knockdown oocytes mimicked some of the phenotypes observed in MOS and GDF9 knockouts [25]. Similar to the *Xenopus* model, mouse CPEB is phosphorylated by Aurora kinase to promote meiotic maturation [26]. Interestingly, a recent study identified the RNA-binding protein DAZL (deleted in azoospermia-like) as a target of CPEB regulation translationally activated in meiotic resumption [27]. DAZL was previously shown to interact with PABP and stimulate translation initiation [28]. Indeed, the global analysis of polysome occupancy during mouse meiotic maturation revealed that 3'UTRs of transcripts recruited to polysomes upon the resumption of meiosis are enriched for the DAZL-binding element. Furthermore, DAZL depletion during maturation reduced the levels of the TPX2 protein required for spindle assembly, which is encoded by a transcript containing multiple DAZL-binding motifs. This is consistent with compromised meiotic maturation and severe spindle defects observed in DAZL-depleted eggs. Thus, a model was proposed in which CPEB activates the translation of *Dazl* mRNA upon the resumption of meiosis. Subsequently, DAZL

stimulates its own translation via a positive reinforcing loop as well as translation of other transcripts later in meiotic maturation [27].

In addition to the tight translational regulation, maternal mRNAs are also subject to a highly organized sequence specific control at the level of mRNA stability. However, unlike the mechanisms regulating maternal mRNA recruitment for translation, which are slowly becoming apparent, the regulatory processes responsible for mRNA stability during mouse oocyte growth and the switch to massive mRNA degradation during oocyte-to-zygote transition remain largely unknown.

1.3 Control of maternal mRNA stability and degradation

The generation of a large maternal mRNA pool and its subsequent rapid and selective elimination is a conserved feature of the metazoan oocyte-to-zygote transition. The fraction of the protein-coding genome present in the maternal mRNA pool ranges from 35% in *C. elegans* to 40% in the mouse, and up to 65% in *Drosophila*. 30-40% of the transcripts constituting the maternal mRNA pool are degraded during the oocyte-to-zygote transition in a sequence specific and temporally controlled manner. The major waves of degradation occur during meiotic maturation, after fertilization and upon ZGA (reviewed in [29]). The relatively short period of massive mRNA clearance is preceded by a long period of significant mRNA stability during oocyte growth. Depending on the organism, this period, during which the maternal transcripts remain stable, can range from days to weeks or even months. As mentioned above, one of the mechanisms that keep the maternal mRNAs stored in a translationally inactive state during oocyte growth is deadenylation by PARN. Dormant maternal mRNAs generally possess a shortened poly(A) tail, which is under normal circumstances a signal for mRNA elimination. Therefore, an mRNA stabilizing environment during oocyte growth is essential to prevent premature maternal mRNA degradation.

In the mouse, MSY2 (also known as Y box protein YBX2) is the best characterized example of an RNA-binding protein controlling mRNA stability. MSY2 is expressed at high levels in both male and female mouse germ cells. During spermatogenesis, MSY2, which can also act as a DNA-binding transcription factor, co-transcriptionally marks the transcripts selected to be stored in the cytoplasm in an MSY2-containing RNP complex

[30]. Knockout experiments showed that MSY2 is involved in the maintenance of mRNA stability in postmeiotic spermatids [31]. In oocytes, MSY2 was calculated to constitute 2% of the total protein content. Similarly to spermatids, MSY2 also confers stability to maternal mRNAs, and its deletion in oocytes leads to dramatic changes in the transcriptome, decreasing the total amount of polyadenylated mRNA by 25%. In addition, stability of an exogenous RNA injected into MSY2 knockout oocytes is also lower in comparison with wild type oocytes [32]. Reminiscent of CPEB regulation, MSY2 was found to be a subject to CDK1-mediated phosphorylation during meiotic maturation. It has been suggested that phosphorylation of MSY2 might be a trigger for the global switch from mRNA stabilizing to a degradation-prone environment. Interestingly, the stimulation of MSY2 phosphorylation is sufficient to overcome the PDE3A-mediated meiotic arrest in fully-grown GV oocytes. In line with this, the expression of non-phosphorylatable dominant-negative form of MSY2 inhibits the maturation-associated decrease in mRNAs, while the expression of constitutively active form induces mRNA degradation in the absence of maturation [33]. This further supports the model in which MSY2 functions as a general mRNA stabilizing factor during mouse oocyte growth and its phosphorylation renders maternal mRNAs prone to degradation. These data characterizing mouse MSY2 are consistent with previous findings from *Xenopus* oocytes. FRGY2, a *Xenopus* ortholog of MSY2, binds maternal mRNAs in a sequence-independent manner and 'masks' them from translational machinery [34]. Similar to the observation in mouse spermatids, FRGY2-regulated masking of *Xenopus* mRNAs in the ooplasm also requires FRGY2-dependent marking of the mRNA during transcription [35]. FRGY2 represents a major constituent of maternal storage mRNPs, in which it associates with other translational repressors CPEB, RAP55 and Xp54 [36].

Xp54 (DDX6 in mammals, CGH-1 in *C. elegans*) is a well characterized DEAD box helicase conserved in all eukaryotes from yeast to human. In *Xenopus* oocytes, Xp54 binds nascent transcripts on chromosome loops and targets them to the storage mRNPs in the cytoplasm. It was shown through tethering assays that Xp54 exerts a translational repressor activity similar to FRGY2 [37]. Although the studies in *Xenopus* oocytes focused solely on the role of Xp54 in translational repression, recent data from *C. elegans* provide a comprehensive overview of CGH-1 role in the maintenance of maternal mRNA stability [38, 39]. In *C. elegans* somatic cells, CGH-1 forms Processing bodies (P-bodies, see below) together with another RNA-binding protein PATR-1 and promotes decapping and

degradation of target mRNAs. During oogenesis, however, CGH-1 is found in CAR-1 (RAP55 ortholog)-containing granules that are independent of PATR-1 and the decapping complex, and therefore distinct from somatic P-bodies. This localization of CGH-1 into domains containing translational repressors and devoid of the decapping complex suggests that CGH-1 plays a different, probably stabilizing role in *C. elegans* germ cells. Indeed, RNA immunoprecipitation identified a subset of maternal mRNAs associated with CGH-1 that are significantly destabilized upon CGH-1 depletion. Interestingly, the group of CGH-1-interacting mRNAs is rather small and contains mostly germ cell-specific transcripts [39]. This suggests that in contrast to MSY2, which confers stability to a large fraction of maternal mRNAs during mouse oocyte growth, CGH-1 protects a specific set of mRNAs, probably in a sequence-dependent manner. Whether this feature of CGH-1 helicase is common to its orthologs in other systems, particularly in mammals, and eventually to what extent the maternal mRNA targets of CGH-1 would be conserved across species remains to be determined.

The above examples make it apparent that the same RNA-binding proteins are involved in the regulation of mRNA stability and translational activity during metazoan oocyte growth. The findings from various model organisms can therefore be complemented to gain a detailed image of maternal mRNA control. Accordingly, the mechanisms of maternal mRNA clearance during oocyte-to-zygote transition also share similar features in various species. Deadenylation appears to be the dominant process responsible for triggering maternal mRNA clearance. Various RNA-binding proteins orchestrate the recruitment of the deadenylase complex to maternal transcripts directed for degradation in different model systems. Thus, Smaug is a specificity factor for deadenylation in *Drosophila*, in which Pumilio and AU-rich element (ARE)-binding proteins also contribute to specific mRNA destabilization. ARE-binding proteins also play an important role during maternal mRNA destabilization in *Xenopus* and *C. elegans*. In mammals, homologs of both Smaug and ARE-binding proteins exist, and a putative ARE-binding protein ZFP36L2 has been implicated in mRNA degradation (reviewed in [29]). Another recently discovered class of regulatory molecules involved in maternal mRNA degradation in several organisms is represented by small non-coding microRNAs.

1.4 MicroRNAs and Processing bodies

The tiny non-coding microRNAs (miRNAs), exhibiting the potential to downregulate target mRNAs with partial complementarity, were first described in 1993 as regulators of heterochronic genes in *C. elegans* development [40]. After the discovery of RNA interference (RNAi) [41], miRNAs were revisited at the turn of the millennium. Since then, an immense research has elucidated the principles of miRNA biogenesis and action as well as the role of miRNAs in both physiological and non-physiological processes. miRNAs were identified in all multicellular eukaryotes examined, and hundreds of unique miRNAs have been described in mammals, with the predicted potential to modulate the expression of up to 50% of all protein coding genes (reviewed in [42]). In agreement with this, miRNAs have been implicated in virtually every cellular and developmental process studied. In particular, miRNAs were found to contribute significantly to cell type specification during differentiation. Many miRNAs show tissue specific expression pattern in somatic cells, for example miR-124 in neural cells or miR-122 in liver. These confer robustness to cell type specification and maintenance by controlling the expression levels of critical target mRNAs (reviewed in [43]). Other miRNAs play essential roles in the fundamental cellular processes such as cell cycle regulation and DNA damage response [44]. Among these, several miRNAs were identified as potent oncogenes, notably the members of miR-17~92 cluster, while others can function as tumour suppressors, for instance miR-34, which is a component of the p53-mediated pathway [45]. Yet another group of miRNAs, represented by miR-290 family members in mice, is indispensable for the maintenance of pluripotency in ES cells, and has been successfully used to improve the efficiency of cell reprogramming and production of iPS cells [46]. Taken together, miRNAs have been established as an integral part of the gene regulatory network in multicellular eukaryotes. The functional studies of individual miRNAs as well as further understanding of mechanistic aspects underlying miRNA action remain in the centre of current research focus.

The majority of mammalian miRNAs are encoded in the genome as independent genes. These so called 'canonical' miRNAs are transcribed by RNA polymerase II into capped and polyadenylated long primary miRNA (pri-miRNA) transcripts. Pri-miRNAs harbour one or more regions capable of folding into local hairpin structures recognized by a nuclear RNase III Drosha. Together with its cofactor, a double-stranded RNA (dsRNA)-binding protein DGCR8, Drosha forms the Microprocessor complex which binds to the stem-loop

structure within pri-miRNA and processes it into an approximately 70 nucleotides (nt) long stem-loop precursor miRNA (pre-miRNA), leaving a 2 nt 3'-overhang on the cleaved stem structure. This 2 nt overhang is subsequently recognized by nuclear export factor Exportin-5, and the pre-miRNA is transported to the cytoplasm for further processing. Once in the cytoplasm, pre-miRNA is cleaved by another RNase III Dicer to become a 21-23 nt duplex miRNA consisting of a guide strand (mature miRNA) and a passenger strand, with 2 nt 3' overhangs at both ends (reviewed in [42]). Dicer is a multi-domain protein that is stabilized and also catalytically stimulated by its association with a dsRNA-binding protein TRBP [47]. Together, Dicer and TRBP not only process the pre-miRNA, but they are also involved in loading the mature miRNA duplex on one of the Argonaute (Ago) proteins [48]. During the loading step, the duplex miRNA is unwound and the strand with a lower thermodynamic stability at the 5' end, which corresponds to the mature miRNA, remains associated with the Ago protein. This miRNA-loaded Ago constitutes the core of the effector miRNA-induced silencing complex (miRISC) [42]. The miRNA biogenesis pathway appears to be a highly regulated process, which is not surprising given the impact of miRNAs on protein-coding transcriptome. Individual miRNAs can be regulated at the level of miRNA gene transcription in a way similar to that of protein-coding genes. This type of control is mostly responsible for tissue-specificity and developmental timing of miRNA expression [42]. Some miRNAs are also subject to post-transcriptional regulation at the level of processing, as is the case of the members of a highly conserved Let-7 miRNA family that are enriched in terminally differentiated cells and may function as tumour suppressors [49]. Let-7 processing at both pri-miRNA and pre-miRNA levels is antagonized by an RNA-binding protein LIN28 and its paralog LIN28B, which specifically recognize and bind to the loop sequence of Let-7 precursors, thereby interfering with Drosha and Dicer activity. LIN28 is usually enriched in pluripotent and multipotent self-renewing cells where it helps maintain low levels of Let-7, and its overexpression is frequently observed in various tumours (reviewed in [50]). Canonical miRNA production can also be modulated globally at the level of Drosha and Dicer processing. Drosha activity is compromised by the excess of its partner DGCR8, which in turn is regulated on the transcript level in a negative loop by direct Drosha cleavage. Similarly, the amount of available TRBP is a limiting factor of Dicer activity and altered TRBP levels have been observed in human carcinomas [42]. In addition to canonical miRNAs, the recent advent of sensitive high-throughput deep sequencing techniques enabled the discovery of miRNAs generated by alternative biogenesis pathways. These include miRNAs independent of the

Microprocessor complex, represented by small nucleolar RNA-derived miRNAs, tRNA processing-derived miRNAs and mirtrons, which are short products of mRNA splicing that spontaneously form a stem-loop structure of a pre-miRNA. A Dicer-independent miRNA was also discovered that is processed to its mature form directly by the Argonaute protein AGO2 (reviewed in [51]). Although these recently discovered alternative miRNAs add to the complexity of the metazoan miRNAome, it should be stressed that the canonical miRNAs still account for the vast majority of miRNAs present in animal cells.

In mammals, a single Dicer protein is responsible for both pre-miRNA processing and generation of small interfering RNAs (siRNAs) from long dsRNA substrates. Likewise, the mechanism of Dicer-processed short RNA loading onto Ago proteins is supposed to be similar for both miRNAs and siRNAs [52]. Therefore, sequence complementarity between the short RNA and its mRNA target is the only parameter distinguishing whether a short RNA will act as a miRNA or a siRNA. There are four Ago proteins encoded in mammalian genomes, of which AGO2 is the dominant form and the only one to possess a short RNA-directed endonucleolytic activity. When the short RNA loaded on AGO2 is perfectly complementary to its target, typically in case of a siRNA, AGO2 directly cleaves the target at the position corresponding to nucleotides 10 and 11 of the short RNA. In contrast, short RNA with only partial complementarity acts as a miRNA and requires additional protein components to form a fully functional miRISC complex capable of repressing translation and inducing indirect degradation of the target mRNA (reviewed in [52]). Nucleotides at positions 2-7 of the miRNA constitute the 'seed region', and their complementarity with the target is a critical determinant of the miRNA function [53]. The precise mechanisms by which miRNAs control translational activity and stability of target mRNAs and levels of corresponding proteins remain a matter of debate [54]. However, it was suggested that decreased protein levels resulting from miRNA activity are predominantly due to miRNA-induced destabilization of targeted transcripts [55]. This is achieved by miRISC-mediated recruitment of deadenylation and decapping enzymes. During the last decade, a number of protein factors required for miRNA activity have been identified [42]. Among these, a trinucleotide repeat-containing protein GW182 (TNRC6A) was shown to be an essential part of the miRISC complex. GW182 interacts directly with AGO2 on one side and with PABP and components of the CCR4-NOT deadenylation complex on the other, thereby promoting deadenylation of the miRNA target, which in turn stimulates decapping by the DCP1-DCP2 complex and subsequent 5'→3' degradation by XRN1 exonuclease (reviewed

in [56]). Interestingly, all the factors involved in miRNA-mediated mRNA destabilization localize to distinct microscopically visible cytoplasmic foci called Processing bodies (P-bodies). The discovery of P-bodies has revolutionized the research of post-transcriptional mRNA regulation and led to the identification of many novel protein factors involved in translational repression and mRNA decay (reviewed in [57]). Notably, miRNAs were established as the integral part of P-bodies. All components of miRISC complex, such as AGO2, GW182, or the above mentioned RNA helicase DDX6, localize to P-bodies together with miRNAs themselves and their mRNA targets [57]. Disruption of the miRNA pathway by downregulation of crucial biogenesis or miRISC factors results in P-body loss. However, the opposite is not true and microscopic P-bodies are dispensable for the miRNA function as downregulation of a structural P-body component unrelated to miRNAs can disintegrate P-bodies without affecting miRNA activity. Therefore, the formation of P-bodies is a consequence rather than the cause of miRNA-mediated repression [58]. Given that P-bodies are highly dynamic structures, their presence or absence can be used as a robust readout for the evaluation of miRNA activity.

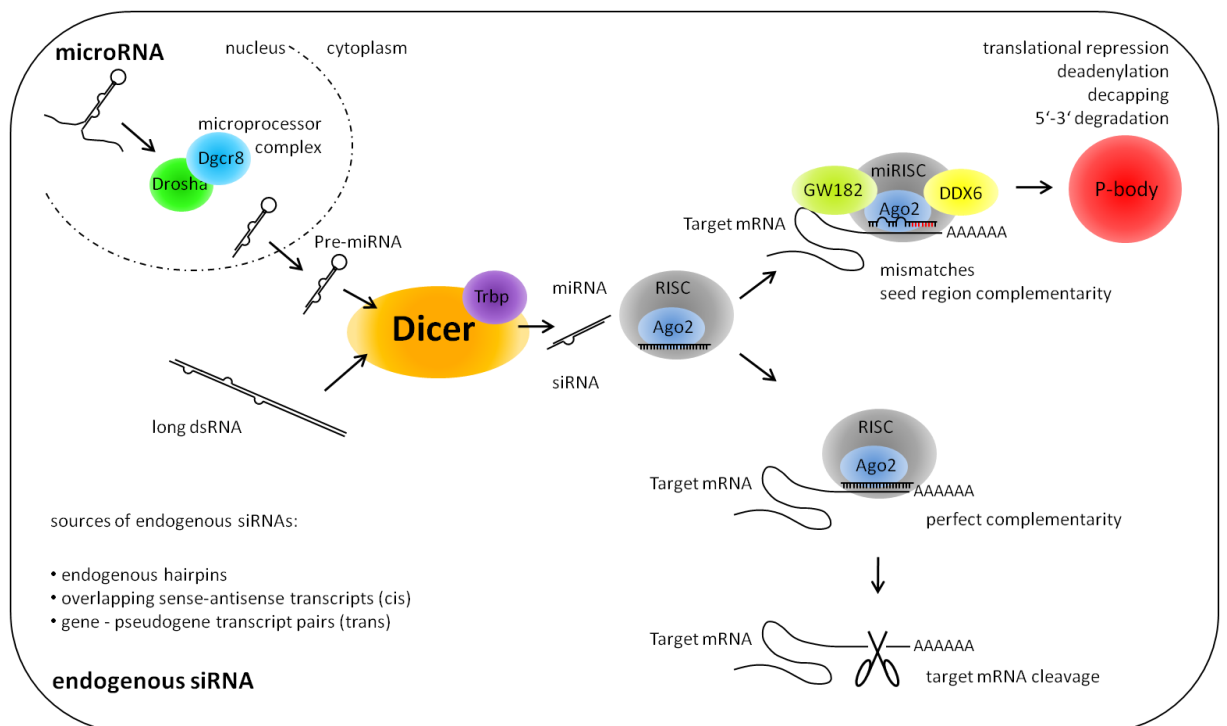


Figure 2. Dicer-dependent small RNA pathways in mammalian cells

1.5 MicroRNAs and other small RNAs in the oocyte-to-zygote transition

The fact that miRNAs recognize their targets in a sequence-dependent manner makes them ideal candidates for the selective post-transcriptional control of maternal mRNAs. Indeed, several studies on invertebrate and vertebrate models established specific miRNAs as the effectors of maternal mRNA clearance. In *Drosophila*, miRNAs from the zygotically expressed miR-309 cluster contribute to the second wave of maternal mRNA degradation during the maternal-to-zygotic transition. Mutant flies lacking the miR-309 cluster accumulate a significant portion of maternal transcripts normally downregulated at the early stages of embryogenesis, which leads to delayed larval development and compromised viability of the mutant embryos [59]. This zygotic miRNA action is consistent with the dynamic rearrangement of *Drosophila* P-bodies during oogenesis, where P-body component-containing granules in late stage oocytes are devoid of 5' decapping machinery and the re-formation of decapping-containing P-bodies occurs in early embryogenesis [60]. Interestingly, another class of small RNAs, the 24-30 nt long Piwi-associated RNAs (piRNAs) produced by the Piwi-type of Argonaute proteins, has been found to trigger maternal mRNA deadenylation in *Drosophila*. Typically, piRNAs function as guardians of genome integrity by controlling the expression of repetitive elements and retrotransposons from which they originate [61]. A recent study has revealed that piRNAs specifically target an mRNA encoding the embryonic posterior morphogen Nanos through transposon-derived sequences in its 3'UTR, and that piRNA-associated factors interact with Smaug protein to promote *Nanos* deadenylation [62]. Thus, the transposon-derived regions, which are generally abundant in 3'UTRs of protein coding transcripts, might serve as regulatory elements in maternal mRNAs. However, a broader evidence for piRNA-mediated maternal mRNA clearance in *Drosophila* or other systems is currently lacking.

In vertebrates, evolutionarily related zygotically expressed miRNAs with a conserved seed region AAGUGC orchestrate maternal mRNA degradation. The finding that miR-430 promotes maternal mRNA clearance during the maternal-to-zygotic transition in zebrafish was the first evidence of miRNA involvement in maternal mRNA control. Similar to the situation in *Drosophila*, miR-430 is expressed at the onset of zygotic genome activation, and it induces the deadenylation and decay of a large fraction of maternal transcripts [63]. The aberrant accumulation of these transcripts is possibly the cause of the developmental delay and gastrulation defects observed in mutant fish lacking maternally and zygotically provided Dicer [64]. Likewise, high levels of miR-427 generating from zygotic

transcription are responsible for the deadenylation and degradation of maternal mRNAs encoding cyclin A1 and cyclin B1 during the *Xenopus* midblastula transition (MBT), which is a period in *Xenopus* embryogenesis when the major wave of zygotic activation occurs, maternal program is suppressed and the embryo becomes autonomous [65]. Interestingly, a recent study suggests that Ago proteins are the limiting factor for miRNA activity at MBT. Injection of exogenous siRNAs leads to the saturation of endogenous Ago proteins, which in turn results in lower levels of miR-427 and relief of miR-427 target repression. Furthermore, neither the exogenous siRNAs nor the endogenous miRNAs are able to elicit miRISC-mediated repression or RNAi in *Xenopus* oocytes, the latter only being restored by the overexpression of catalytically active human AGO2 [66]. These data suggest that oocyte-provided Ago proteins are developmentally controlled in the *Xenopus* maternal-to-zygotic transition to become active only at MBT.

All the above mentioned cases of miRNA involvement in maternal mRNA clearance describe the action of zygotically expressed miRNAs. However, in mammals the major wave of maternal mRNA degradation embarks during oocyte meiotic maturation before fertilization, raising a question to what extent the miRNA-mediated mRNA clearance is conserved during mammalian oocyte-to-zygote transition. Mouse oocytes contain significant amounts of mature miRNAs. Among the most abundant are the members of differentiation-associated Let-7 and miR-30 families, supporting the notion that oocytes are terminally differentiated cells [67, 68]. A large portion of maternal miRNAs is downregulated during the oocyte-to-zygote transition and exchanged upon ZGA, with the miR-290 family miRNAs possessing the AAGUGC seed region, consistent with the expression pattern observed in *Xenopus* and zebrafish [67]. In order to study the role of miRNAs in the control of mouse maternal mRNAs, knockout mice with oocyte-specific deletion of Dicer were analyzed. The evaluation of miRNA contribution to maternal mRNA clearance turned out to be impossible due to dramatic phenotypes observed during meiotic maturation of Dicer knockout oocytes. Although the oocyte growth was not perturbed and the numbers of fully-grown GV oocytes were comparable to the wild type, the majority of knockout oocytes were unable to proceed through meiosis I, which was mainly due to severe spindle defects, chromosome misalignments and the related inability to extrude the first polar body [67, 68]. Originally, these abnormalities were attributed to the loss of maternal miRNAs since no other Dicer-dependent regulatory mechanisms were known to function in mammalian cells at that time [67]. However, the development of

‘next generation sequencing’ techniques allowed for more thorough analyses of small RNAs in mouse oocytes and identified abundant endogenous siRNAs (endo-siRNAs) as a novel class of Dicer-produced mammalian regulatory RNAs [69, 70]. Endo-siRNAs arise from Dicer processing of long dsRNA. The sources of long dsRNA in mouse oocytes include transcripts harbouring long regions of complementarity capable of folding into a long hairpin structure, and natural antisense transcripts originating in *cis* via transcription of overlapping genomic loci or in *trans* via interactions of transcripts encoded by genes and their pseudogenes transcribed in reverse orientation. Even though the majority of endo-siRNAs in oocytes correspond to repetitive sequences and retroelements, a significant portion arises from overlapping transcripts or gene-pseudogene pairs of protein coding genes. These endo-siRNAs have the potential to regulate the expression of cognate transcripts [69, 70]. Strikingly, many predicted endo-siRNA targets encode for genes involved in microtubule formation, microtubule dynamics and cell cycle regulation, arguing for the actual cause of Dicer knockout phenotype. Therefore, the extent to which miRNAs contribute to the regulation of mouse meiotic maturation and maternal mRNA clearance remained to be tested.

2. AIMS OF THE PROJECT

The primary focus of the presented work was to determine the contribution of mouse oocyte miRNAs to meiotic maturation and maternal mRNA degradation, and to monitor the distribution of P-bodies during the oocyte-to-zygote transition.

After the initial surprising finding that fully-grown GV oocytes are devoid of microscopically visible P-bodies, we addressed the following objectives:

- monitor the presence of P-bodies and the dynamics of P-body disassembly during oocyte growth
- ascertain the distribution of P-body components in fully-grown oocytes and their potential role in dormant maternal mRNA regulation
- evaluate the contribution of the decapping complex, which was found to be translated only during meiotic maturation, to the initial wave of maternal mRNA degradation
- test the miRNA pathway activity in fully-grown oocytes

3. SUMMARY OF RESULTS AND DISCUSSION

3.1 Optimization of methods to study ribonucleoprotein complexes in mouse oocytes (Supplement 1)

Meiotic maturation in mouse oocytes and oocyte-to-zygote transition (OZT) proceed without transcription and depend entirely on the post-transcriptional regulation of maternal mRNAs. These mRNAs need to be recruited for translation and subsequently also degraded in a tightly controlled spatial and temporal manner. Such regulation is achieved through the interaction of maternal mRNAs with regulatory RNA-binding proteins. Elucidating the composition and dynamics of ribonucleoprotein (RNP) complexes in mouse oocytes is therefore vital for understanding the post-transcriptional control of maternal mRNAs during OZT.

The composition of RNP complexes is usually studied on the level of protein-protein and RNA-protein interactions using biochemical techniques such as protein-immunoprecipitation followed by western blotting, or RNA-immunoprecipitation followed by RT-PCR or sequencing. These techniques generally require large amounts of input material. However, the total protein content of a single fully-grown mouse oocyte is only approximately 30 ng [71]. Given the limited number of oocytes per mouse, work with mouse oocytes does not enable the use of biochemical techniques mentioned above. Therefore, the studies of RNP complexes in oocytes rely heavily on microscopic techniques such as immunofluorescence and RNA in situ hybridization, which allow to study the composition and subcellular localization of RNPs at the single cell level. Successful use of microscopic techniques depends on accurate sample preservation which is mostly achieved by correct fixation, permeabilization and handling of the specimen during these procedures.

We revisited the previously published protocols for whole mount immunofluorescence on mouse oocytes [72]. A striking observation, which had not been previously described in the literature, was a considerable shrinkage of oocytes during fixation in 4% paraformaldehyde (PFA) in PBS. The size of a fully-grown mouse oocyte is approximately 80 μm in diameter and its large volume makes the cell very sensitive to osmolarity changes. Although the shrinkage observed during fixation was mostly reversible, it was not

clear whether this transient change in morphology might have any impact on protein distribution after fixation. We performed a set of control experiments to confirm that the observed shrinkage does not affect protein localization and that 4% PFA in PBS is a suitable fixative for RNP immunofluorescence studies in mouse oocytes (Suppl.1, Fig.1). In addition, we found that the oocyte 3D structure can be damaged during mounting in dense glycerol-based solutions. A series of successive washes in washing solution with increasing glycerol concentration prior to mounting can overcome this problem. Finally, a proper manipulation of oocytes prior to fixation also turned out to be a critical factor in maintaining oocyte morphology. Due to their size, oocytes need to be manipulated under a microscope and a mouth-operated hand-drawn glass micropipette is typically used to transfer oocytes between solutions. We noticed that using pipettes with a diameter close to the size of the oocyte renders shrinkage during fixation irreversible. This is likely due to a pressure generated in a narrow pipette, which might lead to a significant damage of oocyte cytoskeleton. Therefore, a minimal pipette diameter double the size of the oocyte was suggested for all manipulation steps prior to fixation in order to preserve the original oocyte morphology.

After optimizing the conditions of oocyte manipulation, we focused our efforts on developing a whole-mount RNA fluorescence in situ hybridization (WM-FISH) protocol for the capture of RNA localization at the subcellular level. Although WM-FISH has been used to detect transcripts in preimplantation embryos [73], no such protocol had previously been described for oocytes. We found fixation and permeabilization to be the crucial steps in this procedure. In oocytes, a large fraction of maternal mRNAs is stored in the cytoplasm in a translationally inactive state. This is likely achieved by a tight association of mRNAs with RNA binding proteins possessing translational repressor function. A controlled proteinase K treatment of fixed oocytes turned out to be essential for disrupting such RNPs, making the targeted maternal mRNAs accessible for FISH probe hybridization. Subsequent post-fixation of proteinase-treated oocytes with glutaraldehyde was necessary to preserve the oocyte architecture and RNA levels. By applying these conditions we managed to detect a highly abundant dormant maternal mRNA transcript *c-Mos* with fluorescein-labelled oligodeoxyribonucleotide probe (Suppl.1, Fig.3). The combination of our WM-FISH protocol with immunofluorescence for simultaneous visualization of RNA and proteins was not successful, possibly due to the damage of protein epitopes during the proteinase K treatment. We were nevertheless able to co-stain

RNA binding proteins and poly(A) RNA in oocytes using a fluorescently labelled oligo(dT)₁₈ probe. Hybridization with this probe required no special sample processing and could be performed during a standard immunofluorescence staining. Surprisingly, we found that the signal of fluorescent oligo(dT)₁₈ probe increased significantly when oocytes were pretreated with RNase A for a limited time period (Suppl.1, Fig.4). Possible explanation of this observation could be that the limited RNase A digestion loosens the densely packed RNPs and makes poly(A) tails more accessible for the probe.

With the battery of optimized staining methods mentioned above we proceeded to study cytoplasmic RNP localization and dynamics in mouse oocytes, with an emphasis on P-bodies and miRNA associated factors.

3.2 P-body dynamics during oocyte growth and mRNA storage domains in fully-grown oocytes (Supplement 2)

In order to address the initial topic of the presented PhD project, the role of miRNAs during OZT, we first focused on the distribution and dynamics of P-bodies in mouse oocytes. We got access to autoimmune human index serum 18033 previously described as a robust P-body marker in mammalian cells [74]. The 18033 serum was shown to recognize mainly two P-body components, GW182 (TNRC6A) and EDC4 [75]. The human origin of this serum enabled colocalization studies with other P-body markers, for which commercial and non-commercial antibodies raised in mouse or rabbit were available. The 18033 serum stained large P-bodies in oocytes at primordial and primary follicle stages, together with antibodies against DCP1A, DDX6 and AGO2 (Suppl.2, Fig.1). Surprisingly, the detected P-bodies gradually decreased in size as the oocytes entered the growth phase, and eventually disassembled completely in secondary oocytes (Suppl.2, Fig.2). No P-body-like structures were observed later in oocyte development or in preimplantation embryos until the early blastocyst stage. The lack of P-bodies implies possible perturbations of the miRNA pathway and also raises a question regarding the localization and fate of canonical P-body components. Closer inspection of P-body components in fully-grown oocytes revealed two interesting features. The 18033 signal and DDX6 were enriched in the cortex of fully-grown oocytes, while DCP1A levels dramatically increased during meiotic maturation, suggesting that *Dcp1a* mRNA could represent a dormant maternal mRNA recruited for translation only upon the resumption of

meiosis (Suppl.2, Fig.3). The distribution of cortically enriched DDX6 and 18033 signal underwent dynamic changes in fully-grown oocytes. In surrounded nucleolus (SN) oocytes the proteins detected by these antibodies accumulated in transiently forming irregularly shaped foci, which we termed subcortical aggregates (SCAs). DDX6 homologs in other model organisms have previously been shown to serve as translational repressors [37]. Furthermore, in *C. elegans* oocytes DDX6 homolog CGH-1 was shown to stabilize stored maternal mRNAs [39]. This prompted us to investigate whether the SCAs observed in mouse SN oocytes might represent maternal mRNA storage domains. To this end we analyzed the localization of additional RNA binding proteins. We reproduced the previously described cortical staining of YBX2 (MSY2) protein [72] and found YBX2 localizing into SCAs in SN oocytes (Suppl.2, Fig.4). YBX2 has been involved in the control of mRNA stability and cytoplasmic storage in mouse male germ cells [30]. A recent study implies the role of YBX2 in the control of mRNA stability also in oocytes [32]. Another protein localizing to SCAs was the regulator of cytoplasmic polyadenylation CPEB (Suppl.2, Fig.7). CPEB recognizes short U-rich sequences (CPE elements) in 3'UTRs of dormant maternal mRNAs and supports the translationally inactive state of these mRNAs through association with the deadenylation enzyme. Only upon the resumption of meiosis CPEB phosphorylation promotes cytoplasmic polyadenylation of dormant mRNAs and their translation [19]. Together, the protein composition of SCAs strongly suggested that these might be cytoplasmic storage domains for maternal mRNAs.

We then focused on mRNA localization in fully-grown oocytes. In non-surrounded nucleolus (NSN) oocytes the vast majority of poly(A) mRNA localized to the nucleus. This is in agreement with the fact that NSN oocytes are highly transcriptionally active. As expected, the poly(A) signal in transcriptionally quiescent SN oocytes was almost exclusively cytoplasmic. Interestingly, poly(A) RNA created two distinct populations in SN oocytes, forming a perinuclear ring on one side and localizing into SCAs on the other (Suppl.2, Fig.4). It remains to be determined whether the perinuclear population of mRNAs in SN oocytes consists of translationally active transcripts. It will be interesting to test this hypothesis and explore possible spatial regulation of the translational activity in SN oocytes, with the ooplasm divided to the translationally active inner part and the translationally inactive periphery. One approach might be to monitor the distribution of polysomes in SN oocytes. We pursued the poly(A) mRNAs localizing in SCAs in order to better characterize their properties. We found that apart from the above mentioned RNA

binding proteins, SCAs were also enriched in eIF4AIII (Suppl.2, Fig.7). eIF4AIII is a component of the exon junction complex (EJC), which associates with mRNAs during splicing. It was shown that EJC remains associated with processed mRNAs until the first round of translation and therefore the EJC staining can be used to localize stored untranslated transcripts in the cytoplasm [76]. Localization of eIF4AIII in SCAs further confirmed their mRNA storage function. Finally, we also performed RNA-FISH with a specific probe targeting a classical dormant maternal transcript *c-Mos*. Even though it was not technically possible to colocalize the *c-Mos* signal with SCA protein markers, *c-Mos* showed subcortical distribution reminiscent of SCAs in SN oocytes (Suppl.2, Fig.7). Taken together, we established the transiently forming SCAs in SN oocytes as storage domains for untranslated maternal mRNAs. It remains to be determined whether the formation of SCAs has any functional relevance in terms of maintaining the translationally inactive state and mRNA stability prior to meiotic resumption in mouse oocytes. As DDX6 helicase has been shown to be an essential building block of P-bodies in somatic cells [77], it is possible that DDX6 may play a similar role in the SCA architecture. If that is the case, oocytes from knockout mice depleted of endogenous DDX6 might elucidate the role of SCAs in the post-transcriptional regulation of maternal mRNAs. Also, the DDX6 deficient oocytes might reveal the group of maternal mRNAs directly stabilized by this helicase. It would be interesting to compare these mRNAs with maternal transcripts specifically stabilized by DDX6 homologs in other systems [39], which might provide new insights into the general understanding of oocyte meiotic maturation. The mechanism of SCA formation and mRNA transport to the cortex is also currently unknown. SCA appearance was not affected in oocytes treated with microtubule or microfilament inhibitors, suggesting potential involvement of intermediate filaments in the control of SCA dynamics (Suppl.2, Fig.6). However, more profound studies are needed to expose the role of cytoskeleton components in mRNA transport and SCA formation. Our experiments with microtubule and actin depolymerizing agents were performed on fully-grown oocytes. Although the overall poly(A) signal in the subcortical region increases in SN oocytes compared to NSN, most of the protein constituents of SCAs are already dispersedly enriched in the cortex of NSN oocytes. This might indicate that the proper formation of SCAs does not directly require any long distance transport of its components, and that it may be induced by a local cortical signal. Novel techniques enabling fluorescent *in vivo* tracking of RNA transport will be helpful in dissecting the regulation of maternal mRNA deposition in SCAs [78]. While the generation of SCAs remains a mystery, we were able

to monitor SCA disappearance during meiotic maturation. We followed the fate of SCAs early after the germinal vesicle breakdown (GVBD). Consistent with their role of dormant maternal mRNA storage sites, SCAs began to detach from the cortex and move towards the centre of the oocyte soon after the GVBD. Simultaneously SCAs started to loosen and disperse, likely reflecting the release of stored mRNAs. Within 8 hours after GVBD, no remaining SCAs could be detected and the poly(A) signal was completely diffused and enriched in the oocyte center (Suppl.2, Fig.8). Interestingly, at the same time period after GVBD the DCP1A signal started to appear in the oocyte center. This observation may serve as a proof of spatial regulation of maternal mRNA translation. DCP1A translational activation temporally coincides with the onset of maternal mRNA degradation. This link between mRNA degradation and decapping activation led us to study the role of decapping in maternal mRNA clearance in more detail.

3.3 Role of decapping in maternal mRNA degradation (Supplement 3)

As mentioned above, while studying the P-body component distribution in fully-grown oocytes, we noticed that the level of DCP1A protein increases dramatically during meiotic maturation. However, data from the BioGPS gene expression atlas [79], which we confirmed by RT-PCR, showed that *Dcp1a* transcript is highly abundant in fully-grown oocytes. Likewise, *Dcp2* mRNA coding for the catalytically active component of the decapping complex was also present in a significant amount in fully-grown oocytes, while DCP2 protein started to accumulate only after the resumption of meiosis (Suppl.3, Fig.1). This observation led us to speculate that the decapping machinery is attenuated in growing oocytes on the post-transcriptional level. Such repression of the decapping activity would contribute to the maintenance of a mRNA stabilizing environment, which is necessary for the accumulation of the maternal mRNA pool during oocyte growth.

The nature of *Dcp1a* and *Dcp2* transcript regulation resembled the classical dormant maternal transcripts controlled by CPEB-dependent cytoplasmic polyadenylation. Indeed, a closer inspection of *Dcp1a* and *Dcp2* 3'UTRs revealed multiple candidate CPE elements in the vicinity of the polyadenylation site in both transcripts. We cloned the *Dcp1a* and *Dcp2* 3'UTRs and fused them with the firefly luciferase coding sequence. As expected, injection of these fusion constructs in the form of non-polyadenylated RNA into fully-grown oocytes did not produce any distinct luciferase activity, while the luciferase signal

markedly increased when the injected oocytes were matured to MII eggs. Moreover, mutations introduced into the CPE elements of *Dcp1a* and *Dcp2* 3'UTRs significantly reduced the luciferase activity in MII eggs. In both cases the strongest effect was observed after mutating the CPE closest to the polyadenylation site (Suppl.3, Fig.2). These results confirmed that *Dcp1a* and *Dcp2* are bona fide dormant maternal mRNAs. The CPE elements in *Dcp1a* and *Dcp2* 3'UTRs are well conserved among vertebrates. Therefore, the CPEB-regulated dormancy of decapping is likely a common strategy to establish an mRNA stabilizing environment in vertebrate oocytes. This idea is supported by the compromised decapping activity previously reported in *Xenopus* oocytes [80]. Decapping typically follows deadenylation of mRNAs designated for degradation, making the 5' end of mRNAs accessible to 5'→3' exonucleases [81]. Dormant mRNAs are resting in oocytes in deadenylated form maintaining only a short poly(A), which prevents their precocious translation [11]. In light of this, CPEB-dependent dormancy of the decapping itself presents an elegant way for the switch between stabilizing and degradation-prone environments at the point when maternal mRNAs need to be degraded. We thereby focused on the potential role of decapping activation in the initiation of maternal mRNA clearance.

As decapping components are present almost exclusively in the form of mRNAs in fully-grown oocytes, we used an siRNA approach to downregulate both DCP1A and DCP2 during meiotic maturation. Oocytes injected with siRNAs targeting *Dcp1a* and *Dcp2* as well as control oocytes injected with scrambled siRNAs were matured *in vitro* to the MII stage, and the effect of decapping depletion on MII egg transcriptome was assessed using microarrays. We found that only the simultaneous downregulation of both *Dcp1a* and *Dcp2* induced significant changes in mRNA levels. This can be explained by incomplete degradation of the targeted transcripts using siRNAs (Suppl.3, Fig.3). Thereby, downregulation of individual components of decapping might be insufficient to induce consistent measurable changes. Depletion of DCP1A and DCP2 during meiotic maturation had a generally stabilizing effect, as evidenced by upregulation of hundreds of transcripts compared to only 35 transcripts significantly downregulated. This trend is in good agreement with our hypothesis that decapping participates in the initial wave of maternal mRNA degradation. We compared our microarray data with previously published microarrays monitoring mRNA degradation during meiotic maturation [82]. Interestingly, the majority of transcripts significantly upregulated in *Dcp1a* and *Dcp2* knockdown eggs

fell into the group of significantly downregulated under normal conditions during meiotic maturation (Suppl.3, Fig.4). Although only a fraction of the MII egg degradome was stabilized upon decapping suppression, we may conclude that decapping contributes to the initiation of maternal mRNA degradation. Given the incomplete degradation of *Dcp1a* and *Dcp2* using siRNAs and a potential low level of persisting decapping activity in knockdown eggs, the number of decapping sensitive transcripts identified through our microarrays is probably an underestimate of the real situation. Generation of knockout mice with oocytes lacking one or both decapping factors will shed light on the actual contribution of decapping to maternal mRNA degradation. Knockout mice will also clarify whether alternative mRNA degradation pathways independent of decapping act during oocyte meiotic maturation. It is noteworthy that a gene ontology analysis of transcripts naturally degraded during meiotic maturation and stabilized upon decapping suppression revealed a significant enrichment for genes involved in ribosome biogenesis and components of the respiratory chain (Suppl.3, Tab.1). It will be interesting to test the functional relevance of this decapping-dependent depletion of transcripts coding for ribosome and respiratory chain constituents early during the oocyte-to-zygote transition. One hypothesis could be that the biogenesis of maternal ribosomes has to be discontinued in order to enable replacement with zygotic ribosomes upon the zygotic genome activation (ZGA). Downregulation of respiratory chain components might account for the global metabolic changes during fertilization.

Given the growing evidence for the requirement of maternal mRNA degradation to allow proper preimplantation development [83], we also wanted to know whether the suppression of maternal decapping activity interferes with zygotic activation. To this end we downregulated maternal DCP1A and DCP2 either by siRNA or morpholino injection in fully-grown oocytes. After *in vitro* maturation and strontium induced parthenogenetic activation we monitored the ZGA in 2-cell parthenogenotes. We observed decreased BrUTP incorporation and lower levels of active promoter marker histone H3Lys4me3 methylation in decapping deficient parthenogenotes, indicating compromised ZGA in these embryos (Suppl.3, Fig.7). These data suggest that decapping-dependent maternal mRNA clearance is required for flawless ZGA. However, the molecular mechanism linking maternal mRNA degradation with ZGA remains unclear. Again, it will be interesting to reproduce these experiments in physiologically fertilized knockout embryos lacking maternal decapping activity. It can be expected that complete removal of decapping

activity in knockout oocytes will have a much stronger impact on ZGA and therefore the knockout system will be more suitable for mechanistical studies.

On the whole, our studies of maternal decapping activity during oocyte meiotic maturation proved that decapping is involved in the initial wave of maternal mRNA degradation, and that this contribution to mRNA clearance is required for subsequent proper zygotic activation. In addition, we confirmed that decapping complex constituents DCP1A and DCP2 are attenuated in growing oocytes at the post-transcriptional level in a CPEB-dependent manner, thereby supporting the general mRNA stabilizing environment during oocyte growth. With this in mind, the last piece to add to our mosaic of studying mRNA stability in mouse oocytes remained the investigation of miRNA activity during the oocyte-to-zygote transition.

3.4 MicroRNA pathway suppression in mouse oocytes (Supplement 4)

The observation that P-bodies are absent at later stages of oocyte growth and through the most part of preimplantation development was striking with regard to potential perturbation of the miRNA pathway. It was shown previously that P-bodies arise as a consequence of miRNA pathway activity [58]. Furthermore, the interaction of an Ago protein with GW182 was found to be essential for miRNA mediated translational repression [84]. We noticed that together with P-body disassembly the colocalization of AGO2 with GW182-staining serum 18033 was also lost during oocyte growth (Suppl.2, Fig.2). We therefore monitored the localization of a reporter mRNA harbouring two Let-7 miRNA binding sites in the 3'UTR. The reporter was visualized using the MS2 tethering system with a YFP-tagged MS2 protein fused to a nuclear localization sequence. We detected a strong signal in cytoplasmic P-bodies when this system was introduced in cultured NIH3T3 cells. However, no P-body resembling structures appeared after injection of this system in fully-grown oocytes (Suppl.4, Fig.4), further supporting the hypothesis that maternal miRNAs do not function properly.

It was previously documented that fully-grown oocytes express mature forms of miRNAs [67, 68]. Members of Let-7 and miR-30 families, which are typically enriched in terminally differentiated cells, were among the most abundant miRNAs. We selected Let-7a and miR-30c miRNAs, two of the most abundant in oocytes, to develop our luciferase-

based reporter system for the measurement of miRNA activity. We introduced one site perfectly complementary to Let-7a or miR-30c to the 3'UTR region following the renilla luciferase coding sequence to generate a 'perfect' reporter. As the miRNA recognizes this reporter with perfect complementarity, it should stimulate AGO2 slicer activity and direct cleavage of the reporter mRNA. The perfect reporter thereby serves to assess the efficiency of miRNA loading on AGO2 and the RISC complex formation. Next, we inserted three or four binding sites for Let-7 or miR-30c respectively, with mismatches at positions 10 and 11 to generate a 'bulged' reporter. The central mismatches interfere with short RNA-guided slicer activity of AGO2 and target the reporter for repression through the classical miRNA pathway. Thus, the bulged reporter monitors the capability of endogenous miRNAs to induce translational repression and indirect target mRNA degradation. Finally, we mutated two nucleotides in the seed region of each miRNA binding site in the bulged reporter to generate a 'mutated' reporter. Due to the mismatches in the seed region this reporter should not be recognized by the miRNA and serves as a control (Suppl.4, Fig.3). It should be noted that the Let-7 reporters were derived from the constructs previously published [85].

We first tested our luciferase systems in cultured cells of human or mouse origin. In all the cells tested, the perfect reporter was downregulated by more than 80% compared to controls. The bulged reporter was a target to an even stronger repression in case of miR-30c (Suppl.4, Fig.S3). Even though siRNA-mediated cleavage of a perfectly complementary target is generally more efficient than miRNA-mediated repression, the stronger effect on the bulged reporter in cultured cells can be explained by a higher number of binding sites, which might act synergistically to repress the target. We then injected the reporters in the form of *in vitro* transcribed mRNA into small growing oocytes and fully-grown oocytes prevented from or allowed to undergo meiotic maturation *in vitro*. In small oocytes from 12 day old mice, approximately at the stage when P-bodies disassemble (see part 3.2), both perfect and bulged reporters were repressed significantly compared to mutated control, though the repression of bulged reporters was weaker than that of perfect reporters. However, the repression of bulged reporters was largely relieved in fully-grown oocytes and MII eggs, while perfect reporters remained repressed (Suppl.4, Fig.3). These data indicate that the miRNA pathway is perturbed in fully-grown mouse oocytes, likely at the level of translational repression and recruitment of mRNA degradation factors to the target mRNA. Overall repression of Let-7 reporters was weaker in all injected oocytes

compared to miR-30c. Given that Let-7 is a highly conserved and tightly regulated miRNA family, it is possible that an additional regulatory mechanism specifically suppresses Let-7 activity in mouse oocytes.

Our luciferase reporter experiments showed that two of the most abundant miRNAs in oocytes failed to repress target mRNAs efficiently. To confirm these results suggesting the miRNA pathway suppression on a large scale, we compared transcriptomes of the wild type and Dicer deficient oocytes using microarrays. We found 489 upregulated and 628 downregulated transcripts upon Dicer deletion (Suppl.4, Fig.1). These numbers are low compared to changes in transcriptomes of other cell types, in which the deletion of Dicer typically affects thousands of transcripts. For example, in mouse ES cells more than 2000 transcripts are misregulated in either direction upon loss of Dicer [86]. Interestingly, rescue by a mature miRNA from the miR-290 family, which is a prominent class of miRNAs in ES cells, reduces the transcriptome changes induced by the loss of Dicer to levels comparable with the situation in oocytes (Suppl.4, Fig.1)[86]. We next performed a bioinformatic analysis searching for heptamer sequences enriched in 3'UTRs of transcripts upregulated in Dicer knockout oocytes. None of the overrepresented heptamers corresponded to the seed regions of annotated miRNAs, except for miR-1195 (Suppl.4, Fig.1 and Tab.S1). However, miR-1195 is not expressed in mouse oocytes [69, 70] and we found no software-predicted miR-1195 targets among the upregulated transcripts. The lack of miRNA seed footprint in the transcriptome of Dicer deficient oocytes was further confirmed by Sylamer analysis, which enables identification of enriched motifs in sorted gene lists and is commonly used for tracking the miRNA contribution to changes in transcriptome profiles (Suppl.4, Fig.S1)[87].

Together, our data showed that miRNA activity is compromised in fully-grown mouse oocytes. Luciferase reporter assays indicated that the miRNA pathway is probably suppressed downstream of RISC loading. In agreement with this, loss of maternal miRNAs has no impact on the oocyte transcriptome. Our conclusions were supported by a parallel study analyzing DGCR8 knockout oocytes [88]. Deletion of DGCR8 led to a complete loss of canonical maternal miRNAs. However, there were no significant changes in the transcriptome of DGCR8 depleted oocytes compared to the wild type controls. DGCR8 knockout oocytes did not show any detrimental meiotic phenotype, they could be fertilized and could give rise to a healthy fertile offspring [88]. In light of these results, the previous conclusions explaining the phenotype of Dicer knockout oocytes should be reconsidered

[67]. Instead of miRNAs, the spindle defects during meiotic maturation observed in Dicer knockout oocytes are probably due to the lack of endogenous siRNAs (endo-siRNAs), which were identified as another Dicer dependent small RNA class in mouse oocytes [69, 70]. Indeed, a closer inspection of our microarray data identified numerous potential endo-siRNA targets among genes upregulated in Dicer knockout oocytes (Suppl.4,Tab.S4).

3.5 Regulation of Dicer-dependent pathways during mouse oocyte-to-zygote transition (Supplement 5)

Our findings, supported by the results of a parallel study, showed that miRNA activity is suppressed in mouse oocytes and that canonical miRNAs are dispensable during the oocyte-to-zygote transition (Suppl.4)[88]. Yet it remains to be tested whether miRNA pathway suppression is required in this largest reprogramming event of mammalian development. It has been postulated that miRNAs play key roles in various differentiation processes during animal development by defining and strengthening the differentiated state [43]. Since the oocyte-to-zygote transition is the only naturally occurring process during which a differentiated cell is reprogrammed to a pluripotent cell, it is possible that miRNAs ensuring the differentiated state need to be silenced to enable the reprogramming. It is well documented that the self-renewal vs. differentiation fate of mouse pluripotent ES cells is dictated by the proportion between two opposing miRNA families miR-290 and Let-7 [89]. Let-7 directs the cells towards differentiation while miR-290 supports the self-renewing potential. Members of the Let-7 family are among the most abundant miRNAs in mouse oocytes [67, 68], which is consistent with the assumption that oocytes are terminally differentiated cells. The majority of maternal Let-7 is degraded before ZGA and Let-7 levels remain low throughout preimplantation stages. In contrast, the miR-290 cluster is activated during ZGA and miR-290 members accumulate during preimplantation development (Suppl.5, Fig.3)[67]. Therefore, it is possible that transient suppression of the miRNA pathway during reprogramming creates a window in which differentiation supporting miRNAs are disengaged from regulating their target mRNAs, and are replaced by pluripotency-promoting miRNAs. Both Let-7 and miR-290 are well conserved among vertebrates (Suppl.5, Fig.1). It will be interesting to test whether the same strategy of transient miRNA pathway suppression is applied during the oocyte-to-zygote transition in other mammals as well. Paralogs of miR-290 were found to participate in maternal mRNA

clearance in zebrafish and *Xenopus* [63, 65]. However, the major wave of maternal mRNA degradation in these organisms occurs after ZGA, allowing the zygotic miRNAs to accumulate and target maternal transcripts (Suppl.5, Fig.5). In mouse, the zygotic expression of miR-290 starts at the point when the majority of maternal mRNAs has already been removed. Furthermore, the data from our P-body dynamics studies suggest that miRNA activity is not restored before the early blastocyst stage (Suppl.5, Fig.4). This is supported by the observation that DGCR8 deficiency does not interfere with preimplantation development [88]. Hence the role of miRNAs in maternal mRNA degradation during the mammalian oocyte-to-zygote transition does not reflect the situation in other vertebrates.

The molecular mechanism responsible for miRNA pathway suppression currently remains unclear. Strikingly, mouse oocytes are the first mammalian cell type reported where miRNAs are expressed, but their function is globally suppressed. As mentioned above, we did not observe any colocalization of AGO2 with GW182 in oocytes and preimplantation embryos. Given that the interaction of these proteins is required for a proper miRNA function [84], the mechanism of miRNA inactivity may lie in preventing AGO2-GW182 association. This might be achieved by post-translational modifications of these proteins. However, the absence of AGO2-GW182 interaction might as well be caused by other factors involved in miRNA loading on AGO2, or by RNA binding proteins that would coat the target mRNA and prevent formation of a fully functional miRISC. The strong suppression of miRNA activity could also result from a combination of the proposed mechanisms. In any case, mouse oocytes represent an interesting model for studying the molecular basis of miRNA-mediated translational repression which is still far from being completely understood. Moreover, perturbation of the miRNA pathway is often linked to non-physiological processes in mammalian cells, such as carcinogenesis. Understanding the cause of miRNA pathway suppression in oocytes might thereby provide new insights into tumour biology.

Finally, our finding that miRNAs are inactive in mouse oocytes sheds new light on the interpretation of Dicer knockout phenotype during meiotic maturation and brings endo-siRNAs in the centre of research focus. Mouse oocytes and preimplantation embryos are the only mammalian cells in which abundant endo-siRNAs originating from both transposon sequences and protein coding mRNAs were identified by deep sequencing [69, 70, 90]. Interestingly, a bioinformatic analysis of small RNA populations in these

developmental stages revealed that endo-siRNAs are a dominant class of Dicer-dependent small RNAs in oocytes and embryos until the 8-cell stage, while miRNAs become the most abundant class in later stages of preimplantation development concomitant with the proposed restoration of the miRNA function [90]. It is currently not known whether the miRNA pathway activity and endo-siRNA production are mutually exclusive processes in mammalian cells. Some unique endo-siRNAs derived from repetitive sequences accumulate at levels similar to miRNAs in oocytes [69, 70]. As mammalian Ago proteins are thought to utilize short RNAs in the same manner regardless of their origin, it is possible that the miRNA pathway in oocytes needs to be suppressed in order to prevent endo-siRNAs from modulating the transcriptome in a miRNA-like fashion. Whether disrupting endo-siRNA-dependent regulation of target mRNA levels could explain spindle defects in Dicer null mouse oocytes is a subject to ongoing research. Strikingly, comparison of genes upregulated in Dicer and AGO2 knockout oocytes [91] with the genes matching endo-siRNAs [69] revealed numerous microtubule-associated genes as potential endo-siRNA targets. Upregulation of these genes upon Dicer or AGO2 deletion might lead to defects in the microtubule function and thereby represent the cause of misaligned chromosomes and abnormal spindles observed during meiosis I in knockout oocytes. From an evolutionary point of view, it will be interesting to use deep sequencing approach to estimate the potential of other mammalian oocytes to generate endo-siRNAs. The majority of mouse oocyte endo-siRNAs targeting protein coding transcripts arise from gene-pseudogene pairs [69, 70]. Since pseudogenes are generally not well conserved across species, potential endo-siRNAs in other mammals could originate from different sources and target different mRNAs, thus changing the outcome of oocyte Dicer knockout.

4. CONCLUSIONS

Studies in various model organisms strengthen our knowledge concerning the general principles of post-transcriptional regulation during the oocyte-to-zygote transition. While most of the currently known mechanisms controlling maternal mRNA stability and degradation have been uncovered using *Xenopus*, zebrafish and invertebrate systems, the data constituting this thesis represent progress in the understanding of post-transcriptional processes in a mammalian system. The identification of maternal mRNA storage domains in fully-grown oocytes sets the basis for future functional studies of individual components. Similarities in the protein composition of these domains between invertebrates, vertebrates and mouse indicate that the function of at least some of these proteins might be conserved in metazoans. Following up on the results presented in this work, the function of DDX6 helicase in the regulation of maternal mRNA stability is currently being addressed. It has become evident that an mRNA stabilizing environment needs to be created in growing oocytes to permit maternal mRNA accumulation. Our data on the dormancy of decapping and its activation during meiotic maturation offer one of the first insights into the mechanisms underlying the global switch from mRNA stability to degradation. In addition, suppression of the miRNA pathway might also contribute to stabilizing conditions during oocyte growth. Future work will clarify whether the reduction of miRNA activity is a prerequisite for a successful oocyte-to-zygote transition, and eventually for cell reprogramming in general. In such a case, deciphering the mechanisms of miRNA pathway suppression would provide invaluable penetration into the processes by which differentiated cells acquire the self-renewing potential, with possible application in the iPSC technology and cancer research.

5. REFERENCES

1. Harveus, G. (1651). *Exercitationes de generatione animalium*, (Londini: Typis Du-Gardianis).
2. Gurdon, J.B., Elsdale, T.R., and Fischberg, M. (1958). Sexually mature individuals of *Xenopus laevis* from the transplantation of single somatic nuclei. *Nature* 182, 64-65.
3. Wilmut, I., Schnieke, A.E., McWhir, J., Kind, A.J., and Campbell, K.H. (1997). Viable offspring derived from fetal and adult mammalian cells. *Nature* 385, 810-813.
4. Takahashi, K., and Yamanaka, S. (2006). Induction of pluripotent stem cells from mouse embryonic and adult fibroblast cultures by defined factors. *Cell* 126, 663-676.
5. Barrilleaux, B., and Knoepfler, P.S. (2011). Inducing iPSCs to escape the dish. *Cell Stem Cell* 9, 103-111.
6. Maekawa, M., Yamaguchi, K., Nakamura, T., Shibukawa, R., Kodanaka, I., Ichisaka, T., Kawamura, Y., Mochizuki, H., Goshima, N., and Yamanaka, S. (2011). Direct reprogramming of somatic cells is promoted by maternal transcription factor Glis1. *Nature* 474, 225-229.
7. Bui, H.T., Wakayama, S., Kishigami, S., Kim, J.H., Van Thuan, N., and Wakayama, T. (2008). The cytoplasm of mouse germinal vesicle stage oocytes can enhance somatic cell nuclear reprogramming. *Development* 135, 3935-3945.
8. Edson, M.A., Nagaraja, A.K., and Matzuk, M.M. (2009). The mammalian ovary from genesis to revelation. *Endocr Rev* 30, 624-712.
9. Pan, H., O'Brien M, J., Wigglesworth, K., Eppig, J.J., and Schultz, R.M. (2005). Transcript profiling during mouse oocyte development and the effect of gonadotropin priming and development in vitro. *Dev Biol* 286, 493-506.
10. De La Fuente, R. (2006). Chromatin modifications in the germinal vesicle (GV) of mammalian oocytes. *Dev Biol* 292, 1-12.
11. Zuccotti, M., Merico, V., Cecconi, S., Redi, C.A., and Garagna, S. (2011). What does it take to make a developmentally competent mammalian egg? *Hum Reprod Update* 17, 525-540.
12. Zuccotti, M., Ponce, R.H., Boiani, M., Guizzardi, S., Govoni, P., Scandroglia, R., Garagna, S., and Redi, C.A. (2002). The analysis of chromatin organisation allows selection of mouse antral oocytes competent for development to blastocyst. *Zygote* 10, 73-78.
13. Inoue, A., Nakajima, R., Nagata, M., and Aoki, F. (2008). Contribution of the oocyte nucleus and cytoplasm to the determination of meiotic and developmental competence in mice. *Hum Reprod* 23, 1377-1384.
14. Zuccotti, M., Merico, V., Sacchi, L., Bellone, M., Brink, T.C., Bellazzi, R., Stefanelli, M., Redi, C.A., Garagna, S., and Adjaye, J. (2008). Maternal Oct-4 is a potential key regulator of the developmental competence of mouse oocytes. *BMC Dev Biol* 8, 97.

15. Solc, P., Schultz, R.M., and Motlik, J. (2010). Prophase I arrest and progression to metaphase I in mouse oocytes: comparison of resumption of meiosis and recovery from G2-arrest in somatic cells. *Mol Hum Reprod* 16, 654-664.
16. Burns, K.H., and Matzuk, M.M. (2006). Preimplantation embryogenesis. In Knobil and Neill's physiology of reproduction, 3rd ed., J.D. Neill, ed. (Elsevier).
17. McGrew, L.L., Dworkin-Rastl, E., Dworkin, M.B., and Richter, J.D. (1989). Poly(A) elongation during *Xenopus* oocyte maturation is required for translational recruitment and is mediated by a short sequence element. *Genes Dev* 3, 803-815.
18. Radford, H.E., Meijer, H.A., and de Moor, C.H. (2008). Translational control by cytoplasmic polyadenylation in *Xenopus* oocytes. *Biochim Biophys Acta* 1779, 217-229.
19. Richter, J.D. (2007). CPEB: a life in translation. *Trends Biochem Sci* 32, 279-285.
20. Villalba, A., Coll, O., and Gebauer, F. (2011). Cytoplasmic polyadenylation and translational control. *Curr Opin Genet Dev* 21, 452-457.
21. Minshall, N., Thom, G., and Standart, N. (2001). A conserved role of a DEAD box helicase in mRNA masking. *RNA* 7, 1728-1742.
22. Pique, M., Lopez, J.M., Foissac, S., Guigo, R., and Mendez, R. (2008). A combinatorial code for CPE-mediated translational control. *Cell* 132, 434-448.
23. Gebauer, F., and Richter, J.D. (1996). Mouse cytoplasmic polyadenylation element binding protein: an evolutionarily conserved protein that interacts with the cytoplasmic polyadenylation elements of *c-mos* mRNA. *Proc Natl Acad Sci U S A* 93, 14602-14607.
24. Tay, J., Hodgman, R., and Richter, J.D. (2000). The control of cyclin B1 mRNA translation during mouse oocyte maturation. *Dev Biol* 221, 1-9.
25. Racki, W.J., and Richter, J.D. (2006). CPEB controls oocyte growth and follicle development in the mouse. *Development* 133, 4527-4537.
26. Hodgman, R., Tay, J., Mendez, R., and Richter, J.D. (2001). CPEB phosphorylation and cytoplasmic polyadenylation are catalyzed by the kinase IAK1/Eg2 in maturing mouse oocytes. *Development* 128, 2815-2822.
27. Chen, J., Melton, C., Suh, N., Oh, J.S., Horner, K., Xie, F., Sette, C., Belloch, R., and Conti, M. (2011). Genome-wide analysis of translation reveals a critical role for deleted in azoospermia-like (*Dazl*) at the oocyte-to-zygote transition. *Genes Dev* 25, 755-766.
28. Collier, B., Gorgoni, B., Loveridge, C., Cooke, H.J., and Gray, N.K. (2005). The DAZL family proteins are PABP-binding proteins that regulate translation in germ cells. *EMBO J* 24, 2656-2666.
29. Walser, C.B., and Lipshitz, H.D. (2011). Transcript clearance during the maternal-to-zygotic transition. *Curr Opin Genet Dev* 21, 431-443.
30. Yang, J., Medvedev, S., Reddi, P.P., Schultz, R.M., and Hecht, N.B. (2005). The DNA/RNA-binding protein MSY2 marks specific transcripts for cytoplasmic storage in mouse male germ cells. *Proc Natl Acad Sci U S A* 102, 1513-1518.

31. Yang, J., Medvedev, S., Yu, J., Tang, L.C., Agno, J.E., Matzuk, M.M., Schultz, R.M., and Hecht, N.B. (2005). Absence of the DNA-/RNA-binding protein MSY2 results in male and female infertility. *Proc Natl Acad Sci U S A* *102*, 5755-5760.
32. Medvedev, S., Pan, H., and Schultz, R.M. (2011). Absence of MSY2 in mouse oocytes perturbs oocyte growth and maturation, RNA stability, and the transcriptome. *Biol Reprod* *85*, 575-583.
33. Medvedev, S., Yang, J., Hecht, N.B., and Schultz, R.M. (2008). CDC2A (CDK1)-mediated phosphorylation of MSY2 triggers maternal mRNA degradation during mouse oocyte maturation. *Dev Biol* *321*, 205-215.
34. Bouvet, P., and Wolffe, A.P. (1994). A role for transcription and FRGY2 in masking maternal mRNA within *Xenopus* oocytes. *Cell* *77*, 931-941.
35. Sommerville, J., and Lodomery, M. (1996). Transcription and masking of mRNA in germ cells: involvement of Y-box proteins. *Chromosoma* *104*, 469-478.
36. Tanaka, K.J., Ogawa, K., Takagi, M., Imamoto, N., Matsumoto, K., and Tsujimoto, M. (2006). RAP55, a cytoplasmic mRNP component, represses translation in *Xenopus* oocytes. *J Biol Chem* *281*, 40096-40106.
37. Weston, A., and Sommerville, J. (2006). Xp54 and related (DDX6-like) RNA helicases: roles in messenger RNP assembly, translation regulation and RNA degradation. *Nucleic Acids Res* *34*, 3082-3094.
38. Noble, S.L., Allen, B.L., Goh, L.K., Nordick, K., and Evans, T.C. (2008). Maternal mRNAs are regulated by diverse P body-related mRNP granules during early *Caenorhabditis elegans* development. *J Cell Biol* *182*, 559-572.
39. Boag, P.R., Atalay, A., Robida, S., Reinke, V., and Blackwell, T.K. (2008). Protection of specific maternal messenger RNAs by the P body protein CGH-1 (Dhh1/RCK) during *Caenorhabditis elegans* oogenesis. *J Cell Biol* *182*, 543-557.
40. Lee, R.C., Feinbaum, R.L., and Ambros, V. (1993). The *C. elegans* heterochronic gene *lin-4* encodes small RNAs with antisense complementarity to *lin-14*. *Cell* *75*, 843-854.
41. Fire, A., Xu, S., Montgomery, M.K., Kostas, S.A., Driver, S.E., and Mello, C.C. (1998). Potent and specific genetic interference by double-stranded RNA in *Caenorhabditis elegans*. *Nature* *391*, 806-811.
42. Krol, J., Loedige, I., and Filipowicz, W. (2010). The widespread regulation of microRNA biogenesis, function and decay. *Nat Rev Genet* *11*, 597-610.
43. Bushati, N., and Cohen, S.M. (2007). microRNA functions. *Annu Rev Cell Dev Biol* *23*, 175-205.
44. Hu, H., and Gatti, R.A. (2011). MicroRNAs: new players in the DNA damage response. *J Mol Cell Biol* *3*, 151-158.
45. Lujambio, A., and Lowe, S.W. (2012). The microcosmos of cancer. *Nature* *482*, 347-355.
46. Judson, R.L., Babiarez, J.E., Venere, M., and Blelloch, R. (2009). Embryonic stem cell-specific microRNAs promote induced pluripotency. *Nat Biotechnol* *27*, 459-461.

47. Jaskiewicz, L., and Filipowicz, W. (2008). Role of Dicer in posttranscriptional RNA silencing. *Curr Top Microbiol Immunol* 320, 77-97.
48. Ender, C., and Meister, G. (2010). Argonaute proteins at a glance. *J Cell Sci* 123, 1819-1823.
49. Bussing, I., Slack, F.J., and Grosshans, H. (2008). let-7 microRNAs in development, stem cells and cancer. *Trends Mol Med* 14, 400-409.
50. Viswanathan, S.R., and Daley, G.Q. (2010). Lin28: A microRNA regulator with a macro role. *Cell* 140, 445-449.
51. Yang, J.S., and Lai, E.C. (2011). Alternative miRNA biogenesis pathways and the interpretation of core miRNA pathway mutants. *Mol Cell* 43, 892-903.
52. Carthew, R.W., and Sontheimer, E.J. (2009). Origins and Mechanisms of miRNAs and siRNAs. *Cell* 136, 642-655.
53. Bartel, D.P. (2009). MicroRNAs: target recognition and regulatory functions. *Cell* 136, 215-233.
54. Djuranovic, S., Nahvi, A., and Green, R. (2011). A parsimonious model for gene regulation by miRNAs. *Science* 331, 550-553.
55. Guo, H., Ingolia, N.T., Weissman, J.S., and Bartel, D.P. (2010). Mammalian microRNAs predominantly act to decrease target mRNA levels. *Nature* 466, 835-840.
56. Huntzinger, E., and Izaurralde, E. (2011). Gene silencing by microRNAs: contributions of translational repression and mRNA decay. *Nat Rev Genet* 12, 99-110.
57. Kulkarni, M., Ozgur, S., and Stoecklin, G. (2010). On track with P-bodies. *Biochem Soc Trans* 38, 242-251.
58. Eulalio, A., Behm-Ansmant, I., Schweizer, D., and Izaurralde, E. (2007). P-body formation is a consequence, not the cause, of RNA-mediated gene silencing. *Mol Cell Biol* 27, 3970-3981.
59. Bushati, N., Stark, A., Brennecke, J., and Cohen, S.M. (2008). Temporal reciprocity of miRNAs and their targets during the maternal-to-zygotic transition in *Drosophila*. *Curr Biol* 18, 501-506.
60. Lin, M.D., Jiao, X., Grima, D., Newbury, S.F., Kiledjian, M., and Chou, T.B. (2008). *Drosophila* processing bodies in oogenesis. *Dev Biol* 322, 276-288.
61. Ghildiyal, M., and Zamore, P.D. (2009). Small silencing RNAs: an expanding universe. *Nat Rev Genet* 10, 94-108.
62. Rouget, C., Papin, C., Boureux, A., Meunier, A.C., Franco, B., Robine, N., Lai, E.C., Pelisson, A., and Simonelig, M. (2010). Maternal mRNA deadenylation and decay by the piRNA pathway in the early *Drosophila* embryo. *Nature* 467, 1128-1132.
63. Giraldez, A.J., Mishima, Y., Rihel, J., Grocock, R.J., Van Dongen, S., Inoue, K., Enright, A.J., and Schier, A.F. (2006). Zebrafish MiR-430 promotes deadenylation and clearance of maternal mRNAs. *Science* 312, 75-79.

64. Giraldez, A.J., Cinalli, R.M., Glasner, M.E., Enright, A.J., Thomson, J.M., Baskerville, S., Hammond, S.M., Bartel, D.P., and Schier, A.F. (2005). MicroRNAs regulate brain morphogenesis in zebrafish. *Science* *308*, 833-838.
65. Lund, E., Liu, M., Hartley, R.S., Sheets, M.D., and Dahlberg, J.E. (2009). Deadenylation of maternal mRNAs mediated by miR-427 in *Xenopus laevis* embryos. *RNA* *15*, 2351-2363.
66. Lund, E., Sheets, M.D., Imboden, S.B., and Dahlberg, J.E. (2011). Limiting Ago protein restricts RNAi and microRNA biogenesis during early development in *Xenopus laevis*. *Genes Dev* *25*, 1121-1131.
67. Tang, F., Kaneda, M., O'Carroll, D., Hajkova, P., Barton, S.C., Sun, Y.A., Lee, C., Tarakhovskiy, A., Lao, K., and Surani, M.A. (2007). Maternal microRNAs are essential for mouse zygotic development. *Genes Dev* *21*, 644-648.
68. Murchison, E.P., Stein, P., Xuan, Z., Pan, H., Zhang, M.Q., Schultz, R.M., and Hannon, G.J. (2007). Critical roles for Dicer in the female germline. *Genes Dev* *21*, 682-693.
69. Tam, O.H., Aravin, A.A., Stein, P., Girard, A., Murchison, E.P., Cheloufi, S., Hodges, E., Anger, M., Sachidanandam, R., Schultz, R.M., et al. (2008). Pseudogene-derived small interfering RNAs regulate gene expression in mouse oocytes. *Nature* *453*, 534-538.
70. Watanabe, T., Totoki, Y., Toyoda, A., Kaneda, M., Kuramochi-Miyagawa, S., Obata, Y., Chiba, H., Kohara, Y., Kono, T., Nakano, T., et al. (2008). Endogenous siRNAs from naturally formed dsRNAs regulate transcripts in mouse oocytes. *Nature* *453*, 539-543.
71. Sellens, M.H., Stein, S., and Sherman, M.I. (1981). Protein and free amino acid content in preimplantation mouse embryos and in blastocysts under various culture conditions. *J Reprod Fertil* *61*, 307-315.
72. Yu, J., Hecht, N.B., and Schultz, R.M. (2001). Expression of MSY2 in mouse oocytes and preimplantation embryos. *Biol Reprod* *65*, 1260-1270.
73. Chazaud, C., Yamanaka, Y., Pawson, T., and Rossant, J. (2006). Early lineage segregation between epiblast and primitive endoderm in mouse blastocysts through the Grb2-MAPK pathway. *Dev Cell* *10*, 615-624.
74. Eystathioy, T., Chan, E.K., Tenenbaum, S.A., Keene, J.D., Griffith, K., and Fritzler, M.J. (2002). A phosphorylated cytoplasmic autoantigen, GW182, associates with a unique population of human mRNAs within novel cytoplasmic speckles. *Mol Biol Cell* *13*, 1338-1351.
75. Bloch, D.B., Gulick, T., Bloch, K.D., and Yang, W.H. (2006). Processing body autoantibodies reconsidered. *RNA* *12*, 707-709.
76. Giorgi, C., Yeo, G.W., Stone, M.E., Katz, D.B., Burge, C., Turrigiano, G., and Moore, M.J. (2007). The EJC factor eIF4AIII modulates synaptic strength and neuronal protein expression. *Cell* *130*, 179-191.
77. Serman, A., Le Roy, F., Aigueperse, C., Kress, M., Dautry, F., and Weil, D. (2007). GW body disassembly triggered by siRNAs independently of their silencing activity. *Nucleic Acids Res* *35*, 4715-4727.
78. Paige, J.S., Wu, K.Y., and Jaffrey, S.R. (2011). RNA mimics of green fluorescent protein. *Science* *333*, 642-646.

79. Wu, C., Orozco, C., Boyer, J., Leglise, M., Goodale, J., Batalov, S., Hodge, C.L., Haase, J., Janes, J., Huss, J.W., 3rd, et al. (2009). BioGPS: an extensible and customizable portal for querying and organizing gene annotation resources. *Genome Biol* *10*, R130.
80. Gillian-Daniel, D.L., Gray, N.K., Astrom, J., Barkoff, A., and Wickens, M. (1998). Modifications of the 5' cap of mRNAs during *Xenopus* oocyte maturation: independence from changes in poly(A) length and impact on translation. *Mol Cell Biol* *18*, 6152-6163.
81. Franks, T.M., and Lykke-Andersen, J. (2008). The control of mRNA decapping and P-body formation. *Mol Cell* *32*, 605-615.
82. Su, Y.Q., Sugiura, K., Woo, Y., Wigglesworth, K., Kamdar, S., Affourtit, J., and Eppig, J.J. (2007). Selective degradation of transcripts during meiotic maturation of mouse oocytes. *Dev Biol* *302*, 104-117.
83. Tadros, W., and Lipshitz, H.D. (2009). The maternal-to-zygotic transition: a play in two acts. *Development* *136*, 3033-3042.
84. Eulalio, A., Huntzinger, E., and Izaurralde, E. (2008). GW182 interaction with Argonaute is essential for miRNA-mediated translational repression and mRNA decay. *Nat Struct Mol Biol* *15*, 346-353.
85. Pillai, R.S., Bhattacharyya, S.N., Artus, C.G., Zoller, T., Cougot, N., Basyuk, E., Bertrand, E., and Filipowicz, W. (2005). Inhibition of translational initiation by Let-7 MicroRNA in human cells. *Science* *309*, 1573-1576.
86. Sinkkonen, L., Hugenschmidt, T., Berninger, P., Gaidatzis, D., Mohn, F., Artus-Revel, C.G., Zavolan, M., Svoboda, P., and Filipowicz, W. (2008). MicroRNAs control de novo DNA methylation through regulation of transcriptional repressors in mouse embryonic stem cells. *Nat Struct Mol Biol* *15*, 259-267.
87. van Dongen, S., Abreu-Goodger, C., and Enright, A.J. (2008). Detecting microRNA binding and siRNA off-target effects from expression data. *Nat Methods* *5*, 1023-1025.
88. Suh, N., Baehner, L., Moltzahn, F., Melton, C., Shenoy, A., Chen, J., and Blelloch, R. (2010). MicroRNA function is globally suppressed in mouse oocytes and early embryos. *Curr Biol* *20*, 271-277.
89. Melton, C., Judson, R.L., and Blelloch, R. (2010). Opposing microRNA families regulate self-renewal in mouse embryonic stem cells. *Nature* *463*, 621-626.
90. Ohnishi, Y., Totoki, Y., Toyoda, A., Watanabe, T., Yamamoto, Y., Tokunaga, K., Sakaki, Y., Sasaki, H., and Hohjoh, H. (2010). Small RNA class transition from siRNA/piRNA to miRNA during pre-implantation mouse development. *Nucleic Acids Res* *38*, 5141-5151.
91. Tang, F., Barbacioru, C., Wang, Y., Nordman, E., Lee, C., Xu, N., Wang, X., Bodeau, J., Tuch, B.B., Siddiqui, A., et al. (2009). mRNA-Seq whole-transcriptome analysis of a single cell. *Nat Methods* *6*, 377-382.

SUPPLEMENT 1

Matyas Flemr and Petr Svoboda

Ribonucleoprotein localization in mouse oocytes

(reprint from *Methods*. 2011 Feb;53(2):136-41)

My contribution to this work:

I generated all the experimental data and wrote the manuscript.

Ribonucleoprotein localization in mouse oocytes

Matyas Flemr, Petr Svoboda

Institute of Molecular Genetics, Academy of Sciences of the Czech Republic, Videnska 1083, 142 20 Prague 4, Czech Republic

Accepted 6 August 2010. Available online 12 August 2010.

Abstract

RNA molecules rarely function alone in cells. For most RNAs, their function requires formation of various ribonucleoprotein (RNP) complexes. For example, mRNP composition can determine mRNA localization, translational repression, level of translation or mRNA stability. RNPs are usually studied by biochemical methods. However, biochemical approaches are unsuitable for some model systems, such as mammalian oocytes and early embryos, due to the small amounts that can be obtained for experimental analysis. In such cases, microscopic techniques are often used to learn about RNPs. Here, we present a review of immunostaining, fluorescence *in situ* hybridization with subcellular resolution and a combination of both, with emphasis on the mouse oocyte and early embryos models. Application of these techniques to whole-mount fixed oocytes and early embryos can provide information about RNP composition and localization with three-dimensional resolution.

Keywords

Mouse oocyte; Whole-mount; *In situ* hybridization; Immunofluorescence; RNP

1. Introduction

The function of RNA molecules is also determined by the proteins that bind to them. Ribonucleoprotein (RNP) complexes are functional units that must be analyzed in order to understand the role of a given RNA, such as mRNA, microRNA or other RNA molecules. For example, mRNAs form mRNPs immediately after transcription and different mRNPs regulate mRNA transport, localization, translation and degradation (reviewed for example in [1] and [2]). Cytoplasmic control of mRNA metabolism occurs within RNPs that frequently form RNA granules, focal points visible by light microscopy, where different pathways meet that are involved in mRNA translation control and decay (reviewed in [3] and [4]). Biochemical analysis is a common approach for studying an RNP. There are a number of strategies that can be used, such as pull-down

of a specific RNA and analysis of bound proteins or immunoprecipitation of an RNP by antibodies recognizing one of the RNP proteins. Cross-linking immunoprecipitation (CLIP) approach utilizes RNA cross-linking to its binding proteins [5]. This method seems to be extremely powerful when combined with massive parallel sequencing as it allows one to determine specific sites bound by specific proteins to specific mRNAs.

However, there are model systems where biochemical studies are very difficult, if not impossible to perform, such as mammalian oocytes and early embryos, which can be obtained only in limited numbers. Their analysis typically involves microscopy and techniques allowing for amplification of the rare material. At the same time, understanding RNP biology in mouse oocytes and early embryos is essential for

understanding their biology as post-transcriptional mechanisms are critical for proper oocyte development and its transition into a pluripotent early embryo.

Growing mouse oocytes possess high transcriptional activity and generate a large amount of maternal mRNAs that must be properly utilized during oocyte-to-zygote transition, which includes a relatively long transcriptionally quiescent phase between the resumption of meiosis and activation of the zygotic genome at the 2-cell stage [6]. In addition to translated mRNAs, the maternal transcriptome contains stable untranslated transcripts, dormant maternal mRNAs that are recruited during meiotic maturation and/or early embryogenesis. Reversible polyadenylation is a common mechanism regulating recruitment and stability of dormant maternal mRNAs [7] and [8].

In addition to the protein composition of maternal mRNPs, the spatial distribution of these complexes in the cytoplasm may also play a biologically important role. Well known examples of localized mRNAs are the *Drosophila* transcripts *oskar*, *bicoid*, *gurken* or *nanos*, which accumulate at the anterior or posterior poles of the oocyte. This spatial separation is implicated in the differential patterning occurring during embryogenesis [9]. In a similar way, the maternal transcripts *Vg1* and *VegT* encoding for mesoderm-specifying factors localize to the vegetal cortex of late stage *Xenopus* oocytes [10]. In contrast, not much is known about RNP localization in mouse oocytes, particularly about maternal mRNPs.

Here, we present an overview of techniques for immunostaining, fluorescence *in situ* hybridization with subcellular resolution and a combination of both that can be used for RNP analysis in mouse oocytes and early embryos. Since the immunostaining protocol for mouse oocytes has been well established, we cover it rather briefly, discussing mainly points that might improve the quality of immunofluorescent images of mouse oocytes and early embryos. Most of the text is focused on the whole-mount RNA-fluorescence *in situ* hybridization (FISH) protocol for obtaining a three-dimensional (3D) view of mRNAs in oocytes and early

embryos. The FISH approach has been used to analyze DNA/chromatin [11] and [12] and monoallelic and biallelic gene expression previously [13]. However, preservation of the spherical shape has been reported only for DNA-FISH [11] which differs from the RNA-FISH procedure. The RNA-FISH procedure is typically performed on dried-up flattened oocytes (e.g.[13]) or on ovarian sections (e.g.[14]) not allowing for more precise spatial localization of RNPs. The combination of RNA-FISH and immunofluorescence discussed here provides a tool for analyzing RNPs in mouse oocytes and early embryos as well as, in principle, in a number of other model systems.

2. Methods

2.1. Oocyte morphology preservation

When performing immunostaining or *in situ* hybridization on a whole-mount specimen, the preservation of the cell and tissue morphology is of major importance. Preserving cell and tissue morphology depends on two main factors: (1) an appropriate fixation method and (2) careful handling of the specimen during the procedure. A solution of 3.7% (or 4%) paraformaldehyde (PFA) in 1x phosphate buffered saline (PBS) buffer has become a ‘golden standard’ among the fixatives used in immunocytochemistry regardless of the cell type or the exact staining protocol. Formaldehyde is a cross-linking agent that promotes covalent bond formation between proteins, nucleic acids and other cellular components. PFA is currently considered a good option for cell fixation with regard to the compromise between cell morphology preservation and antigen retrieval, a process employing non-ionic detergents or specific enzymes to reexpose the recognized parts of the targeted molecule and to allow for antibody or probe penetration into fixed cells. On the other hand, the high osmolarity of PFA solution represents a considerable disadvantage. The 3.7% PFA in 1x PBS solution has the osmolarity of approximately 1500 mOsm (experimentally estimated) as compared with 290 mOsm for 1x PBS alone, or 300 mOsm of the M2 medium used for mouse oocyte collection. The osmolarity is particularly important when working with

larger structures like blastocysts. Indeed, when transferred from collection medium or PBS directly to 3.7% PFA in PBS solution (pH 7.5., 9.5 or not adjusted), mouse oocytes shrink or crumble considerably. This shape deformation is reversible and the oocytes regain their original shape after a few minutes in PFA (Fig. 1A–C).

morphological damages during the staining or mounting procedures including the loss of nuclear envelope integrity and repositioning of the nuclei. Alternatively, one can lower the osmolarity of PFA by using 0.5x PBS. In this case, however, the increasing salt concentration during transfer from 3.7% PFA in 0.5x PBS to a solution containing 1x PBS can cause a collapse of the oocyte, especially

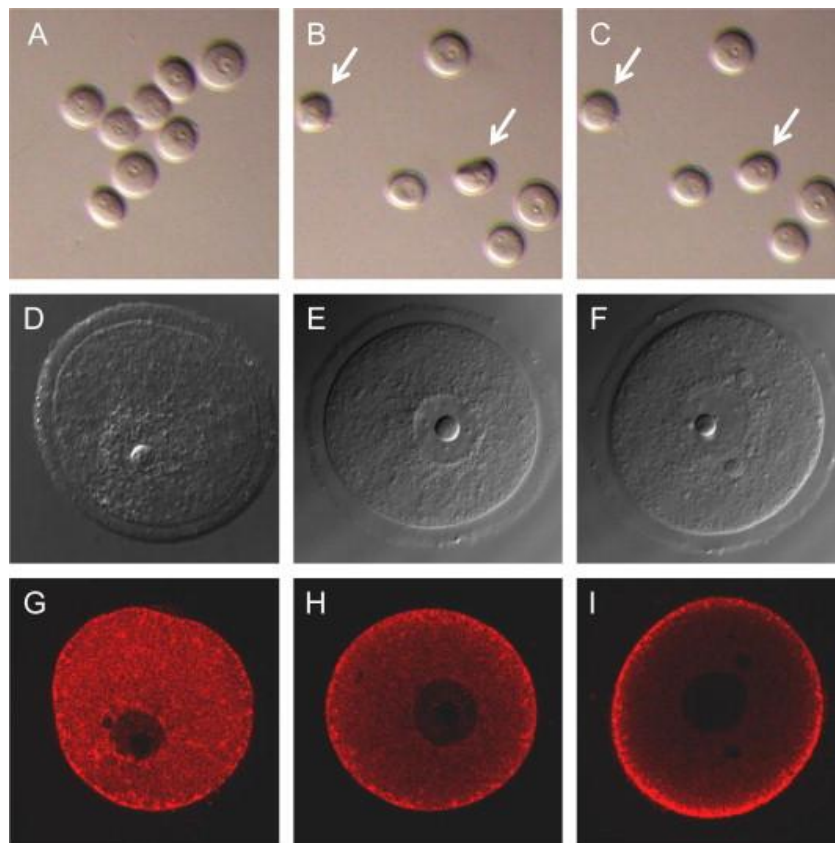


Fig. 1. The effect of PFA on oocyte shape during fixation and a comparison of cytoplasmic protein distribution under different fixation conditions. (A) The oocytes before fixation. (B) The oocytes crumble when transferred directly from PBS to 3.7% PFA in PBS solution with high osmolarity. Arrows depict two oocytes, which were still deformed when the image of oocytes transferred to 3.7% PFA in PBS was taken. (C) The original shape is restored after approximately 5 min in the PFA solution. Arrows depict the same oocytes five minutes later. (D–F) Different fixation strategies may overcome the oocyte shrinkage. However, fixation in only 2% PFA in PBS is not sufficient to retain oocyte morphology (D) and a transfer through a graded series of increasing PFA concentration (E) does not bring any additional benefit to the oocyte morphology compared to direct fixation in 3.7% PFA (F). (G–I) Confocal laser-scanning microscopy of oocytes stained with an antibody against an RNA-binding protein DDX6. DDX6 localization to the subcortical cytoplasmic region is not affected by the fixation procedure, as shown in images G–I, which correspond to the conditions described in D–F, respectively. However, nuclear morphology is somewhat different and stronger cytoplasmic staining is found when 2% PFA in PBS is used.

We were concerned whether the crumbling during fixation could affect protein distribution in the ooplasm and cause experimental artifacts. The shrinkage during fixation can be avoided when a lower concentration of PFA (e.g. 2%) is used. However, we found this milder fixation to be rather insufficient, often leading to

when working with small meiotically incompetent oocytes.

In our experience, the best way to avoid oocyte shrinkage during fixation while preserving its shape is to successively transfer oocytes through 1% and 2% PFA in 1x PBS (3 min each) prior to treatment in

3.7% PFA in PBS. However, upon reviewing data from a number of experiments, it seems that the cytoplasmic distribution of the monitored proteins is not markedly affected by the oocyte shrinkage occurring during fixation (Fig. 1B). This suggests that a direct transfer of oocytes from the medium or PBS to 3.7% PFA in 1x PBS and 1 h incubation at room temperature (RT), as used by many laboratories, is an acceptable fixation method for mRNP analysis in mouse oocytes in most cases.

Proper manipulation of oocytes during immunostaining is another factor affecting the resulting oocyte morphology. A fully-grown mouse oocyte is around 80 μm in diameter. Thus, its manipulation is performed under a microscope and requires fine hand-drawn glass pipettes for transferring oocytes between different solutions. We noticed that the size of the glass pipette used to manipulate living oocytes prior to fixation may affect the shape of the fixed oocytes. When a narrow pipette with a diameter of around 100 μm is used for transfer to PFA solution, the crumbling may become irreversible. This is likely due to the pressure acting on the oocyte in the pipette during aspiration and expiration, which may cause additional damage to the cytoskeletal network and/or other structural changes in the oocyte. Thus, we recommend to use hand-drawn glass pipettes with a diameter at least double the size of that of the oocyte for all pre-fixation manipulations. In addition, the narrow part of the pipette should be devoid of any impurities as these may lead to the generation of air bubbles, which can also increase the pressure in the pipette. Once the oocytes are fixed, a fine pipette can be used for subsequent steps in order to minimize the volume of solution transferred along with the oocytes.

Finally, oocyte mounting in a glycerol-based solution is also a potential source of oocyte shape deformation. We and others routinely use commercial Vectashield medium (Vector Laboratories, Inc.) for oocyte mounting as it is ideal for performing laser-scanning confocal microscopy. Vectashield is stable, optically clear, and reduces photobleaching. Furthermore, being a highly viscous solution,

it ensures immobilization of the oocytes on the microscope slide well.

During mounting, four drops of vaseline are placed on the slide, one in each corner of the cover slip area, whilst a 15 μl drop of Vectashield is placed in the center. The oocytes are then transferred into the Vectashield and a 15 \times 15 mm square cover slip placed carefully on the vaseline drops and pressed slightly to immobilize oocytes without breaking them. The Vectashield volume is adequate for this size of the cover slip, ensuring that the oocytes are only slightly squeezed and that their spherical structure can be analyzed. The transfer of oocytes from a PBS-containing solution to the mounting medium often leads to massive oocyte crumbling. As this process is usually reversible, we strongly recommend transferring oocytes and other early embryonic materials (in particular blastocysts to preserve their cavity) through a series of 5%, 20%, 50% and 70% glycerol with a minimum 10 min incubation at each step before mounting in Vectashield. This is not necessary for oocytes after *in situ* hybridization as these have been dehydrated in ethanol during the procedure, which makes their structure more rigid and prevents shrinkage during direct mounting in Vectashield.

2.2. Immunofluorescent staining

The protocol for immunofluorescent protein detection in mouse oocytes is similar to those applied to other cell types. However, several specific points should be taken into account. All solutions used during the staining should contain a non-ionic detergent (Tween 20 or Triton-X 100) or polyvinyl alcohol and/or a blocking protein, otherwise the oocytes will become sticky and could strongly adhere to the transferring glass pipette. We use a blocking solution containing 0.1% bovine serum albumin (BSA) and 0.05% Tween 20 in PBS for all post-fixation steps of the staining protocol except for 15 min of permeabilization in 0.1% Triton-X 100 in PBS, which is generally sufficient for good antibody penetration. The blocking solution described above is usually sufficient to block non-specific binding of a fluorescently labeled secondary antibody. When the

background staining is unacceptable, it may help to replace BSA with 3% serum from the species in which the secondary antibody was raised. The optimal conditions for primary antibody staining (dilution, incubation length, and temperature) should be determined empirically for each primary antibody. However, an overnight incubation with a primary antibody at 4 °C usually results in a reduced background staining when compared with shorter incubations at RT.

Incubations with antibodies and post-incubation washes can be performed in 96-well conical microplates with a flat bottom (Nunc/Thermo Fisher Scientific), which offers several advantages. The conical shape of the well facilitates manipulation with the transferring pipette, whilst the 96-well mode enables multiple staining in one experiment without the risk of mixing samples, and is compatible with the use of very small incubation volumes. We use as little as 10 µl of the blocking solution with a diluted antibody, which markedly reduces the consumption of antibodies. Importantly, incubations and washes must be performed in a humidified chamber and all oocyte manipulations under the microscope must be performed quickly to avoid evaporation of the blocking solution.

Anti-mouse secondary antibodies tend to accumulate in the zona pellucida. Consequently, when a mouse primary antibody is used for IF staining, the zona pellucida should be removed prior to fixation by brief incubation in acid tyrode solution. We use Alexa-labeled secondary antibodies (Invitrogen) because they produce a strong and stable signal. The stability of the fluorescent signal is especially important when a z-stack serial imaging is performed on a confocal laser-scanning microscope to obtain a 3D reconstruction of the spherical shape. The high number of stacks needed to cover the whole oocyte requires prolonged laser exposure, which may result in the bleaching of less stable fluorophores. For colocalization studies, fluorophores with non-overlapping emission spectra (depending on the available laser these can be, for example, Alexa488 and Alexa594) are employed to minimize channel cross-talk. In addition, the secondary antibodies should ideally be raised

in the same species to reduce potential cross-reactivity.

2.3. Fluorescence *in situ* hybridization

For mouse oocytes, the RNA-FISH protocol for whole-mount with a good subcellular resolution of the spherical oocyte has yet to be defined. The FISH protocols established for cultured cells (see, e.g., [15]) and whole-mount embryos [16] differ in several aspects. Notably, the permeabilization step is critical in whole-mount FISH and requires treatment with proteinase K to allow for a deep and efficient penetration of the FISH probe, while the proteinase step can be omitted in fixed cultured cells where a short dehydration in methanol or ethanol is sufficient for cell permeabilization. Other differences between the FISH protocols include the composition of the hybridization mix and the conditions for post-hybridization washing.

The first of the important factors for a successful FISH experiment is probe selection and design. Long *in vitro* transcribed end-labeled riboprobes have traditionally been used for RNA-FISH. However, the popularity of shorter DNA oligonucleotides with incorporated labeled deoxynucleotides as probes for *in situ* detection of mRNAs has increased in recent years [15], and they are for us the probes of choice for FISH on mouse oocytes. DNA oligonucleotide probes are usually about 50 nucleotides long, which enables efficient penetration through the fixed material and reduces the time required for probe hybridization as compared with traditional several hundred nucleotides long riboprobes. DNA oligonucleotide probes can be obtained from a commercial supplier with all desired modifications already incorporated, thus avoiding time-consuming and laborious home-made probe labeling. When designing an oligonucleotide probe for RNA-FISH, the following rules should be followed. The probe should ideally have a 50% GC content since a high GC content may lead to increased non-specific binding while a low GC content will result in a weaker hybridization efficiency. However, if necessary, this issue can also be addressed by adjusting the hybridization temperature and stringency. The specificity of the designed

probe should be verified by searching the probe sequence against an mRNA sequence database, so that no additional targets with less than five mismatches or more than 30 consecutive base-pairing nucleotides are found in a 50 nt probe. It is also recommended to check the accessibility of the target site within the targeted mRNA with a secondary structure prediction tool (e.g. Mfold [17]) and avoid regions of strong self-folding.

Finally, a critical parameter for FISH probe design is the choice of the label molecule, which is used for further detection of the oligonucleotide probe. Three main detection systems are employed in FISH protocols. These include probes labeled with digoxigenin (DIG), biotin or with a fluorescent molecule (e.g. cyanine derivatives (Cy3 or Cy5) or fluorescein (FITC)). We strongly recommend avoiding biotin labeled probes for FISH experiments in mouse oocytes. The biotin–avidin detection system is based on the interaction of the biotinylated probe with fluorescently labeled streptavidin, which will also bind endogenous biotin present mainly in mitochondria. The distribution of mitochondria in mouse oocytes is similar to that of mRNA, as shown by poly(A) visualization with a fluorescently labeled oligo(dT) probe (Fig. 2) and, although the

endogenous biotin can be blocked with a commercially available biotin blocking kits (e.g. from Invitrogen) to some extent, results of a FISH experiment in mouse oocytes using biotinylated probes can be confusing. Therefore, we use either DIG-labeled probes (which are visualized by incubation with an anti-DIG primary antibody followed by a fluorescently labeled secondary antibody) or direct FITC-labeled probes carrying five FITC molecules per probe. The advantage of FITC-labeled probes is that the hybridization signal can be obtained directly from the probe without introducing any additional background. However, depending on the abundance of the targeted mRNA, the FITC signal can be weak, thus requiring amplification of the signal with an anti-FITC antibody.

Another possible way of increasing sensitivity for low abundance targets is to use the recently introduced Locked Nucleic Acid (LNA) oligos as probes for mRNA-FISH. LNA modification of DNA oligonucleotides strengthens the probe-target RNA interaction and has been shown to dramatically improve RNA-FISH sensitivity [18].

The pre-hybridization in FISH involves fixation of the specimen, which preserves morphology and retains localization of the target, followed by permeabilization, which

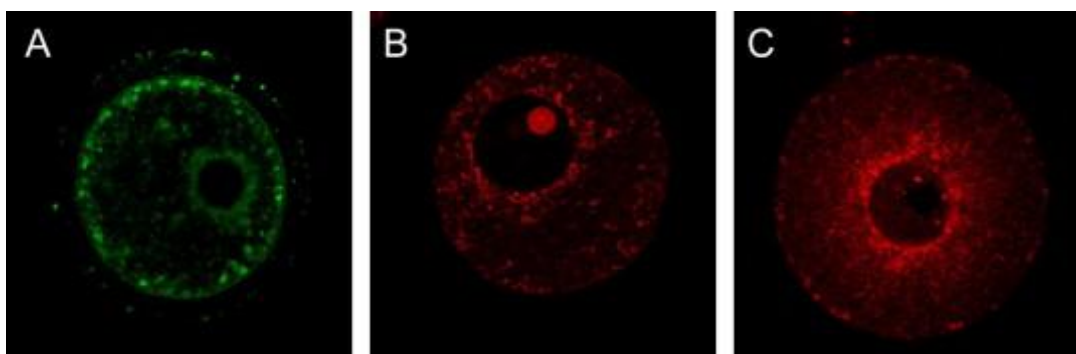


Fig. 2. Biotin is not a suitable probe label for FISH on mouse oocytes. Biotinylated probes do not generally work well in cells with high levels of endogenous biotin, which is mostly found in mitochondria. (A) The distribution pattern of mitochondria in mouse oocytes visualized by MitoTracker Green FM (Invitrogen) can to some extent be recapitulated by (B) the staining with Alexa 594-conjugated Streptavidin (Invitrogen) even in oocytes treated with endogenous biotin blocking kit (Invitrogen). Importantly, mRNA distribution within the oocyte, as seen with TAMRA-labeled oligo dT probe (C), is similar to the mitochondrial pattern and thus the streptavidin–biotin detection system may lead to confusing results. The nucleolus staining in B is an artifact caused by the proteinase K digestion. All images were obtained by confocal laser-scanning microscopy of mouse oocytes.

unmasks the target RNAs and allows for efficient probe penetration and cognate RNA recognition. The same fixation procedure as described above for immunofluorescent staining (Section 2.2) can be used for FISH analysis of mouse oocytes. After fixation, the oocytes are permeabilized in 70% ethanol and can be stored at this stage at -20°C for several days. Oocytes are subsequently rehydrated in a graded series of ethanol–PBT (0,1% Tween 20 in PBS). The rehydration is best performed in a glass dish by successive addition of PBT until the concentration of PBT reaches 75% (in dilutions with higher ethanol concentration the oocytes tend to

dormant maternal mRNAs. In a localization study of the dormant maternal transcript *Mos*, we observed that a very mild and short proteinase K treatment ($1\ \mu\text{g}/\text{ml}$ in PBT for 3 min) was both necessary and sufficient to obtain a detectable signal with the FITC-labeled probe alone (Fig. 3). Such proteinase-treated oocytes become however fragile and must be post-fixed in a solution of 3.7% PFA and 0.25% glutaraldehyde in PBT in order to preserve the shape and retain the target during hybridization. The ethanol step is usually sufficient for the detection of translationally active mRNAs and no further permeabilization with proteinase K is needed.

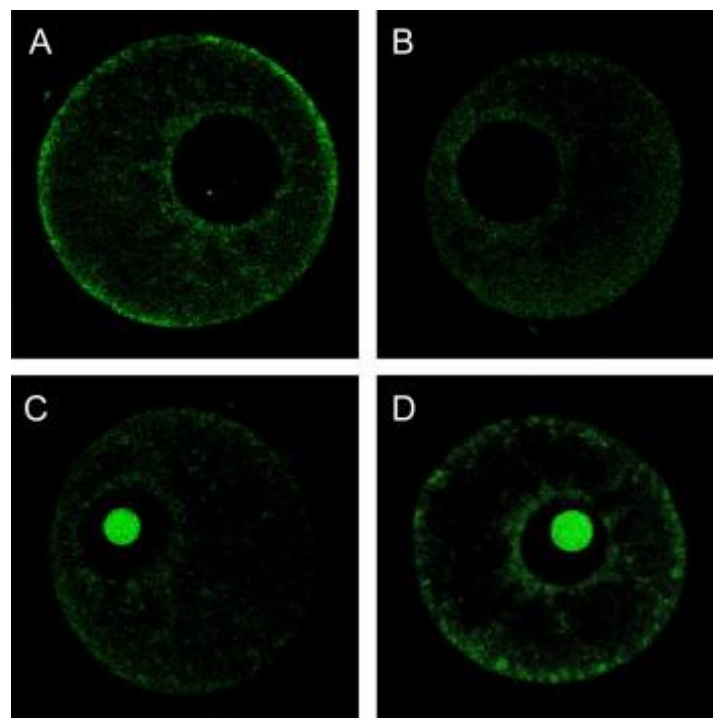


Fig. 3. Proteinase K digestion is necessary for the FISH detection of dormant maternal mRNAs in mouse oocytes. When the proteinase step is not included in the procedure, no significant difference in the signal intensity between a 5 FITC-containing nonsense control probe (A) and a probe targeting the *Mos* mRNA (B) can be seen. In contrast, when the oocytes are treated for 3 min with $1\ \mu\text{g}/\text{ml}$ proteinase K in PBT prior to hybridization, the non-specific signal in the control sample (C) is much lower than the specific signal of the *Mos* probe (D). All images were obtained by confocal laser-scanning microscopy of mouse oocytes.

float in the solution and are difficult to manipulate with a micropipette). The rate of oocyte permeabilization for RNA-FISH depends on the nature of the analyzed RNA. For example, translationally repressed mRNAs deposited in storage mRNPs are likely to form compact complexes with RNA-binding proteins. A proteinase K digestion step should be included prior to hybridization when performing FISH on such

Regardless of the proteinase treatment, all oocytes are quenched before hybridization by incubation with $2\ \text{mg}/\text{ml}$ glycine in PBT. Glycine treatment prevents enhanced autofluorescence resulting from the use of aldehyde-based fixatives, which may interfere with the FISH signal especially when glutaraldehyde is employed. This step is particularly important when using FITC-labeled probes as these often generate a very

weak signal and the lowest possible background is desirable.

The composition of the hybridization mixture and the strategy of post-hybridization washes for mouse oocyte RNA-FISH are generally the same as described in literature for protocols using short oligo DNA probes [15] and [19]. We use hybridization and washing conditions as described by Grunwald et al. [15] and [19]. Slight modifications and optimization may be required depending on the length and GC content of the probe. The control probe used to ensure specificity of the FISH signal should be of the same length and contain the same amount of GC content as the FISH probe. This can be either a sense oligo complementary to the FISH probe, a probe targeting an artificial nonsense sequence, or an oligo against mRNA that is not expressed in oocytes (we use EGFP-derived oligonucleotide).

The manipulation of oocytes during hybridization and subsequent washes is very important. The oocytes become sticky during post-hybridization washes in diluted SSC (sodium citrate/sodium chloride) solution. Thus, the transfer of oocytes between washing solutions with a micropipette is not suitable as it may lead either to oocyte damage or their complete loss. Due to the small size of oocytes, the hybridization and washes cannot be carried out in 2 ml tubes, as in whole-mount FISH protocols for later-stage embryos because the oocytes will not settle at the bottom of the tube and are easily lost during the change of washing solutions. Several systems based on membranes with small-size pores (less than 20 μm) have been introduced to circumvent the technical difficulties involved in oocyte and preimplantation embryo manipulation [20] and [21]. In the chamber system developed by Yoshikawa and colleagues, the oocytes are placed on a transwell membrane with 8 μm pores (Corning Inc.) and the entire *in situ* hybridization procedure is performed in an aluminium device where the solutions are added to the transwell by pipetting and removed by capillary-force-driven drainage [21]. This system allows for simultaneous hybridization of many different probes, which makes it convenient for large scale

experiments. However, after testing various membrane systems, we found that the oocytes deposited on membranes tend to flatten even when a careful drainage method is used for solution exchange. Consequently, the transwell membranes should only be employed in experiments when precise spatial localization is not required.

When the spatial distribution of a transcript within the oocyte is being studied, hybridization and post-hybridization washes should leave the oocytes intact and any mechanical pressure affecting the oocyte shape should be avoided. We recommend using small glass staining blocks for the hybridization procedure, which works well in our hands. Oocytes are transferred to the staining block with a small volume of hybridization mixture containing the FISH probe, and left at the hybridization temperature (usually 37 °C for short DNA oligonucleotide probes) in a humidified chamber. When using fluorescently labeled probes, hybridization and all subsequent incubations should be carried out in the dark. Washing solutions are added to the staining block by pipetting and removed with a glass pipette under the microscope. The micropipette diameter should be around 0.5 mm. This enables fast solution removal and, at the same time, allows for good control of the oocyte position in the staining block, so that no oocytes are aspirated and lost while exchanging solutions. Although this method is more laborious when compared to transwell membranes, it results in perfect preservation of oocyte spherical shape and it is thus optimal for RNA localization studies.

After the last post-hybridization wash in PBT, the oocytes are either directly mounted in Vectashield, if a fluorescently labeled probe has been used and only the FISH signal is being examined, or processed further by antibody staining for visualization of non-fluorescently labeled probes and/or co-immunostaining of proteins of interest.

2.4. Combined immunofluorescence and *in situ* hybridization

Colocalization of an RNA-binding protein with specific RNAs may reveal important

functional properties of the RNP complexes being analyzed. Because the use of biochemical approaches is limited in mouse oocytes and early embryos, combined IF and FISH represents an alternative for studying RNPs. Different strategies are pursued depending on which RNA species is studied.

For the visualization of polyA RNAs within the oocyte, we use a fluorescently labeled 18 nt long oligo dT probe. When performing colocalization with a protein, an unmodified immunofluorescent staining protocol (see above) is followed and the oligo dT probe is simply added to the secondary antibody mixture at a concentration of 0.1 μ M. Due to the high polyA RNA content of the oocyte, a single fluorescent label per probe is sufficient to obtain a detectable signal (Fig. 4A). Interestingly, we found that the oligo dT signal could be significantly enhanced by a short treatment in diluted RNase A (Fig. 4B). This is likely because the limited RNA digestion by RNase A in fixed oocytes makes polyA sequences more accessible, a principle similar to antigen retrieval upon proteinase K treatment during immunostaining [22]. It should be noted, however, that the improved oligo dT hybridization signal of oocytes after RNase treatment is rather a specific case. The RNase treatment is included in the staining protocol after the permeabilization step with 0.1% Triton X-100 in PBS. A 10-min incubation in 0.1 mg/ml RNase A diluted in the blocking solution is sufficient to enhance the oligo dT signal, and no further post-

fixation is needed as the RNase digestion does not affect oocyte morphology. To ensure specificity of the oligo dT signal, an oligo dA probe of the same length and with the same fluorescent label can be used as a negative control. Alternatively, various commercially available nucleic acid stains allow the global visualization of RNA in oocytes. For example TOTO-3 iodide stain (Invitrogen) at a concentration of 0.2 μ M in the mounting medium yields a signal comparable to that of the oligo dT probe (Fig. 4C). However, except for acridine orange which emits different spectra upon binding to DNA or RNA, commercial nucleic acid dyes cannot be employed for nuclear RNA detection as they also stain DNA.

When colocalization of a specific transcript with an RNA-binding protein is studied, the immunofluorescent staining follows the FISH procedure. After post-hybridization washes, the oocytes are briefly washed in PBT and then transferred to the blocking solution prior to primary antibody incubation and the application of the rest of the immunofluorescent staining protocol. However, the quality of protein staining after FISH has to be determined in each specific case because some epitopes can be destroyed during the FISH procedure. In such cases, the primary antibody may be applied before post-fixation or even before hybridization, when proteinase K treatment is omitted. It should be noted, that the proteinase K digestion step, as described above, usually does not have a

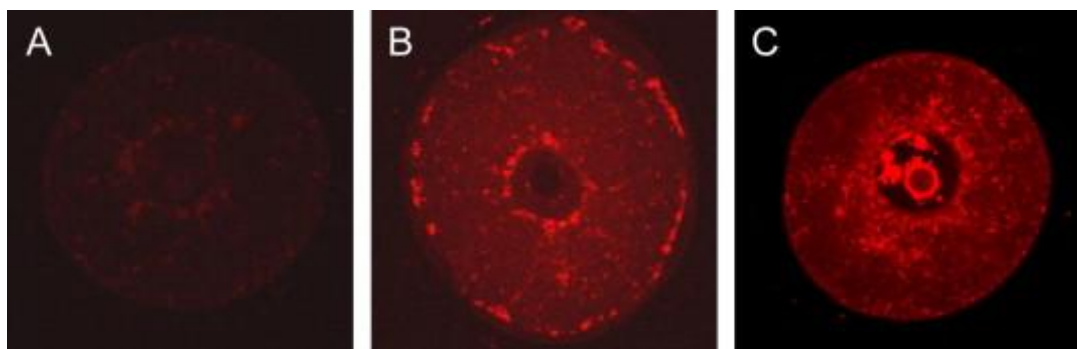


Fig. 4. Mild RNase A treatment enhances the signal of the oligo dT probe. (A) Very weak signal is obtained when the polyA mRNA is visualized by the TAMRA oligo dT probe hybridization step included in the unmodified immunostaining procedure. (B) TAMRA oligo dT signal can be increased several fold by a short incubation of the fixed and permeabilized oocytes in 0.1 mg/ml RNase A in blocking solution. (C) A pronounced perinuclear signal and cortical aggregates are observed in the oocyte also upon staining with commercially available nucleic acid stain TOTO-3 Iodide (Invitrogen). All images were obtained by confocal laser-scanning microscopy of mouse oocytes.

strong effect on epitope integrity.

When a DIG-labeled probe is used for FISH or the signal from a FITC-labeled probe is too weak, a primary antibody against the probe label is applied together with the primary antibody against the protein of interest, and the protocol for double immunofluorescent staining is followed. For such antibody amplification of the FISH signal, it is necessary to perform appropriate controls. These include control samples where no probe was hybridized as well as samples where the primary antibody was excluded. Such controls should allow minimization of false positive non-specific signals of the fluorescently labeled secondary antibody. It is especially important when secondary antibodies are not raised in the same host, as these may cross-react, thus causing artifacts. Where needed, the cross-reactivity problem can be reduced by using separate sequential incubation of the secondary antibodies.

3. Concluding remarks

The experience and observations presented in this review come from our studies of dormant maternal mRNA and their storage RNPs in fully-grown mouse oocytes. However, these protocols should also work for other types of RNP complexes in mammalian oocytes and preimplantation embryos, although slight modifications may be required in each particular case. The whole-mount FISH of mouse oocytes combined with immunostaining is technically demanding and requires considerable practice to obtain satisfying results. We hope that this review provides useful information for our colleagues trying to establish this kind of RNP analysis in their laboratories.

Acknowledgments

Our research is supported by the EMBO SDIG program, GACR grants 204/09/0085 and P305/10/2215, ME09039 grant of the Czech Ministry of Education, and the Purkynje Fellowship to P.S.

References

- [1] G. Dreyfuss, V.N. Kim, N. Kataoka, *Nat. Rev. Mol. Cell Biol.* 3 (2002) 195–205.
- [2] N.L. Garneau, J. Wilusz, C.J. Wilusz, *Nat. Rev. Mol. Cell Biol.* 8 (2007) 113–226.
- [3] P. Anderson, N. Kedersha, *J. Cell Biol.* 172 (2006) 803–808.
- [4] A. Eulalio, I. Behm-Ansmant, E. Izaurralde, *Nat. Rev. Mol. Cell Biol.* 8 (2007) 9–22.
- [5] J. Ule, K.B. Jensen, M. Ruggiu, A. Mele, A. Ule, R.B. Darnell, *Science* 302 (2003) 1212–1215.
- [6] M.L. Stitzel, G. Seydoux, *Science* 316 (2007) 407–408.
- [7] J.D. Richter, *Trends Biochem. Sci.* 32 (2007) 279–285.
- [8] T. Sakurai, M. Sato, M. Kimura, *Biochem. Biophys. Res. Commun.* 336 (2005) 1181–1189.
- [9] O. Johnstone, P. Lasko, *Annu. Rev. Genet.* 35 (2001) 365–406.
- [10] M.L. King, T.J. Messitt, K.L. Mowry, *Biol. Cell.* 97 (2005) 19–33.
- [11] D. Koehler, V. Zakhartchenko, L. Froenicke, G. Stone, R. Stanyon, E. Wolf, T. Cremer, A. Brero, *Exp. Cell Res.* 315 (2009) 2053–2063.
- [12] A.V. Probst, F. Santos, W. Reik, G. Almouzni, W. Dean, *Chromosoma* 116 (2007) 403–415.
- [13] M. Puschendorf, R. Terranova, E. Boutsma, X. Mao, K. Isono, U. Brykczynska, C. Kolb, A.P. Otte, H. Koseki, S.H. Orkin, M. van Lohuizen, A.H. Peters, *Nat. Genet.* 40 (2008) 411–420.
- [14] X. Wu, M.M. Viveiros, J.J. Eppig, Y. Bai, S.L. Fitzpatrick, M.M. Matzuk, *Nat. Genet.* 33 (2003) 187–191.
- [15] D. Grunwald, R.H. Singer, K. Czaplinski, *Methods Enzymol.* 448 (2008) 553–577.
- [16] D. Piette, M. Hendrickx, E. Willems, C.R. Kemp, L. Leyns, *Nat. Protoc.* 3 (2008) 1194–1201.
- [17] M. Zuker, *Nucleic Acids Res.* 31 (2003) 3406–3415.

[18] R. Thomsen, P.S. Nielsen, T.H. Jensen, RNA 11 (2005) 1745–1748.

[19] G. Seydoux, A. Fire, Development 120 (1994) 2823–2834.

[20] E.D. Newman-Smith, Z. Werb, Development 121 (1995) 2069–2077.

[21] T. Yoshikawa, Y. Piao, J. Zhong, R. Matoba, M.G. Carter, Y. Wang, I. Goldberg, M.S. Ko, Gene Expr. Patterns 6 (2006) 213–224.

[22] F. D’Amico, E. Skarmoutsou, F. Stivala, J. Immunol. Methods 341 (2009) 1–18.

SUPPLEMENT 2

Matyas Flemr, Jun Ma, Richard M. Schultz and Petr Svoboda

P-body loss is concomitant with formation of a messenger RNA storage domain in mouse oocytes

(reprint from *Biology of Reproduction*. 2010 May;82(5):1008-17)

My contribution to this work:

I generated all the experimental data used in this publication except Fig.1B and I helped prepare the manuscript.

P-Body Loss Is Concomitant with Formation of a Messenger RNA Storage Domain in Mouse Oocytes¹

Matyas Flemr⁴, Jun Ma⁵, Richard M. Schultz^{3,5} and Petr Svoboda^{2,4}

Author Affiliations

1. *Institute of Molecular Genetics,⁴ Academy of Sciences of the Czech Republic, Prague, Czech Republic*
2. *Department of Biology,⁵ University of Pennsylvania, Philadelphia, Pennsylvania*

1. ²Correspondence: Petr Svoboda, Institute of Molecular Genetics, Academy of Sciences of the Czech Republic, Videnska 1083, 142 20 Prague 4, Czech Republic. FAX: 420 224310955; e-mail: svobodap@img.cas.cz
2. ³Correspondence: FAX: 215 898 8780; e-mail: rschultz@sas.upenn.edu

Abstract

In mammalian somatic cells, several pathways that converge on deadenylation, decapping, and 5'-3' degradation are found in cytoplasmic foci known as P-bodies. Because controlled mRNA stability is essential for oocyte-to-zygote transition, we examined the dynamics of P-body components in mouse oocytes. We report that oocyte growth is accompanied by loss of P-bodies and a subcortical accumulation of several RNA-binding proteins, including DDX6, CPEB, YBX2 (MSY2), and the exon junction complex. These proteins form transient RNA-containing aggregates in fully grown oocytes with a surrounded nucleolus chromatin configuration. These aggregates disperse during oocyte maturation, consistent with recruitment of maternal mRNAs that occurs during this time. In contrast, levels of DCP1A are low during oocyte growth, and DCP1A does not colocalize with DDX6 in the subcortical aggregates. The amount of DCP1A markedly increases during meiosis, which correlates with the first wave of destabilization of maternal mRNAs. We propose that the cortex of growing oocytes serves as an mRNA storage compartment, which contains a novel type of RNA granule related to P-bodies.

DDX6; gene regulation; maternal mRNA; miRNA; oocyte; oocyte development; P-body; RNA granule; YBX2

INTRODUCTION

Transformation of a differentiated mouse oocyte into pluripotent blastomeres of the two-cell embryo (oocyte-to-embryo transition) is largely controlled by maternal mRNAs. In addition to translated mRNAs, which are very stable in the growing oocyte [1], the maternal transcriptome contains stable untranslated transcripts—dormant maternal mRNAs—that are recruited during meiotic maturation or early embryogenesis. A common mechanism regulating recruitment and stability of dormant maternal mRNAs is reversible polyadenylation that is controlled by cytoplasmic polyadenylation

elements (CPEs) (reviewed in [2]). CPEs are specific sequences in 3'-untranslated regions (3'UTRs) of dormant maternal mRNAs that serve as the binding platform for the CPE-binding protein (CPEB), which controls polyadenylation-induced translation.

Cytoplasmic control of mRNA metabolism occurs within ribonucleoprotein particles (RNPs) that frequently form focal points visible by light microscopy where different pathways involved in mRNA translation control and decay are assembled. There are several classes of cytoplasmic RNA granules, such as processing bodies (P-bodies), stress granules, or germ cell granules (reviewed in

[3–5]). P-bodies are cytoplasmic granules associated with repression of translation and mRNA decay. Stress granules are dense aggregates that appear in cells exposed to environmental stress and regulate translational repression and mRNA recruitment to preserve cell integrity. Germ cell granules (GCGs) are RNPs that regulate maternal mRNAs required for germ cell specification. Notably, the composition of all three types of granules overlaps to some extent. For example, the RNA helicase DDX6 (RCK/p54) and translation factor EIF4E are found in all three, whereas the decapping complex DCP1/2 is found in P-bodies and germ cell granules but not in stress granules [3, 4].

P-bodies are the most common type of RNA granules in mammalian cells. They were originally discovered as cytoplasmic foci containing 5'-3' RNA degradation pathway protein XRN1 and the decapping complex [6–8]. Other P-body components, TNRC6 (GW182), LSM14A (RAP55), and EDC4 (also known as Ge-1 and HEDLS), were discovered in parallel when analyzing human autoimmune sera, which stained discrete cytoplasmic foci [9–11]. Subsequently, P-bodies were connected to several pathways, including nonsense-mediated mRNA decay (NMRD) and microRNA (miRNA) pathway/translational repression; P-body components represent an ever-growing list of proteins involved in RNA metabolism, including CPEB, CCR4-NOT deadenylase complex, translational repressor DDX6, translation initiation factors EIF4E and EIF4ET, and Argonaute proteins (reviewed in detail in [4, 5]).

From a structural point of view, several P-body components, such as TNRC6, EDC4, LSM14A, and DDX6 are essential for the integrity of P-bodies, and depletion of any of these proteins results in loss of P-bodies (reviewed in [4]). It has been also shown that an intact miRNA pathway is required for the formation of P-bodies [12], whereas P-bodies are not required for mRNA decay in NMRD [13]. The observation that inhibiting the miRNA pathway at any step prevents P-body formation has led to a proposal that, even though P-body components play crucial roles in mRNA silencing and decay, aggregation of

the protein constituents to P-bodies is not required for miRNA function and mRNA degradation but rather is a consequence of miRNA activity [12].

RNA granules in oocytes of *Xenopus*, *Drosophila*, and *Caenorhabditis* are well characterized [14–18]. In contrast, little is known about the dynamics of RNA granules during mammalian oocyte growth and maturation. Early postnatal mouse oocytes contain granulofibrillar material reminiscent of GCGs in association with transiently appearing Balbiani bodies [19]; but the oocytes lack detectable GCGs [20]. When compared to somatic cells, mouse germinal vesicle (GV) oocytes contain markedly increased transcript levels of many components of RNA granules [21], probably a consequence of an increased demand for posttranscriptional control during the oocyte-to-embryo transition. How these factors contribute to the control of translational repression and mRNA degradation is unknown.

Here, we report an unexpected behavior of P-body proteins during mouse oocyte growth where P-bodies, present in small, meiotically incompetent oocytes, disappear and their components adopt spatially and temporarily separated functions. Moreover, the amount of DCP1A, a component of the decapping complex and a P-body-associated protein, is low during oocyte growth but displays a massive increase during meiotic maturation. In contrast, several RNA-binding proteins, including DDX6, YBX2 (MSY2), and CPEB, localize to the cortex, where they form transient RNP aggregates containing maternal mRNAs. Consistent with their function as a storage compartment, the aggregates detach from the cortex upon resumption of meiosis, relocate toward the center of the oocyte, and disperse. We propose that mouse oocytes store maternal mRNAs in a novel type of RNA granule that shares components with P-bodies.

MATERIALS AND METHODS

Oocyte and Embryo Collection and Culture

Oocytes and embryos were obtained from C57BL/6 mice. Meiotically incompetent oocytes were isolated from ovaries of 2- or 12-day-old mice by incubation in PBS with 1 mg/ml collagenase (Sigma) at 37°C and collected in CZB medium (Chemicon). Fully grown GV oocytes were liberated from ovaries of 6- to 14-wk-old mice by puncturing the antral follicles with syringe needles and collecting in M2 medium (Sigma) containing 0.2 mM isobutylmethylxanthine (IBMX; Sigma) to prevent resumption of meiosis. To study the role of microfilaments and microtubules, oocytes were incubated in 10 μ M cytochalasin D (Sigma) in M2 with IBMX at 37°C, 5% CO₂ for 4 h to disrupt actin microfilaments or in 67 μ M nocodazole. To obtain MII (oocyte in metaphase II) eggs and embryos, 6- to 14-wk-old mice were superovulated with 5 units of equine chorionic gonadotropin (eCG) followed by stimulation with 5 units of human chorionic gonadotropin (hCG) 48 h post-eCG; for embryo collection, the mice were mated with 8- to 20-wk-old males immediately after hCG injection. MII eggs were isolated from mice 12 h post-hCG injection by tearing the oviduct ampulla in M2 medium containing 3 mg/ml hyaluronidase (Sigma) and collected in M2 medium. Blastocysts were isolated by flushing oviducts or uteri of mice 96 h post-hCG injection. All animal experiments were approved by the Institutional Animal Use and Care Committees and were consistent with Czech laws and NIH guidelines.

Immunofluorescent Staining

Oocytes collected in culture medium were washed briefly in PBS and fixed in 3.7% paraformaldehyde (PFA) in PBS for 1 h at room temperature (RT). Oocytes were permeabilized for 15 min in 0.1% Triton X-100 in PBS, washed extensively in blocking solution (0.01% Tween-20 and 0.1% bovine serum albumin in PBS), and incubated with the primary antibody diluted in blocking solution for 1 h. Oocyte transfer during fixation and permeabilization of oocytes was performed with a glass pipette whose inner diameter was \sim 250 μ m.

Mouse anti-AGO2 antibody (Abnova) was used at 1:100, rabbit anti-DDX6 (Bethyl

Laboratories) at 1:500, rabbit anti-DCP1A (a kind gift from Jens Lykke-Andersen) at 1:200, rabbit anti-MSY2 (YBX2) at 1:500 [22], rabbit anti-CPEB (Santa Cruz Biotechnology) at 1:100, rabbit anti- α -tubulin (Santa Cruz Biotechnology) at 1:200, human index serum 18033 (a kind gift from Marvin J. Fritzler) at 1:500, rabbit anti-eIF4a3 (a kind gift from Nahum Sonenberg) at 1:100, and rabbit anti-MATER (NLRP5, a kind gift from Jurrien Dean) at 1:1000 dilution. For AGO2 detection, the zona pellucida was removed before staining by brief incubation in acidic Tyrode solution (Chemicon) because the secondary antibody cross-reacted with the zona.

After four washes in blocking solution (10 min each), oocytes were incubated for 1 h with Alexa488- or Alexa594-conjugated secondary antibody (Invitrogen) diluted 1:500 in blocking solution. For poly(A) mRNA colocalization with proteins, 1 μ M tetramethylrhodamine-oligo(dT)₁₈ probe (TAMRA-oligo(dT)₁₈; Sigma) was included in the secondary antibody mixture. Following another 4 \times 10 min wash, oocytes were mounted in Vectashield with 4', 6-diamidino-2-phenylindole (DAPI; Vector Laboratories).

Confocal Microscopy

Fluorescent images were acquired using a Leica TCS SP5 inverted confocal laser scanning microscope equipped with HCX PL APO 40x/1.25 oil immersion objective. Sequential scanning of DAPI, fluorescein isothiocyanate (FITC) and Alexa488, and TAMRA and Alexa594 were performed by excitation using a 405-nm blue diode laser, a 488-nm argon laser, and a 561-nm helium-neon laser, respectively. The emitted light was collected in a bandwidth of 415–495 nm for DAPI, 498–578 nm for FITC and Alexa488, and 594–692 nm for TAMRA and Alexa 594. The photomultiplier tube (PMT) gain value was set at 950 V maximum, and the excitation laser intensity was adjusted to obtain a few saturated pixels in areas of the strongest signal, while keeping the signal in the control samples below detection limit. The offset was applied to cut the background signal in the space surrounding the oocytes. All the images were collected and merged using Leica LAS AF software. When better

reproduction of the data in printed materials were needed, the contrast and brightness of related images were identically linearly enhanced. The original Leica acquisition files are available upon request.

In Situ Hybridization

A modified version of Robert Singer's laboratory protocol [23] was used. Oligonucleotide probes (50-nucleotides long) were designed using Vector NTI software (Invitrogen), and the probe specificity was verified with Ensembl BlastView tool. The probe for *Mos*, that is, [Flc]AAAAGAGTAGA[FlcdT]GTCAGCTT TGGGCG[FlcdT]GGCAATCTCTCC[FlcdT] TTCAGGATCT[Flc], and the control probe targeting the EGFP-coding region, that is, [Flc]TCGATGTTG[FlcdT]GGCGGATCTT GAAGT[FlcdT]CACCTTGATGCCG[FlcdT] TCTTCTGCTT[Flc], contained 5-fluorescein (Flc) tags at the indicated positions and were obtained from Sigma. For the in situ procedure, oocytes were fixed for 1 h in 3.7% PFA in PBS at RT, washed in PBT (0.1% Tween-20 in PBS), and stored in 70% ethanol at 4°C overnight. After rehydration in PBT, oocytes were treated for 3 min with 1 µg/ml proteinase K in PBT, washed in 2 mg/ml glycine in PBT, and postfixed for 20 min in 3.7% PFA in PBT. Oocytes were initially incubated for 1 h in hybridization mix (HM; 50% formamide, 5× saline-sodium citrate [SCC] 1× Denhardt solution, 200 µg/ml yeast tRNA, 500 µg/ml salmon sperm DNA, and 2% blocking reagent [Roche]) at 37°C and then hybridized 2 h or overnight in HM with 40 nM probe at 37°C. Posthybridization washes consisted of 3 × 15 min in 30% formamide/2x SSC at 50°C, 1 × 15 min in 2x SSC at RT, and 1 × 15 min in 0.2x SSC at RT. After a wash in PBT, oocytes were either mounted in Vectashield with DAPI or incubated for 1 h in blocking solution followed by immunostaining as described in the text.

RESULTS

Loss of P-Bodies Early in Oocyte Growth

Because transcripts of many P-body components are overrepresented in fully

grown GV mouse oocytes relative to somatic cells [21], we examined by confocal microscopy the structure of P-bodies in oocytes using antibodies against AGO2, DCP1A, and DDX6, and the human antiserum 18033 that recognizes P-body components GW182 (TNRC6 paralogs) and EDC4 [24]. *Ecd4* mRNA is apparently several times more abundant than that of *Tnrc6* [21], and therefore a larger fraction of the 18033 signal may come from EDC4. Because there are no specific antibodies that distinguish the contribution of TNRC6 to the 18033 fluorescent signal, we refer to corresponding stainings as “18033.”

Oocytes and embryos at the following developmental stages were analyzed: meiotically incompetent oocytes from 2- and 12-day-old females, fully grown GV oocytes with nonsurrounded nucleolus (NSN) and surrounded nucleolus (SN) chromatin, MII eggs, and blastocysts. The SN chromatin configuration appears in the final stages of GV oocyte development and correlates with higher developmental competence than that of oocytes with NSN chromatin, which is found during oocyte growth [25, 26]; fully grown GV oocytes with a NSN chromatin configuration complete meiosis at reduced incidence. Developmental competence is also associated with cytoplasmic factors because only 4% of SN nuclei transferred to enucleated NSN oocytes support development to the blastocyst stage [25]. Importantly, SN and NSN oocytes are isolated as a mixed population, and the NSN/SN phenotype is recognized only following staining of the DNA.

Immunostaining with antibodies recognizing AGO2, DCP1A, DDX6, and 18033 yielded bright spots of colocalizing signal in meiotically incompetent oocytes from 2 dpp (days postpartum) and 12 dpp animals (Fig. 1A). Specificity of the staining is supported by the fact that the DDX6 antibody detected only a single band in a Western blot from mouse oocytes (Fig. 1B). Thus, P-bodies are present in differentiated mouse oocytes before they enter the growth phase. Surprisingly, P-bodies were not present in fully grown GV oocytes (Fig. 2A). Detailed analysis of 12 dpp oocytes of different diameters revealed that oocytes with a

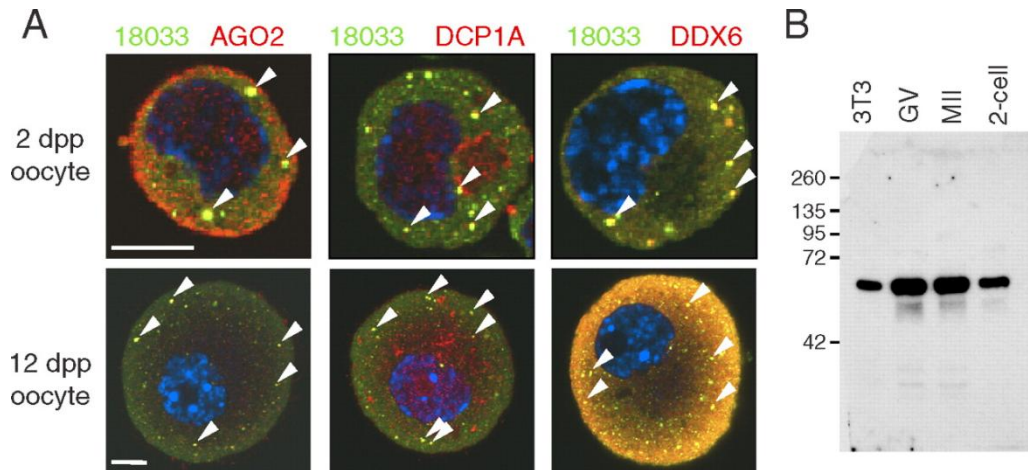


FIG. 1. P-bodies are present in small incompetent oocytes. **A)** Confocal images of mouse meiotically incompetent oocytes from 2 dpp and 12 dpp females after staining with 18033, AGO2, DCP1A, and DDX6 antibodies. Staining with 18033 is green colored, other proteins are shown in red, and DNA staining (DAPI) is shown in blue. Colocalization yields yellow color. The arrowheads depict P-bodies. For each sample, at least 10 oocytes were examined, and representative images are shown. Bar = 10 μ m. **B)** DDX6 antibody specificity analyzed by Western blot analysis. DDX6 antibody used in this work detects a single band corresponding to the size of DDX6 (RCK/p54).

diameter of ~ 50 μ m or larger exhibited a loss of colocalization of 18033 and AGO2 (Fig. 2, B and C). Interestingly, P-bodies appeared larger in the smallest oocytes (35–40 μ m) whereas in larger oocytes (~ 50 μ m), their size decreased while more colocalizing spots were found in confocal sections (Fig. 2C).

To gain more insight into P-body dynamics, we performed immunostaining of fully grown GV oocytes, MII eggs, and early embryo stages. In fully grown GV oocytes and MII eggs, P-bodies were absent, and we found three distinct patterns (Fig. 3). AGO2 staining showed a low granular signal uniformly distributed throughout the cytoplasm of GV oocytes and MII eggs and did not colocalize with other P-body components (see also Fig. 2A). DCP1A staining of GV NSN and GV SN oocytes revealed a low uniform signal throughout the cytoplasm, which strongly increased in MII eggs, suggesting that *Dcp1a* mRNA is recruited following resumption of meiosis. DDX6 and 18033 antibodies yielded enhanced subcortical staining, which contained distinct subcortical aggregates (SCAs) in fully grown GV SN oocytes. SCAs emerged during formation of SN chromatin

and disappeared during meiotic maturation, resulting in homogenous subcortical staining in MII eggs (Fig. 3). SCAs appear as domains of irregular shapes up to several micrometers in diameter and are reminiscent of stress granules. However, a component of stress granules, HuR [3], is not found in SCAs (data not shown).

It is unlikely that the staining patterns were an artifact because the same antibodies visualized P-bodies in other cell types, such as fibroblasts or cumulus cells (Fig. 3). In addition, SN oocytes and NSN oocytes were fixed and stained together, and the same patterns were reproduced in both collaborating laboratories and were observed under different fixation conditions (data not shown). Thus, our data suggest that components of dispersed P-bodies are differently regulated in growing and maturing oocytes, at least for the decapping complex (DCP1A), miRNA-mediated repression (AGO2), and translational repression (DDX6 and 18033). Notably, DDX6 and 18033 signal remained colocalized in the cortex suggesting some P-body proteins still remain functionally linked.

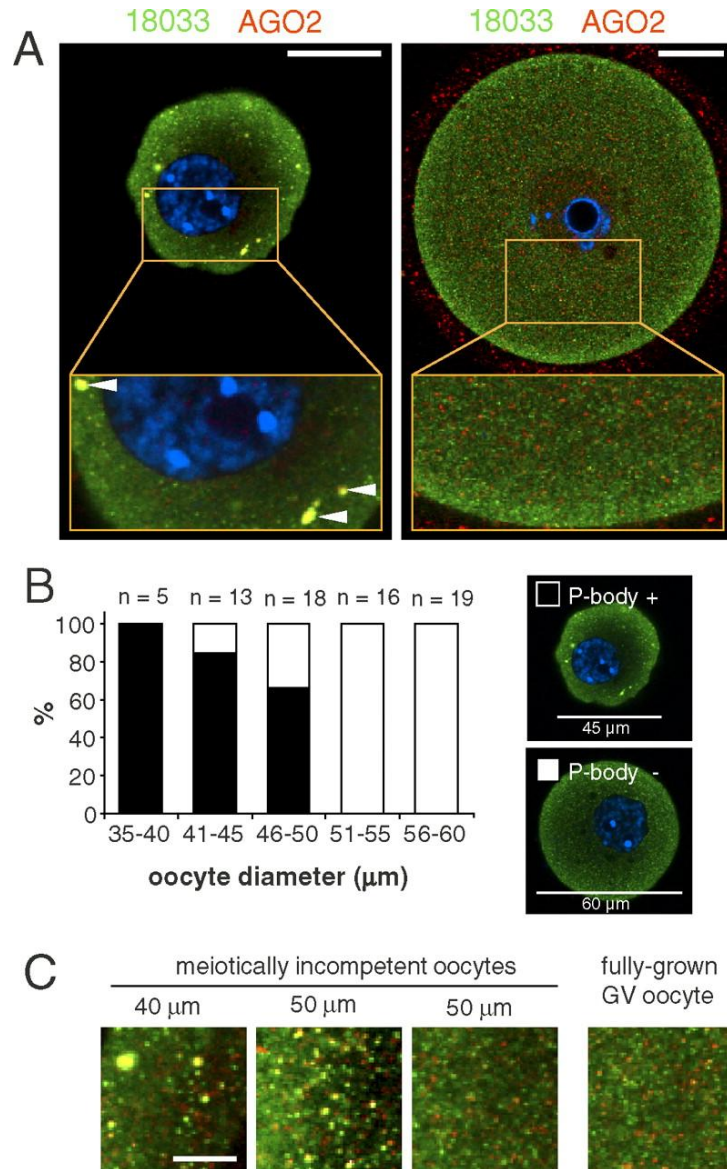


FIG. 2. P-bodies disappear as oocytes increase in size. **A**) Representative confocal images showing colocalization of 18033 and AGO2 in small, meiotically incompetent (12 dpp; left panel) and fully grown GV SN oocytes (right panel). Staining with 18033 is green colored, AGO2 is shown in red, and DNA staining (DAPI) is shown in blue. Colocalization of 18033 and AGO2 yields yellow color. Horizontal arrowheads depict P-body-like structures. AGO2 signal was enhanced in the fully grown GV oocyte to visualize the lack of AGO and 18033 colocalization. It should be noted that the observed intensity of the subcortical staining depends on setting the dynamic range of the image acquisition. Bars = 20 μm . **B**) Quantification of P-body presence/absence in incompetent oocytes (12 dpp). Oocyte diameter was estimated by image analysis of the central confocal sections. The numbers of incompetent oocytes within each group are indicated above the columns. The representative images show what was classified as a P-body-containing oocyte (shown in the solid bars in the histogram) and an oocyte not containing P-bodies (shown as the open bars in the histogram). These images were acquired in one experiment with the same confocal microscope settings. **C**) A detail of cytoplasmic staining from incompetent and fully grown oocytes showing the loss of 18033 and AGO2 colocalization in larger oocytes. Staining with 18033 is green colored, and staining with AGO2 is shown in red. Colocalization yields yellow color. Bar = 5 μm .

Finally, we analyzed early embryo stages because we hypothesized that P-bodies may assemble following zygotic genome activation when zygotic miRNAs are expressed [27]. P-bodies were found in

blastocysts (Fig. 3) whereas their presence was not consistently detected in earlier embryo stages (data not shown). Taken together, our data show that P-bodies are dispersed early in oocyte growth and

reappear only during later stages of preimplantation development.

A Novel Subcortical RNP Complex in GV Oocytes

We next focused on the subcortical region where DDX6 and 18033 formed subcortical aggregates in GV SN oocytes (Fig. 3). A

subcortical staining pattern is observed for a number of proteins, including the subcortical maternal complex (SCMC) [28] and RNA binding protein YBX2 [29].

YBX2 is a highly abundant mRNA-binding protein involved in RNA metabolism, which is essential for formation of meiotically and developmentally competent oocytes [22, 30].

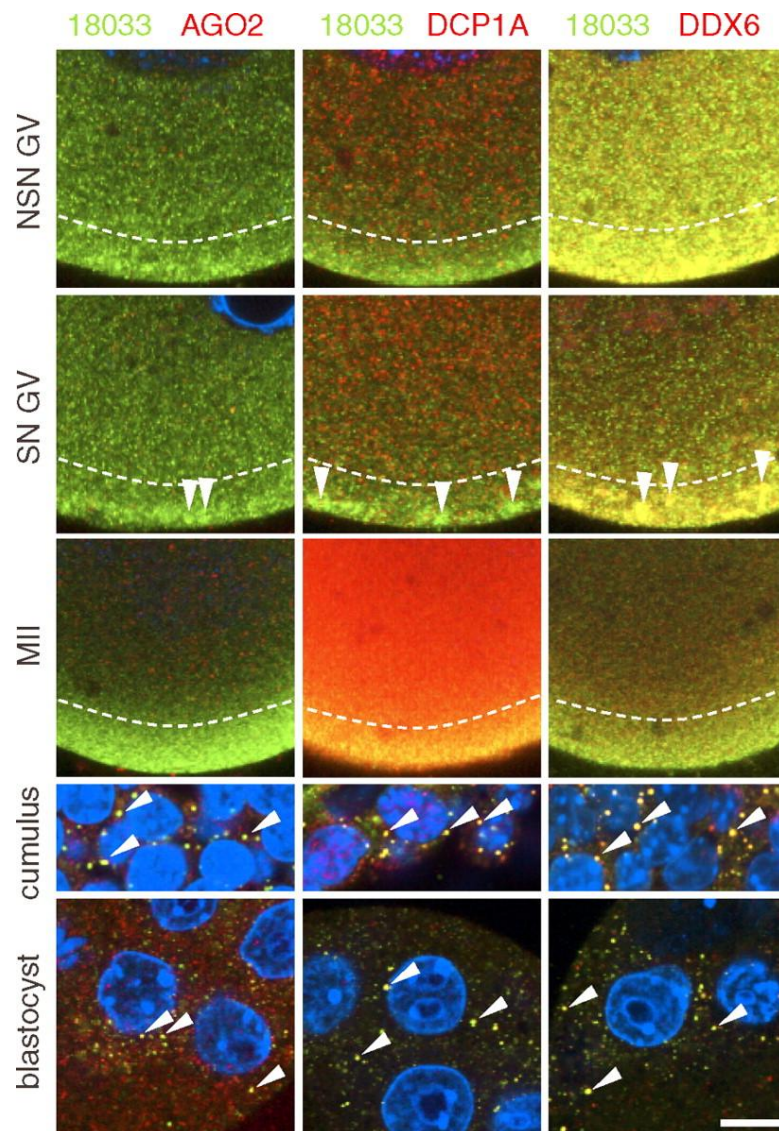


FIG. 3. Expression of P-body components during oocyte development. Confocal images of mouse GV NSN and SN oocytes, MII eggs, cumulus cells, and blastocysts after staining with 18033, AGO2, DCP1A, and DDX6 antibodies. A representative region of a whole specimen is shown. Staining with 18033 is green colored, other proteins are shown in red, and DNA staining (DAPI) is shown in blue. Colocalization yields yellow color. Diagonal arrowheads depict P-bodies in blastocysts and somatic cells. Vertical arrowheads depict subcortical aggregates found in SN GV oocytes. Dashed lines border the subcortical domain with enhanced staining of 18033 and DDX6. Note low colocalization of DDX6 and 18033 outside of the subcortical domain. Staining with the same primary antibodies were performed independently in both the United States and Czech laboratories with similar results; a representative staining is shown. GV and MII samples in each column come from the same staining experiment and were scanned with identical confocal microscope settings. SN, surrounded nucleolus; NSN, nonsurrounded nucleolus; GV, fully grown germinal-vesicle oocyte; MII, oocyte in meiosis II. Bar = 10 μ m. For each sample, at least 10 oocytes, eggs, blastocysts, or cumulus cells were examined; representative images are shown.

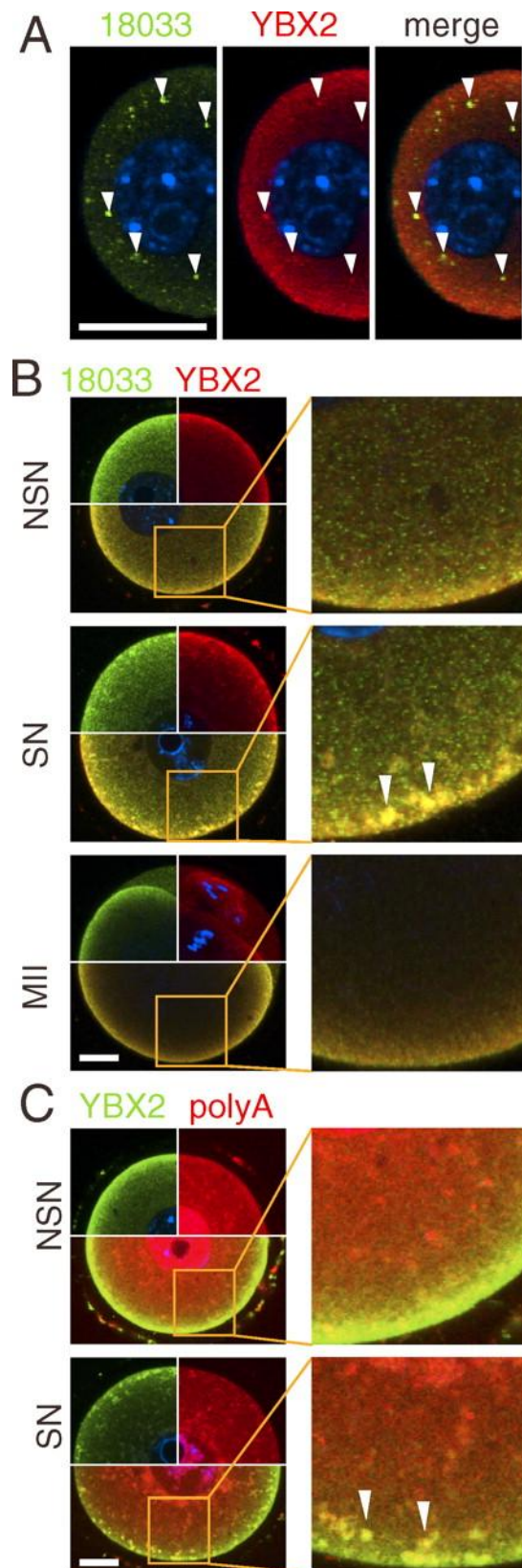
Accordingly, we analyzed YBX2 colocalization with DDX6 and TNRC6/EDC4. YBX2 was detectable in P-bodies in incompetent oocytes (Fig. 4A), and we also found overlapping staining in the subcortical domain including colocalization

of YBX2 and 18033 in subcortical aggregates in SN oocytes (Fig. 4B).

To test if subcortical aggregates also contain mRNA, we used the TAMRA-oligo(dT)₁₈ probe and found a distinct localization of the TAMRA signal in both the cytoplasm and the nucleus of NSN and SN oocytes (Fig. 4C). In NSN GV oocytes, the TAMRA signal was very high in the nucleus but lower in chromocenters. There was also a stronger perinuclear signal and an increased homogeneous subcortical staining that overlapped with YBX2 staining. In SN GV oocytes, the nuclear TAMRA signal partially overlapped with DNA staining whereas the rest of the nucleoplasm showed little or no staining. The nuclear pattern likely reflects cessation of transcription and translocation of most mRNAs to the cytoplasm during NSN and SN transition. In the cytoplasm of SN oocytes, the TAMRA signal was found in subcortical aggregates colocalizing with YBX2 (Fig. 4C).

Thus, DDX6, YBX2, 18033, and RNA define a novel compartment that we name the subcortical RNP domain (SCRD). The SCRD is apparently established in oocytes from primary follicles, and it does not mutually exclude the presence of P-bodies as

FIG. 4. Poly(A) RNA and RNA-binding protein YBX2, but not the SCMC complex, form subcortical RNP aggregates with P-body components. **A**) YBX2 (MSY2) is also present in P-bodies. Confocal images showing colocalization of 18033 and YBX2 in small, meiotically incompetent oocytes (12 dpp). The arrowheads point to subcortical P-bodies. The blue signal is DNA staining (DAPI). **B**) Confocal images showing colocalization of 18033 and YBX2 in fully grown GV NSN and SN oocytes and MII eggs. **C**) Confocal images of colocalization of YBX2 and poly(A) RNA, visualized by TAMRA-oligo(dT)₁₈, in fully grown GV NSN and SN oocytes. Contrast of poly(A) samples was linearly enhanced for better presentation of colocalization in SCRCD and SCAs. The identities of green and red channels are indicated above each panel, colocalization yields yellow color. The blue signal is DNA staining (DAPI). The area in the merged image outlined by solid lines is magnified in the adjacent image. The arrowheads point to subcortical RNP aggregates. For each sample, at least 10 oocytes were examined, and representative images are shown. SN, surrounded nucleolus GV oocyte; NSN, nonsurrounded nucleolus GV oocyte. Bars = 20 μm.



evidenced by an enhanced subcortical signal of 18033 and DDX6 in populations of smaller 12 dpp oocytes (Fig. 1A). The prominent feature of the SCRD are SCAs, which appear in fully grown GV SN oocytes. The SCRD could physically interact with the SCMC complex, perhaps via OOEP (MOEP19), which is a putative RNA-binding protein [28, 31]. To test this hypothesis, we performed immunocolocalization testing of SCRD (18033) and SCMC (NLRP5) in GV SN oocytes and found little, if any, overlap of the signal in the cortex and absence of the SCMC in most of the SCAs (Fig. 5). The structural basis of SCRD is presently unclear but, like YBX2 localization [22], it does not depend on the actin or tubulin cytoskeleton (Fig. 6). Treatment of fully grown GV oocytes with nocodazole or cytochalasin D caused clear changes in microtubules (loss of fibrillar structures) or microfilaments (disruption of cortical actin and appearance of phalloidin-positive foci in the cytoplasm), respectively. Nevertheless, SCAs were still found intact in the cortex, and changes in DDX6 and 18033 staining patterns were not observed.

SCAs Store Untranslated mRNAs in the Oocyte

One of the components of the SCRD and SCAs is the translational repressor DDX6 (Rck/p45), an ortholog of CGH-1 in *C. elegans*, Me31B in *Drosophila*, and Xp54 in *X. laevis* that is implicated in the control of maternal mRNAs in these organisms [32]. CGH-1 and its orthologs are found in a number of different RNA granules regulating mRNA stability and translation throughout the female germ cell development and in the soma [32]. We hypothesized that SCAs might also contain untranslated maternal mRNAs, such as dormant maternal mRNAs. Therefore, we performed in situ hybridization to visualize the classical dormant maternal mRNA encoding MOS kinase [33]. Indeed, *Mos* mRNA staining of SN oocytes revealed a strong subcortical staining that was concentrated into aggregates similar to SCAs (Fig. 7). We were unable to demonstrate, however, that *Mos* mRNA colocalized with SCA proteins because all attempts for in situ hybridization combined with immunofluorescent staining failed. *Mos*, like other dormant maternal mRNAs, contains a CPE,

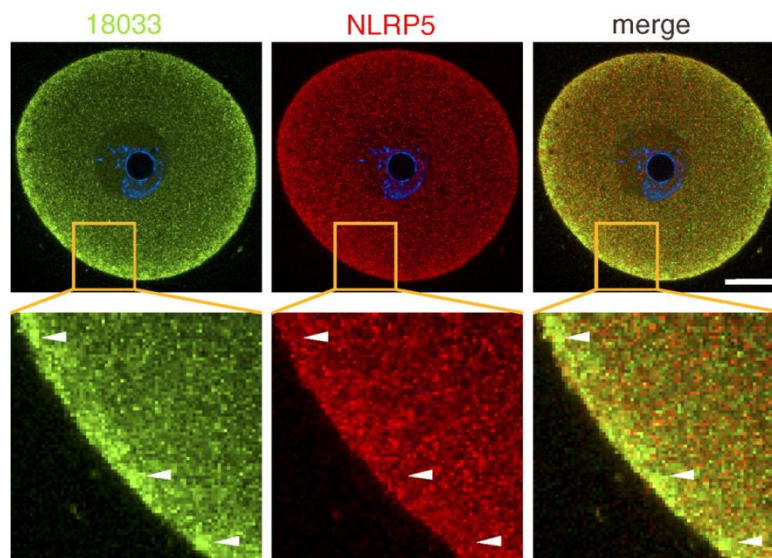


FIG. 5. Confocal images showing immunolocalization of 18033 and NLRP5 in GV SN oocytes. Identities of green and red channels are indicated above each panel, and colocalization yields yellow color. The blue signal is DNA staining (DAPI). The area in the merged image outlined by solid lines is magnified in the adjacent image. The arrowheads point to subcortical RNP aggregates. Ten oocytes were examined, and representative images are shown. SN, surrounded nucleolus GV oocyte; NSN, nonsurrounded nucleolus GV oocyte. Bar = 20 μ m.

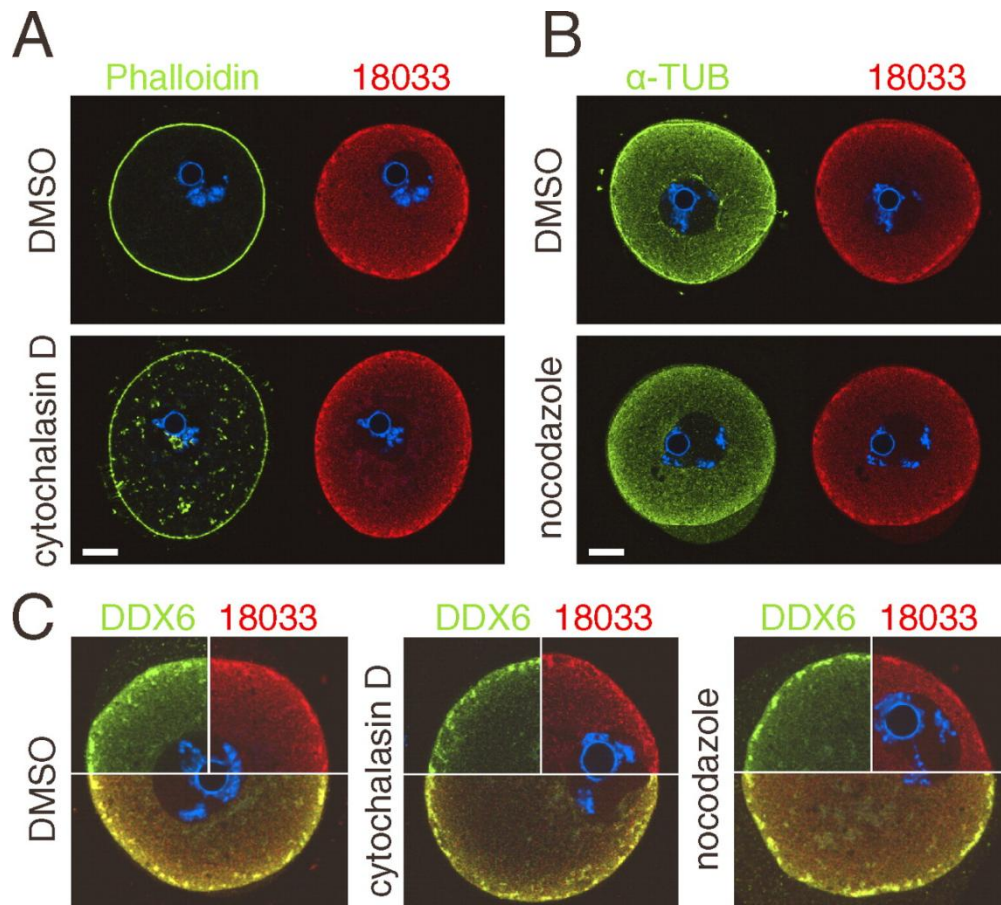


FIG. 6. SCR and SCAs are independent on actin and tubulin cytoskeleton. **A**) Immunolocalization of 18033 and actin (Phalloidin-A488) in oocytes treated with cytochalasin D. **B**) Immunolocalization of 18033 and α -tubulin in oocytes treated with nocodazole. Staining of DNA (DAPI) is shown in blue. **C**) SCAs remain unchanged upon cytochalasin D and nocodazole treatments. Confocal images showing colocalization of 18033 and DDX6 in oocytes treated with cytochalasin D and nocodazole. Staining of DNA (DAPI) is shown in blue. Dimethyl sulfoxide (DMSO)-treated oocytes serve as a control. Bars = 20 μ m.

which is bound by the CPEB protein [33]. Thus, CPEB should be present in SCAs if these store untranslated maternal mRNAs. In fact, CPEB staining, which showed a slightly enhanced subcortical signal, was clearly localized to the SCAs (Fig. 7B).

Spliced mRNAs remain associated with exon junction complex (EJC) until the first round of translation. If SCAs hold translationally repressed maternal mRNAs, which were never translated, EJC components, such as EIF4A3 [34], should be also present in the SCAs. As predicted, analysis of SN oocytes identified EIF4A3 presence in SCAs (Fig. 7C), further supporting the idea of SCAs being a store of untranslated maternal mRNAs.

Finally, we addressed the behavior of SCAs upon resumption of meiosis when

untranslated maternal mRNAs are recruited for translation. We found that SCAs were uncoupled from the SCR 2 h after initiation of the germinal vesicle breakdown (GVBD) when SCAs are detached from their position close to the cytoplasmic membrane and relocated more centrally (Fig. 8). A considerable amount of 18033 and DDX6 still remained in the SCR during meiosis. SCAs assumed a more diffuse and expanded appearance during GVBD. DDX6, 18033, CPEB, EJC, and poly(A) RNA were still found in the more centrally positioned SCAs at 4 h, but not 8 h, after GVBD, while CPEB became reduced in the SCR 4 h after GVBD (Fig. 8) and barely detectable there in MII eggs (data not shown). Thus, SCAs relocate and disintegrate in a manner consistent with release of untranslated maternal mRNAs for translation during meiosis.

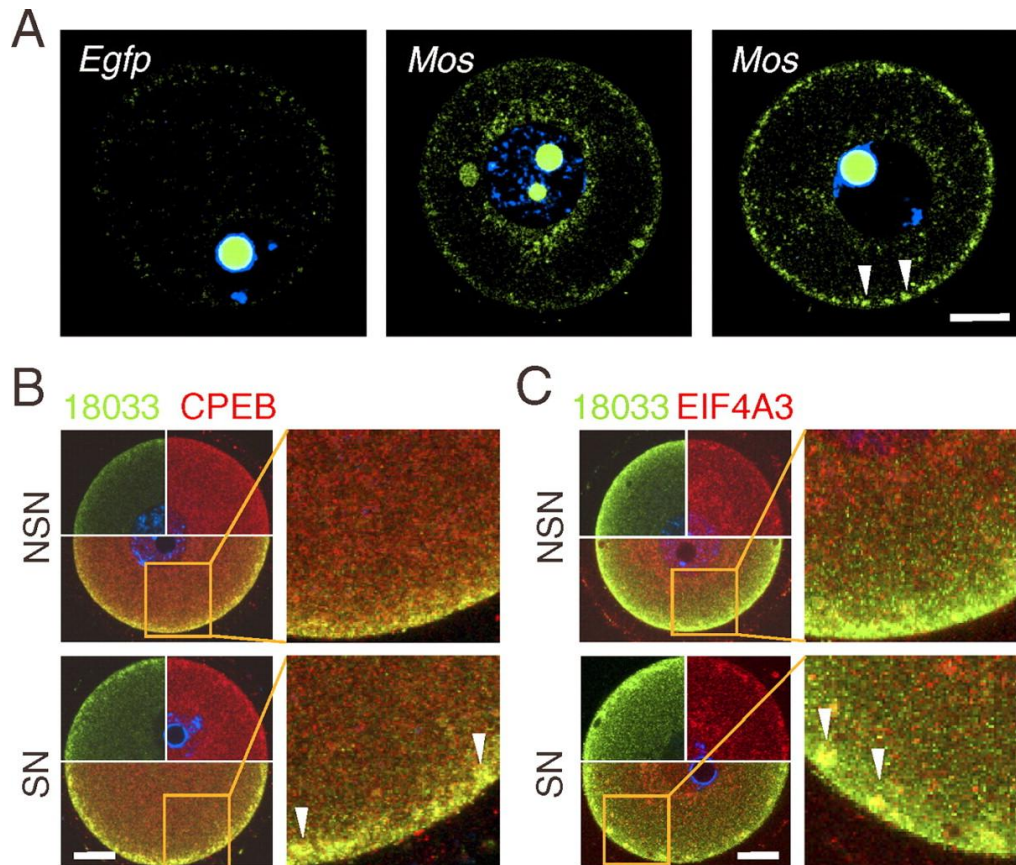


FIG. 7. Subcortical RNP domain holds dormant maternal mRNAs. **A)** In situ detection of *Mos* mRNA in the SCRD. The arrowheads depict SCA-like structures in SN oocytes, which are similar to the SCAs shown in Figures 2 and 3. Bright nucleolar signal is caused by nonspecific binding of hybridization probes. The left image shows an oocyte stained with a probe complementary to the *Egfp*-coding sequence, which served as a control for nonspecific background. For each sample, at least five oocytes were examined, and representative images are shown. **B)** Confocal images showing colocalization of 18033 and CPEB in fully grown GV SN and NSN oocytes. **C)** Confocal images showing colocalization of 18033 and EIF4A3 in fully grown GV SN and NSN oocytes. Areas in the merged images outlined by solid lines in **B** and **C** are magnified in the adjacent images. DNA staining (DAPI) is shown in blue. For each sample, at least 10 oocytes were examined, and representative images are shown. SN, surrounded nucleolus GV oocyte; NSN, nonsurrounded nucleolus GV oocyte; MII, oocyte in meiosis II. Bars = 20 μ m.

DISCUSSION

Here, we report that oocyte growth is accompanied by loss of P-bodies and subcortical accumulation of several RNA-binding proteins, including DDX6, CPEB, YBX2, and the exon junction complex. These proteins form transient, RNA-containing aggregates in fully grown oocytes with surrounded nucleolus chromatin configuration, which disperse during meiotic maturation. At the same time, levels of DCP1A, another P-body component, are low during oocyte growth, and DCP1A is absent in the aggregates. Abundance of DCP1A strongly increases during meiosis, which correlates with the first wave of destabilization of maternal mRNAs.

An enhanced subcortical signal has been reported for several proteins, including YBX2 [29], and DDX6 expression is detected in oocytes and early embryos [35]. The published images, however, do not have sufficient resolution to be compared with the data presented here. Interestingly, a recent report by Swetloff et al. [36] detected enhanced subcortical localization of DDX6 whereas the enhanced CPEB localization to the cortex was unclear. Our CPEB staining (Fig. 7B) shows stronger subcortical staining than the published data [36] but the overall pattern is similar; it is likely that the slightly stronger subcortical staining becomes more visible when using a wide dynamic range for image acquisition. The published DDX6 pattern [36] overlaps with the pattern for DDX6 we observe, and the slight differences

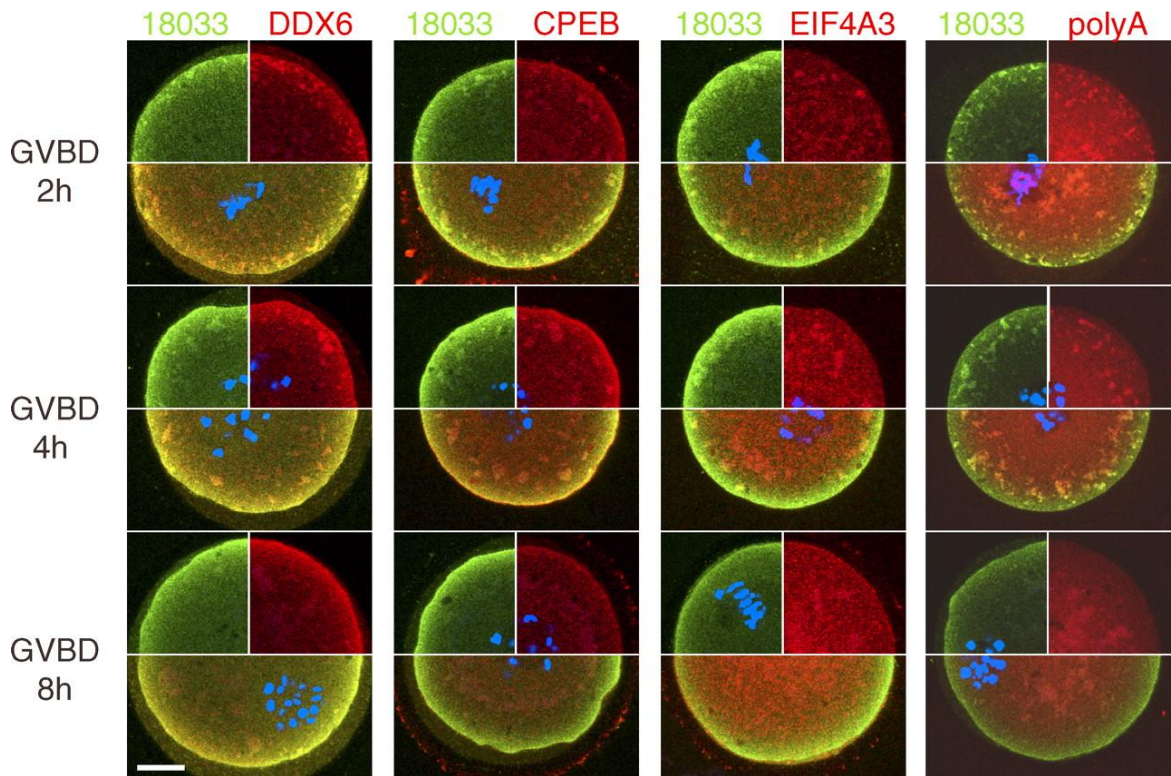


FIG. 8. Dynamics of SCRD during GVBD. Confocal images of oocytes undergoing GVBD were examined by immunofluorescent staining with 18033, DDX6, CPEB, and EIF4A3 antibodies and TAMRA-oligo(dT)₁₈ at 2, 4, and 8 h after release from the first meiotic block. Individual green- and red-colored stainings are shown in upper quadrants, DNA staining (DAPI) is shown in blue. The lower half of each oocyte shows a merged image where colocalization of the red and green signal yields yellow color. For each sample, at least five oocytes were examined, and representative images are shown. Bar = 20 μ m.

may be attributed to use of a different DDX6 antibody and different dynamic range used for image acquisition.

Interestingly, Swetloff et al. [36] also reported enhanced subcortical staining for LSM14A, another P-body component [10], which is a potential additional component of the RNP complexes reported here. Because the authors focused on analysis of granules formed upon overexpression of EGFP-DCP1A, they do not comment on the subcortical localization of endogenous LSM14A and DDX6.

Our results show that P-bodies are absent from growing oocytes to early embryo stages. This result contrasts with two other studies of P-body components in oocytes and early embryos. In one study, P-body-like structures were found in two-cell embryos [37]. However, these structures were observed following overexpression of AGO2-EGFP and DCP1A-DSRED and may not reflect the normal situation.

The majority of the data reported in Swetloff et al. [36] are based on overexpressed EGFP-DCP1A in GV oocytes [36], which might result in a nonphysiological formation of P-bodies. We observed that, in contrast to the transcript level, the DCP1A protein levels are low in the oocyte and sharply rise during meiotic maturation (Fig. 3) suggesting that *Dcp1a* encodes a dormant maternal mRNA. It should be noted the DCP1A signal in MII eggs in Figure 3 is partially saturated, and when the laser power was set so that a subsaturating signal is obtained in MII eggs, the DCP1A signal becomes barely detectable in GV oocytes. Dormancy of *Dcp1a* is further supported by RNA interference (RNAi)-mediated targeting of maternal *Dcp1a* mRNA and mutation analysis of *Dcp1a* 3'UTR (Ma et al., unpublished results). In addition, YFP-tagged miRNA-targeted mRNA shows a uniform cytoplasmic distribution in fully grown GV oocytes (Ma et al., unpublished results), further suggesting that P-bodies observed upon overexpression of EGFP-DCP1A are nonphysiological.

Thus, differences in behavior of endogenous and artificially expressed proteins likely account for the aforementioned inconsistencies.

The loss of P-bodies early in oocyte growth is the first case of which we are aware where P-bodies disappear from a mammalian cell under bona fide physiological conditions. Because the population of oocytes, which shows a correlation between oocyte size and the loss of P-bodies, was isolated from 12-day-old mice, the loss of P-bodies in the oocyte seems to occur during the transition between primary and secondary follicles. Although the mechanistic explanation for the loss of P-bodies is unknown, it could be related to the function of the miRNA pathway. As miRNA-mediated translational repression involves binding of TNRC6 to AGO proteins [38], the loss of AGO2 and 18033 colocalization at the beginning of the oocyte growth might reflect down-regulation of the miRNA pathway. In fact, results of experiments to be reported elsewhere indicate that miRNA-mediated mRNA repression is very inefficient in oocytes [39] and suggest that the meiotic failure observed in *Dicer1*^{-/-} oocytes [27, 40] is due to misregulation of genes controlled by endogenous small interfering RNAs (endo-siRNAs) [41, 42] and not miRNAs [27, 43]. Moreover, maternal depletion of *Dgcr8*, which inhibits miRNA biogenesis, but not endo-siRNA biogenesis, does not result in infertility [44]. The loss of P-bodies during oocyte growth may provide the molecular underpinnings for the aforementioned results.

We show that several proteins, including P-body components DDX6, 18033, and CPEB, form a subcortical RNP domain that contains untranslated maternal mRNAs. The SCRD might represent a spatial and temporal separation of the storage function, which in P-bodies is combined with mRNA degradation [5]. The SCRD structure changes during oocyte growth, the most prominent feature being the appearance of SCAs in fully grown SN GV oocytes. The appearance of SCAs is reminiscent of stress granules, but we did not find HuR in the SCRD, thus excluding the possibility that SCAs are stress granules.

We also tested a potential link between the SCRD and the SCMC complex. The SCMC complex, which is composed of OOEP (FLOPED), NLRP5 (MATER), Filia, and TLE6 proteins, localizes to the oocyte cortex and is required during early embryo cleavage [28]. The complex has not been associated with mRNA metabolism, although OOEP is a putative RNA-binding protein [31]. Maternal loss of Filia causes defects in spindle assembly and chromosomal segregation [45]. Oocytes lacking OOEP or NLRP5 do not form the SCMC but develop normally and can be fertilized. These data indicate that the SCMC is likely not essential for maternal mRNA metabolism and is distinct from the SCRD. This notion is supported by results of our immunocytochemical experiments. Although the staining of oocytes with NLRP5 antibody is much weaker, when compared to published results, we observed increased subcortical staining, which did not colocalize well with the SCRD and, particularly, with SCAs. Furthermore, SCMC localizes to the outer cortex of preimplantation embryos where it is excluded from cell-to-cell contact regions [28], a pattern not observed for SCRD components (data not shown). Thus, similar localization of SCMC and SCRD to the cortex rather reflects a common strategy of mouse oocytes to use the cortex for deposition of mRNAs and proteins of different functions. This proposal is further supported by subcortical localization reported for DNMT1o, an oocyte-specific isoform of DNMT1, which also localizes to the cortex [46] but is functionally unrelated to maternal mRNA metabolism.

The mechanism of the SCRD and SCAs formation remains unknown. The SCRD is not lost upon disruption of actin or tubulin cytoskeleton (Fig. 6), which also does not perturb the localization of YBX2 [22]. Unfortunately, the stability of proteins in the SCRD precluded attempts to disrupt the SCRD by RNAi. Analysis of the maternal YBX2 knockout also does not show disruption of the SCRD, suggesting that YBX2 is not an essential structural component of the SCRD (data not shown). This result is not surprising because YBX2 localization and cytoplasmic retention depends on its RNA-binding activity [22].

One of the components of the SCRD is DDX6 (Rck/p54), an ortholog of CGH-1 in *C. elegans*, Me31B in *Drosophila*, and Xp54 in *X. laevis*, that is implicated in control of maternal mRNAs in these organisms [32]. CGH-1 and its orthologs are found in a number of different RNA granules regulating mRNA stability and translation throughout the female germ cell development and in the soma [32]. The SCRD fits a model of the maternal mRNA stabilization and translational repression where CGH-1 has a conserved germline-specific role in mRNA repression and protection [17]. The subcortical localization of the SCRD perhaps denotes a suitable peripheral storage place in apparently nonpolarized mouse oocytes.

Our data offer new insights into how mRNA accumulation and assembly of mRNA decay machinery, two seemingly opposing tasks, are achieved. We propose a model in which DDX6, an unidentified 18033 antibody-interacting protein, and maternal mRNA bound by proteins such as YBX2, CPEB, and the EJC form the SCRD, a maternal mRNA storage domain, which matures into SCAs as an oocyte reaches its full developmental competence. Although growing mouse oocytes do not contain GCGs or P-bodies, the SCAs appear related to RNA storage granules observed in invertebrates [14, 15]. SCAs disperse during meiotic maturation and release maternal mRNAs, which become available for translation. While SCAs disperse, the amount of DCP1A increases and the first wave of maternal mRNA degradation begins. These data provide another example of diversity of mammalian RNA granules, which exhibit overlapping composition but different structures and functions.

Acknowledgments

We thank Jens Lykke-Andersen, Jurrien Dean, Witold Filipowicz, Marvin J. Fritzler, and Nahum Sonenberg for antibodies and Witold Filipowicz and Andrej Susor for useful discussions.

Footnotes

¹ Supported by the EMBO SDIG program, ME09039 grant, and the Purkynje Fellowship to P.S. and the NIH grant HD22681 to R.M.S.

Received October 20, 2009.

Revision received November 9, 2009.

Accepted December 23, 2009.

References

1. Brower PT, Gizang E, Boreen SM, Schultz RM. Biochemical studies of mammalian oogenesis: synthesis and stability of various classes of RNA during growth of the mouse oocyte in vitro. *Dev Biol* 1981; 86:373–383.
2. Richter JD. CPEB: a life in translation. *Trends Biochem Sci* 2007; 32: 279–285.
3. Anderson P, Kedersha N. RNA granules. *J Cell Biol* 2006; 172:803–808.
4. Eulalio A, Behm-Ansmant I, Izaurralde E. P bodies: at the crossroads of post-transcriptional pathways. *Nat Rev Mol Cell Biol* 2007; 8:9–22.
5. Parker R, Sheth U. P bodies and the control of mRNA translation and degradation. *Mol Cell* 2007; 25:635–646.
6. Bashkirov VI, Scherthan H, Solinger JA, Buerstedde JM, Heyer WD. A mouse cytoplasmic exoribonuclease (mXRN1p) with preference for G4 tetraplex substrates. *J Cell Biol* 1997; 136:761–773.
7. Ingelfinger D, Arndt-Jovin DJ, Luhrmann R, Achsel T. The human LSM1–7 proteins colocalize with the mRNA-degrading enzymes Dcp1/2 and Xrn1 in distinct cytoplasmic foci. *RNA* 2002; 8:1489–1501.
8. van Dijk E, Cougot N, Meyer S, Babajko S, Wahle E, Seraphin B. Human Dcp2: a catalytically active mRNA decapping enzyme located in specific cytoplasmic structures. *EMBO J* 2002; 21:6915–6924.

9. Eystathioy T, Chan EK, Tenenbaum SA, Keene JD, Griffith K, Fritzler MJ. A phosphorylated cytoplasmic autoantigen, GW182, associates with a unique population of human mRNAs within novel cytoplasmic speckles. *Mol Biol Cell* 2002; 13:1338–1351.
10. Yang WH, Yu JH, Gulick T, Bloch KD, Bloch DB. RNA-associated protein 55 (RAP55) localizes to mRNA processing bodies and stress granules. *RNA* 2006; 12:547–554.
11. Yu JH, Yang WH, Gulick T, Bloch KD, Bloch DB. Ge-1 is a central component of the mammalian cytoplasmic mRNA processing body. *RNA* 2005; 11:1795–1802.
12. Eulalio A, Behm-Ansmant I, Schweizer D, Izaurralde E. P-body formation is a consequence, not the cause, of RNA-mediated gene silencing. *Mol Cell Biol* 2007; 27:3970–3981.
13. Stalder L, Muhlemann O. Processing bodies are not required for mammalian nonsense-mediated mRNA decay. *RNA* 2009; 15:1265–1273.
14. Lin MD, Jiao X, Grima D, Newbury SF, Kiledjian M, Chou TB. Drosophila processing bodies in oogenesis. *Dev Biol* 2008; 322:276–288.
15. Noble SL, Allen BL, Goh LK, Nordick K, Evans TC. Maternal mRNAs are regulated by diverse P body-related mRNP granules during early *Caenorhabditis elegans* development. *J Cell Biol* 2008; 182:559–572.
16. Radford HE, Meijer HA, de Moor CH. Translational control by cytoplasmic polyadenylation in *Xenopus* oocytes. *Biochim Biophys Acta* 2008; 1779:217–229.
17. Rajyaguru P, Parker R. CGH-1 and the control of maternal mRNAs. *Trends Cell Biol* 2009; 19:24–28.
18. Standart N, Minshall N. Translational control in early development: CPEB, P-bodies and germinal granules. *Biochem Soc Trans* 2008; 36: 671–676.
19. Pepling ME, Wilhelm JE, O'Hara AL, Gephardt GW, Spradling AC. Mouse oocytes within germ cell cysts and primordial follicles contain a Balbiani body. *Proc Natl Acad Sci U S A* 2007; 104:187–192.
20. McLaren A. Primordial germ cells in the mouse. *Dev Biol* 2003; 262:1–15.
21. Svoboda P. RNA silencing in mammalian oocytes and early embryos. *Curr Top Microbiol Immunol* 2008; 320:225–256.
22. Yu J, Hecht NB, Schultz RM. Requirement for RNA-binding activity of MSY2 for cytoplasmic localization and retention in mouse oocytes. *Dev Biol* 2003; 255:249–262.
23. Grunwald D, Singer RH, Czaplinski K. Cell biology of mRNA decay. *Methods Enzymol* 2008; 448:553–577.
24. Bloch DB, Gulick T, Bloch KD, Yang WH. Processing body autoantibodies reconsidered. *RNA* 2006; 12:707–709.
25. Inoue A, Nakajima R, Nagata M, Aoki F. Contribution of the oocyte nucleus and cytoplasm to the determination of meiotic and developmental competence in mice. *Hum Reprod* 2008; 23:1377–1384.
26. Zuccotti M, Piccinelli A, Giorgi Rossi P, Garagna S, Redi CA. Chromatin organization during mouse oocyte growth. *Mol Reprod Dev* 1995; 41: 479–485.
27. Tang F, Kaneda M, O'Carroll D, Hajkova P, Barton SC, Sun YA, Lee C, Tarakhovskiy A, Lao K, Surani MA. Maternal microRNAs are essential for mouse zygotic development. *Genes Dev* 2007; 21:644–648.
28. Li L, Baibakov B, Dean J. A subcortical maternal complex essential for preimplantation mouse embryogenesis. *Dev Cell* 2008; 15:416–425.
29. Yu J, Hecht NB, Schultz RM. Expression of MSY2 in mouse oocytes and preimplantation embryos. *Biol Reprod* 2001; 65:1260–1270.
30. Yu J, Deng M, Medvedev S, Yang J, Hecht NB, Schultz RM. Transgenic RNAi-mediated reduction of MSY2 in mouse oocytes results in reduced fertility. *Dev Biol* 2004; 268:195–206.

31. Herr JC, Chertihin O, Digilio L, Jha KN, Vemuganti S, Flickinger CJ. Distribution of RNA binding protein MOEP19 in the oocyte cortex and early embryo indicates pre-patterning related to blastomere polarity and trophectoderm specification. *Dev Biol* 2008; 314:300–316.
32. Weston A, Sommerville J. Xp54 and related (DDX6-like) RNA helicases: roles in messenger RNP assembly, translation regulation and RNA degradation. *Nucleic Acids Res* 2006; 34:3082–3094.
33. Gebauer F, Richter JD. Mouse cytoplasmic polyadenylation element binding protein: an evolutionarily conserved protein that interacts with the cytoplasmic polyadenylation elements of c-mos mRNA. *Proc Natl Acad Sci U S A* 1996; 93:14602–14607.
34. Chan CC, Dostie J, Diem MD, Feng W, Mann M, Rappsilber J, Dreyfuss G. eIF4A3 is a novel component of the exon junction complex. *RNA* 2004; 10:200–209.
35. Matsumoto K, Kwon OY, Kim H, Akao Y. Expression of rck/p54, a DEAD-box RNA helicase, in gametogenesis and early embryogenesis of mice. *Dev Dyn* 2005; 233:1149–1156.
36. Swetloff A, Conne B, Huarte J, Pitetti JL, Nef S, Vassalli JD. Dcp1-bodies in mouse oocytes. *Mol Biol Cell* 2009; 20:4951–4961.
37. Lykke-Andersen K, Gilchrist MJ, Grabarek JB, Das P, Miska E, Zernicka-Goetz M. Maternal Argonaute 2 is essential for early mouse development at the maternal-zygotic transition. *Mol Biol Cell* 2008; 19:4383–4392.
38. Eulalio A, Huntzinger E, Izaurralde E. GW182 interaction with Argonaute is essential for miRNA-mediated translational repression and mRNA decay. *Nat Struct Mol Biol* 2008; 15:346–353.
39. Ma J, Flemr M, Stein P, Berninger P, Malik R, Zavolan M, Svoboda P, Schultz RM. MicroRNA activity is suppressed in mouse oocytes. *Curr Biol* 2010; 20:265–270.
40. Murchison EP, Stein P, Xuan Z, Pan H, Zhang MQ, Schultz RM, Hannon GJ. Critical roles for Dicer in the female germline. *Genes Dev* 2007; 21: 682–693.
41. Tam OH, Aravin AA, Stein P, Girard A, Murchison EP, Cheloufi S, Hodges E, Anger M, Sachidanandam R, Schultz RM, Hannon GJ. Pseudogene-derived small interfering RNAs regulate gene expression in mouse oocytes. *Nature* 2008; 453:534–538.
42. Watanabe T, Totoki Y, Toyoda A, Kaneda M, Kuramochi-Miyagawa S, Obata Y, Chiba H, Kohara Y, Kono T, Nakano T, Surani MA, Sakaki Y, Sasaki H. Endogenous siRNAs from naturally formed dsRNAs regulate transcripts in mouse oocytes. *Nature* 2008; 453:539–543.
43. Kaneda M, Tang F, O’Carroll D, Lao K, Surani MA. Essential role for Argonaute2 protein in mouse oogenesis. *Epigenetics Chromatin* 2009; 2:9.
44. Suh N, Baehner L, Moltzahn F, Melton C, Shenoy A, Chen J, Blelloch R. MicroRNA function is globally suppressed in mouse oocytes and early embryos. *Curr Biol* 2010; 20:271–277.
45. Zheng P, Dean J. Role of Filia, a maternal effect gene, in maintaining euploidy during cleavage-stage mouse embryogenesis. *Proc Natl Acad Sci U S A* 2009; 106:7473–7478.
46. Doherty AS, Bartolomei MS, Schultz RM. Regulation of stage-specific nuclear translocation of Dnmt1o during preimplantation mouse development. *Dev Biol* 2002; 242:255–266.

SUPPLEMENT 3

Jun Ma, Matyas Flemr, Hynek Strnad, Jing Chen, Petr Svoboda
and Richard M. Schultz

Maternally-recruited DCP1A and DCP2 regulate mRNA degradation during
oocyte maturation and genome activation in mouse

(under revision for submission to *Development*.)

My contribution to this work:

I performed the immunofluorescence staining experiment that initiated this work. I generated the bioinformatic data for Fig.3, Fig.4A and B, Fig.5 and Tab.1.

Maternally-recruited DCP1A and DCP2 regulate mRNA degradation during oocyte maturation and genome activation in mouse

Jun Ma¹, Matyas Flemr², Hynek Strnad², Jing Chen³, Petr Svoboda², and Richard M. Schultz¹

¹ Department of Biology, University of Pennsylvania Philadelphia, PA 19104

² Institute of Molecular Genetics AS CR, Videnska 1083, 142 20 Prague 4, Czech Republic

³ Center for Reproductive Sciences, University of California at San Francisco, San Francisco, California 94143, USA.

Address all correspondence to:

Richard Schultz
Department of Biology
University of Pennsylvania
433 South University Avenue
Philadelphia, PA 19104-6018
Tel. # 215-898-7869
Email: rschultz@sas.upenn.edu

or

Petr Svoboda
Institute of Molecular Genetics,
Academy of Sciences of the Czech Republic
Videnska 1083, 142 20 Prague 4, Czech Republic
Tel. # +420 241063147
Email: Petr.Svoboda@img.cas.cz

Summary

The oocyte-to-zygote transition entails transforming a highly differentiated oocyte into totipotent blastomeres and represents one of the earliest obstacles that must be successfully hurdled for continued development. Degradation of maternal mRNAs, which likely lies at the heart of this transition, is characterized by a transition from mRNA stability to instability during oocyte maturation. Although phosphorylation of the oocyte-specific RNA-binding protein MSY2 during maturation is implicated in making maternal mRNAs more susceptible to degradation, mechanisms underlying mRNA degradation during oocyte maturation remain poorly understood. We report that DCP1A and DCP2, proteins responsible for decapping mRNA, are encoded by maternal mRNAs recruited for translation during maturation via cytoplasmic polyadenylation elements located in their 3' UTRs. Moreover, inhibiting accumulation of DCP1A and DCP2 by RNAi or morpholinos not only decreases degradation of mRNAs during meiotic maturation but also transcription of the zygotic genome. These results provide new mechanistic insights into the transition from mRNA stability to instability during meiotic maturation and highlight the importance of maternal mRNA degradation for the successful execution of the oocyte-to-zygote transition.

Introduction

The balance between mRNA synthesis and mRNA turnover determines steady-state mRNA levels. Regulation of mRNA degradation is gaining increased attention because the process is highly regulated and therefore has significant impact on the overall pattern of gene expression (Coller and Parker, 2005). In eukaryotic cells, functional mRNAs have a 5' cap structure and a 3' poly(A) tail that control translation and mRNA stability. mRNA degradation usually involves deadenylation of the 3' poly(A) tail in which the CCR4-NOT complex plays a central role (Tucker et al., 2001); mRNAs with very short poly(A) tails are degraded either from the 5' or 3' end (Coller and Parker, 2004).

Removal of the 5'-monomethyl guanosine cap (decapping) is the critical step in the 5'-3' mRNA degradation pathway. Decapping exposes mRNAs to exonucleases (e.g., XRN1) that rapidly degrade the mRNA from the 5' end. The decapping complex was first identified in yeast in which Dcp2p possesses catalytic activity and Dcp1p is a regulatory unit that stimulates Dcp2p decapping activity (Beelman et al., 1996; Floor et al., 2010; LaGrandeur and Parker, 1998). The mammalian orthologs of Dcp2 and Dcp1 are Dcp2 and Dcp1a/Dcp1b (Lykke-Andersen, 2002; van Dijk et al., 2002; Wang et al., 2002). Although mammalian DCP2 possesses decapping activity, the ability of mammalian DCP1A/B to stimulate directly the decapping activity of DCP2 has not been demonstrated (Cougot et al., 2004; Lykke-Andersen, 2002; van Dijk et al., 2002). Several other proteins that are present in the decapping complex also modulate decapping activities and have mammalian orthologs, including the Lsm1-7 complex, Dhh1 (also known in mammals as Ddx6/Rck/p54), Edc3 and Edc4 (Coller and Parker, 2005; Fenger-

Gron et al., 2005; Ingelfinger et al., 2002; Kshirsagar and Parker, 2004).

Stockpiles of mRNAs are synthesized and accumulated during oocyte growth and serve as the maternal contribution that supports early embryo development before zygotic genome activation. Maternal mRNAs in mouse oocytes are unusually stable during the growth phase, which takes about 2.5 weeks, with an average half-life of ~10-14 days as compared to hours or minutes in somatic cells (Bachvarova et al., 1985; Bachvarova and DeLeon, 1980; Brower et al., 1981; Jahn et al., 1976). The oocyte-to-zygote transition entails coordinate removal of the maternal transcriptome and its replacement with a zygotic transcriptome. Oocyte maturation, i.e., resumption of meiosis, triggers a transition from mRNA stability to instability in which many maternal mRNAs are extensively degraded (Bachvarova and DeLeon, 1980; Su et al., 2007). There is growing consensus that degradation of maternal mRNA is essential for the oocyte-to-zygote transition (DeRenzo and Seydoux, 2004; Stitzel and Seydoux, 2007) that entails transforming a highly differentiated oocyte into totipotent blastomeres. Maternal mRNA degradation accelerates loss of oocyte identity and facilitates a totipotent identity of blastomeres.

The transition to mRNA instability is facilitated by MSY2, an abundant germ-cell specific RNA-binding protein that mediates global mRNA stability in mouse oocytes (Medvedev et al., 2011; Medvedev et al., 2008; Yu et al., 2004). During oocyte maturation, MSY2 is phosphorylated by CDC2A, a consequence being that maternal mRNAs become more accessible to the oocyte's mRNA decay machinery (Medvedev et al., 2008). It is unclear, however, whether the mRNA decay machinery becomes activated during meiotic

maturation and how it targets maternal transcripts.

While studying the role of P-bodies in mRNA degradation in mouse oocytes, we noted that the abundance of DCP1A protein substantially increases during oocyte maturation (Flemr et al., 2010). This finding prompted us to examine how post-transcriptional control of the mRNA decay machinery regulates the transition from maternal mRNA stability to instability. We report that Dcp1a and Dcp2 are maternal mRNAs that are recruited during maturation via cytoplasmic polyadenylation elements (CPE) (Mendez and Richter, 2001; Pique et al., 2008; Radford et al., 2008), thus providing a mechanism for induction of maternal mRNA degradation. Inhibiting the maturation-associated increase in DCP1A and DCP2 protein not only prevents degradation of a large population of maternal mRNAs but also affects activation of the embryonic genome during the 2-cell stage.

Material and Methods

Mouse oocyte/egg/embryo collection, cell culture, and microinjection

Full-grown, germinal vesicle (GV)-intact oocytes, MII eggs, fertilized eggs and 2-cell embryos were collected as previously described (Schultz et al., 1983). GV oocytes were cultured in CZB medium containing 2.5 μ M milrinone (Sigma) to inhibit GV breakdown; MII eggs were cultured in CZB medium (Chatot et al., 1989) and fertilized eggs in KSOM medium (Erbach et al., 1994). MI eggs were collected 8 h after transferring oocytes to milrinone-free CZB medium and 2-cell embryos were isolated by flushing oviducts of super-ovulated and mated mice 42-44 h post-hCG injection. NIH 3T3 cells were grown in Dulbecco Modified Eagle medium plus 10% fetal bovine serum in an atmosphere of 5% CO₂ in air at 37° C. All animal experiments were approved by the Institutional Animal Use and Care

Committee and were consistent with National Institutes of Health guidelines.

GV oocytes were microinjected with ~5 μ l of either siRNAs or morpholinos in bicarbonate-free Whitten's medium (Whitten, 1971) supplemented with 10 mM Hepes, 0.01% polyvinylalcohol and 2.5 μ M milrinone as previously described (Kurasawa et al., 1989). The Dcp1a siRNA was 25 μ M and that of Dcp2 was 50 μ M. When morpholinos were injected, the concentration was 1 mM.

DNA constructs

To generate a luciferase reporter with a Dcp1a or Dcp2 3' UTR, firefly luciferase coding sequence was excised from pGL4.10 (Promega) by a Xho I and Xba I double digestion and inserted into pIVT vector containing T7 and T3 promoters in tandem at the 5' flanking region, followed by a Xenopus β -globin 5' UTR and a multiple cloning site, (plasmid map is available upon request) to generate pIVT-Luc. The last 0.5 kb Dcp1a 3' UTR with a poly(A) site was amplified using 5'-TACTCTAGAAAGGCCACTCACGAG GAGAGTT-3' and 5'-CGTGAATTCTAGG TGCTAAACTTGGTT-3'; Dcp2 3' UTR (NM_027490.1) was amplified by PCR using primers 5'-TACTCTAGATGCTTGGGCA CAGTTACTGCT-3' and 5'-CGTGAATT CTTTATTTGGTTGTCTTCACATACAGC-3'. Amplified Dcp1a or Dcp2 3' UTRs were digested by Xba I and EcoR I and inserted downstream of the coding sequence of the pIVT-Luc vector. pIVT-Luc with mouse Ccnb1 3' UTR was a kind gift from Dr. Shin Murai (Toho University, Japan).

To generate luciferase reporter/Dcp1a or Dcp2 3' UTR with mutated CPEs, pairs of oligonucleotides were synthesized with the desired mutated sequences, annealed, extended by Klenow 3'-5' exo- polymerase, digested by EcoR I and Xba I, and inserted into EcoR I/Xba I digested pIVT-Luc.

The following oligonucleotides were used in the construction of these pIVT/Dcp1a 3' UTR variants: 5'-GGCTCTAGAAGCATT TTCATCCTAAATTTTATATGTTTGCAA ATATATTTTTTTAA-3' & 5'-ACTGAATT CCTAAACTTGGTTTTGAAATTTTATT AAAAAATATATTTGCAAACAT-3' were used to generate pIVT-Luc with shortened version of wild-type Dcp1a 3' UTR; 5'-GGCTCTAGAAGCATTTCATCCTAAA TTTTATATGTTTGCAAATATATTTTTT AA-3' & 5'-ACTGAATTCCTAAACTTGG TTTTGAAATTTCTTAAAAAATATAT TTGCAAACAT-3' were used to generate pIVT-Luc /Dcp1a 3' UTR/ mutated polyA signal(AAUAAA to AAGAAA mutation); 5'-ACTGAATTCCTAAACTTGG TTTTGAAATTTTATTAATAAAAAATATA TTTGCAAACAT-3' & 5'-GGCTCTAGAAG CATTGGCATCCTAAATTTTATATGTT TGCAAATATATTTTTTTAA-3' were used to generate pIVT-Luc /Dcp1a 3' UTR/mutated CPE1 (UUUUUCAU to UUUGGCAU mutation); 5'-ACTGAATTC TAAACTTGGTTTTGAAATTTTATTAA AAAAATATATTTGCAAACAT-3' & 5'-GGCTCTAGAAGCATTTCATCCTAAA TTGGATATGTTTGCAAATATATTTTTT TAA-3' were used to generate pIVT-Luc /Dcp1a 3' UTR/mutated CPE2(UUUUUUA to UUUGGAUA); 5'-GCTCTAGAAGCATT TTCATCCTAAATTTTATATGTTTGCAA ATATATTTGGGTAA-3' & 5'-ACTGAATT CCTAAACTTGGTTTTGAAATTTTATT ACCCAAATATATTTGCAAACAT-3' were used to generate pIVT-Luc /Dcp1a 3' UTR/mutated CPE3(UUUUUUUAU to UUUGGGUAAU); 5'-ACTGAATTCCTAA AACTTGGTTTTGAAATTTTATTAATAA AATATATTTGCAAACAT-3' & 5'-GGCTC TAGAAGCATTGGCATCCTAAATTGG ATATGTTTGCAAATATATTTTTTTAA-3' were used to generate pIVT-Luc /Dcp1a 3' UTR/mutated CPE1+2; 5'-ACTGAATTC TAAACTTGGTTTTGAAATTTTATTAC CCAAATATATTTGCAAACAT-3' & 5'-GG CTCTAGAAGCATTTCATCCTAAATT GGATATGTTTGCAAATATATTTGGTA

A-3' were used to generate pIVT-Luc/Dcp1a 3' UTR/mutated CPE2+3; 5'-ACTGAATT CCTAAACTTGGTTTTGAAATTTTATT ACCCAAATATATTTGCAAACAT-3' & 5'-GGCTCTAGAAGCATTGGCATCCTAA ATTTTATATGTTTGCAAATATATTTGG GTAA-3' were used to generate pIVT-Luc/Dcp1a 3' UTR/mutated CPE1+3; 5'-ACTGAATTCCTAAACTTGGTTTTGAA ATTTTATTACCAAATATATTTGCAA ACAT-3' & 5'-GGCTCTAGAAGCATTGGC ATCCTAAATTGGATATGTTTGCAAATA TATTTGGGTAA-3' were used to generate pIVT-Luc/Dcp1a 3' UTR / mutated CPE1+2 +3.

The following oligonucleotides were used in the construction of these pIVT/Dcp2 3' UTR variants. 5'-AGCTCTAGAGTTTAGA CTTCTTGAAACTTTTTTCTGTTTTCA GTAGAGAACTTCTGTTTATGCTGTA- 3' & 5'-TCCGAATTCTTCTCATTATCA TCAATTTTTATTTGGTTGTCTTCACATA CAGCATAAACAGAAGTTT-3' were used to generate pIVT-Luc with shortened version of wild-type Dcp2 3' UTR; 5'-AGCTC TAGAGTTTAGACTTCTTGAAACTTTTT TTCTGTTTTCAGTAGAGAACTTCTG TTTATGCTGTA-3' & 5'-TCCGAATTCTT CTCATTTATCATCAATTTTTCTTTGGTT GTCTTCACATACAGCATAAACAGAAG TTT-3' were used to generate pIVT-Luc/Dcp2 3' UTR/ mutated polyA signal(AAUAAA to AAGAAA mutation); 5'-TCCGAATTCTTCTCATTATCATCAAT TTTTATTTGGTTGTCTTCACATACAGC ATAAACAGAAGTTT-3' & 5'-AGCTCTAG AGTTTAGACTTCTTGAAACTTGGGTTC CTGTTTTCAGTAGAGAACTTCTGTTT ATGCTGTA-3' were used to generate pIVT-Luc/Dcp2 3' UTR/mutated CPE1 (UUUUU UU to UUUGGUU mutation); 5'-AGCT CTAGAGTTTAGACTTCTTGAAACTTTTT TTCTGTTTTTTCAGTAGAGAACTTCT GTGGATGCTGTA-3' & 5'-TCCGAATTCT TCTCATTATCATCAATTTTTATTTGGT TGTCTTCACATACAGCATCCACAGAA GTTT-3' were used to generate pIVT-

Luc/Dcp2 3' UTR/mutated CPE2(UUUUAU to UGGAU); 5'-TCCGAATTCTTCTCATT TATCATCAATTTTTATTTGGTTGTCTTC ACATACAGCATCCACAGAAGTTT-3' & 5'-AGCTCTAGAGTTTAGACTTCTTGAA ACTTGGGTTCTGTGTTTTTCAGTAGAGAA ACTTCTGTGGATGCTGTA-3' were used to generate pIVT-Luc/Dcp2 3' UTR/mutated CPE1+2.

In vitro transcription

All above generated pIVT-Luc/Dcp1a or Dcp2 3' UTR variants were verified by DNA sequencing and then linearized by EcoR I digestion. Capped cRNAs were made using in vitro transcription with T7 mMESSAGE Mmachine (Ambion) according to the manufacturer's instruction. Following in vitro transcription, template DNAs were digested by adding RNase-free DNase and synthesized cRNA was purified by MEGAclear kit (Ambion), precipitated and re-dissolved in RNase-free water. A single mRNA band of the expected size was observed for each RNA sample on 1% formaldehyde denaturing agarose gel.

For microinjection controls, Renilla luciferase based vector phRL-SV40 (Promega) was linearized by Not I, in vitro transcribed by T7, and polyadenylated by Poly(A) tailing kit (Ambion) following the manufacturer's instruction. ~150bp polyA tail was added to the 3' terminal of synthesized Renilla luciferase mRNA after polyadenylation as estimated by electrophoresis on 1% denaturing agarose gel.

Immunocytochemistry and immunoblotting

Oocyte, egg or embryo samples were fixed in 2.5% paraformaldehyde for 40 min at room temperature. The cells were then permeabilized for 15 min in PBS containing 0.2% Triton X-100, blocked in PBS containing 0.2% IgG-free BSA and 0.01%

Tween-20 for 30min (blocking solution), and then incubated with the primary antibody for 1 h at room temperature. The following antibodies/antisera were used at the following dilutions: rabbit anti-DCP1A antisera (a kind gift from Jens Lykke-Anderson, University of Colorado) at 1:150; rabbit anti-DCP2 (kindly provided by Dr. Megerditch Kiledjian, Rutgers University) at 1:150; rabbit anti-tri-methyl-Histone H3 (lys4) (H3K4me3, Cell Signaling) was used at 1:300 dilution. After four 15-min washes in blocking medium, samples were incubated for 1 h with the appropriate cy5-conjugated secondary antibody (Jackson ImmunoResearch) diluted 1:100 in blocking solution. After an additional three 15-min washes in blocking solution, the samples were mounted in the Vectashield solution containing DAPI (Vector Laboratories). Images were captured by a Leica TCS SP laser-scanning confocal microscope. For each experiment, all samples were processed in parallel and the intensity of fluorescence was quantified using NIH Image J software. Antibody specificity for DCP1A and DCP2 was verified by immunofluorescence (Fig. 3A).

For immunoblotting, equal numbers of GV oocytes, MI eggs, MII eggs, fertilized eggs, and 2-cell embryos were lysed in SDS loading buffer (Laemmli, 1970), run in a 10% SDS-PAGE and transferred to PVDF membrane (Amersham). The following antibodies were used: rabbit anti-DCP1A antisera (1:3,000 dilution); rabbit anti-DCP2 antisera (1:2,000 dilution). Immunodetection was performed using horseradish peroxidase-conjugated secondary antibodies and ECL Advance reagents (Amersham) according to the manufacturer's instructions. As a loading control, membranes were stripped and re-probed with a mouse anti β -tubulin (TUBB) antibody (Sigma) at 1:20,000 dilution.

RNA isolation and quantitative real-time PCR (qPCR)

Total RNA was isolated from 20~50 oocytes/eggs/embryos using an RNAqueous-Micro kit (Ambion) and reverse-transcribed with Superscript II reverse transcriptase (Invitrogen) using random hexamers as primers. The cDNA was quantified by qPCR using an ABI Prism 7000 thermocycler (Applied Biosystems). The ABI TaqMan Assay-on-Demand probe/primer sets used were Mm00460131_m1 for Dcp1a; Mm01264059_m1 for Dcp2; Mm00510343_m1* for Ppil3; Mm00457212_m1* for Upp1; Mm01300991_g1 for Rpl10a; Mm02601635_g1* for Rpl28; Mm04213524_gH for Rpl18a; and Mm01198491_g1* for Rpl6. PCR conditions were 40 cycles of 95°C for 15 sec, and 60°C for 60 sec. Each sample was analyzed in three independent samples except for the experiments assaying for Ppil3 and Upp1 transcripts, which were performed on two independent samples. Prior to RNA isolation, each sample was spiked with 2.5 ng of Gfp cRNA and quantification was normalized to the spiked Gfp cRNA using the comparative Ct method (ABI Prism 7700 Sequence Detection System).

Luciferase reporter assay

Full-grown GV oocytes were microinjected with ~5 pl of the mixture of pIVT-firefly Luc cRNA with Dcp1a or Dcp2 3' UTR variants (0.5 µg/µl) and control Renilla luciferase cRNA (0.075 µg/µl). Injected oocytes were transferred to milrinone-free medium and matured in vitro for 18 h. Controls were injected GV oocytes cultured for 18 h in CZB containing 2.5 µM milrinone. Luciferase activity was assayed by lysing oocytes/eggs in 1x passive lysis buffer and analyzed using a dual-luciferase reporter assay system (Promega) according to the manufacturer's instructions. For signal normalization, firefly/Renilla luciferase activity readout from non-injected oocytes/eggs was subtracted as background and firefly

luciferase activity was then normalized to that of the co-injected Renilla luciferase reporter.

siRNA mediated knockdown of Dcp1a and Dcp2 and microarray analysis

Full-grown GV oocytes were injected with Dcp1a siRNA (Dharmacon, On-TARGETplus SMARTpool, L-065144-01) or Dcp2 siRNA (Dharmacon, On-TARGETplus SMARTpool L-040353-01) as described above. Dcp1a&Dcp2 double knockdown were achieved by injecting a mixture of the above siRNAs. Microinjected oocytes were cultured in CZB with milrinone for 20 h and then transferred to milrinone-free medium and allowed to mature to MII for 18 h and total RNA extracted from 30 eggs using a Pico-Pure RNA Isolation kit (Acturus) and amplified for microarray analysis as previously described (Pan et al., 2005). Microarray analyses were performed on three independent samples obtained from Dcp1a siRNA-injected, Dcp2 siRNA-injected, Dcp1a&Dcp2 siRNAs-injected, and scrambled siRNA-injected control samples. Samples were hybridized to Affymetrix MOE430 2.0 GeneChips and processed according to Affymetrix instructions. Raw microarray data were analyzed as previously described (Pan et al., 2005) and were deposited in the GeneExpression Omnibus database (GSE27049).

Inhibition of maturation-associated increase in DCP1A and DCP2 by morpholinos

Full-grown GV oocytes were microinjected with ~ 5 pl of 1 mM Dcp1a morpholino or Dcp2 morpholino (GeneTools) or a mixture of Dcp1a&Dcp2 morpholino in bicarbonate-free Whitten's medium supplemented with 10mM Hepes, 0.01% polyvinylalcohol and 2.5 mM milrinone as previously described (Kurasawa et al., 1989). A morpholino with a scrambled sequence served as the control. Following microinjection, oocytes were

cultured in CZB medium with 2.5 mM milrinone for 3 h before in vitro maturation to MII in CZB medium without milrinone. The MII eggs were activated with 5 mM SrCl₂ in mCZB containing 2mM EGTA and 5 µg/ml cytochalasin B for 6 h (Kishigami and Wakayama, 2007) and then cultured in KSOM at 37° C in 5% CO₂ in air.

Global transcription assay

Global transcription was assayed by Click-iT® RNA Imaging Kit (Invitrogen) according to the manufacturer's instruction. Briefly, 2-cell embryos were cultured with 2 mM 5-ethynyl uridine (EU) in CZB medium for 1 h before fixation in 3.7% paraformaldehyde for 1 h at room temperature. After washing and permeabilization, incorporated EU was detected using the Click-iT® detection molecule (Invitrogen) and visualized by confocal microscopy.

Results and Discussion

DCP1A and DCP2 are encoded by dormant maternal mRNAs

First, we used immunocytochemistry to examine expression of DCP1A and DCP2 during oocyte maturation (oocytes apparently do not express Dcp1b (Pan et al., 2005; Wang et al., 2004; Zeng et al., 2004)). In addition to accumulation of DCP1A during oocyte maturation, consistent with our previous report (Flemer et al., 2010) and a recent report that Dcp1a mRNA is mobilized during maturation (Chen et al., 2011), the amount of DCP2 also markedly increased (Fig. 1A). Immunocytochemistry results were confirmed by western blot analysis of oocytes and early embryos (Fig. 1B). Although DCP1A and DCP2 were barely detectable in full-grown oocytes their amounts increased dramatically during meiotic maturation. Interestingly, an increase in the amount of DCP2 was observed before DCP1A, with DCP2 being readily detected

by MI, whereas the bulk of DCP1A accumulation occurred after meiosis I. The delayed appearance of DCP1A suggests that the majority of the decapping complex forms after meiosis I, further suggesting that the bulk of the decapping-dependent mRNA degradation occurs relatively late during meiotic maturation.

It should be noted that DCP1A showed a reduced electrophoretic mobility in MII when compared to GV-intact oocytes and later stages (Fig. 1B). In contrast to a previous report that detected a maturation-associated electrophoretic shift in DCP1A following injection of a cRNA encoding Egfp-hDcp1a but did not attribute the shift to phosphorylation (Swetloff et al., 2009), we find that the shift was apparently due to phosphorylation because phosphatase treatment converted the slower migrating form to the faster form (Fig. 1C). The responsible kinase(s), sites of phosphorylation and role of DCP1A phosphorylation in degradation of maternal mRNAs in the context of other published data (Blumenthal et al., 2009; Dephoure et al., 2008; LaGrandeur and Parker, 1998; Swetloff et al., 2009; Zeng et al., 2004; Zeng and Schultz, 2005) are currently under investigation and will be published elsewhere.

In contrast to the protein levels, the relative amount of Dcp1a and Dcp2 transcripts were little changed during the transition of full-grown oocytes to 1-cell embryos, but were negligible in 2-cell and 8-cell embryos (Fig. 1D). This expression pattern is also observed by microarray analyses which, in addition, showed that neither Dcp1a nor Dcp2 becomes expressed during zygotic genome activation (Wang et al., 2004; Zeng et al., 2004; Zeng and Schultz, 2005). These data imply that maternally recruited DCP1A and DCP2 function not only during meiotic maturation but are also the source of decapping activity

in the preimplantation embryo, because the maternal mRNAs are degraded and not replaced by zygotic transcripts during this period of time. Dormancy of Dcp1a and Dcp2 transcripts provides a simple mechanism for switching from an environment that fosters mRNA stability to one that promotes mRNA degradation. Minimal levels of DCP1A and DCP2 would presumably enhance mRNA stability during oocyte growth, perhaps even facilitating accumulation of dormant maternal mRNAs,

which are deadenylated without being degraded. The switch to mRNA instability during meiotic maturation also involves MSY2, which stabilizes mRNAs before resumption of meiosis, but whose phosphorylation during maturation makes maternal mRNAs more accessible to the mRNA decay machinery (Medvedev et al., 2011; Medvedev et al., 2008; Yu et al., 2004).

3' UTR elements drive Dcp1a and Dcp2 mRNA recruitment

Recruitment of dormant maternal mRNAs is typically driven by 3' UTR cis elements near the AAUAAA polyadenylation signal sequence (Mendez and Richter, 2001; Pique et al., 2008). To confirm that Dcp1a and Dcp2 encode classic dormant maternal mRNAs, we first verified that 3'UTRs of Dcp1a and Dcp2 transcripts regulate recruitment during maturation by injecting oocytes with a cRNA composed of the terminal 0.5 kb of the Dcp1a or Dcp2 3' UTR fused downstream of firefly luciferase coding sequence (Fig. 2A). Injected oocytes were then matured in vitro and the MII eggs

Figure 1

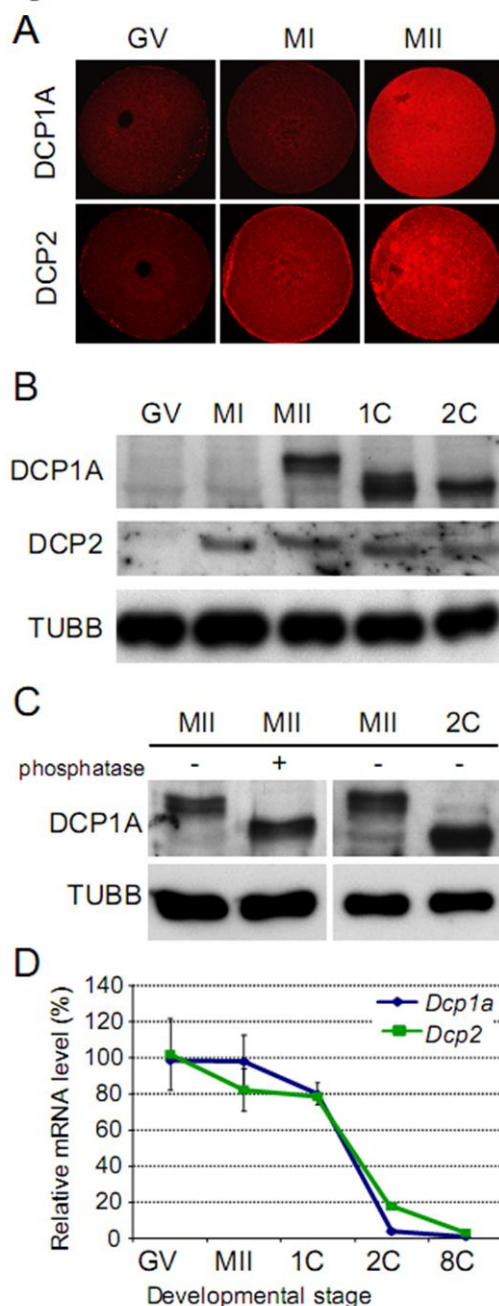


Figure 1. Maturation-associated increase of DCP1A and DCP2 protein and relative transcript abundance. (A) Immunofluorescent analysis of decapping complex components DCP1A and DCP2 in full-grown oocytes (GV), metaphase I eggs (MI) and metaphase II eggs (MII). (B) Immunoblot analysis of decapping complex components DCP1A and DCP2 during oocyte maturation and early embryonic development. The blot was stripped and re-probed with an anti- β -tubulin (TUBB) antibody as a loading control. The experiment was conducted two times and similar results were obtained in each case. (C) Phosphatase treatment of DCP1A in MII eggs. An MII egg extract was incubated with (+) or without (-) lambda protein phosphatase. As a control, an MII egg or 2C embryo lysate without phosphatase treatment was run in parallel. The experiment was reproduced three times, and a representative image is shown. (D) Temporal expression profile of Dcp1a and Dcp2 transcripts during oocyte maturation and pre-implantation embryogenesis. Relative abundance of Dcp1a and Dcp2 transcripts was determined by qPCR. GV, GV-intact oocyte; MII, MII egg; 1C, 1-cell embryo; 2C, 2-cell embryo; 8C, 8-cell embryo. The experiment was performed three times and the data are expressed as mean \pm SEM.

assayed for luciferase activity. Control oocytes were injected with the cRNA but cultured in the presence of milrinone, a phosphodiesterase inhibitor, to prevent spontaneous maturation (Wiersma et al., 1998). Each cRNA was recruited during maturation as evidenced by the large increase in luciferase activity following maturation (Fig. 2A). This increase was even significantly higher than that directed by the Cyclin B1 (*Ccnb1*) 3' UTR, a maternal mRNA known to be recruited during maturation (Fig. 2A) (Tay et al., 2000).

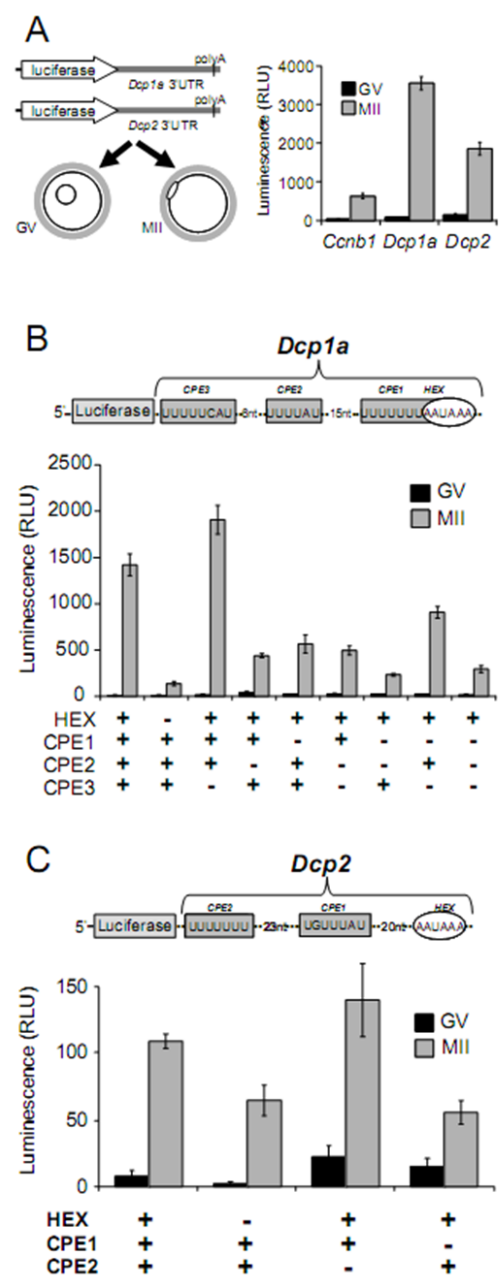
Different 3'UTR sequence motifs, including cytoplasmic polyadenylation elements (CPEs), Musashi/polyadenylation response elements (PREs), Pumilio-binding elements (PBEs) and DAZL-binding sequences regulate translation of mRNAs (Chen et al., 2011; Nakahata et al., 2003; Padmanabhan and Richter, 2006; Sheets et al., 1994). The terminal 3' 0.5 kb of *Dcp1a* and *Dcp2* 3' UTR contains three putative CPEs for *Dcp1a* and two putative CPEs for *Dcp2* (Fig. 2B and C). To identify which putative CPE/CPEs are functional in vivo, all putative CPEs were mutated and Luc reporter cRNAs containing mutated CPE/CPEs were injected into oocytes and tested for luciferase

Figure 2. Functional analysis of 3' UTR of *Dcp1a* and *Dcp2* mRNA. (A) Schematic representation of *Dcp1a* and *Dcp2* mRNA and luciferase reporter construct (upper panel). Luc reporter cRNAs with the terminal 0.5 kb of *Dcp1a* or *Dcp2* 3' UTRs were injected into GV oocytes. Following maturation, luciferase activity was analyzed in individual eggs. Injected oocytes cultured in milrinone-containing medium to inhibit maturation served as controls. The experiment was performed three times and the data are expressed as mean \pm SEM. (B) Schematic of the Luc reporter cRNA used to identify functional CPEs in *Dcp1a* 3' UTR. Three putative CPEs and one HEX were mutated. (C) Schematic of the Luc reporter cRNA used to identify functional CPEs in *Dcp2* 3' UTR. Two putative CPEs and one HEX were mutated. For these experiments, firefly luciferase reporter activities were normalized to a co-injected Renilla luciferase control and are expressed relative to the activity in oocytes injected with the same non-mutated reporter cRNA. The experiment was conducted three times and the data are presented as the mean \pm SEM.

activity following maturation.

Mutating the CPE1 or CPE2, but not CPE3, significantly reduced *Dcp1a* reporter activity, with the double mutation of CPE1 and CPE2 further reducing luciferase activity (Fig. 2B). These results suggest both CPE1 and CPE2 are required for recruitment of *Dcp1a* translation during oocyte maturation. As expected, mutating the polyadenylation hexanucleotide (HEX) AAUAAA substantially reduced luciferase activity, a

Figure 2



finding consistent with a requirement for CPEs and HEX to initiate cytoplasmic polyadenylation (Pique et al., 2008). Mutating CPE1, but not CPE2, significantly reduced Dcp2 reporter activity to a level similar to that for the mutated HEX reporter (Fig. 2C), suggesting that CPE1, the CPE closer to the HEX, is the functional cis element largely responsible for recruitment of Dcp2 mRNA. Thus, Dcp1a and Dcp2 are canonical dormant maternal mRNAs recruited during oocyte maturation.

Elimination of Dcp1a and Dcp2 transcripts stabilizes maternal mRNAs

We used RNA interference (RNAi) to

address the role of maturation-associated accumulation of DCP1A and DCP2. RNAi efficiently prevented the maturation-associated increase of DCP1A or DCP2 without affecting the meiotic maturation or metaphase II arrest (Fig. 3A). Next, we analyzed transcriptome changes associated with the loss of maturation-associated increase of DCP1A and DCP2. Full-grown oocytes were microinjected with either Dcp1a or Dcp2 siRNAs or their combination, hereafter referred as Dcp1a&Dcp2; controls were injected with non-targeting, scrambled siRNAs. The oocytes were then cultured for 20 h in the presence of milrinone to permit extensive degradation of targeted mRNAs

Figure 3

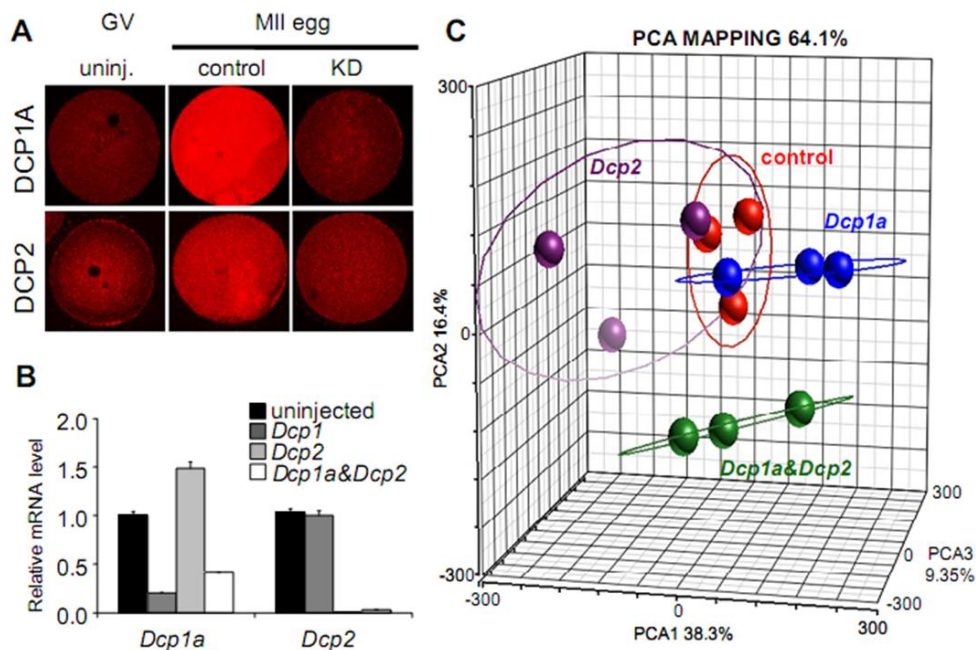


Figure 3. Effects of Dcp1a and Dcp2 knock-down on maternal mRNA stability. (A) The effect of siRNA treatment on inhibiting the maturation-associated increase in DCP1A and DCP2. Control; oocytes injected with scrambled siRNA and matured to MII. KD, knock-down oocytes injected with appropriate siRNA and matured to MII. (B) qPCR analysis of Dcp1a and Dcp2 down-regulation in MII eggs after microinjection of Dcp1a, Dcp2 and DCP1&2 siRNA pools. GV oocytes were microinjected, cultured for 20 h in milrinone-containing medium and then transferred to milrinone-free medium to initiate maturation; MII eggs were then collected for qPCR analysis. The relative transcript abundance of Dcp1a and Dcp2 are relative to un-injected controls. The experiment was performed three times and the data are expressed as mean \pm SEM. (C) Principal component analysis (PCA) of microarray profiles of MII eggs depleted of Dcp1a or Dcp2 or both transcripts. Each color-coded sphere represents projection of a complete microarray dataset in a three-dimensional space formed by the top three principal components. The amount of variation covered by the top three principle components is indicated along each corresponding axis. Color-coded ovals encompass an area corresponding to the mean \pm 2 S.D. of the corresponding samples. Clustering of individual arrays from Dcp1a and Dcp2 knockdowns together with controls suggests that transcriptome changes upon individual knockdowns are minimal. Double knockdown samples cluster apart from the other three samples suggesting that knockdown of both Dcp1a and Dcp2 transcripts causes significant transcriptome changes, which differ from individual knockdowns of these two transcripts.

(Fig. 3B) prior to maturation for additional 18 h when the MII eggs were collected for microarray analysis.

Analysis of differentially expressed transcripts, including principal component analysis (PCA) of the microarray data revealed little perturbation of the transcriptome when either Dcp1a or Dcp2 were targeted but a marked difference when both Dcp1a and Dcp2 mRNAs were targeted (Fig. 3C). That degradation of maternal mRNAs was relatively normal when only a single component of the decapping complex was targeted could reflect that RNAi reduced but not completely eliminated Dcp1a and Dcp2 transcripts (Fig. 3B). Thus, only when both decapping complex components were targeted was decapping activity reduced enough to impair mRNA degradation during maturation.

The perturbation on the transcriptome when both Dcp1a and Dcp2 were targeted was unlikely due to off-targeting effects. First, ON-TARGET SMARTpool siRNAs have minimized off-targeting effects, because of the covalent siRNA modifications and their pooling (Jackson et al., 2006; Myers et al., 2006; Parsons et al., 2009). Second, the miRNA pathway, which forms the basis of off-targeting (Anderson et al., 2008; Birmingham et al., 2006; Saxena et al., 2003), is suppressed in oocytes (Ma et al., 2010; Suh et al., 2010). Third, the transcriptome was not significantly perturbed when Dcp1a and Dcp2 siRNA pools were used individually. Last, bioinformatic analysis of the oligonucleotide motifs associated with transcriptome changes (Schmitter et al., 2006; van Dongen et al., 2008) did not provide any evidence for off-targeting either (data not shown).

ANOVA analysis of differentially expressed transcripts revealed a predominant increase in the relative abundance of transcripts when Dcp1a and Dcp2 mRNAs were targeted (Fig. 4A). Whereas the relative

abundance of 45 transcripts (probe sets) was significantly decreased >1.5 -fold (false discovery rate (FDR) p -value < 0.05), the relative abundance of 380 transcripts was significantly increased > 1.5 fold (FDR p -value < 0.05), suggesting a mainly stabilizing effect on maternal mRNAs following Dcp1a&Dcp2 double knockdown. Transcripts whose relative abundance significantly decreased following Dcp1a&Dcp2 knockdown were typically stable during meiotic maturation (Fig. 4B, blue points). Destabilization upon Dcp1a&Dcp2 knockdown could reflect a secondary effect induced by stabilization of other mRNAs or an accelerated selective decapping-independent mRNA degradation. The majority (70.3%) of the 380 transcripts stabilized in Dcp1a&Dcp2 double knockdown oocytes are common to those that are normally degraded during maturation (Su et al., 2007) as shown by a combined display of relative transcriptome changes during maturation and following maturation in Dcp1a&Dcp2 knockdown (Fig. 4B, red points).

Notably, transcripts stabilized in Dcp1a&Dcp2 knockdown oocytes included many ribosomal RNA proteins, translation factors, and components of the respiratory chain, confirmed by Gene Ontology analysis (Table 1). The same observation had been made during analysis of transcripts normally degraded during maturation (Su et al., 2007) and provides further evidence that inhibition of maturation-associated production of the decapping complex has a global effect on transcripts normally degraded during meiotic maturation. We selected four genes encoding ribosomal proteins (Rpl6, Rpl10a, Rpl18a, and Rpl28) and analyzed by random hexamer-primed qPCR their transcript abundance during meiotic maturation and following inhibition of maturation-associated increase in DCP1A and DCP2. We observed significant stabilization of three of the four transcripts upon inhibition of decapping (Fig.

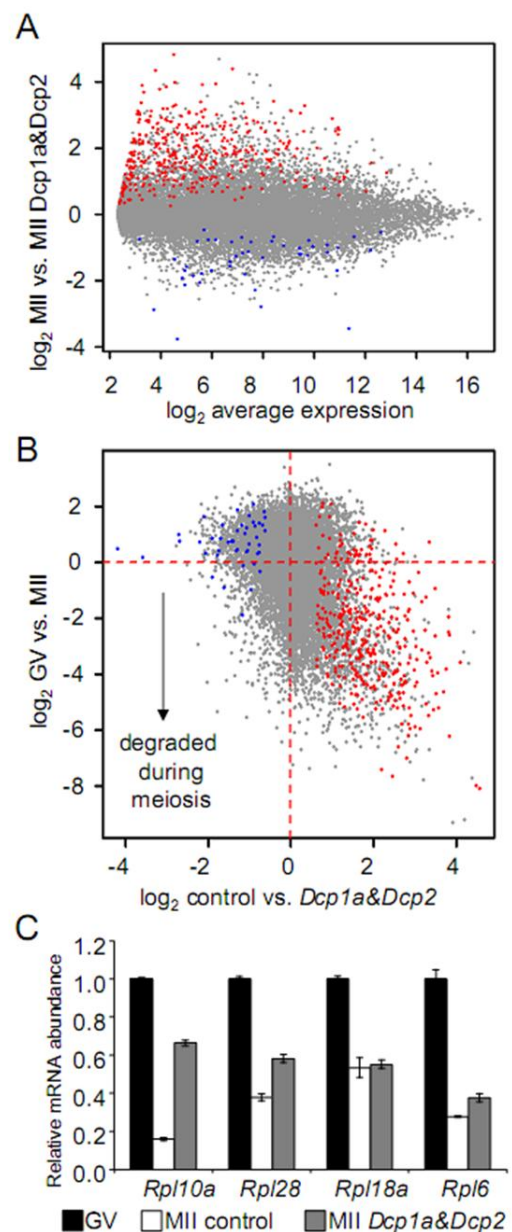
4C). The most pronounced stabilization was observed for *Rpl10a*, which whose transcript was reduced by 84% during normal meiotic maturation but only 33% upon inhibition of decapping. These results indicate that, whereas decapping is involved in meiotic mRNA degradation, the 3'-5' degradation likely contributes to the process in a partially redundant manner. This notion is supported by the combined display of relative transcriptome changes following maturation when *Dcp1a*&*Dcp2* were knocked down, because many transcripts are degraded without an apparent contribution of decapping (Fig.4B, lower left quadrant). Nevertheless, decapping is widely employed in degradation of maternal mRNAs during maturation (Fig.4B, lower right quadrant).

The contribution of decapping to mRNA degradation during maturation is likely larger

Figure 4. Transcriptome analysis of MII eggs following knock-down of *Dcp1a* and *Dcp2*. (A) MII egg transcriptome changes upon *Dcp1a*&*Dcp2* knockdown. The X-axis shows the average probe set hybridization signal and the Y-axis is the relative expression change upon inhibition of decapping. Probe sets whose relative signal was significantly increased or decreased (>1.5-fold, FDR<0.05) in MII eggs following knockdown of *Dcp1a* and *Dcp2* are shown as red and blue points, respectively. (B) Extensive *Dcp1a* and *Dcp2*-dependent degradation of maternal mRNAs during maturation. The graph shows the relationship between transcriptome changes during oocyte maturation (displayed on the Y-axis) and changes following *Dcp1a*&*Dcp2* double-knockdown (shown on the X-axis). Each point displays relative behavior of one Affymetrix probe set. Microarray data for oocyte maturation were taken from the literature (Su et al., 2007). The contribution of *DCP1A* and *DCP2* to the maturation-associated mRNA degradation is clearly visible in the lower right quadrant. Transcripts whose degradation is independent of *DCP1A* and *DCP2* are in the lower left quadrant. Probe sets whose relative signal was increased or decreased in MII eggs following knockdown of *Dcp1a*&*Dcp2* (see also panel B) are shown as red and blue points, respectively. (C) Validation of microarray data using a set of ribosomal protein-encoding transcripts and qRT-PCR. GV, GV-intact oocytes. MII control; oocytes injected with scrambled siRNA and matured to MII. MII *Dcp1a*&*Dcp2*, oocytes injected with siRNAs to *Dcp1a* and *Dcp2* and matured to MII. The data are expressed as mean \pm SEM, where n=3.

than the conservative estimate based on statistical filtering of the microarray analysis (Fig. 4A). First, the knock-down approach cannot completely prevent decapping-dependent mRNA degradation, resulting in underestimating of the number of transcripts degraded in decapping-dependent manner. Second, a number of transcripts, whose apparent abundance increased upon inhibition of decapping, did not pass the statistical filtering. That many of these represent false negatives is indicated by

Figure 4



comparison with an independent microarray analysis of maternal mRNA degradation (Su et al., 2007). Without statistical filtering, there were 848 transcripts whose degradation (>2-fold decrease) was reversed upon inhibition of decapping (>2-fold increase). Third, as mentioned above, inhibition of decapping could be partially compensated by 3'-5' degradation. The accelerated degradation of a small population of transcripts when the maturation-associated increase in DCP1A and DCP2 is inhibited points to involvement of 3'-5' degradation pathway.

It should be pointed out that we used oligo-dT priming to amplify mRNA for our microarray analyses while Su et al. (2007) used random priming. Thus, it is formally possible that the different methods would compromise comparing the two data sets and that oligo-dT priming would be strongly biased by changes in polyA tails of maternal mRNAs. There are, however, several lines of evidence that the comparison is valid and our data reflect mRNA turnover during maturation. First, we do not compare normalized hybridization intensities but relative changes. It is known that oligo-dT priming for mRNA amplification introduces a bias towards 3' ends of transcripts, which is evident from Affymetrix control probe sets.

This bias does not allow for a direct comparison of hybridization intensities from arrays hybridized with oligo-dT and random hexamer-primed amplified mRNA. However, this problem is eliminated when relative changes are compared. It has been shown that even for different microarray platforms that different RNA preparation protocols yield highly reproducible relative changes (Shi et al., 2006). Second, polyadenylation and deadenylation during maturation might affect oligo-dT-primed mRNA amplification and result in different relative changes than would be observed during hexamer-primed mRNA analysis. Dormant maternal transcripts with very short polyA tails, however, yield comparable hybridization intensities as transcripts with longer polyA tails (Wu et al., 2009; Zeng et al., 2004) suggesting that oligo-dT priming generates biases mainly when the poly(A) tail is reduced beyond a minimal length required for oligo-dT priming. Such shortening of the poly(A) tail would be indicative of mRNA degradation and would not compromise our results. The remarkable concordance between transcripts stabilized during maturation following inhibiting the maturation-associated increase in DCP1A and DCP2 with those that are normally degraded during maturation (Su et al., 2007)

Table 1 EASE analysis

Gene Category	System	EASE score	Bonferroni
GO 0003735 structural constituent of ribosome	GO 0003674 Molecular Function	3.08E-09	2.41E-06
GO 0005739 mitochondrion	GO 0005575 Cellular Component	1.19E-06	9.27E-04
GO 0006412 protein biosynthesis	GO 0008150 Biological Process	1.15E-05	8.99E-03
GO 0016659 oxidoreductase activity, acting on NADH or NADPH, other acceptor	GO 0003674 Molecular Function	1.37E-05	1.07E-02
GO 0003954 NADH dehydrogenase activity	GO 0003674 Molecular Function	1.37E-05	1.07E-02
GO 0005737 cytoplasm	GO 0005575 Cellular Component	1.69E-05	1.32E-02
GO 0009058 biosynthesis	GO 0008150 Biological Process	2.03E-05	1.59E-02
GO 0016651 oxidoreductase activity, acting on NADH or NADPH	GO 0003674 Molecular Function	3.30E-05	2.58E-02
GO 0005198 structural molecule activity	GO 0003674 Molecular Function	6.65E-05	5.19E-02
GO 0009059 macromolecule biosynthesis	GO 0008150 Biological Process	9.78E-05	7.63E-02
GO 0005840 ribosome	GO 0005575 Cellular Component	9.80E-05	7.65E-02
GO 0007046 ribosome biogenesis	GO 0008150 Biological Process	1.01E-04	7.89E-02
GO 0042254 ribosome biogenesis and assembly	GO 0008150 Biological Process	1.37E-04	1.07E-01
GO 0005489 electron transporter activity	GO 0003674 Molecular Function	1.54E-04	1.20E-01
GO 0005622 intracellular	GO 0005575 Cellular Component	2.68E-04	2.09E-01
GO 0030529 ribonucleoprotein complex	GO 0005575 Cellular Component	2.76E-04	2.16E-01
GO 0015078 hydrogen ion transporter activity	GO 0003674 Molecular Function	6.25E-04	4.88E-01
GO 0015399 primary active transporter activity	GO 0003674 Molecular Function	6.39E-04	4.99E-01
GO 0015077 monovalent inorganic cation transporter activity	GO 0003674 Molecular Function	7.01E-04	5.47E-01

Table 1. EASE analysis of the 380 probe sets significantly upregulated upon Dcp1a and Dcp2 knockdown (FDR < 0.05, 1.5-fold up) compared to the population of 11,648 probe sets detecting expression in MII eggs.

also suggests that such a comparison is valid. Finally, random hexamer-primed qPCR analysis of mRNAs encoding ribosomal proteins suggest that relative changes observed by microarray analysis upon inhibiting decapping during meiosis reflect inhibition of mRNA degradation and not poly(A) length variability (Fig. 4C).

Noteworthy is that mRNAs whose degradation is perturbed following inhibition of decapping are stable and highly abundant in full-grown GV oocytes (Puschendorf et al., 2006) (Fig. 5A). There is a minimal overlap between transcripts degraded during meiotic maturation and mRNAs that are intrinsically unstable in full-grown oocytes (Puschendorf et al., 2006; Su et al., 2007). This observation highlights the contribution of recruiting dormant maternal Dcp1a and Dcp2 mRNAs to the first wave of induced maternal mRNA degradation during meiosis.

To resolve further the population of transcripts that are degraded during oocyte maturation in decapping-dependent manner, we addressed their translation status. A recent study of polysome-associated mRNAs identified mRNAs that are continuously translated, recruited for translation or are not translated during maturation (Chen et al., 2011). Remarkably, whereas translation of about one fifth of maternal mRNAs is activated during meiosis (Chen et al., 2011), these transcripts were depleted among mRNAs targeted by decapping (Fig. 5B). This finding suggests that the decapping-dependent mRNA degradation during maturation targets transcripts that were either continuously translated or repressed from the onset of resumption of meiosis.

We also performed a bioinformatic analysis of the 3'UTRs of maternal transcripts. Notably, although we failed to identify specific 3'UTR sequence motifs associated with destabilization, we did note that transcripts which are stabilized in MII eggs when the increase in DCP1A and DCP2

Figure 5

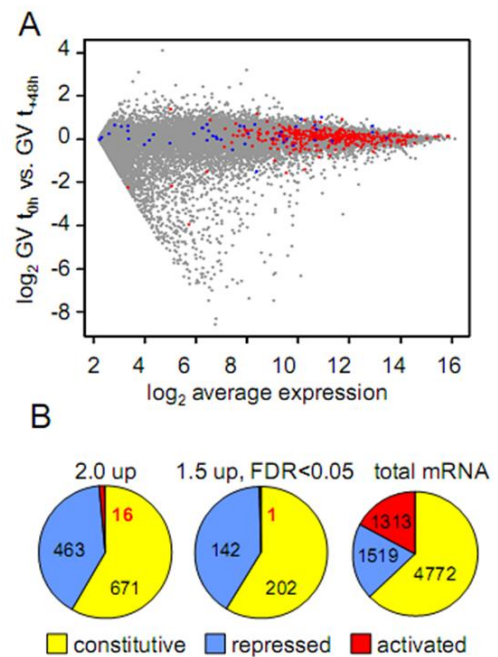


Figure 5. Features of transcripts stabilized following Dcp1a&Dcp2 double knock-down (A) Transcripts targeted by the decapping complex during oocyte maturation are stable in GV oocytes. The graph is based on published microarray data profiling transcriptome changes following extended culture of GV oocytes (Puschendorf et al., 2006). The X-axis shows the average expression level of a particular transcript in GV oocytes and the Y-axis is the change in abundance following 48h of culture of GV oocytes in the presence of milrinone. Each point represents one Affymetrix probe set. Red and blue points highlight probe sets whose hybridization signal was significantly increased or decreased in MII eggs following knockdown of both Dcp1a and Dcp2 transcripts, respectively. (B) Relationship between decapping-dependent degradation during meiosis and translation. Maternal mRNAs were classified according to Chen et al. (Chen et al., 2011) as constitutively translated (yellow, constitutive), repressed (blue, repressed), and recruited for translation during meiotic maturation (red, activated). The distribution of the normal transcriptome into these categories is represented by the pie graph on the right (adapted from Chen et al. (2011)). The other two pie graphs indicate how many of the transcripts in the three categories from the left graph are found among transcripts, which are stabilized upon inhibition of decapping at least 2-fold (2.0 up) and significantly (FDR p-value < 0.05) at least 1.5-fold (1.5 up, FDR<0.05). Note the strong reduction of the category of activated transcripts among mRNAs, which are up-regulated upon inhibition of decapping.

Figure 6

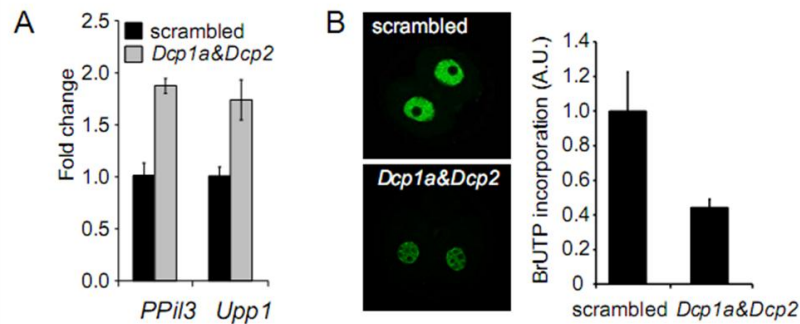


Figure 6. Effect of inhibiting maturation-associated increase in DCP1A and DCP2 on 2-cell embryos. (A) Increased levels of maternal mRNAs Ppil3 and Upp1, which are normally degraded during oocyte maturation, when the maturation-associated increase in DCP1A and DCP2 is inhibited by RNAi. The qPCR experiment was performed two times and the data are presented as mean \pm range. (B) Global transcription in Dcp1a&Dcp2 knockdown 2-cell embryos. Representative staining images of control, scrambled siRNA-injected and Dcp1a&Dcp2 knockdown 2-cell embryos (left panel) and quantification of the data (right panel). The experiment was performed three times and the data are presented as mean \pm SEM.

is inhibited or are normally degraded during maturation have shorter 3'UTRs (Figs. S1 and S2). These results raise the question to what extent is the selectivity of maternal mRNA degradation during oocyte maturation driven by sequence-specific recruitment of the degradation machinery and to what extent is it driven by the loss of protection of a large portion of the transcriptome against degradation, e.g., protection conferred by RNA-binding proteins such as MSY2.

In yeast, deadenylation is the major locus of control that regulates mRNA degradation and is linked to decapping (Muhlrad et al., 1994). A similar situation appears to exist in mammalian cells (Yamashita et al., 2005), but the molecular basis for the linkage is not well understood. Oocytes may differ, however, in the role that deadenylation serves in triggering decapping. In *Xenopus* oocytes, deadenylation is uncoupled from decapping (Gillian-Daniel et al., 1998). A similar situation may exist in mouse oocytes. If deadenylation is the primary trigger for meiotic mRNA degradation, it is hard to envision why inhibiting the increase in DCP1A and DCP2 would stabilize mRNAs as seen by microarrays because our transcriptome profiling relies on the presence

of a polyA tail. This finding also suggests that degradation from the 5' end of transcripts is the dominant pathway for mRNA degradation during oocyte maturation.

Inhibition of decapping affects zygotic genome activation

To ascertain whether degradation of maternal mRNAs is essential for oocyte-to-zygote transition, the maturation-associated increase in both DCP1A and DCP2 was inhibited by microinjecting full-grown oocytes with Dcp1a and Dcp2 siRNAs, and after maturation in vitro the MII eggs were activated by SrCl₂ and diploidized by treatment with cytochalasin B (Kubiak et al., 1991). Activated MII eggs normally undergo zygotic genome activation as shown by microarray profiling (Vassena et al., 2007).

Inhibiting the maturation-associated increase in DCP1A and DCP2 should cause in 2-cell embryos elevated levels of transcripts normally degraded during maturation. We tested this hypothesis by analyzing expression of Ppil3 and Upp1, which are two maternal mRNAs that are extensively degraded during oocyte maturation in decapping-dependent manner.

Consistent with the expected extended survival of maternal mRNAs, *Ppil3* and *Upp1* transcript abundance was increased approximately two-fold increase in 2-cell embryos (Fig. 6A). Furthermore, genome activation, as assessed by BrUTP incorporation was compromised being reduced by ~50% (Fig. 6B).

To further confirm that the extent of the zygotic genome activation is reduced when the maturation associated increase in DCP1A and DCP2 is inhibited, we repeated the experiment using *Dcp1a* and *Dcp2* morpholinos. Microinjection of *Dcp1a* and *Dcp2* morpholinos also prevented the maturation-associated increase in DCP1A and DCP2 (Fig. 7A) and genome activation,

as assessed by BrUTP incorporation was also compromised being reduced by ~50% (Fig. 7B). The reduced BrUTP incorporation also correlated with a similar reduction in the amount of H3K4me3 methylation, which marks active promoters (Shilatifard, 2006) (Fig. 7C). The molecular basis for the linkage between inhibiting maternal mRNA degradation and genome activation, however, remains unclear.

The following model emerges for the transition from mRNA stability to instability that occurs during oocyte maturation. During oocyte growth, mRNAs are relatively stable because binding of MSY2 confers mRNA stability, miRNA activity is suppressed, and the activity of the mRNA degradation machinery is low. Maturation is associated with phosphorylation of MSY2, which makes mRNAs more susceptible to degradation, and recruitment of maternal mRNAs encoding DCP1A and DCP2 increases the mRNA degradation capacity of the maturing oocyte. That most of the increase in DCP1A occurs between MI and MII further suggests that degradation of the bulk of maternal mRNAs occurs late in maturation. The net result is the transition from mRNA stability to instability and degradation of maternal mRNAs. This transcriptome remodeling subsequently enables the full extent of the

Figure 7

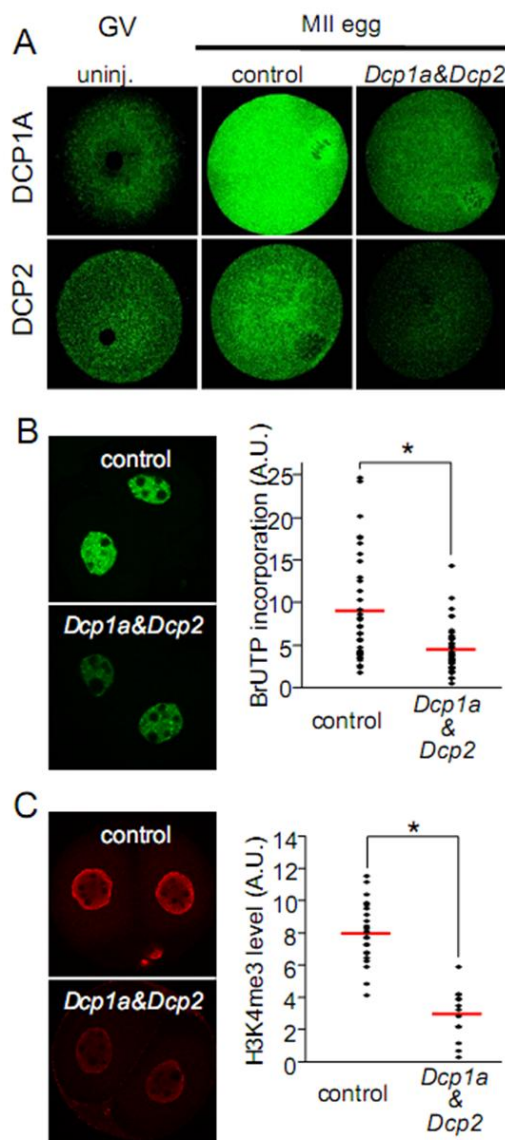


Figure 7. Morpholino-mediated inhibition of the maturation-associated increase in DCP1A and DCP2 affects zygotic genome activation. (A) Morpholinos targeting *Dcp1a* and *Dcp2* mRNAs inhibit maturation-associated increase in DCP1A and DCP2. Oocytes were injected with the appropriate morpholino (a scrambled morpholino was used in control samples) and following maturation to MII, DCP1A or DCP2 was detected by immunocytochemistry. (B) Global transcription in 2-cell embryos following inhibiting the maturation-associated increase in DCP1A and DCP2 using morpholinos. Representative staining images of control and experimental 2-cell embryos and quantification of the data are shown. The experiment was performed four times. The difference between the two groups is significant, $p < 0.001$. (C) H3K4me3 methylation is reduced following inhibition of the maturation-associated increase in DCP1A and DCP2. Representative staining images of control and experimental 2-cell embryos and quantification of the data are shown. The experiment was performed two times. The difference between the two groups is significant, $p < 0.001$.

zygotic genome activation during the 2-cell stage.

Acknowledgments

This research was supported by an NIH grant HD022681 to RMS and EMBO SDIG program, ME09039 grant, and the Purkynje Fellowship to PS. JM thanks Shin Murai (Toho University School of Medicine) for the luciferase reporter plasmid.

References

- FigurAnderson, E. M., Birmingham, A., Baskerville, S., Reynolds, A., Maksimova, E., Leake, D., Fedorov, Y., Karpilow, J. and Khvorova, A. (2008). Experimental validation of the importance of seed complement frequency to siRNA specificity. *RNA* 14, 853-61.
- Bachvarova, R., De Leon, V., Johnson, A., Kaplan, G. and Paynton, B. V. (1985). Changes in total RNA, polyadenylated RNA, and actin mRNA during meiotic maturation of mouse oocytes. *Dev.Biol.* 108, 325-331.
- Bachvarova, R. and DeLeon, V. (1980). Polyadenylated RNA of mouse ova and loss of maternal RNA in early development. *Dev.Biol.* 74, 1-8.
- Beelman, C. A., Stevens, A., Caponigro, G., LaGrandeur, T. E., Hatfield, L., Fortner, D. M. and Parker, R. (1996). An essential component of the decapping enzyme required for normal rates of mRNA turnover. *Nature* 382, 642-6.
- Birmingham, A., Anderson, E. M., Reynolds, A., Ilsley-Tyree, D., Leake, D., Fedorov, Y., Baskerville, S., Maksimova, E., Robinson, K., Karpilow, J. et al. (2006). 3' UTR seed matches, but not overall identity, are associated with RNAi off-targets. *Nat Methods* 3, 199-204.
- Blumenthal, J., Behar, L., Elliott, E. and Ginzburg, I. (2009). Dcp1a phosphorylation along neuronal development and stress. *FEBS Lett* 583, 197-201.
- Brower, P. T., Gizang, E., Boreen, S. M. and Schultz, R. M. (1981). Biochemical studies of mammalian oogenesis: synthesis and stability of various classes of RNA during growth of the mouse oocyte in vitro. *Dev Biol* 86, 373-83.
- Chatot, C. L., Ziomek, C. A., Bavister, B. D., Lewis, J. L. and Torres, I. (1989). An improved culture medium supports development of random-bred 1-cell mouse embryos in vitro. *J. Reprod. Fertil.* 86, 679-688.
- Chen, J., Melton, C., Suh, N., Oh, J. S., Horner, K., Xie, F., Sette, C., Billelloch, R. and Conti, M. (2011). Genome-wide analysis of translation reveals a critical role for deleted in azoospermia-like (*Dazl*) at the oocyte-to-zygote transition. *Genes Dev* 25, 755-66.
- Coller, J. and Parker, R. (2004). Eukaryotic mRNA decapping. *Ann. Rev. Biochem.* 73, 861-890.
- Coller, J. and Parker, R. (2005). General translational repression by activators of mRNA decapping. *Cell* 122, 875-886.
- Cougot, N., Babajko, S. and Seraphin, B. (2004). Cytoplasmic foci are sites of mRNA decay in human cells. *J Cell Biol* 165, 31-40.
- Dephoure, N., Zhou, C., Villén, J., Beausoleil, S., Bakalarski, C., Elledge, S. and Gygi, S. (2008). A quantitative atlas of mitotic phosphorylation. *Proceedings of the National Academy of Sciences* 105, 10762.
- DeRenzo, C. and Seydoux, G. (2004). A clean start: degradation of maternal proteins at the oocyte-to-embryo transition. *Trends Cell Biol* 14, 420-6.
- Erbach, G. T., Lawitts, J. A., Papaioannou, V. E. and Biggers, J. D. (1994). Differential growth of the mouse preimplantation embryo in chemically defined media. *Biol Reprod* 50, 1027-33.
- Fenger-Gron, M., Fillman, C., Norrild, B. and Lykke-Andersen, J. (2005). Multiple processing body factors and the ARE binding protein TTP activate mRNA decapping. *Mol Cell* 20, 905-15.
- Flemer, M., Ma, J., Schultz, R. M. and Svoboda, P. (2010). P-body loss is concomitant with formation of a messenger RNA storage domain in mouse oocytes. *Biol Reprod* 82, 1008-17.

- Floor, S. N., Jones, B. N., Hernandez, G. A. and Gross, J. D. (2010). A split active site couples cap recognition by Dcp2 to activation. *Nat Struct Mol Biol* 17, 1096-101.
- Gillian-Daniel, D. L., Gray, N. K., Astrom, J., Barkoff, A. and Wickens, M. (1998). Modifications of the 5' cap of mRNAs during *Xenopus* oocyte maturation: independence from changes in poly(A) length and impact on translation. *Mol Cell Biol* 18, 6152-63.
- Ingelfinger, D., Arndt-Jovin, D., Lührmann, R. and Achsel, T. (2002). The human LSM1-7 proteins colocalize with the mRNA-degrading enzymes Dcp1/2 and Xrn1 in distinct cytoplasmic foci. *RNA* 8, 1489.
- Jackson, A. L., Burchard, J., Leake, D., Reynolds, A., Schelter, J., Guo, J., Johnson, J. M., Lim, L., Karpilow, J., Nichols, K. et al. (2006). Position-specific chemical modification of siRNAs reduces "off-target" transcript silencing. *RNA* 12, 1197-205.
- Jahn, C., Baran, M. and Bachvarova, R. (1976). Stability of RNA synthesized by the mouse oocyte during its major growth phase. *Journal of Experimental Zoology* 197, 161-171.
- Kishigami, S. and Wakayama, T. (2007). Efficient strontium-induced activation of mouse oocytes in standard culture media by chelating calcium. *J Reprod Dev* 53, 1207-15.
- Kshirsagar, M. and Parker, R. (2004). Identification of Edc3p as an enhancer of mRNA decapping in *Saccharomyces cerevisiae*. *Genetics* 166, 729-39.
- Kubiak, J., Paldi, A., Weber, M. and Maro, B. (1991). Genetically identical parthenogenetic mouse embryos produced by inhibition of the first meiotic cleavage with cytochalasin D. *Development* 111, 763-9.
- Kurasawa, S., Schultz, R. M. and Kopf, G. S. (1989). Egg-induced modifications of the zona pellucida of mouse eggs: effects of microinjected inositol 1,4,5-trisphosphate. *Dev Biol* 133, 295-304.
- Laemmli, U. K. (1970). Cleavage of structural proteins during the assembly of the head of bacteriophage T4. *Nature* 227, 680-685.
- LaGrandeur, T. E. and Parker, R. (1998). Isolation and characterization of Dcp1p, the yeast mRNA decapping enzyme. *EMBO J* 17, 1487-96.
- Lykke-Andersen, J. (2002). Identification of a human decapping complex associated with hUpf proteins in nonsense-mediated decay. *Mol Cell Biol* 22, 8114-21.
- Ma, J., Flemr, M., Stein, P., Berninger, P., Malik, R., Zavolan, M., Svoboda, P. and Schultz, R. M. (2010). MicroRNA activity is suppressed in mouse oocytes. *Curr Biol* 20, 265-70.
- Medvedev, S., Pan, H. and Schultz, R. M. (2011). Absence of MSY2 in Mouse Oocytes Perturbs Oocyte Growth and Maturation, RNA Stability, and the Transcriptome. *Biol Reprod*.
- Medvedev, S., Yang, J., Hecht, N. B. and Schultz, R. M. (2008). CDC2A (CDK1)-mediated phosphorylation of MSY2 triggers maternal mRNA degradation during mouse oocyte maturation. *Dev Biol* 321, 205-15.
- Mendez, R. and Richter, J. D. (2001). Translational control by CPEB: a means to the end. *Nat Rev Mol Cell Biol* 2, 521-9.
- Muhlrad, D., Decker, C. J. and Parker, R. (1994). Deadenylation of the unstable mRNA encoded by the yeast MFA2 gene leads to decapping followed by 5'→3' digestion of the transcript. *Genes Dev* 8, 855-66.
- Myers, J. W., Chi, J. T., Gong, D., Schaner, M. E., Brown, P. O. and Ferrell, J. E. (2006). Minimizing off-target effects by using diced siRNAs for RNA interference. *J RNAi Gene Silencing* 2, 181-94.
- Nakahata, S., Kotani, T., Mita, K., Kawasaki, T., Katsu, Y., Nagahama, Y. and Yamashita, M. (2003). Involvement of *Xenopus* Pumilio in the translational regulation that is specific to cyclin B1 mRNA during oocyte maturation. *Mech Dev* 120, 865-80.
- Padmanabhan, K. and Richter, J. D. (2006). Regulated Pumilio-2 binding controls RINGO/Spy mRNA translation and CPEB activation. *Genes Dev* 20, 199-209.
- Pan, H., O'Brien M, J., Wigglesworth, K., Eppig, J. J. and Schultz, R. M. (2005). Transcript

- profiling during mouse oocyte development and the effect of gonadotropin priming and development in vitro. *Dev Biol* 286, 493-506.
- Parsons, B. D., Schindler, A., Evans, D. H. and Foley, E. (2009). A direct phenotypic comparison of siRNA pools and multiple individual duplexes in a functional assay. *PLoS One* 4, e8471.
- Pique, M., Lopez, J. M., Foissac, S., Guigo, R. and Mendez, R. (2008). A combinatorial code for CPE-mediated translational control. *Cell* 132, 434-48.
- Puschendorf, M., Stein, P., Oakeley, E. J., Schultz, R. M., Peters, A. H. and Svoboda, P. (2006). Abundant transcripts from retrotransposons are unstable in fully grown mouse oocytes. *Biochem Biophys Res Commun* 347, 36-43.
- Radford, H. E., Meijer, H. A. and de Moor, C. H. (2008). Translational control by cytoplasmic polyadenylation in *Xenopus* oocytes. *Biochim Biophys Acta* 1779, 217-
- Saxena, S., Jonsson, Z. O. and Dutta, A. (2003). Small RNAs with imperfect match to endogenous mRNA repress translation. Implications for off-target activity of small inhibitory RNA in mammalian cells. *J Biol Chem* 278, 44312-9.
- Schmitter, D., Filkowski, J., Sewer, A., Pillai, R. S., Oakeley, E. J., Zavolan, M., Svoboda, P. and Filipowicz, W. (2006). Effects of Dicer and Argonaute down-regulation on mRNA levels in human HEK293 cells. *Nucleic Acids Res* 34, 4801-15.
- Schultz, R. M., Montgomery, R. R. and Belanoff, J. R. (1983). Regulation of mouse oocyte meiotic maturation: implication of a decrease in oocyte cAMP and protein dephosphorylation in commitment to resume meiosis. *Dev Biol* 97, 264-73.
- Sheets, M. D., Fox, C. A., Hunt, T., Vande Woude, G. and Wickens, M. (1994). The 3'-untranslated regions of *c-mos* and cyclin mRNAs stimulate translation by regulating cytoplasmic polyadenylation. *Genes Dev* 8, 926-38.
- Shi, L. Reid, L. H. Jones, W. D. Shippy, R. Warrington, J. A. Baker, S. C. Collins, P. J. de Longueville, F. Kawasaki, E. S. Lee, K. Y. et al. (2006). The MicroArray Quality Control (MAQC) project shows inter- and intraplatform reproducibility of gene expression measurements. *Nat Biotechnol* 24, 1151-61.
- Shilatifard, A. (2006). Chromatin modifications by methylation and ubiquitination: implications in the regulation of gene expression. *Annu Rev Biochem* 75, 243-69.
- Stitzel, M. L. and Seydoux, G. (2007). Regulation of the oocyte-to-zygote transition. *Science* 316, 407-8.
- Su, Y. Q., Sugiura, K., Woo, Y., Wigglesworth, K., Kamdar, S., Affourtit, J. and Eppig, J. J. (2007). Selective degradation of transcripts during meiotic maturation of mouse oocytes. *Dev Biol* 302, 104-17.
- Suh, N., Baehner, L., Moltzahn, F., Melton, C., Shenoy, A., Chen, J. and Blelloch, R. (2010). MicroRNA function is globally suppressed in mouse oocytes and early embryos. *Current Biology* 20, 271-277.
- Swetloff, A., Conne, B., Huarte, J., Pitetti, J. L., Nef, S. and Vassalli, J. D. (2009). Dcp1-bodies in mouse oocytes. *Mol Biol Cell* 20, 4951-61.
- Tay, J., Hodgman, R. and Richter, J. D. (2000). The control of cyclin B1 mRNA translation during mouse oocyte maturation. *Dev Biol* 221, 1-9.
- Tucker, M., Valencia-Sanchez, M., Staples, R., Chen, J., Denis, C. and Parker, R. (2001). The transcription factor associated Ccr4 and Caf1 proteins are components of the major cytoplasmic mRNA deadenylase in *Saccharomyces cerevisiae*. *Cell* 104, 377-386.
- van Dijk, E., Cougot, N., Meyer, S., Babajko, S., Wahle, E. and Seraphin, B. (2002). Human Dcp2: a catalytically active mRNA decapping enzyme located in specific cytoplasmic structures. *EMBO J* 21, 6915-24.
- van Dongen, S., Abreu-Goodger, C. and Enright, A. J. (2008). Detecting microRNA binding and siRNA off-target effects from expression data. *Nat Methods* 5, 1023-5.
- Vassena, R., Han, Z., Gao, S., Baldwin, D. A., Schultz, R. M. and Latham, K. E. (2007). Tough

beginnings: alterations in the transcriptome of cloned embryos during the first two cell cycles. *Dev Biol* 304, 75-89.

Wang, Q.T., Piotrowska, K., Ciemerych, M.A., Milenkovic, L., Scott, M.P., Davis, R.W., Zernicka-Goetz, M. (2004). A genome-wide study of gene activity reveals developmental signaling pathways in the preimplantation mouse embryo. *Dev Cell* 4, 133-44.

Wang, Z., Jiao, X., Carr-Schmid, A. and Kiledjian, M. (2002). The hDcp2 protein is a mammalian mRNA decapping enzyme. *Proc Natl Acad Sci U S A* 99, 12663-8.

Whitten, W. K. (1971). Nutrient requirements for the culture of preimplantation mouse embryo in vitro. *Adv. Biosci.* 6, 129-139.

Wiersma, A., Hirsch, B., Tsafiriri, A., Hanssen, R. G., Van de Kant, M., Kloosterboer, H. J., Conti, M. and Hsueh, A. J. (1998). Phosphodiesterase 3 inhibitors suppress oocyte maturation and consequent pregnancy without affecting ovulation and cyclicity in rodents. *J Clin Invest* 102, 532-7.

Wu, C., Orozco, C., Boyer, J., Leglise, M., Goodale, J., Batalov, S., Hodge, C. L., Haase, J., Janes, J., Huss, J. W., 3rd et al. (2009). BioGPS: an extensible and customizable portal for querying and organizing gene annotation resources. *Genome Biol* 10, R130.

Yamashita, A., Chang, T. C., Yamashita, Y., Zhu, W., Zhong, Z., Chen, C. Y. and Shyu, A. B. (2005). Concerted action of poly(A) nucleases and decapping enzyme in mammalian mRNA turnover. *Nat Struct Mol Biol* 12, 1054-63.

Yu, J., Deng, M., Medvedev, S., Yang, J., Hecht, N. B. and Schultz, R. M. (2004). Transgenic RNAi-mediated reduction of MSY2 in mouse oocytes results in reduced fertility. *Dev Biol* 268, 195-206.

Zeng, F., Baldwin, D. A. and Schultz, R. M. (2004). Transcript profiling during preimplantation mouse development. *Dev. Biol.* 272, 483-496.

Zeng, F. and Schultz, R. M. (2005). RNA transcript profiling during zygotic gene activation in the preimplantation mouse embryo. *Dev Biol* 283, 40-57.

Supplemental Material

Bioinformatic analysis of 3' UTRs

Global profiling of gene expression: Affymetrix CEL files were either generated during this study or were downloaded (Puschendorf et al., 2006; Su et al., 2007) from the GEO database (<http://www.ncbi.nlm.nih.gov/gds>). CEL files were processed by gcRMA algorithm in the Partek Genomics Suite package (Partek, Missouri, USA). Differentially expressed genes (>1.5-fold change) were detected using ANOVA (FDR < 0.05). Data were plotted using the R environment (<http://www.r-project.org/>).

Retrieval of a non-redundant set of 3'UTRs: Information about genes, transcripts and mapping of individual probes from GeneChip Mouse Genome 430 2.0 (Affymetrix) were obtained from EnsEMBL (Flicek et al., 2010) mouse genome annotation build 54 (genome assembly m37). Acquisition and filtering of data employed perl scripts using EnsEMBL API. Downloaded data were stored in a MySQL database. For each gene, all exons were merged into one “synthetic” transcript. The start position of each 3'UTR was defined as the most frequent stop codon position among known gene transcripts. Probesets were associated with genes only if their all 11 probes were mapped in the corresponding “synthetic” transcript.

Assignment of expression values to 3'UTRs: All CEL files were processed in R environment using Bioconductor. The data were background corrected using the gcRMA and normalized using quantile normalization. Only probesets with average expression exceeding value of 7.64 in Dcp1a&Dcp2 siRNA-treated MII eggs and full-grown GV oocytes (Puschendorf et al., 2006; Su et al., 2007) were retained. Differential expression was detected using the Limma package (Wettenhall and Smyth, 2004). Probe set annotation was provided by the Bioconductor (Gentleman et al., 2004) package mouse4302.db.

3'UTR sequences of protein coding genes (defined as biotype qualifier in EnsEMBL annotation) longer than 50 nt were assigned to expression values using probe sets identifiers. In cases where multiple probe sets mapped to one 3'UTR sequence, we selected the one with larger fold-change. In the resulting table was every 3'UTR sequence linked to only one probe set.

3'UTR length analysis: 3'UTR length was analyzed by Mann-Whitney test using the Wilcox test function in R environment. The test was performed between bins of 3'UTR sequences, which corresponded to deciles of fold-change.

Sylamer analysis: Sylamer analysis of sequence motif biases in rank-sorted 3'UTR sequences (according to the fold-change) was performed for hexamer motifs. Analysis was run in a non-cumulative mode in a sliding window with step that corresponded to five percentiles of fold-change. All 3'UTR sequences were used for definition of the analysis universe. The analysis of repetitive pentamer motifs was performed with similar parameters for a minimum of three occurrences of each pentamer motif per 3'UTR.

References

Flicek, P., Aken, B. L., Ballester, B., Beal, K., Bragin, E., Brent, S., Chen, Y., Clapham, P., Coates, G., Fairley, S. et al. (2010). Ensembl's 10th year. *Nucleic Acids Res* 38, D557-62.

Gentleman, R. C., Carey, V. J., Bates, D. M., Bolstad, B., Dettling, M., Dudoit, S., Ellis, B., Gautier, L., Ge, Y., Gentry, J. et al. (2004). Bioconductor: open software development for computational biology and bioinformatics. *Genome Biol* 5, R80.

Puschendorf, M., Stein, P., Oakeley, E. J., Schultz, R. M., Peters, A. H. and Svoboda, P. (2006). Abundant transcripts from retrotransposons are unstable in fully grown mouse oocytes. *Biochem Biophys Res Commun* 347, 36-43.

Su, Y. Q., Sugiura, K., Woo, Y., Wigglesworth, K., Kamdar, S., Affourtit, J. and Eppig, J. J. (2007). Selective degradation of transcripts during meiotic maturation of mouse oocytes. *Dev Biol* 302, 104-17.

Wettenhall, J. M. and Smyth, G. K. (2004). limmaGUI: a graphical user interface for linear modeling of microarray data. *Bioinformatics* 20, 3705-6.

Figure S1

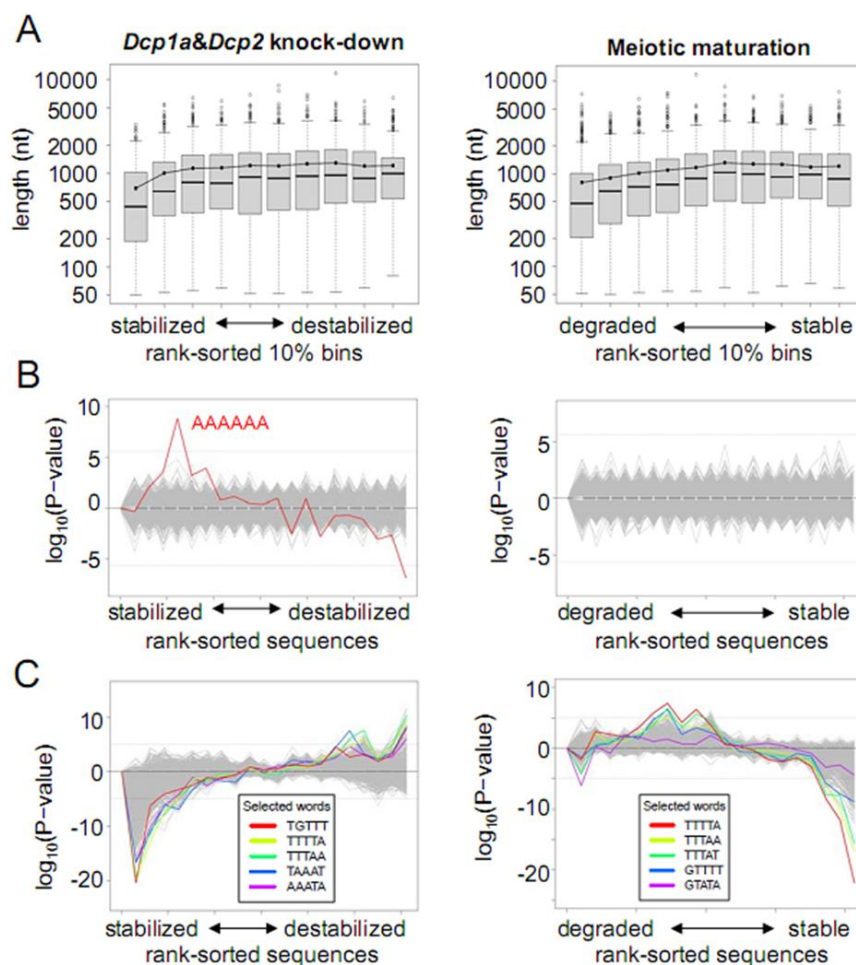


Figure S1. Bioinformatic analysis of transcriptome remodeling during oocyte maturation (graphs on the right) and upon inhibition of decapping (graphs of on the left). (A) Transcripts degraded during meiosis and stabilized upon inhibition of decapping have shorter 3'UTRs. Graphs show distribution of 3'UTR lengths in 10% rank-sorted bins created by dividing transcripts sorted according to the fold-change into ten consecutive groups. Only transcripts that have readily detectable microarray hybridization signals were selected for the analysis; for more details see Material and methods. Transcripts most stabilized upon inhibition of decapping and transcripts most degraded during maturation (the first box plot in each graph) have significantly shorter 3'UTRs than stable transcripts (see Fig. S2 for statistical analysis). (B) Absence of specific hexamer motifs associated with transcripts targeted by decapping and transcripts degraded during maturation. Graphs show results of Sylamer analysis where the X-axis represents transcripts rank-sorted according to their fold-change (the same transcripts as in the panel A) and the Y-axis shows Sylamer $\log_{10}(\text{P-value})$. Each line then represents a

significance landscape plot, which indicates enrichment or depletion of a particular motif in a population of transcripts exhibiting a similar fold-change. In red is highlighted AAAAAA motif, which was the only motif yielding a significant Sylamer $\log_{10}(\text{P-value})$. This motif, however, is apparently not enriched in transcripts most stabilized upon Dcp1a&Dcp2 knockdown. (C) Repetitive AU-rich motifs (pentamer motifs found in three or more copies per transcript) are depleted in transcripts that are most degraded during maturation or stabilized upon inhibition of decapping. Shown is the Sylamer analysis of the same rank-sorted gene list as in panels A and B. Highlighted are motifs reaching local maxima or minima of $\log_{10}(\text{P-value})$.

Figure S2

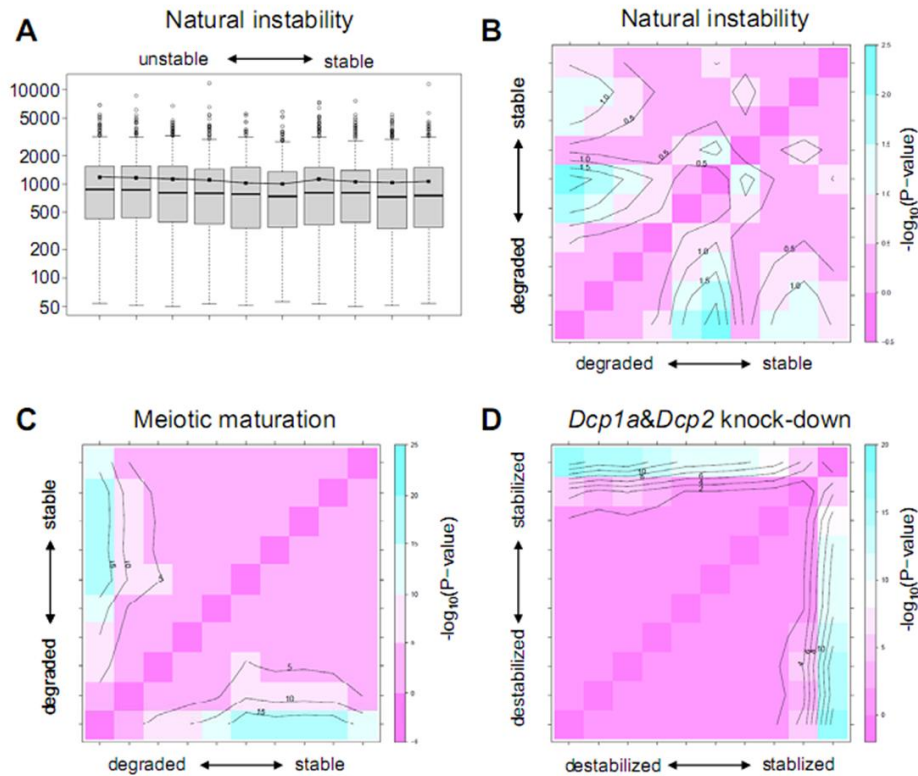


Figure S2. Bioinformatic analysis of correlation between 3'UTR length and stability during meiosis. (A) Absence of correlation between mRNA stability and 3'UTR length in transcripts, which are naturally unstable in full-grown GV oocytes (Puschendorf et al., 2006). Graphs show distribution of 3'UTR lengths in 10% rank-sorted bins created by dividing transcripts sorted according to the fold-change. Only transcripts that yielded readily detectable microarray hybridization signals were selected for the analysis (for more details see Materials and Methods). (B) Statistical analysis of differences of 3'UTR lengths among 10% quintiles. Color of each square indicates statistical significance ($-\log_{10}(\text{P-value})$, Wilcoxon test) of difference of the intersecting quantiles (deciles). Lines indicate courses of $-\log_{10}(\text{P-value})$ for indicated values. (C) Same analysis as in B was applied onto transcriptome changes during meiosis [10]. (D) Same analysis as in B applied onto transcriptome changes upon inhibition of decapping. Note the different scale of $-\log_{10}(\text{P-value})$ in panels B, C, and D.

SUPPLEMENT 4

Jun Ma, Matyas Flemr, Paula Stein, Radek Malik, Philipp Berninger, Mihaela Zavolan, Petr Svoboda and Richard M. Schultz

MicroRNA activity is suppressed in mouse oocytes

(reprint from *Current Biology*. 2010 Feb 9;20(3):265-70)

My contribution to this work:

I designed and prepared the luciferase reporters used for experiments presented in Fig.3, Fig.4B and Fig.S3. I generated the data for Fig.S3 and performed the Sylamer analysis shown in Fig.S1. I helped prepare the manuscript.

MicroRNA Activity Is Suppressed in Mouse Oocytes

Jun Ma¹, Matyas Flemr², Paula Stein¹, Philipp Berninger³, Radek Malik², Mihaela Zavolan³, Petr Svoboda², Richard M. Schultz¹

¹ Department of Biology, University of Pennsylvania, Philadelphia, PA 19104-6018, USA

² Institute of Molecular Genetics, Academy of Sciences of the Czech Republic, Videnska 1083, 142 20 Prague 4, Czech Republic

³ Division of Bioinformatics, Biozentrum, University of Basel and Swiss Institute of Bioinformatics, Klingelbergstrasse 50/70, 4056 Basel, Switzerland

Received 19 October 2009. Revised 2 December 2009. Accepted 16 December 2009. Available online 28 January 2010. Published online: January 28, 2010.

Summary

MicroRNAs (miRNAs) are small endogenous RNAs that typically imperfectly base pair with 3' untranslated regions (3'UTRs) and mediate translational repression and mRNA degradation. Dicer, which generates small RNAs in the miRNA and RNA interference (RNAi) pathways, is essential for meiotic maturation of mouse oocytes. We found that 3'UTRs of transcripts upregulated in *Dicer1*^{-/-} oocytes are not enriched in miRNA binding sites, implicating a weak impact of miRNAs on the maternal transcriptome. Therefore, we tested the ability of endogenous miRNAs to mediate RNA-like cleavage or translational repression of reporter mRNAs. In contrast to somatic cells, endogenous miRNAs in oocytes poorly repressed translation of mRNA reporters, whereas their RNAi-like activity was much less affected. Reporter mRNA carrying let-7-binding sites failed to localize to P body-like structures in oocytes. Our data suggest that miRNA function is downregulated during oocyte development, an idea supported by normal meiotic maturation of oocytes lacking *Dgcr8*, which is required for the miRNA but not the RNAi pathway (Suh et al. [1], this issue of *Current Biology*). Suppressing miRNA function during oocyte growth is likely an early event in reprogramming gene expression during the transition of a differentiated oocyte into pluripotent blastomeres of the embryo.

Highlights

► Transcripts upregulated in *Dicer1*^{-/-} oocytes are not enriched in miRNA binding sites ► Endogenous miRNAs in oocytes poorly repress translation of mRNA reporters ► Reporter mRNAs carrying let-7-binding sites fail to localize to P body-like structures

Keywords

RNA; DEVBIO

Results and Discussion

Minimal Impact of MicroRNAs on Mouse Oocyte Transcriptome

The eight 5'-terminal nucleotides of a microRNA (miRNA) form a "seed," which hybridizes nearly perfectly with the target mRNA and nucleates the miRNA-mRNA interaction [2]. Whereas enrichment of motifs complementary to seeds of highly active miRNAs has been observed in 3' untranslated regions (3'UTRs) of mRNAs whose relative abundance is increased (hereafter referred to as upregulated) upon depletion of *Dicer1* [3], [4] and [5], transcriptome analysis of *Dicer1*^{-/-} metaphase II (MII) eggs did not identify any miRNA-related motifs [6]. Because transcriptome remodeling during meiosis [7] could mask upregulation of primary miRNA targets, we performed an analysis of fully grown germinal vesicle-intact (GV) *Dicer1*^{-/-} oocytes. Microarray profiling revealed a comparable number of upregulated (489, $p < 0.001$) and downregulated (628, $p < 0.001$) transcripts (Figure 1A). The magnitude of these changes was ~5 times smaller when compared to other studies of *Dicer1*-depleted mammalian cells [4] and [5]. In fact, the loss of *Dicer1* in the oocyte caused a transcriptome change comparable to the effect of a single miRNA in embryonic stem (ES) cells (Figure 1A) [5].

We searched for heptamer motifs enriched in 3'UTRs of transcripts that were upregulated in the *Dicer1*^{-/-} oocytes and that could explain the mRNA expression changes. One of the four motifs most significantly enriched (see Table S1 available online) was complementary to the seed of miR-1195 (GAACUCA, Figure 1B). This motif, however, is likely not associated with miRNA function, because miR-1195 was absent in deep sequencing of small RNAs from mouse oocytes [8]. Likewise, none of the predicted miR-1195 targets in the miRBase [9] was upregulated in the *Dicer1*^{-/-} oocytes. Sylamer [10], an alternative approach to analyze miRNA signals in 3'UTRs, showed that none of the high-scoring motifs and none of the top five miRNA-related heptamers (Figure S1) match seed regions of miRNAs with a cloning frequency in oocytes $> 0.1\%$.

We also examined motifs related to abundant miRNAs in transcriptomes of *Dicer1*^{-/-} oocytes and ES cells. These motifs, which were selected based on deep sequencing data [8] and [11], represent binding sites for more than half of all miRNAs cloned from these cells (Table S2). Interestingly, none of the motifs (including those for the let-7 family, which represents ~30% of maternal miRNAs [8] and [12]) showed any enrichment or any statistical bias in 3'UTRs of transcripts upregulated in *Dicer1*^{-/-} oocytes. This contrasts with *Dicer1*^{-/-} ES cells, where the most significant motifs match a family of highly abundant miRNAs (~25% of cloned miRNAs [11]), and several motifs corresponding to other abundant miRNAs also showed enrichment and deviation from the statistical background (Figure 1C; Table S3).

Our data suggest limited miRNA-associated mRNA degradation in the oocyte and do not support the notion that miRNAs extensively modulate gene expression in oocytes [12] and [13]. Our analysis of 3'UTRs of transcripts upregulated in *Dicer1*^{-/-} oocytes does not provide evidence that the upregulation is associated with miRNA function via seed-mediated interaction with 3'UTRs. Likewise, we observed no significant enrichment of miRNA-associated motifs in 3'UTRs of intrinsically unstable mRNAs [14] and mRNAs degraded during meiosis [7]. Although miRNA binding sites were associated with specific transcript isoforms during meiotic mRNA degradation [15], it is unclear whether this observation reflects miRNA effects. It is possible that none of the maternal miRNAs is functionally dominant, and therefore none generates a strong signal, but this does not explain the low number of upregulated transcripts in *Dicer1*^{-/-} oocytes. Alternatively, miRNA-mediated mRNA degradation is not robust, and the transcriptome change reflects the loss of endogenous small interfering RNAs (endo-siRNAs). We found that 42 of 489 upregulated but only 6 of the 628 downregulated transcripts in *Dicer1*^{-/-} oocytes perfectly base pair (Table S4) with endo-siRNAs [16]. Because siRNA-guided cleavage by small RNAs requires less than complete base pairing and can occur without a perfect seed complementarity [17], it is

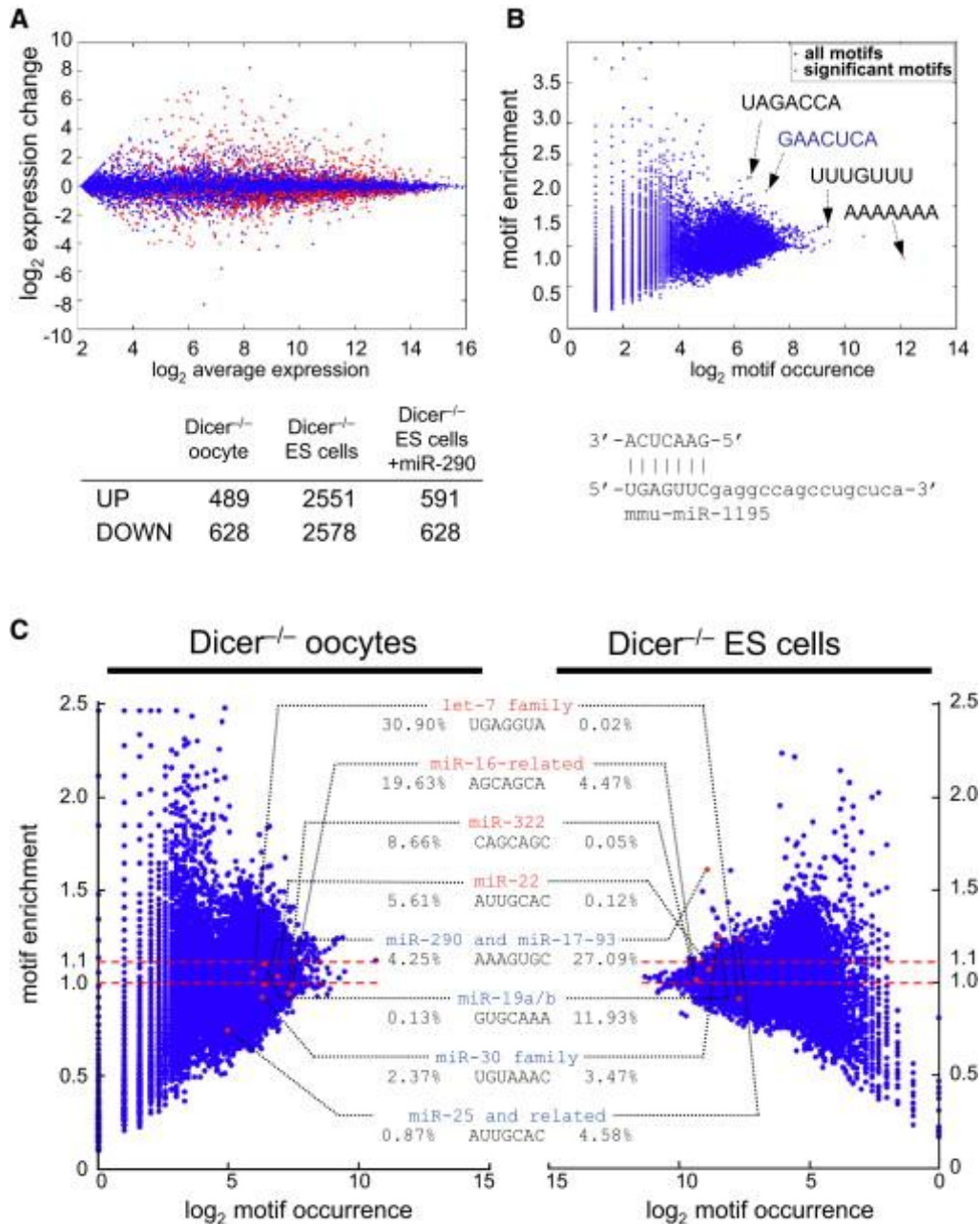


Figure 1. Transcriptome Analysis of *Dicer1*^{-/-} Oocytes(A) M [$\log_2(\text{fold change})$] versus A [average $\log_2(\text{expression level})$] plot for the *Dicer1*^{-/-} versus *Dicer1*^{+/+} fully grown germinal vesicle oocytes. Each dot represents a transcript. Significant expression changes ($p < 0.001$ computed from four replicate experiments) are shown in red.(B) Heptamer motif analysis of upregulated transcripts. The motifs whose frequency in the 3' untranslated regions (3'UTRs) of upregulated transcripts is significantly different from the frequency in the entire set of 3'UTRs are shown in red (see also Experimental Procedures). One of the significantly enriched motifs is complementary to positions 1–7 of the miR-1195.(C) Comparison of heptamer motif analyses of *Dicer1*^{-/-} oocytes (left) and embryonic stem (ES) cells (right, horizontally inverted); most-relevant motifs complementary to seeds of most-abundant microRNAs (miRNAs) in both cell types are highlighted. The most-abundant miRNAs in the oocyte and ES cells are shown in red and blue text, respectively. Note that none of the motifs corresponding to abundant maternal miRNAs is enriched more than 1.1 times in 3'UTRs of transcripts upregulated in *Dicer1*^{-/-} oocytes, whereas all four motifs corresponding to miRNAs abundant in ES cells are enriched in *Dicer1*^{-/-} ES cells. Posterior probability analysis shows a high significance (1.000) only for the GCACUUU motif. However, posterior probability for the other three motifs corresponding to ES cell miRNAs was one to three orders of magnitude higher than all other motifs, which scored within the statistical background ($\sim 10^{-5}$, Table S3). Abundance (%) of miRNAs related to individual motifs in both cell types is indicated next to each motif. Dashed lines mark 1.0- and 1.1-fold motif enrichment.

plausible that inhibition of the RNAi pathway is the major cause of transcriptome changes in *Dicer1*^{-/-} oocytes.

The idea that low activity of miRNA-mediated mRNA degradation is responsible for the absence of a miRNA signature in *Dicer1*^{-/-} oocytes is supported by Suh et al. [1], who analyzed the maternal loss of *Dgcr8*, a component of the microprocessor complex involved in miRNA biogenesis. *Dgcr8*^{-/-} oocytes show the same depletion of miRNAs as *Dicer1*^{-/-} oocytes, yet the transcriptome of *Dgcr8*^{-/-} oocytes is more similar to the wild-type, and mice with *Dgcr8*^{-/-} oocytes are fertile, showing no meiotic spindle defects reported for *Dicer1*^{-/-} and *Ago2*^{-/-} oocytes. Therefore, the sterile phenotype of *Dicer1*^{-/-} oocytes [6] and [12] is likely due to misregulation of genes controlled by endo-siRNAs [8].

Endogenous miRNAs Poorly Repress Cognate mRNAs

To understand the function of maternal miRNAs, we used three sets of reporter mRNAs carrying binding sites for the endogenous miRNAs let-7a and miR-30c. let-7 is the most abundant miRNA family in the oocyte (~30% of maternal miRNAs [8], [12] and [16]). The miR-30 family is less abundant; it represents ~8% of maternal miRNAs, as suggested by reverse transcriptase-polymerase chain reaction (RT-PCR) [12]. The deep-sequencing data suggest a lower abundance (~2.4% [8]), but such estimates are prone to errors [18].

To assess let-7 activity during oocyte growth and meiotic maturation, we used firefly luciferase reporters (Figure 2A) carrying a lin-41 fragment with two natural bulged let-7 binding sites (FL-2xlet-7), which were mutated in the control (FL-control) [19]. Because fully grown GV oocytes and MII eggs are transcriptionally quiescent, we microinjected in vitro-synthesized mRNAs instead of plasmid reporters. First, we compared let-7-mediated repression of FL-2xlet-7 mRNA microinjected into meiotically incompetent oocytes with repression of the FL-2xlet-7 plasmid or synthetic FL-2xlet-7 mRNA transfected into NIH 3T3 cells. FL-

2xlet-7 expression was reduced by ~40% relative to FL-control in oocytes (Figure 2B). Although this was less than repression of FL-2xlet-7 reporters in NIH 3T3 cells (~50%, Figure 2B), it showed that reporter mRNA is repressed by endogenous let-7 in small, growing oocytes.

When FL-2xlet-7 mRNA was microinjected into fully grown GV oocytes, we observed inefficient let-7 repression, which was also found upon meiotic maturation (Figure 2C).

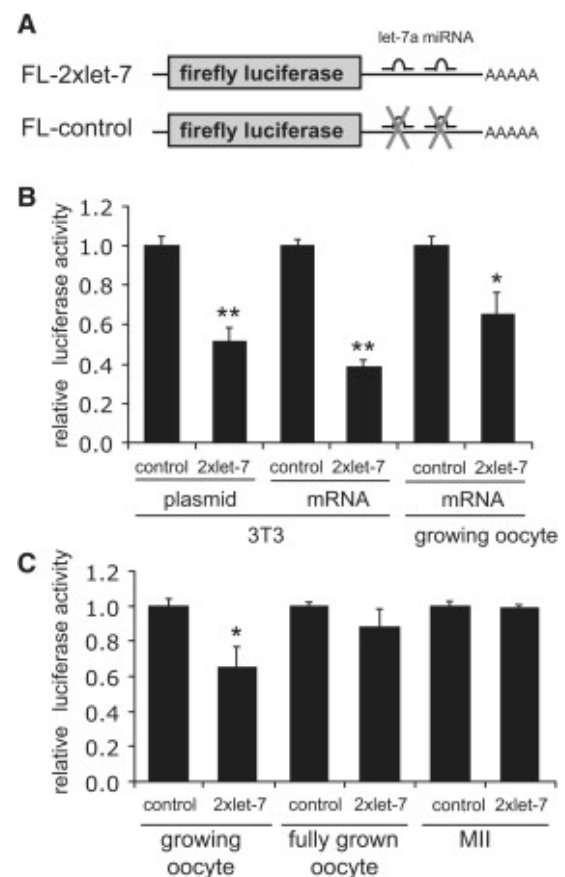


Figure 2. FL-2xlet-7 Reporter Analysis (A) Schematic drawing of reporters used in the experiments presented in Figure 2. (B) Relative firefly luciferase reporter activity in NIH 3T3 cells and growing oocytes. NIH 3T3 cells were transfected with reporter plasmids or mRNAs, and small, growing oocytes obtained from 13-day-old mice were microinjected with reporter mRNAs as described in the Experimental Procedures. Firefly luciferase reporter activities were normalized to the coinjected *Renilla* luciferase control and are shown relative to FL-control, which was set to one. The experiment was performed three times, and similar results were obtained in each case. Shown are data (mean ± standard error of the mean [SEM]) from one experiment. (C) Relative firefly luciferase reporter activity in growing oocytes obtained from 13-day-old mice, fully grown GV oocytes, and oocytes matured to metaphase II (MII). Data are presented as the mean ± SEM from six independent experiments. **p* < 0.05, ***p* < 0.01 compared to control by analysis of variance.

This was unlikely due to insufficient amounts of endogenous let-7 miRNA because delivering the FL-2xlet-7 mRNA with a 50 molar excess of let-7a miRNA did not, in contrast to NIH 3T3 cells, improve reporter repression (Figure S2A). Likewise, a 50 molar excess of let-7a antagomir did not increase FL-2xlet-7 expression in oocytes but did in NIH 3T3 cells (Figure S2B).

To explore further let-7 function in oocytes, we obtained another set of reporters (Figure 3A), which contained three bulged let-7 sites (RL-3xB let-7) or a single perfectly complementary let-7 site (RL-1xP let-7) downstream of the *Renilla* luciferase coding sequence [20]. These two reporters are repressed to the same extent in different cell lines, but by different mechanisms [4]. The RL-1xP let-7 is cleaved by AGO2 loaded with let-7 in the middle of the duplex. The bulged sites of RL-3xB let-7 mediate translational repression and subsequent mRNA degradation. To extend the analysis to other miRNAs, we produced a similar set of reporters for miR-30c (Figure 3A; Supplemental Experimental Procedures).

Our results showed that repression of all miRNA-targeted reporters was reduced during oocyte growth (Figures 3B–3D) despite a 3- and 5-fold increase in the amount of miR-30 and let-7, respectively, during oocyte growth [12]. This repression was presumably miRNA mediated because reporters harboring mutated miRNA binding sites (RL-3xM let-7 and RL-4xM miR-30) were not repressed (Figures 3B–3D). Repression of perfectly complementary reporters was always significantly greater than that of their bulged versions, contrasting with data from cell lines where bulged reporters were repressed either more (Figure S3) or equally as well [4]. This finding suggests that RNAi-like cleavage by miRNAs loaded on the AGO2-RISC complex is less affected during oocyte growth than translational repression, which is typical for most natural mammalian miRNA targets. Target site accessibility probably partially influences reduced repression of all reporters; our data show that siRNAs target

3'UTR sequences less efficiently in the oocyte when compared to somatic cells or siRNAs targeting the coding sequence (Figure S4).

The miR-30 reporter was consistently better repressed than the let-7 reporter. This finding was unexpected because let-7 family constitutes ~30% of maternal miRNAs, whereas miR-30 mRNAs are several times less abundant [8] and [12]. An additional miR-30 binding site in the bulged miR-30 reporter could explain its better repression relative to the bulged let-7 reporter. However, this cannot explain differences between RL-1xP let-7 and RL-1xP miR-30 reporters. This difference may stem from secondary structures of miRNA binding sites or may reflect yet-unknown let-7-specific regulation.

Repression of the RL-4xB miR-30 reporter could involve miRNA-mediated translational repression, miRNA-mediated mRNA degradation, or a combination of both. Thus, we microinjected fully grown GV oocytes with the RL-4xB miR-30 reporter and assayed for luciferase activity and the relative amount of *Luc* mRNA (Figures 4A and 4B). Whereas RL-1xP miR-30 mRNA was reduced at protein and mRNA levels as expected, RL-4xB miR-30 luciferase activity was reduced ~50%, whereas there was negligible reduction in the amount of *Luc* mRNA. This observation suggests that the remaining miRNA-mediated translational repression is uncoupled from mRNA degradation in fully grown GV oocytes. Therefore, we tested whether miRNA-targeted mRNAs localize to P bodies, cytoplasmic foci involved in miRNA-mediated mRNA degradation [19] and [20]. We visualized let-7-targeted and nontargeted mRNAs via a MS2-YFP binding strategy [19]. Whereas the let-7-targeted and nontargeted reporters were uniformly distributed in the oocyte cytoplasm, only the reporter harboring functional let-7 miRNA binding sites was targeted to P bodies in NIH 3T3 cells (Figure 4C). This result is consistent with the loss of P bodies during oocyte growth [21].

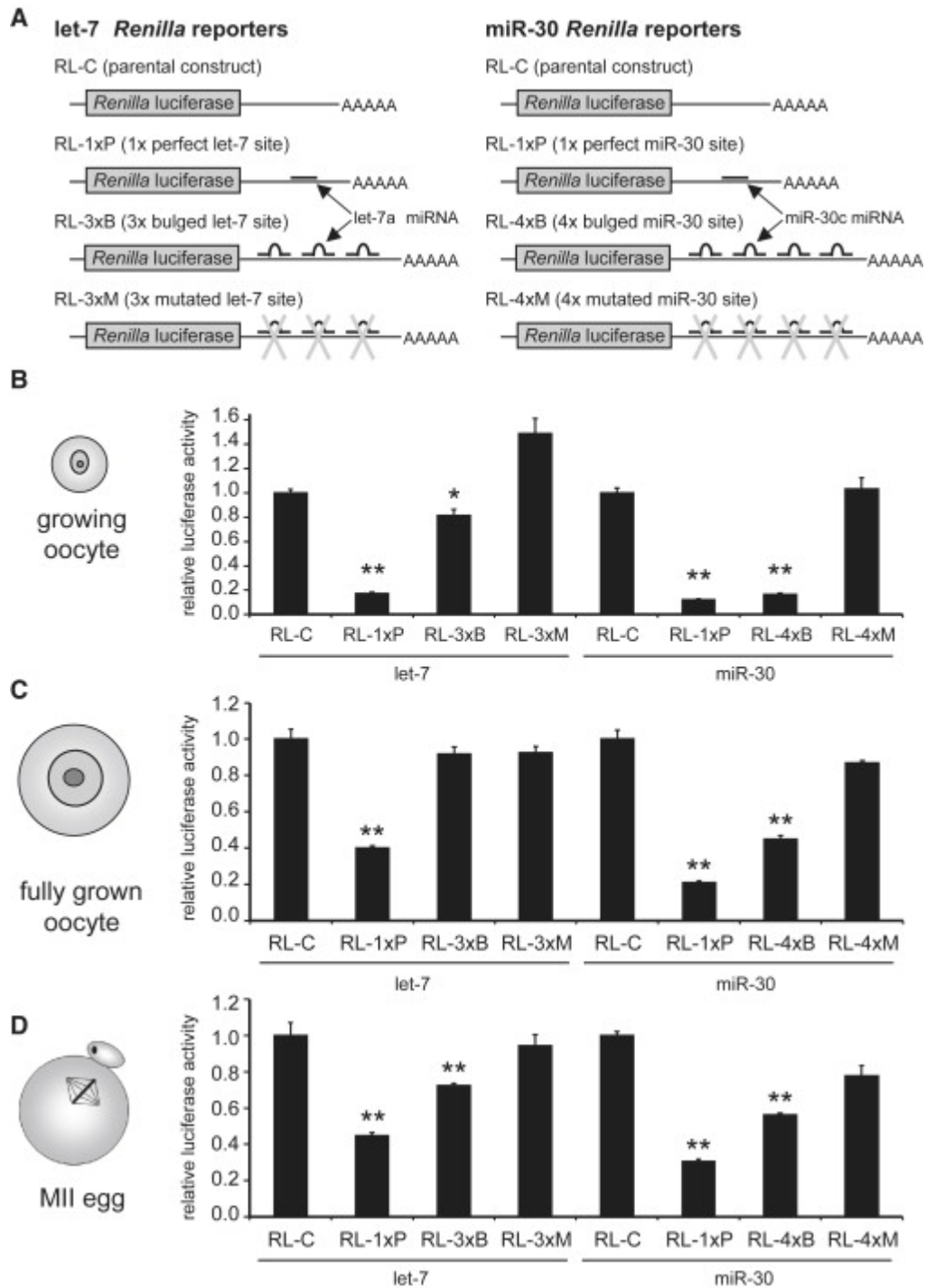


Figure 3. *Renilla* Luciferase let-7 and miR-30 Reporter Analysis (A) Schematic drawing of reporters used in experiments presented in Figure 3. (B–D) Relative *Renilla* luciferase reporter activities in growing oocytes (B), fully grown GV oocytes (C), and MII eggs (D). In vitro-produced reporter mRNAs were microinjected as described in the Experimental Procedures. *Renilla* luciferase reporter activities were normalized to coinjected firefly luciferase control and are shown relative to RL-C control, which was set to one for each studied miRNA. The experiment was performed three times, and similar results were obtained in each case. Shown are data (mean \pm SEM) from one experiment. * $p < 0.05$, ** $p < 0.01$ compared to control by analysis of variance.

Taken together, our data present a puzzling paradox: although mouse oocytes produce abundant RNA-induced silencing complex (RISC)-loaded miRNAs, their mRNA targets

are poorly repressed. Uncoupling the loaded RISC from translational repression, however, may be an elegant solution for selective inhibition of the miRNA pathway in the

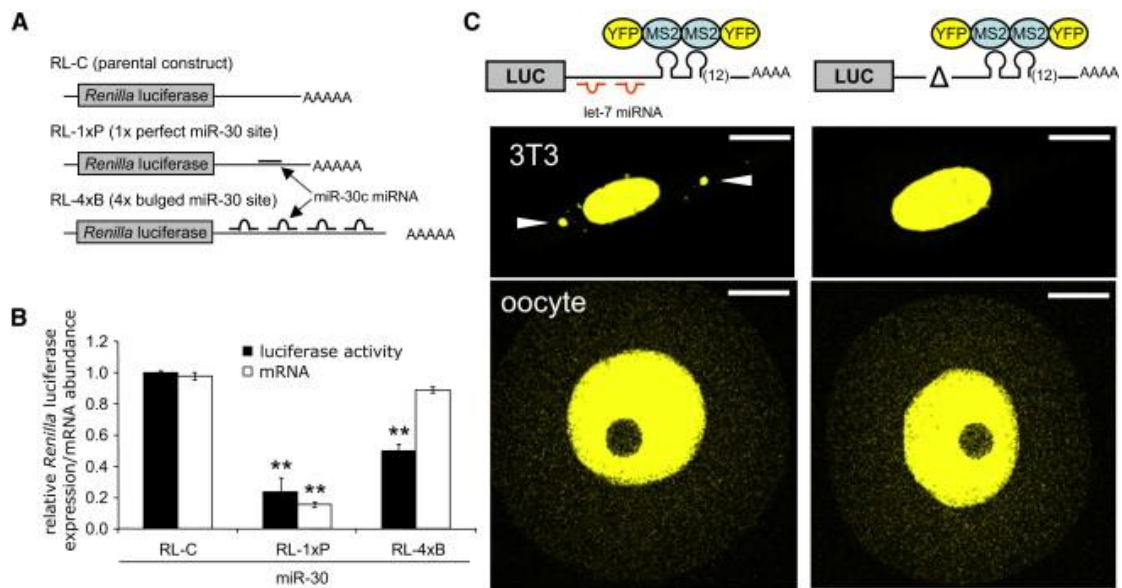


Figure 4. Repressed Bulged Luciferase Transcripts Are Not Degraded and Do Not Localize to P Bodies(A) Schematic of the miR-30 reporters.(B) Oocytes were microinjected with miR-30 reporter mRNAs, shown in (A), and after 1 day of culture, the relative reporter mRNA abundance was measured by quantitative reverse transcriptase-polymerase chain reaction, and reporter mRNA translation efficiency was monitored by the dual luciferase assay. *Renilla* luciferase reporter activities were normalized to coinjected firefly luciferase control and are shown relative to RL-C control, which was set to one. The experiment was performed three times, and similar results were obtained in each case. Shown are data (mean \pm SEM) from one experiment. * $p < 0.05$, ** $p < 0.01$ compared to control by analysis of variance.(C) mRNA harboring a let-7-binding sequence fails to localize to P bodies in oocytes. Schematic depiction of reporters bound and not bound by endogenous let-7 is shown on the top of the figure. Below are confocal images showing cytoplasmic localization of corresponding reporter mRNAs. NIH 3T3 cells (top) were transfected with the corresponding reporter plasmids, and fully grown GV oocytes (bottom) were microinjected with in vitro-transcribed mRNAs as described in the Experimental Procedures. Cotransfected (coinjected) YFP-MS2 fusion protein containing nuclear localization signal is retained in the cytoplasm upon binding to reporter transcripts, thus visualizing their localization [19]. White arrowheads depict P bodies visualized by let-7-targeted reporter mRNA in NIH 3T3 cells. Scale bars represent 20 μ m.

oocyte because the RNAi and miRNA pathways have common components, e.g., Dicer and AGO2. Reducing miRNA activity during oocyte growth may have two roles. First, the low activity of miRNA-mediated mRNA degradation, perhaps linked to the absence of P bodies, may contribute to mRNA stability and accumulation in growing oocytes. Second, downregulation of the miRNA pathway may be required for oocyte-to-zygote transition. Abundant maternal miRNAs, such as let-7, are found in somatic cells [22]. Efficient reprogramming of somatic cells into pluripotent stem cells requires large remodeling of miRNA expression, including downregulation of “somatic” miRNAs like let-7 (reviewed in [23]). Therefore, reducing miRNA activity may be associated with acquisition of developmental competence, and miRNAs may not be required until the zygotic genome activation is completed and the pluripotency program, which also controls miRNA expression [24], is established. From this

perspective, suppression of maternal miRNA function during oocyte growth may be the first event in reprogramming the differentiated oocyte into pluripotent blastomeres of the embryo.

Experimental Procedures

Animals and Oocytes

Fully grown GV *Dicer1*^{-/-} oocytes were obtained from 3A8 *Dicer1* conditional mice as previously described [6]. Meiotically incompetent oocytes; fully grown, GV-intact cumulus-enclosed oocytes; and MII eggs were collected, microinjected, and cultured as described [25], [26], [27] and [28]. All animal experiments were approved by the Institutional Animal Use and Care Committee and were consistent with National Institutes of Health guidelines. A more detailed overview is provided in the Supplemental Experimental Procedures.

mRNA Microarray Analysis

RNA was isolated from 25 fully grown GV-intact mouse oocytes and amplified as previously described [29] and [30]. Oocytes for each sample were collected from an individual mouse, and four samples were generated for each group. Biotinylated complementary RNA (cRNA) was fragmented and hybridized to the Affymetrix MOE430 v2 chip, which contains ~45,000 probe sets. All arrays yielded hybridization signals of comparable intensity and quality. Original CEL files were processed, and 3'UTR heptamer analysis was performed as described previously [4] and [5]. A detailed overview of bioinformatic analyses is provided in the Supplemental Experimental Procedures.

Reporter mRNA Preparation and Microinjection

Meiotically incompetent oocytes and fully grown GV oocytes were injected as described [28]. The same concentration of reporter mRNA was achieved in both stages by microinjecting incompetent oocytes with ~1.7 pl and fully grown GV oocytes with three times that amount (i.e., ~5 pl), because the volume of the meiotically incompetent oocytes used in these studies is about one-third of the fully grown GV oocyte. Five pl contained ~10⁵ molecules of the reporter. Reporter mRNAs were microinjected at the following concentrations: FL-2xlet-7 and FL-control reporter cRNA for let-7 at 0.2 µg/µl with spiked *Renilla* luciferase mRNA at 0.05 µg/µl; RL-C, RL-1xP, RL-3xB, and RL-3xM for let-7 reporter at 0.05 µg/µl with spiked firefly luciferase mRNA at 0.05 µg/µl; RL-C, RL-1xP, RL-4xB, and RL-4xM for miR-30 reporter at 0.05 µg/µl with spiked firefly luciferase mRNA at 0.05 µg/µl; let-7 reporter with 12xMS2-YFP binding sites and MS2-YFP at 1 µg/µl each; let-7 mimic or antagonist at 50:1 molar ratio to FL-2xlet-7 reporter mRNA. After microinjection, oocytes were cultured overnight in CZB containing 2.5 µM milrinone (to maintain meiotic arrest of meiotically competent oocytes) or CZB without milrinone (for meiotically incompetent oocytes) in an atmosphere of 5% CO₂ in air at 37°C before

they were processed for RT-PCR analysis, luciferase assay, or immunocytochemistry. A detailed description of analysis of microinjected oocytes is provided in the Supplemental Experimental Procedures.

Acknowledgments

We thank G.J. Hannon for conditional *Dicer1* knockout mice and firefly luciferase let-7 reporters, W. Filipowicz for *Renilla* luciferase let-7 reporters, and F. Duncan for help in preparing the RNA samples for microarray analysis. This research was supported by NIH grant HD22681 to R.M.S., EMBO SDIG project 1483, GACR P305/10/2215, Kontakt ME09039, and the Purkinje Fellowship to P.S.

References

1. Suh, N., Baehner, L., Moltzahn, F., Melton, C., Shenoy, A., Chen, J., and Blelloch, R. (2010). MicroRNA function is globally suppressed in mouse oocytes and early embryos. *Curr. Biol.*, in press. Published online January 28, 2010. 10.1016/j.cub.2009.12.044.
2. Lewis, B.P., Burge, C.B., and Bartel, D.P. (2005). Conserved seed pairing, often flanked by adenosines, indicates that thousands of human genes are microRNA targets. *Cell* 120, 15–20.
3. Giraldez, A.J., Mishima, Y., Rihel, J., Grocock, R.J., Van Dongen, S., Inoue, K., Enright, A.J., and Schier, A.F. (2006). Zebrafish MiR-430 promotes deadenylation and clearance of maternal mRNAs. *Science* 312, 75–79.
4. Schmitter, D., Filkowski, J., Sewer, A., Pillai, R.S., Oakeley, E.J., Zavolan, M., Svoboda, P., and Filipowicz, W. (2006). Effects of Dicer and Argonaute down-regulation on mRNA levels in human HEK293 cells. *Nucleic Acids Res.* 34, 4801–4815.
5. Sinkkonen, L., Hugenschmidt, T., Berninger, P., Gaidatzis, D., Mohn, F., Artus-Revel, C.G., Zavolan, M., Svoboda, P., and Filipowicz, W. (2008). MicroRNAs control de novo DNAmethylation through regulation of transcriptional repressors in mouse embryonic stem cells. *Nat. Struct. Mol. Biol.* 15, 259–267.

6. Murchison, E.P., Stein, P., Xuan, Z., Pan, H., Zhang, M.Q., Schultz, R.M., and Hannon, G.J. (2007). Critical roles for Dicer in the female germline. *Genes Dev.* 21, 682–693.
7. Su, Y.Q., Sugiura, K., Woo, Y., Wigglesworth, K., Kamdar, S., Affourtit, J., and Eppig, J.J. (2007). Selective degradation of transcripts during meiotic maturation of mouse oocytes. *Dev. Biol.* 302, 104–117.
8. Tam, O.H., Aravin, A.A., Stein, P., Girard, A., Murchison, E.P., Cheloufi, S., Hodges, E., Anger, M., Sachidanandam, R., Schultz, R.M., and Hannon, G.J. (2008). Pseudogene-derived small interfering RNAs regulate gene expression in mouse oocytes. *Nature* 453, 534–538.
9. Griffiths-Jones, S., Grocock, R.J., van Dongen, S., Bateman, A., and Enright, A.J. (2006). miRBase: MicroRNA sequences, targets and gene nomenclature. *Nucleic Acids Res.* 34 (Database issue), D140–D144.
10. van Dongen, S., Abreu-Goodger, C., and Enright, A.J. (2008). Detecting microRNA binding and siRNA off-target effects from expression data. *Nat. Methods* 5, 1023–1025.
11. Calabrese, J.M., Seila, A.C., Yeo, G.W., and Sharp, P.A. (2007). RNA sequence analysis defines Dicer's role in mouse embryonic stem cells. *Proc. Natl. Acad. Sci. USA* 104, 18097–18102.
12. Tang, F., Kaneda, M., O'Carroll, D., Hajkova, P., Barton, S.C., Sun, Y.A., Lee, C., Tarakhovskiy, A., Lao, K., and Surani, M.A. (2007). Maternal microRNAs are essential for mouse zygotic development. *Genes Dev.* 21, 644–648.
13. Kaneda, M., Tang, F., O'Carroll, D., Lao, K., and Surani, M.A. (2009). Essential role for Argonaute2 protein in mouse oogenesis. *Epigenetics Chromatin* 2, 9.
14. Puschendorf, M., Stein, P., Oakeley, E.J., Schultz, R.M., Peters, A.H., and Svoboda, P. (2006). Abundant transcripts from retrotransposons are unstable in fully grown mouse oocytes. *Biochem. Biophys. Res. Commun.* 347, 36–43.
15. Salisbury, J., Hutchison, K.W., Wigglesworth, K., Eppig, J.J., and Graber, J.H. (2009). Probe-level analysis of expression microarrays characterizes isoform-specific degradation during mouse oocyte maturation. *PLoS ONE* 4, e7479.
16. Watanabe, T., Totoki, Y., Toyoda, A., Kaneda, M., Kuramochi-Miyagawa, S., Obata, Y., Chiba, H., Kohara, Y., Kono, T., Nakano, T., et al. (2008). Endogenous siRNAs from naturally formed dsRNAs regulate transcripts in mouse oocytes. *Nature* 453, 539–543.
17. Jackson, A.L., Burchard, J., Schelter, J., Chau, B.N., Cleary, M., Lim, L., and Linsley, P.S. (2006). Widespread siRNA “off-target” transcript silencing mediated by seed region sequence complementarity. *RNA* 12, 1179–1187.
18. Linsen, S.E., de Wit, E., Janssens, G., Heeter, S., Chapman, L., Parkin, R.K., Fritz, B., Wyman, S.K., de Bruijn, E., Voest, E.E., et al. (2009). Limitations and possibilities of small RNA digital gene expression profiling. *Nat. Methods* 6, 474–476.
19. Liu, J., Valencia-Sanchez, M.A., Hannon, G.J., and Parker, R. (2005). MicroRNA-dependent localization of targeted mRNAs to mammalian P-bodies. *Nat. Cell Biol.* 7, 719–723.
20. Pillai, R.S., Bhattacharyya, S.N., Artus, C.G., Zoller, T., Cougot, N., Basyuk, E., Bertrand, E., and Filipowicz, W. (2005). Inhibition of translational initiation by Let-7 MicroRNA in human cells. *Science* 309, 1573–1576.
21. Flemr, M., Ma, J., Schultz, R.M., and Svoboda, P. (2010). P-body loss is concomitant with formation of an mRNA storage domain in mouse oocytes. *Biol. Reprod.*, in press. Published online January 14, 2010. 10.1095/biolreprod.109.082057.
22. Landgraf, P., Rusu, M., Sheridan, R., Sewer, A., Iovino, N., Aravin, A., Pfeffer, S., Rice, A., Kamphorst, A.O., Landthaler, M., et al. (2007). A mammalian microRNA expression atlas based on small RNA library sequencing. *Cell* 129, 1401–1414.
23. Gunaratne, P.H. (2009). Embryonic stem cell microRNAs: Defining factors in induced pluripotent (iPS) and cancer (CSC) stem cells? *Curr. Stem Cell Res. Ther.* 4, 168–177.

24. Marson, A., Levine, S.S., Cole, M.F., Frampton, G.M., Brambrink, T., Johnstone, S., Guenther, M.G., Johnston, W.K., Wernig, M., Newman, J., et al. (2008). Connecting microRNA genes to the core transcriptional regulatory circuitry of embryonic stem cells. *Cell* 134, 521–533.
25. Schultz, R.M., Montgomery, R.R., and Belanoff, J.R. (1983). Regulation of mouse oocyte meiotic maturation: Implication of a decrease in oocyte cAMP and protein dephosphorylation in commitment to resume meiosis. *Dev. Biol.* 97, 264–273.
26. Chatot, C.L., Ziomek, C.A., Bavister, B.D., Lewis, J.L., and Torres, I. (1989). An improved culture medium supports development of random-bred 1-cell mouse embryos in vitro. *J. Reprod. Fertil.* 86, 679–688.
27. Svoboda, P., Stein, P., and Schultz, R.M. (2001). RNAi in mouse oocytes and preimplantation embryos: Effectiveness of hairpin dsRNA. *Biochem. Biophys. Res. Commun.* 287, 1099–1104.
28. Kurasawa, S., Schultz, R.M., and Kopf, G.S. (1989). Egg-induced modifications of the zona pellucida of mouse eggs: Effects of microinjected inositol 1,4,5-trisphosphate. *Dev. Biol.* 133, 295–304.
29. Pan, H., O'Brien, M.J., Wigglesworth, K., Eppig, J.J., and Schultz, R.M. (2005). Transcript profiling during mouse oocyte development and the effect of gonadotropin priming and development in vitro. *Dev. Biol.* 286, 493–506.
30. Zeng, F., Baldwin, D.A., and Schultz, R.M. (2004). Transcript profiling during preimplantation mouse development. *Dev. Biol.* 272, 483–496.

Supplemental Information

MicroRNA Activity Is Suppressed in Mouse Oocytes

Jun Ma, Matyas Flemr, Paula Stein, Philipp Berninger, Radek Malik, Mihaela Zavolan, Petr Svoboda, and Richard M. Schultz

Supplemental Experimental Procedures

Animals and Oocytes

Fully-grown GV-intact mouse *Dicer1*^{-/-} oocytes were obtained from 3A8 *Dicer1* conditional animals [1], which were crossed to *Zp3*-Cre mice (Jackson Laboratories [2]) and their progeny were intercrossed to produce *Dicer1*^{flox/flox}; *Zp3*-Cre animals.

Fully grown, GV-intact cumulus-enclosed oocytes and MII eggs were collected as described [3]. Oocytes were collected in MEM/PVP (bicarbonate-free minimal essential medium [Earle's salt] supplemented with pyruvate [100 µg/ml], gentamicin [10 µg/mL], polyvinylpyrrolidone [PVP; 3 mg/ml], 25 mM HEPES at pH 7.3) containing 2.5 µM milrinone and allowed to mature in milrinone-free CZB [4] in an atmosphere of 5% CO₂ in air at 37°C for 16 h (MII). Meiotically incompetent oocytes were obtained from 13-day-old female mice as described [5]. All animal experiments were approved by the Institutional Animal Use and Care Committee and were consistent with National Institutes of Health guidelines.

Bioinformatic Analysis

The Affymetrix Mouse Genome 430 2.0 Array CEL files were imported into the R software (<http://www.R-project.org>) using the BioConductor affy package [6]. The gcRMA algorithm [7] was used to correct the probe intensities for optical noise, to adjust for nonspecific binding and for quantile normalization. Normalized (gcRMA) microarray data were deposited in the GEO database (GSE17985). We obtained the log₂ fold change per gene as follows: To correct for technical bias of AU content on probe-level log₂ fold change as reported by Elkouss and Agami [8], we first fitted a lowest model of the probe log₂ fold change using the probe AU content. Afterwards, the probe set-level log₂ fold changes were defined as the median probe-level log₂ fold change and probe sets with more than two probes mapping ambiguously (more than one match) to the genome were removed from further analysis, as well as probe sets mapping to multiple genes. We took all remaining probe sets matching a given gene, and averaged their log₂ fold changes to obtain an expression change per gene. For sequence analyses, we selected for each gene the RefSeq [9] transcript with median 3' UTR length corresponding to that gene. Finally, only genes were considered where at least one probe set was called present in the experiment as expressed for further analysis.

To identify motifs whose frequency is significantly different in the 3'-UTRs of transcripts that are up-regulated in *Dicer1*^{-/-} oocytes relative to their frequency in the entire set of 3'-UTRs, we used a Bayesian model that we previously introduced for comparing miRNA frequencies between samples [10, 11]. Briefly, we estimate the posterior probabilities of the model that assumes that the

frequency of a given motif is different between two sets of transcripts (call this "different" model), and the model that assumes that the frequency is the same (call this "same" model), given the observed counts m and n of the motif among M and N total motifs in the two samples. We selected as significant those motifs that were enriched in the up-regulated set with a posterior probability of the "different" model > 0.99 .

Plasmids

FL-2x let-7 and FL Control

These plasmids were published by Liu et al. [12] and obtained from Gregory Hannon (Cold Spring Harbor Laboratory, NY). All reporters are driven by the CMV promoter and contain a T7 promoter allowing in vitro transcription to synthesis mRNAs.

Let-7 RL Reporters (RL-C, RL-1xP, RL-3xB, and RL-3xM Let-7)

These reporters were published by Pillai et al. [10]. Plasmids were obtained from Witold Filipowicz (FMI Basel). All reporters are driven by the CMV promoter and also contain T7 promoter allowing for in vitro transcription. RL-3xB let-7 corresponds to the 3x Bulge A published previously [7, 13].

miR-30 RL Reporters (RL-C, RL-1xP, RL-4xB, and RL-4xM Let-7)

These four reporters were constructed from phRL-SV40 plasmid (Promega). Design miR-30 target sequences are displayed in Figure S3). miR-30 target sites were synthesized as DNA oligonucleotides flanked with Xba I and Not I restriction sites. Annealed fragments were digested and inserted into Xba I/Not I digested and dephosphorylated vector. Cloning oligonucleotides were as follows:

1xmiR-30c_perf_Xba_fwd CTAGAGCTGAGAGTGTAGGATGTTTACAGC

1xmiR-30c_perf_Not_rev GGCCGCTGTAAACATCCTACACTCTCAGCT

4xmiR-30c_bulge_Xba_fwd

CTAGAGCTGAGAGTGTCAATGTTTACAAGTTAGCTGAGAGTGTCAATGTTTACACGAT
TGCTGAGAGTGTCAATGTTTACATGCATGCTGAGAGTGTCAATGTTTACAGC

4xmiR-30c_bulge_Not_rev

GGCCGCTGTAAACATTGACACTCTCAGCATGCATGTAAACATTGACACTCTCAGCAAT
CGTGTAACATTGACACTCTCAGCTAACTTGTAACATTGACACTCTCAGCT

4xmiR-30c_bulge_mut_Xba_fwd

CTAGAGCTACGAGTGTCAATGTTACCAAGTTAGCTACGAGTGTCAATGTTACCACGAT
TGCTACGAGTGTCAATGTTACCATGCATGCTACGAGTGTCAATGTTACCAGC

4xmiR-30c_bulge_mut_Not_rev

GGCCGCTGGTAACATTGACACTCGTAGCATGCATGGTAACATTGACACTCGTAGCAAT
CGTGGTAACATTGACACTCGTAGCTAACTTGTAACATTGACACTCGTAGCT

Clones with inserts were screened by restriction digest and verified by sequencing.

Renilla Luciferase Reporter Plasmid with Mos 3'-UTR

Murine Mos 3'-UTR with the polyA signal was amplified from the mouse genomic DNA and used to replace SV40 PolyA in pHRL_SV40 plasmid (Promega). Mos 3'-UTR cloning primers were: Mos_3UTR_XbaI_Fwd: 5'-GACTCTAGACTCCATCGAGCCGATGTAG and Mos_3UTR_BamHI_Rev: 5'-GTAGGATCCTTAGGAAAAGCACTTCAGGCTG. PCR product was cleaved by BamHI and XbaI, gel extracted. pHRL-vector was digested with BamHI and XbaI to remove the original SV40 polyA sequence, ligated with the digested and purified PCR product and the ligation was transformed into DH5a competent cells. Several clones were screened by restriction digest and the final clone was verified by sequencing.

FL-2x let-7, FL Control with 12x MS2-YFP Binding Sites and MS2-YFP-NLS Construct

These plasmids were published by Liu et al. [12] and obtained from Gregory Hannon (Cold Spring Harbor Laboratory, NY). All reporters are driven by the CMV promoter and also contain T7 promoter allowing for in vitro transcription.

In Vitro Transcription of Reporters

To prepare reporter target mRNAs, plasmids were linearized and capped mRNAs were made by in vitro transcription with T7 mMESSAGE mMACHINE (Ambion) according to the manufacturer's instructions. Following in vitro transcription, template DNA was digested by adding RNase-free DNase and mRNA was polyadenylated by polyA tailing kit (Ambion). mRNA transcribed from pIVT-based construct terminates with a polyA33 tail obviating the need for further polyA tailing. Synthesized mRNA was then purified using a MEGAclear kit (Ambion), precipitated and re-dissolved in RNase-free water and stored at -80°C until use.

Cell Line Transfection with miR-30 Plasmid Reporters

Approximately 30,000 cells (HeLa & NIH 3T3 cells) or 60,000 cells (HEK293 cells) were plated per well in a 24-well plate (in 500 µl). One ng of a RL miR-30 reporter plasmid and 1 ng of the firefly luciferase control plasmid (pGL4, Promega) were transfected per well (the total DNA amount was adjusted with pBluescript to 500 ng per well). Cells were transfected with TurboFect (Fermentas) using ratio 1 µl/1 µg for HEK293 and NIH 3T3 and 2 µl/1 µg for HeLa cells in 100 µl of DMEM and the mixture was added to cells in 500 µl of DMEM + 10%FCS media (without changing media before transfection). Six hours later 1 ml of DMEM + 10%FCS was added and the cells were cultured until harvesting for luciferase activity, which was measured 48 h post-transfection.

Quantitative Real-Time PCR

Total RNA was isolated from 20 oocytes with RNAqueous-Micro kit (Ambion) and reverse transcription was carried out with Superscript II reverse transcriptase (Invitrogen) using random primers. The resulting cDNA was quantified by real-time PCR using an ABI Prism 7000 thermocycler (Applied Biosystems). Quantification was normalized to co-injected firefly luciferase mRNA or spiked GFP mRNA, respectively, within the log-linear phase of the amplification curve obtained for each probe/primer using the comparative CT method (ABI PRISM 7700 Sequence Detection System). The following primers were used: Renilla luciferase (probe 5'CAGGGCGATA TCCTC3'; forward primer 5'CGAGTGGCCTGACATCGA3'; reverse primer 5'ACGAAGAAGTT ATTCTCAAGCACCAT3'); Firefly luciferase (probe 5'CTGGTGGCCACACTAT3'; forward primer 5'GCGCAGCTTGCAAGACTATAAG3'; reverse primer 5'TTGTCGATGAGAGTGCTCT

TAGC3'); Mos (probe 5'CCGAGCCAAACCCTC3'; forward primer 5'GGGAACAGGTATGTCTGATGCA3'; reverse primer 5'CACCGTGGTAAGTAAGTGGCTTTATAACA3'); GFP (probe 5'GCTACCCCGACCACATGAAG3'; forward primer 5'CGGGCATGGCGGACTT3'; reverse primer 5'CAGCACGACTTCTTC3').

Luciferase Assay

Testing miR-30 Reporters in Somatic Cells

Luciferase assay was performed using the Dual Luciferase Reporter Assay kit (Promega) as per manufacturer's instructions. Luciferase activity was measured using the dual-injection Modulus microplate luminometer (Turner Biosystems). Renilla luciferase activity was normalized according to firefly luciferase activity expressed from pGL4.

Analysis of Microinjected Oocytes/Eggs

Oocytes/eggs were lysed directly in 1x passive lysis buffer and analyzed with a dual-luciferase reporter Assay system (Promega) on Monolight 2010 luminometer according to the manufacturer's instructions. For signal normalization, luciferase activity readout from non-injected oocytes/eggs was subtracted as background and Renilla/Firefly reporter luciferase activity was then normalized by co-injected control firefly/Renilla luciferase. On average, 10 oocytes were microinjected with each reporter. Two oocytes/eggs were assayed for luciferase activity and at least 3 measurements were conducted for each sample. Unless stated otherwise, experiments were repeated at least three times.

Visualization of miRNA Reporter mRNA Localization

To trace the localization of let-7 reporter mRNA in somatic cells, the MS2-YFP-NLS construct and plasmids expressing the reporter mRNA with or without let-7 recognition sequences were co-transfected into NIH 3T3 cells. These miRNA reporters also contain 12 copies of MS2-YFP binding sites in their 3' UTR and their intracellular localization can be indirectly visualized by binding of MS2-YFP fluorescence protein; the nuclear localization signal of MS2-YFP-NLS will direct unbound MS2-YFP-NLS into the nucleus. After 1 day of culture cells were fixed in 3.7% paraformaldehyde and reporter mRNA localization was monitored by laser confocal microscopy. To trace let-7 reporter mRNA localization in GV oocytes, let-7 reporter mRNAs and MS2-YFP-NLS mRNA were co-injected into GV oocytes. After 1 day of culture oocytes were fixed and processed for confocal microscopy as described above.

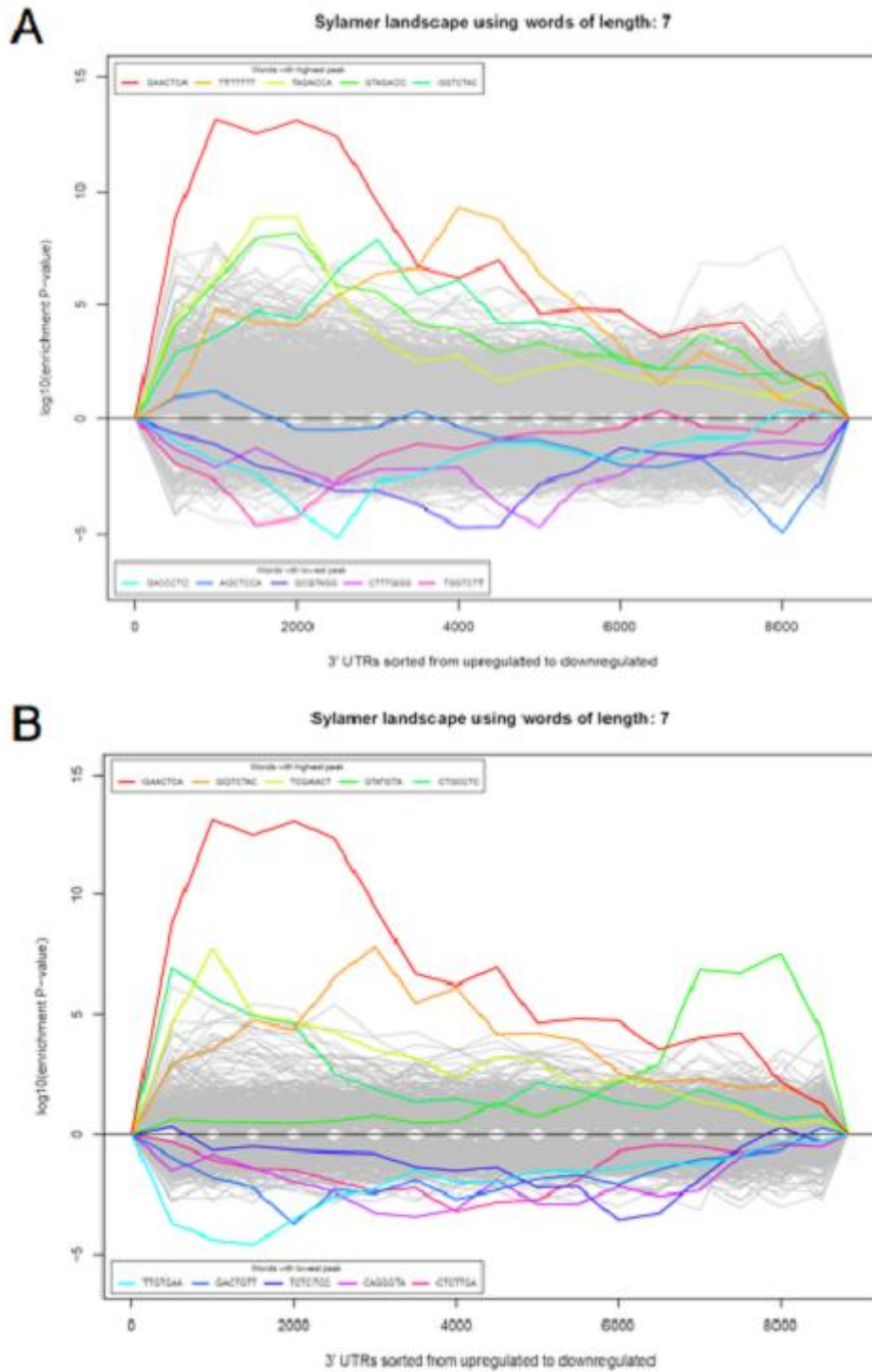


Figure S1. Sylamer Analysis of *Dicer1*^{-/-} Oocytes

(A) Top five motifs.

(B) Top five motifs complementary to known miRNAs. The x-axes represent the 3'UTRs of a fold-change-sorted transcript list from most upregulated to most downregulated (left to right). The y axes show the hypergeometric significance for each 7-mer (Positive values indicate enrichment and negative values indicate depletion).

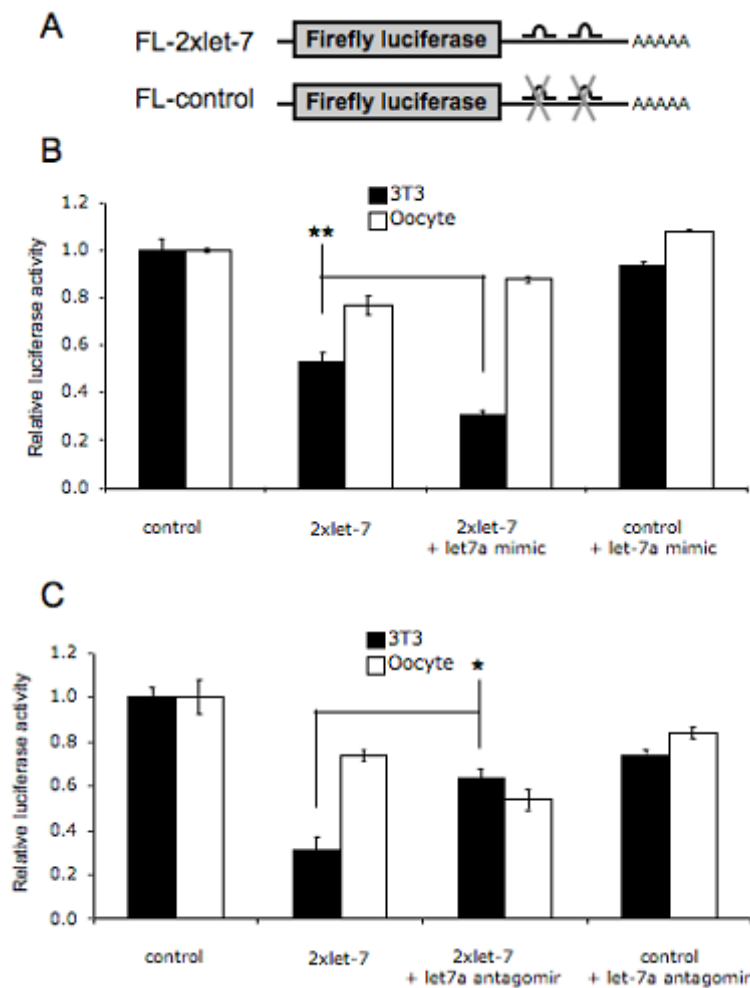


Figure S2. Effect of miRNA Mimic and Antagonist on miRNA-Mediated Repression in Mouse Oocytes and NIH 3T3 Cells

(A) Schematic depiction of FL-2xlet7a reporter and mutated control.

(B) FL-2xlet7a reporter and mutated control were co-injected with a 50 molar excess of a let7 mimic (5×10^6 molecules mimic to 10^5 molecules reporter) to test whether an excess of let7a can further repress let7 reporter expression in oocytes.

(C) FL-2xLet7a reporter and mutated control were co-injected with a 50 molar excess of let7 antagonist (5×10^6 molecules antagonist to 10^5 molecules reporter) to test whether competition for binding to endogenous let7a can relieve the mild repression on let7 reporter in mouse oocytes. As a control, let7a mimic and antagonist were also co-transfected with let7a reporter into NIH 3T3 cells. Shown (B, C) are the luciferase activities normalized to mutated controls, which were set to one. Experiments were performed twice and similar results were obtained in each case. Shown are data (mean \pm SEM) from one experiment.

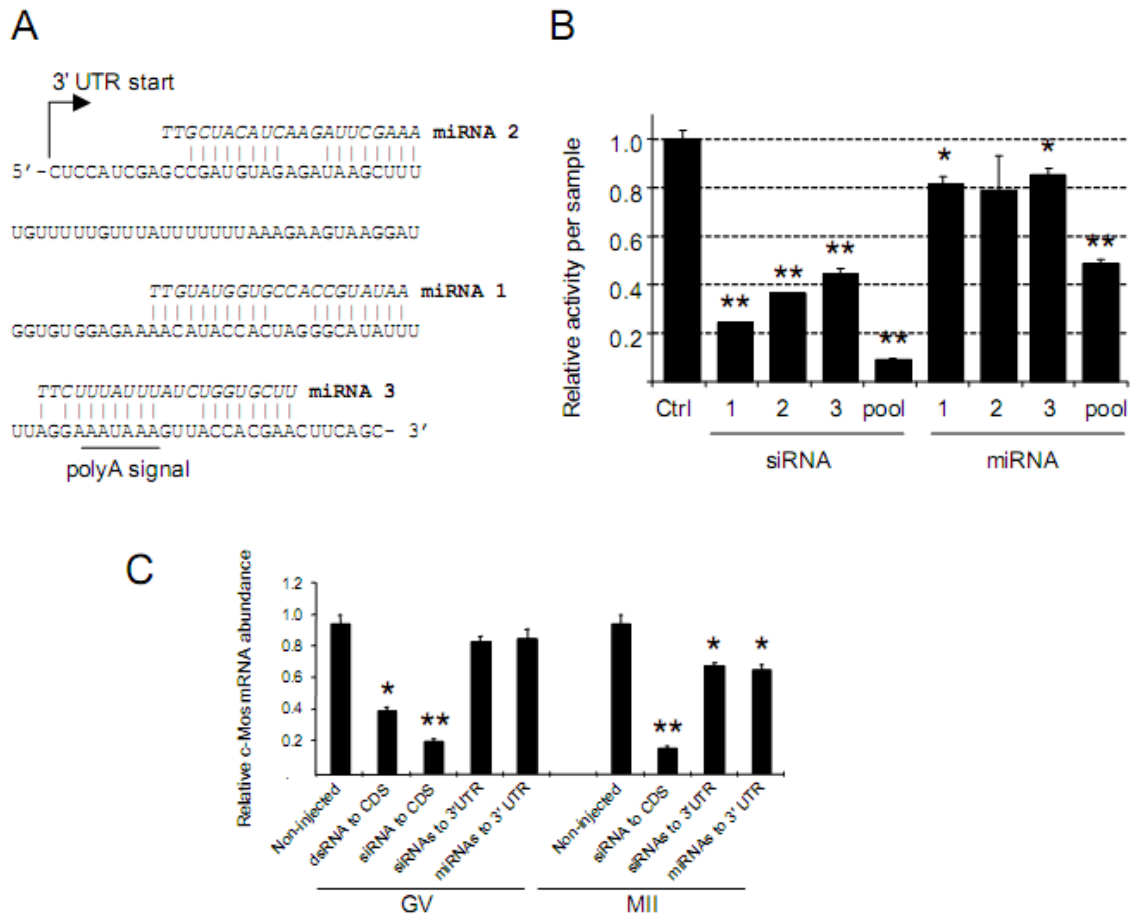


Figure S4. Analysis of miRNA-Like siRNAs Targeting Mos 3' UTR

(A) Positions of three different siRNAs, which were designed using BIOPREDSi (<http://www.biopredsi.org>) and RNAXs (<http://rna.tbi.univie.ac.at/cgi-bin/RNAXs>) prediction algorithms and which contain a central bulge that should prevent direct AGO2-mediated mRNA cleavage.

(B) Relative effect of miRNAs (with the central bulge) and siRNAs (perfectly complementary) on a reporter carrying Renilla luciferase coding sequence followed by Mos 3'UTR. Short RNAs were transfected either individually at 33 nM concentration or as a pool of all three with total siRNA/miRNA concentration of 33 nM. Renilla luciferase activity was assayed 24 h post-transfection and was normalized according to co-transfected firefly luciferase reporter (pGL4) and activity of Renilla-Mos reporter is shown relative to the phRL_SV40 parental construct whose activity was set to one.

(C) To test the effect of miRNAs on stability of endogenous transcripts, three sets of miRNAs and siRNAs targeting the same region of Mos mRNA 3' UTR were designed and synthesized. As a positive control, 0.5 kb dsRNA [1] and siRNA targeting Mos coding sequence (5'-UUUAUACACCGAGCCAAACCCUUU-3') were also prepared in the same manner. Fully-grown GV oocytes were microinjected with ~5 μ l 0.2 μ g/ μ l Mos specific dsRNA/siRNAs/miRNAs. After 1 day of culture in the presence of milrinone-containing medium, a portion of injected oocytes was assayed for the relative abundance of Mos mRNA by qRT-PCR. The remainder were transferred to milrinone-free medium and allowed to mature to MII at which time they were assayed for the relative abundance of Mos mRNA by qRT-PCR.

Table S1. Top 50 Heptamer Motifs from 3'UTR Analysis of Transcripts Upregulated in Dicer1^{-/-} Oocytes and Dicer1^{-/-} ES Cells

motif	oocyte KO			ES KO		
	enrichment	count	posterior probability	enrichment	count	posterior probability
AAAAAAA	0.85849	4340	1.000000	0.95447	23914	0.999999
GAACUCA	1.67718	142	0.991577	0.99911	346	0.000017
UUUGUUU	1.24534	656	0.987467	1.03503	1954	0.000103
UAGACCA	1.84419	96	0.965774	0.96222	194	0.000015
GGAUUAA	1.83863	90	0.912191	0.99047	188	0.000013
UUGUUUU	1.24117	569	0.893747	1.03722	1713	0.000095
UUUUUUU	1.12564	1601	0.768888	0.98133	4923	0.000144
ACACACA	1.22703	537	0.590372	0.95068	1807	0.000307
CACACAC	1.23148	516	0.571013	0.95887	1734	0.000150
UUUUUUU	1.21452	528	0.327921	1.04792	1640	0.000159
GUAGACC	1.80136	72	0.266008	0.89457	140	0.000024
AAAGGCA	1.49510	139	0.276654	1.03941	390	0.000023
AACUCAC	1.63259	97	0.251964	1.00132	234	0.000014
UCAGAAA	1.40871	179	0.222040	1.02944	506	0.000024
GGAACUC	1.62561	90	0.127025	1.04947	241	0.000018
GGGAUUA	1.70811	76	0.125254	0.97470	168	0.000013
AAACCCU	1.49559	124	0.119762	0.95069	317	0.000024
CCUGGAA	1.40771	163	0.107816	0.98609	484	0.000021
GGUGGGG	0.64692	76	0.076881	0.87717	431	0.000546
AUUAAAAG	1.39228	163	0.069947	1.07146	487	0.000052
UGUAGAC	1.53117	104	0.066641	1.00511	265	0.000015
UCGAACU	2.48280	29	0.064763	0.76677	35	0.000018
AUAUAUA	1.61837	79	0.041265	1.04770	190	0.000015
CUGAUGA	0.51502	29	0.037995	0.76881	184	0.005185
CCACCAC	1.41455	136	0.034231	0.95857	372	0.000024
GCAGCAC	0.51750	29	0.033701	1.09469	240	0.000031
UGAGUUC	1.41256	136	0.032566	0.98646	379	0.000018
AUUUCUU	1.31727	201	0.031087	0.97710	565	0.000025
UUUCUUU	1.18642	465	0.028903	0.98113	1435	0.000044
GAUUAAA	1.44469	119	0.027662	0.98653	318	0.000017
UGUUUGU	1.24042	302	0.025641	1.05386	919	0.000077
UUUUCGA	2.40904	27	0.024013	1.05315	49	0.000007
CCUGUCC	0.66454	73	0.021999	0.98890	431	0.000020
GUUUUUU	1.23736	300	0.021576	1.01405	885	0.000029
UAUGUAG	1.50649	95	0.021239	0.99307	241	0.000014
UCUUUCU	1.26561	249	0.020533	0.97393	776	0.000033
AAGGCAA	1.51201	93	0.020393	0.95694	241	0.000018
UCUACAA	1.58397	77	0.019603	1.03892	206	0.000015
GGGUUUC	1.46981	104	0.018975	0.96981	268	0.000017
CUGCCUC	1.26455	247	0.018764	0.97690	725	0.000030
GGCCAGG	0.64118	60	0.018183	0.95392	367	0.000025
GGAGGAC	0.51345	26	0.017890	0.88583	185	0.000043
CUGGCCC	0.63812	57	0.014839	0.98669	373	0.000018
UGGUGGA	0.56078	34	0.014680	1.02945	254	0.000016
AGUGCUG	1.33821	162	0.014433	1.01676	453	0.000020
UAAAGGC	1.49944	90	0.013013	0.99908	237	0.000014
AGGAGGA	0.67062	70	0.012268	0.95350	427	0.000029
GAUAGAU	1.66106	60	0.011299	0.98421	132	0.000011
UAAAGAC	1.55048	76	0.010526	0.97777	193	0.000013
UUGUUUG	1.24316	256	0.010499	1.07518	786	0.000136

rank-sorted

motif	oocyte KO enrichment	count	posterior probability	ES KO enrichment	count	posterior probability
GCACUUU	0.9930	83	0.000032	1.6150	489	1.000000
AGCACUU	1.2508	120	0.000508	1.4954	545	1.000000
AAAAAAA	0.8585	4340	1.000000	0.9545	23914	0.999999
GCACUUA	0.9854	41	0.000023	1.6148	255	0.999928
UGCACUU	1.0039	81	0.000031	1.4025	415	0.998849
AAGCACU	1.1806	88	0.000094	1.3928	406	0.996707
CUCUCUC	0.9862	225	0.000053	0.8245	849	0.983451
UCUCUCU	1.0026	256	0.000056	0.8397	963	0.973735
GGCACUU	1.0137	54	0.000026	1.4354	277	0.903878
CACUUUA	1.1089	84	0.000047	1.3527	375	0.875415
UUACUCG	1.1393	10	0.000012	2.2425	66	0.833120
CUCGCAC	0.4872	5	0.000039	1.9576	69	0.169473
UGGCACU	1.0132	68	0.000029	1.3075	318	0.090182
UACUCGC	0.7878	5	0.000009	2.2410	47	0.078683
GCACUGU	0.8668	69	0.000058	1.2635	377	0.048291
AUGCACU	1.3394	69	0.000343	1.3395	250	0.044010
UUGCACU	1.0105	67	0.000028	1.2922	312	0.030631
CACUUAC	1.0887	43	0.000026	1.3728	210	0.034098
CUGCACU	1.0024	80	0.000031	1.2425	374	0.016254
UUUGCAC	1.1025	83	0.000045	1.2525	349	0.015815
CAGCACU	1.0162	113	0.000037	1.1880	496	0.006690
GCAGUGU	0.8643	81	0.000073	1.2086	413	0.006138
GCACUUG	1.2140	50	0.000056	1.3132	215	0.005745
CUGAUGA	0.5150	29	0.037995	0.7688	184	0.005185
GCACUUG	1.1638	84	0.000074	1.2356	326	0.004777
GAGCCUU	1.0225	70	0.000029	0.7650	210	0.004366
ACUCGCA	0.9793	8	0.000010	1.7771	57	0.004074
AUAUAGA	0.9723	73	0.000030	0.8042	251	0.003781
GUUAUGU	0.9766	48	0.000024	1.2870	230	0.003762
CAAGGGU	1.0547	46	0.000025	0.7374	131	0.003682
GAAGALU	1.0203	89	0.000033	1.1944	425	0.003670
UCCUCCG	1.1292	129	0.000092	0.8409	384	0.003568
AACACAU	0.9515	60	0.000029	0.7865	205	0.003426
AAGAAGA	1.2167	144	0.000464	0.8491	419	0.003176
ACAAAAA	1.0511	186	0.000058	1.1322	778	0.003094
GUUUACA	0.9272	79	0.000038	1.2055	375	0.003004
CCCCACC	0.9048	130	0.000074	0.8629	500	0.002901
UGCACUG	0.9780	83	0.000032	1.2001	386	0.002775
AGUAUUU	1.2304	160	0.000608	1.1605	543	0.002522
UCAAUAA	1.0791	80	0.000038	0.8171	270	0.002505
AGGCACU	0.9141	54	0.000031	1.2326	295	0.002364
UCACACU	1.0407	69	0.000030	1.2187	314	0.001953
AUUGCAC	0.9759	34	0.000020	1.3187	175	0.001940
CAGUAIU	1.0396	93	0.000035	1.1875	397	0.001842
UCGCACA	0.7406	7	0.000013	1.6771	60	0.001821
CCACCCC	0.8165	107	0.000329	0.8650	470	0.001783
UGUCUUU	1.0705	171	0.000065	1.1332	682	0.001696
GAGCACU	1.0039	61	0.000027	1.2249	291	0.001655
GCACUAA	0.4970	15	0.001167	1.3386	155	0.001640
AGCCCCA	0.8949	78	0.000049	0.8344	305	0.001599

rank-sorted

Table S2. Highly Abundant miRNAs and Their Seed Motifs in Mouse Oocytes and ES Cells

miRNA	sequence	oocyte deep sequencing		ES deep sequencing		seed motifs
		# of clones	frequency	# of clones	frequency	
mmu-let-7a	UGAGGUAGUAAGUUGUAUAGUU	20927	4.02%	2	0.00%	UGAGGUA
mmu-let-7b	UGAGGUAGUAAGUUGUGUGUU	17124	3.29%	1	0.00%	GAGGUAG
mmu-let-7c	UGAGGUAGUAAGUUGUAUUGUU	67931	13.07%	9	0.01%	AGGUAGU
mmu-let-7d	AGAGGUAGUAAGUUGCAUAGUU	8601	1.65%	5	0.01%	0.02%
mmu-let-7e	UGAGGUAGUAAGUUGUAUAGUU	3416	0.66%			
mmu-let-7f	UGAGGUAGUAAGUUGUAUAGUU	22877	4.40%			
mmu-let-7g	UGAGGUAGUAAGUUGUACAGUU	13048	2.51%			
mmu-let-7i	UGAGGUAGUAAGUUGUGUGUU	6748	1.30%			
mmu-miR-322	CAGCAGCAAGUC AUGUUUGGA	45012	8.66%	42	0.05%	UAGCAGC
mmu-miR-103	AGCAGCAUUGUACAGGUCUAUGA	12036	2.31%	83	0.09%	AGCAGCA
mmu-miR-15a	UAGCAGCACAUAAUUGUUUGUU	1056	0.20%	234	0.26%	
mmu-miR-15b	UAGCAGCACAUAC AUGUUUACA	2950	0.57%	1961	2.15%	
mmu-miR-16	UAGCAGCACGUA AAUUAUUGUCG	19697	3.77%	1618	1.78%	4.47%
mmu-miR-195	UAGCAGCACAGA AAUUAUUGUC	1089	0.21%	38	0.04%	
mmu-miR-497	CAGCAGCACAUUGUUUGUA	1140	0.22%	80	0.09%	
mmu-miR-503	UAGCAGCGGAA CAGUACUGCAG	19159	3.68%	19	0.02%	
mmu-miR-21	UAGCUUACAGACUGAUGUUUGA	14691	2.83%	4222	4.64%	UAGCUUA
mmu-miR-22	AAGCUGCCAGUU GAAGAACUGU	29153	5.61%	109	0.12%	AAGCUGC
mmu-miR-17	CAAAGUGCUUACAGUGCAGGUG	3535	0.68%	1152	1.26%	AAAGUGC
mmu-miR-106a	CAAAGUGCUAACAGUGCAGGUG			786	0.86%	UAAGUGC
mmu-miR-106b	UAAAGUGCUGACAGUGCAGAU	475	0.09%	599	0.66%	AAGUGCU
mmu-miR-20a	UAAAGUGCUUAGAGUGCAGGUG	10888	2.09%	1002	1.10%	5.42%
mmu-miR-20b	CAAAGUGCUCAUAGUGCAGGUG	11	0.00%	1015	1.11%	
mmu-miR-93	CAAAGUGCUGUU CGUGCAGGUG	5868	1.13%	378	0.42%	
mmu-miR-290	AAAGUGCCGCC UAGUUUAAAGCCC	52	0.01%	2760	3.03%	
mmu-miR-291a	AAAGUGCUUCCACUUUGUGUC	40	0.01%	2161	2.37%	
mmu-miR-291b	AAAGUGCAUCCAUUUUGUUUGU	80	0.02%	154	0.17%	
mmu-miR-292	AAAGUGCCGCCAGGUUUUGAGUGU	453	0.09%	3108	3.41%	21.21%
mmu-miR-293	AGUGCCGCAGAUUUUGUAGUGU	17	0.00%	5744	6.31%	
mmu-miR-294	AAAGUGCUUCCUUUUUGUGUGU	474	0.09%	2902	3.19%	
mmu-miR-295	AAAGUGCUACUACUUUUAGAGUCU	168	0.03%	2488	2.73%	
mmu-miR-302a	UAAAGUCUUCCAUUUUUUGUGA			87	0.07%	
mmu-miR-302b	UAAAGUCUUCCAUUUUUUAGUAG		absent	87	0.10%	0.46%
mmu-miR-302c	AAGUGCUUCCAUUUUUUAGUAG			9	0.01%	
mmu-miR-302d	UAAAGUCUUCCAUUUUUAGAGUGU			254	0.28%	
mmu-miR-30a	UGUAAACAUCUUCGACUGGAAG	2690	0.52%	90	0.10%	UGUAAAC
mmu-miR-30b	UGUAAACAUCUUCACUCAGUCU	813	0.16%	1208	1.33%	GUAAACA
mmu-miR-30c	UGUAAACAUCUUCACUCUCAGC	901	0.17%	1662	1.83%	3.47%
mmu-miR-30d	UGUAAACAUCUUCGACUGGAAG	3232	0.62%	33	0.04%	
mmu-miR-30e	UGUAAACAUCUUCUAGACUGGAAG	4711	0.91%	170	0.19%	
mmu-miR-25	CAUUGCACUUGUCUUGGUCUGA	1386	0.27%	766	0.84%	AUUGCAC
mmu-miR-32	UAUUGCACAUUAUAAGUUGCA	175	0.03%	181	0.20%	
mmu-miR-92	UAUUGCACUUGUCUUGGUCUGU	2962	0.57%	2572	2.82%	4.58%
mmu-miR-363	AAUUGCACGGUAUCCAUUCUGA			350	0.38%	
mmu-miR-367	AAUUGCACUUAUUAUCAUUGUGA			300	0.33%	
mmu-miR-19a	UGUGCAAUUCUAUGCAAACUGA	102	0.02%	1520	1.67%	UGUGCAA
mmu-miR-19b	UGUGCAAUUCUAUGCAAACUGA	584	0.11%	9348	10.26%	11.93%
total number of miRNA clones in deep sequencing:		519929		91082		

individual miRNA frequency > 2%
 group miRNA frequency > 4%

Table S3. Motifs Highly Relevant for Mouse Oocytes and Early Embryos

miRNA (class)	frequency		seed motif	motif	ES KO		posterior probability	oocyte KO		posterior probability
	ES	OO			enrichment	count		enrichment	count	
Let-7 family	0.02	30.90	UGAGGUA	UACCUCA	0.916895	207	0.000027	1.054236	81	0.000029
miR-16 and related	4.47	19.63	AGCAGCA	UGCUGCU	1.021248	651	0.000026	0.99132	169	0.000045
miR-322	0.05	8.66	CAGCAGC	GCUGCUG	1.01444	632	0.000024	0.947575	157	0.000054
miR-22	0.12	5.61	AAGCUGC	GCUGCUU	1.075518	457	0.000052	1.040452	119	0.000041
miR-290 and 17-106	26.63	4.00	AAAGUGC	GCACUUU	1.615044	489	1.000000	0.992993	83	0.000032
miR-30 family	3.47	2.37	UGUAAAC	GUUUACA	1.20555	375	0.003004	0.927164	79	0.000038
miR-25 and related	4.58	0.87	AUUGCAC	GUGCAAU	1.239997	191	0.000388	0.747795	31	0.000076
miR-19 family	11.93	0.13	GUGCAA	UUUGCAC	1.252541	349	0.015815	1.102534	83	0.000045

Table S4. Upregulated and Downregulated mRNAs Matching Endo-siRNAs

endo-siRNA matching in Dicer-/- oocytes					
up-regulated transcripts			down-regulated transcripts		
Gene	RefSeq	hits	Gene	RefSeq	hits
Kif4	NM_008446	83	Rora	NM_013646	17
Ccdc82	NM_025534	48	Dcun1d5	NM_029775	6
Trim71	NM_001042503	44	Neb	NM_010889	4
Optn	NM_181848	25	Cdk7	NM_009874	3
Coro1c	NM_011779	21	Styk1	NM_172891	1
Ptbp1	NM_001077363	20	Braf	NM_139294	1
Prc1	NM_145150	19			
Ube2l3	NM_009456	14			
Traip	NM_011634	12			
1110067D22Rik	NM_173752	11			
Sfrs4	NM_020587	8			
Ppp2r2b	NM_027531	8			
Hmga2	NM_010441	8			
Cdc14b	NM_001122989	8			
Oog4	NM_173773	7			
4930539E08Rik	NM_172450	6			
Rangap1	NM_011241	4			
Cacna1d	NM_028981	3			
Polr3f	NM_029763	2			
Mrpl9	NM_030116	2			
Kctd10	NM_026145	2			
Fbxo5	NM_025995	2			
BC034090	XM_993701	2			
Zmat3	NM_009517	1			
Vamp3	NM_009498	1			
Tubb5	NM_011655	1			
Trove2	NM_013835	1			
Tmlhe	NM_138758	1			
Ston2	NM_175367	1			
Smyd4	NM_001102611	1			
Mdc1	NM_001010833	1			
LOC675709	XM_984471	1			
Gtdc1	NM_172662	1			
Dmtf1	NM_001110327	1			
Cyb5d2	NM_001024926	1			
Bpnt1	NM_011794	1			
BC057893	NM_173033	1			
BC011426	NM_145490	1			
Ag1	NM_001081326	1			
Adsl	NM_009634	1			
9230110C19Rik	NM_199017	1			
2610029I01Rik	XM_001475329	1			

hit = 20 nucleotides of perfect complementarity

Supplemental References

1. Svoboda, P., Stein, P., Hayashi, H., and Schultz, R.M. (2000). Selective reduction of dormant maternal mRNAs in mouse oocytes by RNA interference. *Development (Cambridge, England)* 127, 4147-4156.
2. de Vries, W.N., Binns, L.T., Fancher, K.S., Dean, J., Moore, R., Kemler, R., and Knowles, B.B. (2000). Expression of Cre recombinase in mouse oocytes: a means to study maternal effect genes. *Genesis* 26, 110-112.
3. Schultz, R.M., Montgomery, R.R., and Belanoff, J.R. (1983). Regulation of mouse oocyte meiotic maturation: implication of a decrease in oocyte cAMP and protein dephosphorylation in commitment to resume meiosis. *Developmental biology* 97, 264-273.
4. Chatot, C.L., Ziomek, C.A., Bavister, B.D., Lewis, J.L., and Torres, I. (1989). An improved culture medium supports development of random-bred 1-cell mouse embryos in vitro. *J Reprod Fertil* 86, 679-688.
5. Svoboda, P., Stein, P., and Schultz, R.M. (2001). RNAi in mouse oocytes and preimplantation embryos: effectiveness of hairpin dsRNA. *Biochemical and biophysical research communications* 287, 1099-1104.
6. Gentleman, R.C., Carey, V.J., Bates, D.M., Bolstad, B., Dettling, M., Dudoit, S., Ellis, B., Gautier, L., Ge, Y., Gentry, J., et al. (2004). Bioconductor: open software development for computational biology and bioinformatics. *Genome biology* 5, R80.
7. Wu, Z., and Irizarry, R.A. (2004). Preprocessing of oligonucleotide array data. *Nature biotechnology* 22, 656-658; author reply 658.
8. Elkon, R., and Agami, R. (2008). Removal of AU bias from microarray mRNA expression data enhances computational identification of active microRNAs. *PLoS computational biology* 4, e1000189.
9. Pruitt, K.D., Tatusova, T., and Maglott, D.R. (2005). NCBI Reference Sequence (RefSeq): a curated non-redundant sequence database of genomes, transcripts and proteins. *Nucleic acids research* 33, D501-504.
10. Pillai, R.S., Bhattacharyya, S.N., Artus, C.G., Zoller, T., Cougot, N., Basyuk, E., Bertrand, E., and Filipowicz, W. (2005). Inhibition of translational initiation by Let-7 MicroRNA in human cells. *Science (New York, N.Y)* 309, 1573-1576.

SUPPLEMENT 5

Petr Svoboda and Matyas Flemr

The role of miRNAs and endogenous siRNAs in maternal-to-zygotic reprogramming and the establishment of pluripotency

(reprint from *EMBO Reports*. 2010 Aug;11(8):590-7)

My contribution to this work:

I generated the experimental data for Fig.4, I performed the computational analysis for Fig.1 and I helped prepare the manuscript.

The role of miRNAs and endogenous siRNAs in maternal-to-zygotic reprogramming and the establishment of pluripotency

Petr Svoboda¹ & Matyas Flemr¹

1. Institute of Molecular Genetics AS CR, Videnska 1083, 14220 Praha 4, Czech Republic

Correspondence to:

Petr Svoboda, Tel: +420 241063147; Fax: +420 224310955;

E-mail: svobodap@img.cas.cz

Received 31 March 2010; Accepted 18 June 2010

RNA silencing is a complex of mechanisms that regulate gene expression through small RNA molecules. The microRNA (miRNA) pathway is the most common of these in mammals. Genome-encoded miRNAs suppress translation in a sequence-specific manner and facilitate shifts in gene expression during developmental transitions. Here, we discuss the role of miRNAs in oocyte-to-zygote transition and in the control of pluripotency. Existing data suggest a common principle involving miRNAs in defining pluripotent and differentiated cells. RNA silencing pathways also rapidly evolve, resulting in many unique features of RNA silencing in different taxonomic groups. This is exemplified in the mouse model of oocyte-to-zygote transition, in which the endogenous RNA interference pathway has acquired a novel role in regulating protein-coding genes, while the miRNA pathway has become transiently suppressed.

Keywords:

pluripotency, RNAi, oocyte, Dicer, Dgcr8, miR-290

See Glossary for abbreviations used in this article.

Introduction

Pluripotency is the ability of cells to differentiate into any fetal or adult cell type. Pluripotency is formed during early development and self-renewing pluripotent cells can be maintained in culture under specific conditions. Pluripotency in mammals is most often studied in embryonic stem cells (ESCs), which are derived from the inner cell

mass of the blastocyst (Smith, 2001), and induced pluripotent stem cells (iPSCs), which are formed after reprogramming gene expression in somatic cells with specific pluripotency factors (Takahashi & Yamanaka, 2006). The OCT4 (POU5F1), SOX2 and NANOG transcription factors form the core of a network responsible for the transcriptional control of ESC renewal and pluripotency (Boyer *et al*, 2005; Loh *et al*, 2006). Microarray data indicate that a

similar transcription factor network also forms in a stepwise manner upon mouse zygotic genome activation (ZGA; Zeng *et al*, 2004; Zeng & Schultz, 2005), which starts around 1.0 dpc during the early two-cell stage (the blastocyst, which is the source of ESCs, forms at 3.5 dpc). Thus, reprogramming of an oocyte into pluripotent blastomeres of an early embryo—here referred to as oocyte-to-zygote transition (OZT)—is a physiological analogy of the experimental reprogramming of somatic cells into iPSCs. In fact, the cytoplasm of an enucleated oocyte can induce pluripotency in the nuclei of somatic cells during nuclear transfer (reviewed in Gurdon & Melton, 2008), which is the basis of mammalian cloning (Wilmut *et al*, 1997). As there is no mRNA synthesis between the end of the mouse oocyte growth phase and the first zygotic cleavage, post-transcriptional mechanisms are essential for the natural formation of pluripotency.

Here, we review the role of mammalian miRNA and RNAi during OZT and in the control of pluripotency. MicroRNA and RNAi pathways use small RNA molecules as sequence-specific guides for translational repression and/or mRNA degradation (reviewed in Chapman & Carrington, 2007). Briefly, siRNAs are produced from long dsRNA by cleavage with RNase III Dicer. MicroRNAs originate as long primary transcripts with local hairpin structures, that are cleaved by the Microprocessor complex composed of DGCR8 and RNase III Drosha. MicroRNAs are produced from small hairpin precursors upon cleavage by Dicer. Small interfering RNAs and miRNAs are loaded on Argonaute (AGO) proteins, which mediate silencing effects (reviewed in Kim *et al*, 2009).

Animal miRNAs typically base-pair imperfectly with the 3'-UTR of target mRNAs and induce translational repression and/or mRNA degradation. MicroRNAs are the dominant class of short RNAs in mammalian cells—more than a thousand miRNAs with defined sequences have been identified and implicated in the regulation of many cellular processes (Kloosterman & Plasterk, 2006). It has been estimated that miRNAs could directly target more than half

of all mammalian genes (Friedman *et al*, 2009).

Target mRNA recognition involves the nearly perfect hybridization of the miRNA 5'-end, which nucleates the miRNA–mRNA interaction (Brennecke *et al*, 2005; Lai, 2002). Perfect base-pairing of a miRNA or siRNA results in the AGO2-mediated sequence-specific endonucleolytic cleavage of the target in the middle of the base-pairing sequence (Liu *et al*, 2004; Meister *et al*, 2004). However, miRNAs can induce substantial mRNA degradation even in the absence of extensive base-pairing to their targets (Bagga *et al*, 2005; Lim *et al*, 2005). This is a likely consequence of translational repression and the relocation of repressed mRNAs to cytoplasmic foci known as P-bodies (reviewed in Eulalio *et al*, 2007a). P-bodies harbour mRNAs, translational repressors, mRNA-binding proteins and components of the mRNA degradation machinery. It has been proposed that their formation is a consequence of miRNA activity (Eulalio *et al*, 2007b).

The role of microRNAs in pluripotent stem cells

The well-characterized ESC miRNome is dominated by miRNAs sharing a 5'-proximal AAGUGC motif (Babiarz *et al*, 2008; Houbaviy *et al*, 2003; Landgraf *et al*, 2007; Suh *et al*, 2004). These miRNAs (referred to hereafter as AAGUGC miRNAs) can be divided into three groups (Fig 1): (i) EEmiRC miRNAs, found in placental mammals (Houbaviy *et al*, 2005); (ii) the miR-17-92 cluster (and its paralogues), which is conserved across vertebrates and carries onco-miRs (reviewed in Mendell, 2008); and (iii) the miR-302/miR-467 group, including the miR-302 family in tetrapods and the miR-467 family in the mouse. In addition, there is a closely related group of miRNAs (Fig 1B) that are found in fish (miR-430 cluster) and amphibian embryos (miR-427), where they contribute to the degradation of maternal mRNAs (Giraldez *et al*, 2006; Lund *et al*, 2009). The miR-17-92 cluster group probably evolved independently as these miRNAs—in contrast to the other two groups—derive from the 5' arm of small hairpin and are not as GU-rich in the 3' end.

Two approaches have been taken to address the specific roles of miRNAs in mouse ESCs. Sinkkonen *et al* undertook a bioinformatic analysis of the transcriptome of *Dcr1*^{-/-} ESCs (Sinkkonen *et al*, 2008), while Wang *et al* screened rescue effects of individual miRNAs in *Dgcr8*^{-/-} ESCs (Wang *et al*, 2007). *Dcr1*^{-/-} analysis has revealed that the most significantly enriched motifs in the 3'UTRs of transcripts upregulated in *Dcr1*^{-/-} ESCs are sequences complementary to AAGUGC motifs. This implicates a dominant function for EEmiRC miRNAs among ESC miRNAs. Subsequent analysis has identified around 250 primary targets of EEmiRC miRNAs in ESCs (Sinkkonen *et al*, 2008), and *Rbl2* (*p130*) and *Cdkn1a* (*p21*) were verified as primary targets of EEmiRC miRNAs (Fig 2). RBL2 is a transcriptional repressor that suppresses expression of *de novo* DNA methyltransferases. Thus, in the

absence of EEmiRC miRNAs, elevated levels of RBL2 reduce levels of DNMT3A and DNMT3B. This causes DNA methylation defects during differentiation, whereby the *Oct4* promoter does not accumulate *de novo* DNA methylation (Benetti *et al*, 2008; Sinkkonen *et al*, 2008). Defective *de novo* DNA methylation probably contributes to differentiation defects in ESCs, similarly to a *Dnmt3a* and *Dnmt3b* double knockout (Chen *et al*, 2003). However, differentiation defects are not rescued by EEmiRC miRNAs (Wang *et al*, 2008), suggesting that the cause of differentiation defects includes the loss of other ESC miRNAs or perhaps miRNAs that appear and function during differentiation, such as miR-145 (Xu *et al*, 2009).

Studies of *Dcr1*^{-/-} and *Dgcr8*^{-/-} have also revealed that cell-cycle progression in ESCs is under the control of miRNAs. Sinkkonen

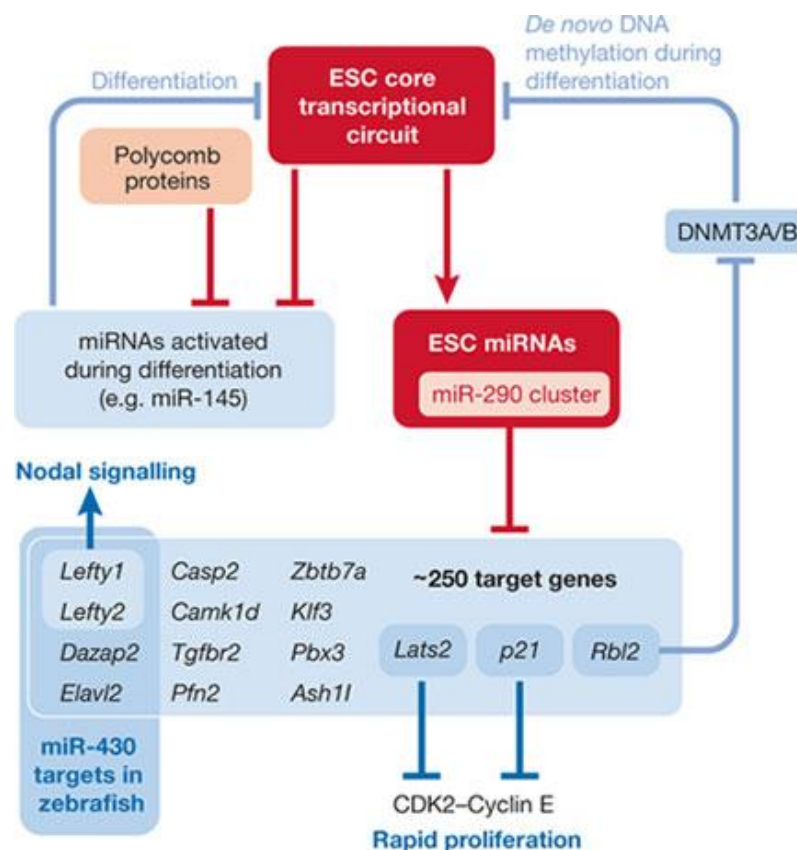


Figure 2. Roles of the miR-290 cluster in undifferentiated mouse embryonic stem cells. Red frames highlight two important components of control of gene expression in ESCs: the core pluripotency transcription factor network (ESC core transcriptional circuit), which also controls expression of the second component, ESC miRNAs. The miR-290 cluster dominates miRNA function in ESCs and regulates ~250 primary targets, some of which are shown here. Murine miR-290 have a role in several processes including cell-cycle regulation, nodal signalling and transcriptional regulation. The miR-290 cluster indirectly regulates *de novo* DNA methylation by targeting RBL2, a transcriptional repressor acting on *Dnmt3* genes. MicroRNAs—including miR-145 and others—also contribute to suppression of the ESC core transcriptional circuit during differentiation. The scheme and listed miR-290 targets are based on published data (Marson *et al*, 2008; Melton *et al*, 2010; Sinkkonen *et al*, 2008; Tay *et al*, 2008; Xu *et al*, 2009). ESC, embryonic stem cell.

et al reported that EEmiRC miRNAs regulate *p21* and that transfection of EEmiRC miRNAs partly rescues growth defects in *Dcr1*^{-/-} cells (Sinkkonen *et al*, 2008). Wang *et al* subsequently showed, in *Dgcr8*^{-/-} cells, that several ESC miRNAs designated ESCC contribute to the rescue of proliferation by the regulation of CDK2–cyclin E-dependent control of G1–S progression (Wang *et al*, 2008). ESCC miRNAs include EEmiRC miRNAs, members of the miR-17-92 cluster and an unrelated miR-223. MicroRNA-mediated control of proliferation also involves cyclin D1, which is targeted by miR-302 in human ESCs (Card *et al*, 2008).

Interestingly, despite the massive transcriptome remodeling in *Dcr1*^{-/-} ESCs, the loss of pluripotency is not accompanied by notable changes in the expression of the core pluripotency circuit factors (Sinkkonen *et al*, 2008). This implies that ESC miRNAs, the transcription of which is largely controlled by core pluripotency factors (Marson *et al*, 2008), do not form a feedback loop to maintain the core pluripotency factors and that the core pluripotency network is insufficient to maintain pluripotency in the absence of miRNAs. In addition to their role in the maintenance of pluripotency, EEmiRC miRNAs can also contribute to the establishment of pluripotency during the formation of iPSCs (Judson *et al*, 2009). miR291-3p, miR-294 and miR-295 increase the efficiency of reprogramming by pluripotency factors *Oct4*, *Sox2* and *Klf4*. Thus, AAGUGC miRNAs dominate miRNA activities in ESCs and have a broader relationship to the control of cell growth and differentiation.

The role of microRNAs and endo-siRNAs in OZT

Mouse ovarian oocytes are highly specialized cells that are arrested in the prophase of the first meiotic division. The fully grown mouse oocyte can resume meiosis during ovulation but arrests again at metaphase II and dies unless fertilized. Even if diploidized and parthenogenetically activated, a zygotic genome of entirely maternal origin cannot support normal embryonic development (Surani *et al*, 1984). The fertilized egg, however, transforms into a cleaving zygote,

the cells of which exhibit pluripotency. The factors required for genome reprogramming during OZT are present in the oocyte cytoplasm. OZT has two essential components: (i) control of stability and translation of maternal mRNAs and (ii) control of the transcriptional activation of zygotic genes. As no new mRNAs are produced before the two-cell stage (Zeng & Schultz, 2005), gene expression during OZT is mostly governed by post-transcriptional mechanisms such as reversible deadenylation coupled with transcriptional repression—which is the basis for controlling storage and recruitment of specific mRNAs for translation during meiosis and later (reviewed in Richter, 2007). RNA silencing pathways—that have essential roles elsewhere—are also involved in the regulation of mammalian OZT, but in a rather unexpected way.

MicroRNAs during OZT

The cloning of small RNAs from mouse oocytes has revealed three classes of small RNA: miRNAs, endo-siRNAs and piRNAs (Tam *et al*, 2008; Watanabe *et al*, 2008). Mammalian piRNAs are small RNAs produced by a *Dcr1*-independent mechanism that are essential for the male but not the female germline (reviewed in Klattenhoff & Theurkauf, 2008). The presence of all three known mammalian RNA silencing pathways in one cell type is unique. Interestingly, mouse oocytes do not contain any abundant oocyte-specific miRNAs and, due to a high abundance of members of the let-7 family and low levels of the miR-290 cluster miRNAs, the miRNA profile appears somatic-like. This is counterintuitive, considering the reprogramming ability of oocyte cytoplasm.

RT-PCR analysis of mouse miRNA expression during OZT (Tang *et al*, 2007) has revealed typical maternal, maternal-zygotic and zygotic expression patterns (Fig 3B). MicroRNA expression patterns are relatively unvarying when compared with mRNA expression patterns during OZT, and essentially depend on the ‘entry’ level of maternal miRNAs and the intensity of zygotic transcription. Maternal miRNAs undergo a common degradation on fertilization, and zygotic miRNAs increase

their abundance from the two-cell stage onwards (Tang *et al*, 2007). This common degradation probably reflects the fact that miRNAs are too short to be selectively degraded on the basis of sequence motifs, but the common transcriptional activation during ZGA is peculiar because miRNA expression is controlled by polymerase II, which allows for variable expression patterns. This is in contrast to maternal mRNAs, which have diverse individual patterns of expression (Zeng *et al*, 2004; Zeng & Schultz, 2005).

The most abundant maternal miRNAs are members of the let-7 family, which account for about one-third of miRNAs in the oocyte (Tam *et al*, 2008; Tang *et al*, 2007; Watanabe *et al*, 2008). Such a high quantity of mature

let-7 miRNAs is surprising considering that let-7 is typically found in adult and differentiated tissues, and its cloning frequency in *Xenopus* eggs is relatively low (Armisen *et al*, 2009). let-7 levels rapidly decline during OZT and let-7 expression is not restored in the early embryo, which is consistent with very low let-7 levels in ESCs. The most pronounced zygotic miRNAs are EEmiRC members (the miR-290 cluster), which are transcribed during the two-cell stage (Zeng & Schultz, 2005) and accumulate throughout preimplantation development (Tang *et al*, 2007). There are also maternal-zygotic miRNAs (for example, the miR-17-92 cluster), which are present at considerably high levels in oocytes and embryos, with a transiently lower expression at the two-cell

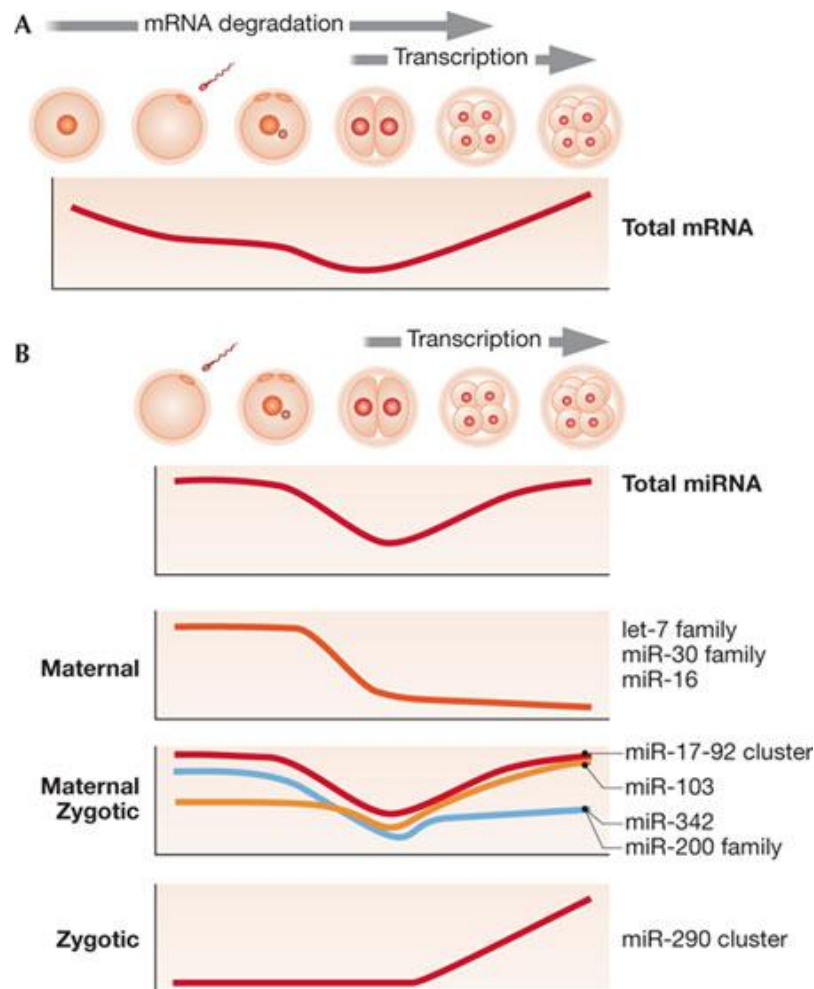


Figure 3. miRNAs during mouse oocyte-to-zygote transition. **(A)** Total mRNA (poly(A) RNA) amount changes during OZT (based on Piko & Clegg, 1982). From left to right the following developmental stages are shown: fully grown oocyte, mature MII egg, one-cell, two-cell, four-cell and eight-cell. **(B)** Schematic miRNA expression profiles during OZT. From left to right the following developmental stages are shown: mature MII egg, one-cell, two-cell, four-cell and eight-cell. Graphs are based on previously published data (Tang *et al*, 2007). miRNA, microRNA; OZT, oocyte-to-zygote transition.

stage (Fig 3B). These data imply that there is a switch between maternal and zygotic miRNAs that involves the rapid degradation of maternal miRNAs between the fertilized egg and the two-cell embryo stages. The active degradation must cease at times during the two-cell stage to allow for expression of zygotic miRNAs. Presumably, the remaining maternal miRNAs that survive the degradation disappear as they are replaced with zygotic miRNAs.

Idling microRNAs

The loss of *Dcr1*-dependent small RNAs during oocyte growth causes defects in meiotic spindle formation and infertility (Murchison *et al*, 2007; Tang *et al*, 2007). This phenotype was originally attributed to the loss of maternal miRNAs, because mature miRNAs were abundant in the wild-type oocyte and it seemed unlikely that the loss of endo-siRNAs would cause a spindle defect (Murchison *et al*, 2007; Tang *et al*, 2007). More recent data, however, questions the activity and role of maternal miRNAs, and changes the view of RNA silencing in mouse oocytes and early embryos. A study of the maternal loss of *Dgcr8*—which is involved in the biogenesis of canonical miRNA—found that *Dgcr8*^{-/-} oocytes develop and ovulate normally, can be fertilized and give rise to viable mice (Suh *et al*, 2010). Although the loss of maternal miRNAs slightly reduced developmental competence, it became clear that oocytes have an impressive tolerance to the loss of miRNAs. This tolerance appears to extend into early development because *Dgcr8*^{-/-} oocytes fertilized with *Dgcr8*^{-/-} sperm develop to the blastocyst stage (Suh *et al*, 2010).

In parallel, a loss of P-bodies in fully grown mouse oocytes was discovered by indirect immunofluorescence and by visualizing mRNAs targeted to P-bodies (Flemer *et al*, 2010; Ma *et al*, 2010). During OZT, P-bodies disappear as meiotically incompetent small postnatal oocytes start to grow in size, and appear again at the morula and blastocyst stages (Fig 4; Flemer *et al*, 2010). Although P-bodies are absent in growing oocytes, their components—TNRC6, DDX6, CPEB—and other proteins are found in subcortical ribonucleoprotein aggregates, which are

thought to be a storage place for maternal mRNAs (Flemer *et al*, 2010).

The absence of P-bodies provoked a more detailed examination of maternal miRNA activities using luciferase-based reporters, which can distinguish between the abilities of endogenous miRNAs to induce RNAi-like cleavage and translational repression (Schmitter *et al*, 2006). Reporters targeted by endogenous let-7 and miR-30 showed that RNAi-like cleavage (that is, loading of miRNA on AGO2 and accessibility of cognate 3' UTRs) is relatively normal, but the ability of miRNAs to repress translation is strongly reduced during oocyte growth and maturation (Ma *et al*, 2010). Interestingly, the less abundant miR-30 apparently retained more silencing activity, suggesting that an additional mechanism or mechanisms suppresses let-7 function in the oocyte (Ma *et al*, 2010). Suppression of miRNA activity is further supported by microarray data from *Dgcr8*^{-/-} and *Dcr1*^{-/-} oocytes (Suh *et al*, 2010). Taken together, this suggests that miRNAs are not only non-essential for OZT, but also that their function is suppressed by the oocyte. Therefore, uncoupling miRNAs from the repression of translation is the earliest known event in OZT in the mouse.

The mechanism and benefits of idling miRNAs are unknown. Suppression of miRNA function seems to take place after AGO2 loading and possibly involves uncoupling of AGO2 and TNRC6 (GW182), the latter being necessary for miRNA-mediated translational repression (Eulalio *et al*, 2008). This model is supported by the loss of colocalization of AGO2 and GW182 in oocytes (Flemer *et al*, 2010). Interestingly, overexpression of AGO2 in early embryos induces formation of P-bodies (Lykke-Andersen *et al*, 2008). At the moment, it is unclear why the miRNA pathway is turned off during the largest genome reprogramming event in the mammalian life cycle. We can only speculate that it might contribute to OZT by facilitating the switch between maternal and zygotic miRNAs. Idling miRNA might be seen as a waste of resources, but such a gearshift mechanism is a simple solution to disengaging maternal miRNAs during oocyte growth and engaging

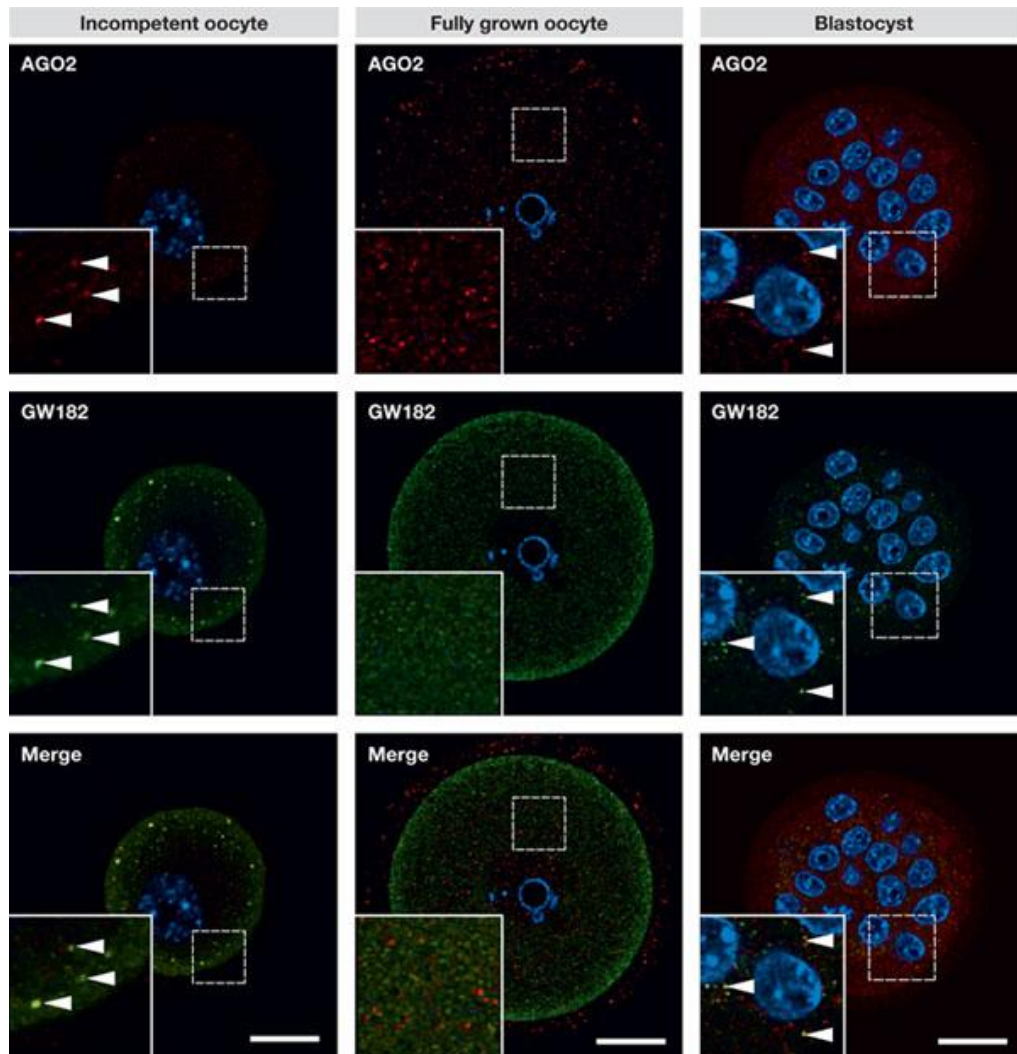


Figure 4. Loss of P-bodies in fully grown oocytes. Confocal images of GW182 (green) and AGO2 (red) in meiotically incompetent mouse oocytes (from 12-day-old mice), fully grown preovulatory oocytes and blastocysts. The inset shows a detail of cytoplasmic staining, the part of the specimen covered by the insert is not any different from the rest of the image. Immunofluorescent staining of GW182 and AGO2 was carried out as previously described (Flemer *et al.*, 2010). DNA is shown in blue (DAPI). Colocalization yields a yellow colour. Arrowheads depict P-bodies in blastocysts and somatic cells. Note the absence of GW182 and AGO2 colocalization and enhanced subcortical staining of GW182 in the subcortical region in fully grown oocytes. Scale bars, 20 μ m.

zygotic miRNAs later in preimplantation development.

As mentioned above, members of the let-7 family constitute about one-third of maternal miRNome, and are negative regulators of pluripotency. Although *Lin-28*, an inhibitor of let-7 (Hagan *et al.*, 2009), has high transcript levels in the oocyte (Zeng *et al.*, 2004), it does not appear to prevent high levels of mature let-7 from accumulating. A global suppression of activity of maternal miRNAs might, therefore, be able to relieve let-7-mediated repression, and allow the expression of maternal factors, which will

promote pluripotency in the zygote. Furthermore, as a considerable amount of let-7 survives maternal miRNA degradation between fertilization and the two-cell stage, continual suppression of the miRNA pathway into preimplantation development would further facilitate replacement of let-7 with zygotic miRNAs, particularly with the miR-290 cluster, which has a let-7 opposing role (Melton *et al.*, 2010). In this situation, LIN28 would prevent zygotic expression of let-7, which could cause problems when the miRNA pathway becomes functional again.

Mammalian RNA interference in the spotlight

One important output of recent studies of maternal miRNAs is new data concerning endogenous RNAi in mammals. The mammalian RNAi pathway has so far been a mystery, as endo-siRNAs were found only in oocytes and ESCs (Babiarz *et al*, 2008; Tam *et al*, 2008; Watanabe *et al*, 2008). Oocyte endo-siRNAs derived from processed pseudogenes suggest that mammalian RNAi, in addition to roles in the suppression of mobile and repetitive sequences known from invertebrates, might also regulate endogenous genes (Tam *et al*, 2008; Watanabe *et al*, 2008). This hypothesis is now supported by the defective spindle phenotype of *Dcr1*^{-/-} and *Ago2*^{-/-} oocytes, which is absent in *Dgcr8*^{-/-} oocytes. Furthermore, the bioinformatic analysis of the *Dcr1*^{-/-} transcriptome shows that many upregulated transcripts have complementary sequences to endo-siRNAs found in the oocyte (Ma *et al*, 2010). Thus, data support a model in which the miRNA pathway becomes disengaged early during oocyte growth and RNAi becomes the dominant RNA silencing pathway essential for OZT. Here, it presumably targets genes that would interfere with proper meiotic spindle assembly. The requirement for endogenous RNAi might extend into early development, because *Ago2* knockdown in early embryos causes arrests at the two-cell stage (Lykke-Andersen *et al*, 2008). The role of endogenous RNAi still needs to be validated by evidence that the ‘slicer’ activity of AGO2 is required for normal oocyte development. At present, it implies that the *Dcr1*^{-/-} and *Ago2*^{-/-} phenotypes might be unique to the mouse and that the role of mammalian RNAi in the oocyte might not be well conserved because it relies on endo-siRNAs produced from transcribed, processed pseudogenes, which evolve rapidly.

MicroRNAs in the zygote

Although we have argued above that mammalian miRNAs are not needed for OZT, it is necessary to put the function of zygotic miRNAs into the context of other vertebrate systems. When such a comparison is made (Fig 5), it becomes apparent that

vertebrate zygotes express AAGUGC miRNAs, but use them in a different spatiotemporal context.

In the mouse, the major reprogramming of the zygote by newly expressed genes initiates at the two-cell stage. Although the one-cell embryo is transcriptionally active, it does not seem to produce functional mRNAs (Zeng & Schultz, 2005). The final stage of degradation of maternal mRNAs is superimposed on the activation of the zygotic genome. It is initiated by the resumption of meiosis and is an integral part of the switch from the maternal to the zygotic programme, although a direct link between maternal mRNA degradation and establishment of pluripotency has not been documented. Maternal mRNA degradation is substantial and, by the two-cell stage, eliminates 75% of the poly(A) RNA that is originally found in the pre-ovulatory oocyte (Piko & Clegg, 1982). The zygotic miR-290 family transcription starts during the two-cell stage, but mature miRNA accumulation is first observed at the four-cell stage (Tang *et al*, 2007; Zeng & Schultz, 2005). Zygotic miRNAs are, therefore, unlikely to contribute significantly to maternal mRNA degradation in the mouse: first, because their activity is suppressed at the early stages of preimplantation development; and second, even if the zygotic miRNAs were active, they would appear when the majority of maternal mRNAs are already degraded.

This situation is different from that in the fish and the frog, in which development is very fast and zygotic miRNAs appear when maternal mRNAs are still abundant (Fig 5). Due to this fast development, there is likely to be greater pressure to eliminate maternal mRNAs so that they do not interfere with differentiation, and zygotic miRNAs offer a way to deal with this problem. A contribution of miRNAs to degradation of maternal mRNA was reported in *Drosophila* (Bushati *et al*, 2008). In the zebrafish, the miR-430 family becomes strongly upregulated a few hours after fertilization and targets up to an estimated 40% of maternal mRNAs (Giraldez *et al*, 2006). This suggests that the miR-430 family significantly contributes to maternal mRNA degradation. A similar role has also

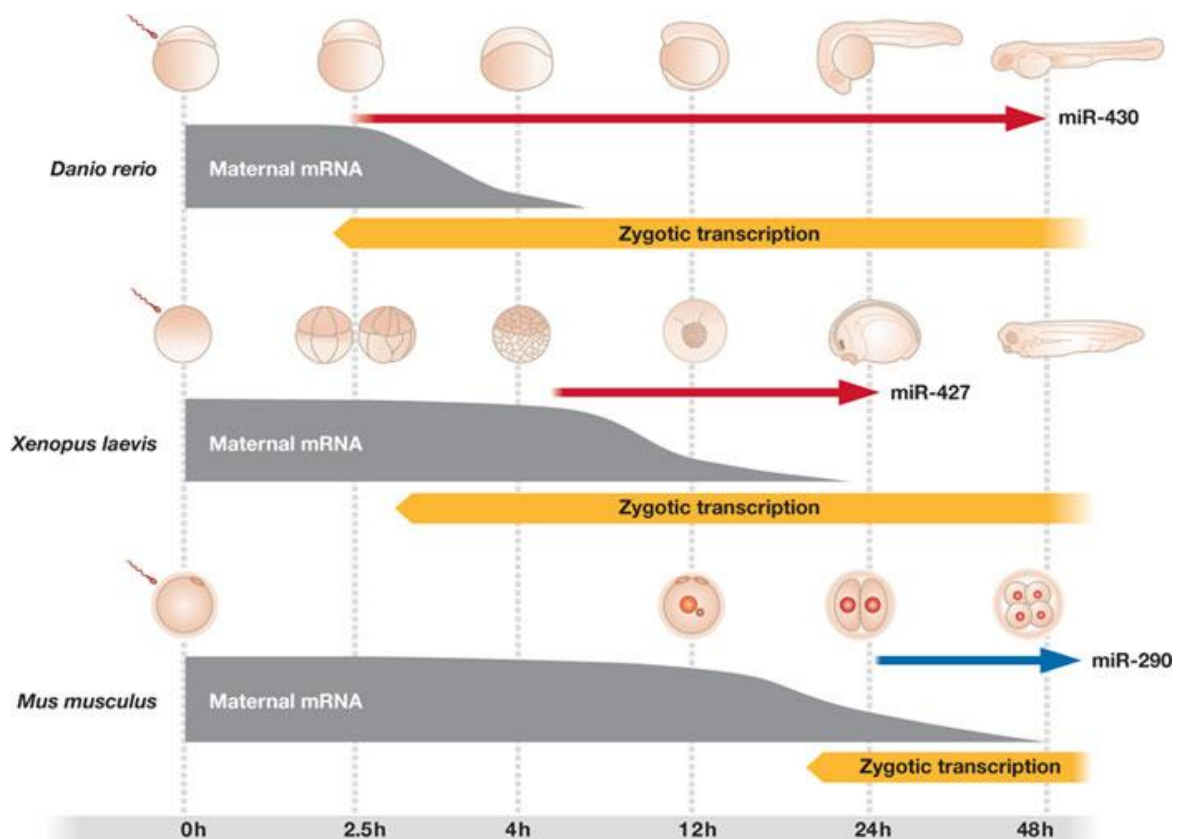


Figure 5. Oocyte-to-zygote transition in the mouse, zebrafish and frog. Specific developmental stages, the course of maternal mRNA degradation, ZGA and expression of zygotic AAGUGC miRNAs in mouse, zebrafish and frog embryos is shown on the same timescale.

been proposed for miR-427 during *Xenopus* embryo development (Lund *et al.*, 2009).

Despite the differences detailed above, there are also notable similarities. One example is a partly conserved role in Nodal signalling, which is important for germ layer specification (Choi *et al.*, 2007; Rosa *et al.*, 2009). Early vertebrate embryos express a set of related AAGUGC miRNAs during ZGA. This suggests that AAGUGC miRNAs have common and evolving roles in the regulation of development. In addition to *Lefty1* and *Lefty2* in Nodal signalling, only a small number of genes—including *Dazap2* and *Elavl2* (*HuB*)—are common among miR-290 and miR-430 targets (Giraldez *et al.*, 2006; Sinkkonen *et al.*, 2008). However, the general role of EEmiRCs and the miR-430 cluster is the same: they support development by targeting genes the expression of which should be kept low in the embryo. From this perspective, the difference is in the context: the miR-290 cluster targets mostly zygotic transcripts, whereas the miR-430 cluster deals also with a large amount of maternal

mRNAs. Variability among targets and specific roles of AAGUGC miRNAs across vertebrates should not be surprising, because early post-zygotic regulations might evolve fast during speciation.

Conclusions

It is remarkable that the molecular mechanisms underlying developmental potential are not strongly conserved. This can be contrasted with the example of let-7 miRNA, which is found in differentiated cells from *Caenorhabditis elegans* to mammals, and zygotic AAGUGC miRNAs, which are found in vertebrates with considerable variation in conservation at the genomic level. RNA silencing mechanisms underlying OZT and pluripotency in mammals should be viewed as unique solutions superimposed on broader general principles. In the mouse, miRNA function is suppressed in oocytes: miRNAs do not contribute to zygotic genome activation, maternal mRNA degradation or establishment of the core pluripotency transcriptional network. However, the

importance of endogenous RNAi in the oocyte has recently become apparent. MicroRNAs are essential for pluripotency, but whether this reflects the activity of ESC miRNAs or the requirement for other miRNAs during differentiation remains to be revealed.

Sidebar A | In need of answers

- i. Which miRNAs are essential for pluripotency in embryonic stem cells?
- ii. How do miRNAs support pluripotency in embryonic stem cells?
- iii. What is the role of RNAi in embryonic stem cells?
- iv. How are miRNAs suppressed in the oocyte?
- v. Would normal miRNA activity interfere with OZT?
- vi. Is mammalian RNAi-mediated control of gene expression essential for meiosis?
- vii. How conserved is the function of RNAi in the germline in mammals?

Glossary

DAZAP2	DAZ (deleted in azoospermia)-associated protein 2
DGCR8	Di George Critical Region 8
DCR	DICER, an RNase III family endoribonuclease
DNMT	<i>de novo</i> DNA methyltransferase
dpc	days post-coitum
dsRNA	double-stranded RNA
EB	embryoid bodies
EemIRC	early embryonic microRNA cluster
ELAVL2	(HuB) A+U-rich sequences binding translational repressor
ESCs	embryonic stem cells
iPSCs	induced pluripotent stem cells
ESCC	ES cell-specific cell cycle-regulating miRNAs
miRNA	microRNA, a small RNA encoded by the genome
OZT	oocyte-to-zygote transition
OCT4	octamer 4, also known as POU class 5 homeobox
oncomiRs	miRNAs with oncogenic potential
piRNA	Piwi-interacting RNA
RBL2	retinoblastoma-like protein 2
RNAi	RNA interference, one of the pathways that uses short RNAs generated from long dsRNA to induce sequence-specific cleavage of cognate mRNAs
RNA silencing	
RT-PCR	reverse transcription PCR

siRNA	small interfering RNA
SOX2	(sex determining region Y)-Box 2 transcription factor
UTR	untranslated region
ZGA	zygotic genome activation

Acknowledgements

The authors thank Richard M. Schultz, Robert Blelloch and Witold Filipowicz for fruitful discussions. P.S. is a holder of the J.E. Purkyne Fellowship and his lab is supported by the following grants: EMBO SDIG project 1483, GACR 204/09/0085, GACR P305/10/2215 and Kontakt ME09039.

Conflict of interest

The authors declare that they have no conflict of interest.

References

- Armisen J, Gilchrist MJ, Wilczynska A, Standart N, Miska EA (2009) Abundant and dynamically expressed miRNAs, piRNAs, and other small RNAs in the vertebrate *Xenopus tropicalis*. *Genome Res* 19: 1766–1775
- Babiarz JE, Ruby JG, Wang Y, Bartel DP, Blelloch R (2008) Mouse ES cells express endogenous shRNAs, siRNAs, and other Microprocessor-independent, Dicer-dependent small RNAs. *Genes Dev* 22: 2773–2785
- Bagga S, Bracht J, Hunter S, Massirer K, Holtz J, Eachus R, Pasquinelli AE (2005) Regulation by let-7 and lin-4 miRNAs results in target mRNA degradation. *Cell* 122: 553–563
- Benetti R *et al* (2008) A mammalian microRNA cluster controls DNA methylation and telomere recombination via Rbl2-dependent regulation of DNA methyltransferases. *Nat Struct Mol Biol* 15: 268–279
- Boyer LA *et al* (2005) Core transcriptional regulatory circuitry in human embryonic stem cells. *Cell* 122: 947–956
- Brennecke J, Stark A, Russell RB, Cohen SM (2005) Principles of microRNA-target recognition. *PLoS Biol* 3: e85
- Bushati N, Stark A, Brennecke J, Cohen SM (2008) Temporal reciprocity of miRNAs and their

- targets during the maternal-to-zygotic transition in *Drosophila*. *Curr Biol* 18: 501–506
- Bussing I, Slack FJ, Grosshans H (2008) let-7 microRNAs in development, stem cells and cancer. *Trends Mol Med* 14: 400–409
- Card DA, Hebbar PB, Li L, Trotter KW, Komatsu Y, Mishina Y, Archer TK (2008) Oct4/Sox2-regulated miR-302 targets cyclin D1 in human embryonic stem cells. *Mol Cell Biol* 28: 6426–6438
- Chapman EJ, Carrington JC (2007) Specialization and evolution of endogenous small RNA pathways. *Nat Rev Genet* 8: 884–896
- Chen T, Ueda Y, Dodge JE, Wang Z, Li E (2003) Establishment and maintenance of genomic methylation patterns in mouse embryonic stem cells by Dnmt3a and Dnmt3b. *Mol Cell Biol* 23: 5594–5605
- Choi WY, Giraldez AJ, Schier AF (2007) Target protectors reveal dampening and balancing of Nodal agonist and antagonist by miR-430. *Science* 318: 271–274
- Eulalio A, Behm-Ansmant I, Izaurralde E (2007a) P bodies: at the crossroads of post-transcriptional pathways. *Nat Rev Mol Cell Biol* 8: 9–22
- Eulalio A, Behm-Ansmant I, Schweizer D, Izaurralde E (2007b) P-body formation is a consequence, not the cause, of RNA-mediated gene silencing. *Mol Cell Biol* 27: 3970–3981
- Eulalio A, Huntzinger E, Izaurralde E (2008) GW182 interaction with Argonaute is essential for miRNA-mediated translational repression and mRNA decay. *Nat Struct Mol Biol* 15: 346–353
- Flemer M, Ma J, Schultz RM, Svoboda P (2010) P-body loss is concomitant with formation of a messenger RNA storage domain in mouse oocytes. *Biol Reprod* 8: 1008–1017
- Friedman RC, Farh KK, Burge CB, Bartel DP (2009) Most mammalian mRNAs are conserved targets of microRNAs. *Genome Res* 19: 92–105
- Fukagawa T, Nogami M, Yoshikawa M, Ikeno M, Okazaki T, Takami Y, Nakayama T, Oshimura M (2004) Dicer is essential for formation of the heterochromatin structure in vertebrate cells. *Nat Cell Biol* 6: 784–791
- Giraldez AJ, Mishima Y, Rihel J, Grocock RJ, Van Dongen S, Inoue K, Enright AJ, Schier AF (2006) Zebrafish miR-430 promotes deadenylation and clearance of maternal mRNAs. *Science* 312: 75–79
- Gurdon JB, Melton DA (2008) Nuclear reprogramming in cells. *Science* 322: 1811–1815
- Hagan JP, Piskounova E, Gregory RI (2009) Lin28 recruits the TUTase Zcchc11 to inhibit let-7 maturation in mouse embryonic stem cells. *Nat Struct Mol Biol* 16: 1021–1025
- Houbaviy HB, Murray MF, Sharp PA (2003) Embryonic stem cell-specific microRNAs. *Dev Cell* 5: 351–358
- Houbaviy HB, Dennis L, Jaenisch R, Sharp PA (2005) Characterization of a highly variable eutherian microRNA gene. *RNA* 11: 1245–1257
- Judson RL, Babiarz JE, Venere M, Blalock R (2009) Embryonic stem cell-specific microRNAs promote induced pluripotency. *Nat Biotechnol* 27: 459–461
- Kanellopoulou C, Muljo SA, Kung AL, Ganesan S, Drapkin R, Jenuwein T, Livingston DM, Rajewsky K (2005) Dicer-deficient mouse embryonic stem cells are defective in differentiation and centromeric silencing. *Genes Dev* 19: 489–501
- Kim VN, Han J, Siomi MC (2009) Biogenesis of small RNAs in animals. *Nat Rev Mol Cell Biol* 10: 126–139
- Klattenhoff C, Theurkauf W (2008) Biogenesis and germline functions of piRNAs. *Development* 135: 3–9
- Kloosterman WP, Plasterk RH (2006) The diverse functions of microRNAs in animal development and disease. *Dev Cell* 11: 441–450
- Lai EC (2002) Micro RNAs are complementary to 3' UTR sequence motifs that mediate negative post-transcriptional regulation. *Nat Genet* 30: 363–364
- Landgraf P *et al* (2007) A mammalian microRNA expression atlas based on small RNA library sequencing. *Cell* 129: 1401–1414
- Lim LP, Lau NC, Garrett-Engle P, Grimson A, Schelter JM, Castle J, Bartel DP, Linsley PS, Johnson JM (2005) Microarray analysis shows

- that some microRNAs downregulate large numbers of target mRNAs. *Nature* 433: 769–773
- Liu J, Carmell MA, Rivas FV, Marsden CG, Thomson JM, Song JJ, Hammond SM, Joshua-Tor L, Hannon GJ (2004) Argonaute2 is the catalytic engine of mammalian RNAi. *Science* 305: 1437–1441
- Loh YH *et al* (2006) The Oct4 and Nanog transcription network regulates pluripotency in mouse embryonic stem cells. *Nat Genet* 38: 431–440
- Lund E, Liu M, Hartley RS, Sheets MD, Dahlberg JE (2009) Deadenylation of maternal mRNAs mediated by miR-427 in *Xenopus laevis* embryos. *RNA* 15: 2351–2363
- Lykke-Andersen K, Gilchrist MJ, Grabarek JB, Das P, Miska E, Zernicka-Goetz M (2008) Maternal Argonaute 2 is essential for early mouse development at the maternal–zygotic transition. *Mol Biol Cell* 19: 4383–4392
- Ma J, Flemer M, Stein P, Berninger P, Malik R, Zavolan M, Svoboda P, Schultz RM (2010) MicroRNA activity is suppressed in mouse oocytes. *Curr Biol* 20: 265–270
- Marson A *et al* (2008) Connecting microRNA genes to the core transcriptional regulatory circuitry of embryonic stem cells. *Cell* 134: 521–533
- Meister G, Landthaler M, Patkaniowska A, Dorsett Y, Teng G, Tuschl T (2004) Human Argonaute2 mediates RNA cleavage targeted by miRNAs and siRNAs. *Mol Cell* 15: 185–197
- Melton C, Judson RL, Blelloch R (2010) Opposing microRNA families regulate self-renewal in mouse embryonic stem cells. *Nature* 463: 621–626
- Mendell JT (2008) miRiad roles for the miR-17-92 cluster in development and disease. *Cell* 133: 217–222
- Murchison EP, Partridge JF, Tam OH, Cheloufi S, Hannon GJ (2005) Characterization of Dicer-deficient murine embryonic stem cells. *Proc Natl Acad Sci USA* 102: 12135–12140
- Murchison EP, Stein P, Xuan Z, Pan H, Zhang MQ, Schultz RM, Hannon GJ (2007) Critical roles for Dicer in the female germline. *Genes Dev* 21: 682–693
- Piko L, Clegg KB (1982) Quantitative changes in total RNA, total poly(A), and ribosomes in early mouse embryos. *Dev Biol* 89: 362–378
- Richter JD (2007) CPEB: a life in translation. *Trends Biochem Sci* 32: 279–285
- Rosa A, Spagnoli FM, Brivanlou AH (2009) The miR-430/427/302 family controls mesendodermal fate specification via species-specific target selection. *Dev Cell* 16: 517–527
- Schmitter D, Filkowski J, Sewer A, Pillai RS, Oakeley EJ, Zavolan M, Svoboda P, Filipowicz W (2006) Effects of Dicer and Argonaute down-regulation on mRNA levels in human HEK293 cells. *Nucleic Acids Res* 34: 4801–4815
- Sinkkonen L, Hugenschmidt T, Berninger P, Gaidatzis D, Mohn F, Artus-Revel CG, Zavolan M, Svoboda P, Filipowicz W (2008) MicroRNAs control *de novo* DNA methylation through regulation of transcriptional repressors in mouse embryonic stem cells. *Nat Struct Mol Biol* 15: 259–267
- Smith AG (2001) Embryo-derived stem cells: of mice and men. *Annu Rev Cell Dev Biol* 17: 435–462
- Suh MR *et al* (2004) Human embryonic stem cells express a unique set of microRNAs. *Dev Biol* 270: 488–498
- Suh N, Baehner L, Moltzahn F, Melton C, Shenoy A, Chen J, Blelloch R (2010) MicroRNA function is globally suppressed in mouse oocytes and early embryos. *Curr Biol* 20: 271–277
- Surani MA, Barton SC, Norris ML (1984) Development of reconstituted mouse eggs suggests imprinting of the genome during gametogenesis. *Nature* 308: 548–550
- Takahashi K, Yamanaka S (2006) Induction of pluripotent stem cells from mouse embryonic and adult fibroblast cultures by defined factors. *Cell* 126: 663–676
- Tam OH *et al* (2008) Pseudogene-derived small interfering RNAs regulate gene expression in mouse oocytes. *Nature* 453: 534–538
- Tang F, Kaneda M, O'Carroll D, Hajkova P, Barton SC, Sun YA, Lee C, Tarakhovsky A, Lao K, Surani MA (2007) Maternal microRNAs are essential for mouse zygotic development. *Genes Dev* 21: 644–648

Tay Y, Zhang J, Thomson AM, Lim B, Rigoutsos I (2008) MicroRNAs to Nanog, Oct4 and Sox2 coding regions modulate embryonic stem cell differentiation. *Nature* 455: 1124–1128

Wang Y, Medvid R, Melton C, Jaenisch R, Blelloch R (2007) DGCR8 is essential for microRNA biogenesis and silencing of embryonic stem cell self-renewal. *Nat Genet* 39: 380–385

Wang Y, Baskerville S, Shenoy A, Babiarz JE, Baehner L, Blelloch R (2008) Embryonic stem cell-specific microRNAs regulate the G1–S transition and promote rapid proliferation. *Nat Genet* 40: 1478–1483

Watanabe T *et al* (2008) Endogenous siRNAs from naturally formed dsRNAs regulate transcripts in mouse oocytes. *Nature* 453: 539–543

Wilmut I, Schnieke AE, McWhir J, Kind AJ, Campbell KH (1997) Viable offspring derived from fetal and adult mammalian cells. *Nature* 385: 810–813

Xu N, Papagiannakopoulos T, Pan G, Thomson JA, Kosik KS (2009) MicroRNA-145 regulates OCT4, SOX2, and KLF4 and represses pluripotency in human embryonic stem cells. *Cell* 137: 647–658

Zeng F, Schultz RM (2005) RNA transcript profiling during zygotic gene activation in the preimplantation mouse embryo. *Dev Biol* 283: 40–57

Zeng F, Baldwin DA, Schultz RM (2004) Transcript profiling during preimplantation mouse development. *Dev Biol* 272: 483–496

LIST OF PUBLICATIONS

Publications related to this thesis:

Flemer, M., Ma, J., Schultz, R.M., and Svoboda, P. (2010). P-body loss is concomitant with formation of a messenger RNA storage domain in mouse oocytes. *Biol Reprod* 82, 1008-17. (IF2010 = 3.87)

Ma, J., Flemer, M., Stein, P., Berninger, P., Malik, R., Zavolan, M., Svoboda, P., and Schultz, R.M. (2010). MicroRNA activity is suppressed in mouse oocytes. *Curr Biol* 20, 265-70. (IF2010 = 10.026)

Svoboda, P., and Flemer, M. (2010). The role of miRNAs and endogenous siRNAs in maternal-to-zygotic reprogramming and the establishment of pluripotency. *EMBO Rep* 11, 590-7. (IF2010 = 7.822)

Flemer, M., and Svoboda, P. (2011). Ribonucleoprotein localization in mouse oocytes. *Methods* 53, 136-41. (IF2010 = 4.527)

Other publications:

Nejepinska, J., Malik, R., Filkowski, J., Flemer, M., Filipowicz, W., and Svoboda, P. (2012). dsRNA expression in the mouse elicits RNAi in oocytes and low adenosine deamination in somatic cells. *Nucleic Acids Res* 40, 399-413.

Nejepinska, J., Flemer, M., and Svoboda, P. (2012). Control of the interferon response in RNAi experiments. *Methods Mol Biol* 820, 133-61.

Vinopal, S., Cernohorska, M., Sulimenko, V., Sulimenko, T., Vosecka, V., Flemer, M., Draberova, E., and Draber, P. (2012) γ -Tubulin 2 nucleates microtubules and is downregulated in mouse early embryogenesis. *PLoS One* 7, e29919.

CURRICULUM VITAE

Matyas Flemr
born June 25, 1983 in Prague

flemrm@img.cas.cz
tel. +420 776 215 500

WORK ADDRESS

Institute of Molecular Genetics
Videnska 1083
14220 - Prague 4
Czech Rep.

PRIVATE ADDRESS

Na Rozhledu 9
14700 - Prague 4
Czech Rep.

EDUCATION

- 2007 - 2012 Charles University Prague, 1st Faculty of Medicine, Ph.D. program in cell and developmental biology
- 2002 - 2007 Institute of Chemical Technology Prague, Faculty of Food and Biochemical Technology, M.Sc. program in general and applied biochemistry, graduated with honours

RESEARCH EXPERIENCE

- Sep 2012 - Friedrich Miescher Institute for Biomedical Research, Basel, Switzerland (Postdoc position in the laboratory of Dr. Marc Bühler)
- 2007 - 2012 Laboratory of Epigenetic Regulations, Institute of Molecular Genetics, Prague (Head: Petr Svoboda Ph.D.) Ph.D. project focused on mechanisms of maternal mRNA degradation during oocyte-to-zygote transition in the mouse
- 2004 - 2007 Laboratory of Plant Biochemistry, Institute of Chemical Technology, Prague (Head: Prof. Olga Valentova Ph.D.) research on phospholipid signalling pathways involved in plant systemic acquired resistance
diploma thesis: Phospholipase D regulated transcriptome of systemic acquired resistance in *Arabidopsis thaliana*.
- 02 - 06/2006 Laboratory of Plant Cellular and Molecular Physiology, University Pierre et Marie Curie, Paris (Head: Prof. Alain Zachowski Ph.D.) Erasmus study stay - research on phospholipid-modifying enzymes involved in plant defence responses
final report: Role of Phospholipase D in Response to Salicylic Acid in *Arabidopsis thaliana*.

ADDITIONAL INFORMATION

- 2007 Josef Hlavka Award dedicated to the best students and talented young investigators from Czech universities and Academy of Sciences
- 2007 Dean's Award for excellence in undergraduate studies, ICT Prague
- 2011 Scientia foundation Award for the best 2010 publication record of PhD students of the 1st Faculty of Medicine, Charles University